ISBN 978-82-326-6448-1 (printed ver.)
ISBN 978-82-326-5990-6 (electronic ver.)
ISSN 1503-8181 (printed ver.)
ISSN 2703-8084 (electronic ver.)

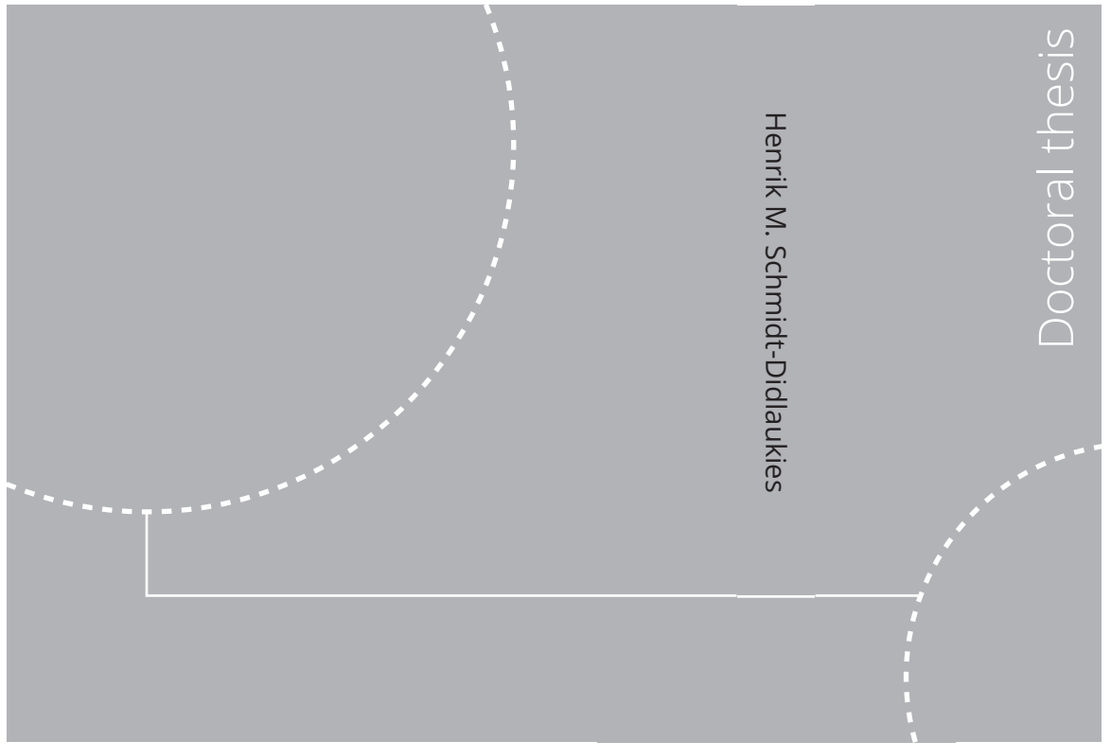

Doctoral theses at NTNU, 2023:130

Henrik M. Schmidt-Didlaukies

Modeling and Hybrid Feedback Control of Underwater Vehicles

NTNU
Norwegian University of
Science and Technology
Thesis for the degree of
Philosophiae Doctor
Faculty of Engineering
Department of Marine Technology

NTNU
Norwegian University of
Science and Technology

Doctoral theses at NTNU, 2023:130

NTNU

NTNU
Norwegian University of
Science and Technology

Henrik M. Schmidt-Didlaukies

Modeling and Hybrid Feedback Control of Underwater Vehicles

Thesis for the degree of Philosophiae Doctor

Trondheim, April 2023

Norwegian University of Science and Technology
Faculty of Engineering
Department of Marine Technology

NTNU
Norwegian University of
Science and Technology

NTNU
Norwegian University of Science and Technology

Thesis for the degree of Philosophiae Doctor

Faculty of Engineering
Department of Marine Technology

ISBN 978-82-326-6448-1 (printed ver.)
ISBN 978-82-326-5990-6 (electronic ver.)
ISSN 1503-8181 (printed ver.)
ISSN 2703-8084 (electronic ver.)

Doctoral theses at NTNU, 2023:130

PRINTED IN NORWAY
NO - 1598

NORDIC SWAN ECOLABEL
Printed matter
2041 0731

Printed by Skipnes Kommunikasjon AS

Summary

This thesis presents contributions to the mathematical modeling of underwater vehicles and nonlinear hybrid feedback control. We present a matrix Lie group formulation of the standard model describing the motion of rigid underwater vehicles. Furthermore, we introduce monotone dissipativity, a specialization of the standard notion of dissipativity, which is useful for the stability analysis of underwater vehicle control systems. It is shown that common formulations of hydrodynamic damping experienced by underwater vehicles are not merely dissipative, but in fact monotonically dissipative. We then investigate a fundamental relationship between convexity properties of Rayleigh dissipation functions and monotonically dissipative hydrodynamic damping models. The Lie group formulation of the underwater vehicle dynamics also makes possible a complete and precise description of vehicle shape symmetry, and its role in simplifying the modeling of hydrodynamic inertia and damping effects.

An extension of the aforementioned modeling framework to underwater vehicles that are multibody systems with a kinematic tree structure is subsequently formulated. This class of underwater vehicles includes not only conventional underwater vehicle-manipulator systems, but also a large number of experimental and prototype designs such as articulated intervention autonomous underwater vehicles. A global matrix-form of the vehicle kinematics and dynamics which is well-suited to stability analysis of model-based control laws is derived. Furthermore, we introduce a generalized inverse dynamics algorithm that simplifies the implementation of such control laws. The forward dynamics problem is addressed in an efficient manner with a composite-rigid-body algorithm.

Hybrid feedback control laws typically comprise a collection of continuous state feedback control laws in conjunction with a state-based switching logic that determines which control law from the collection is utilized. We employ hybrid feedback control to circumvent topological obstructions to robust global stabilization which are associated, for example, with the rotational degrees of freedom of marine vehicles. In particular, we formulate globally asymptotically stabilizing proportional-derivative (PD), output feedback, and proportional-derivative-integral (PID) hybrid feedback control laws, which solve the tracking problem globally and robustly for a class of mechanical control systems defined on matrix Lie groups. These control laws are constructed from so-called synergistic functions, which have already been derived for the Lie groups that describe the configuration space of many important engineering systems. The presented control laws therefore have immediate and wide applicability.

We also present specialized adaptive hybrid feedback control laws for marine surface and underwater vehicles, which we derive from a slightly more general class of functions than the aforementioned synergistic ones. The introduced control laws can

be loosely characterized as being of dynamic sliding-surface type, and ensure global asymptotic path-following for the marine vehicles in the presence of parametric modeling uncertainties. In contrast to conventional synergistic backstepping control laws, the sliding surface formulation results in a switching logic which is independent of the vehicle velocities. While this feature comes at the cost of a minor increase in dynamic order of the control law, it permits the estimation of the vehicle's inertial parameters. Experimental validation of the derived control laws are presented for surface and underwater vehicles.

We subsequently introduce hysteretic control Lyapunov functions (HCLFs). A family of HCLFs consists of several locally defined control Lyapunov functions. A switching logic with hysteresis is encoded in three finite covers of the state-space on which the control Lyapunov functions satisfy certain decrease conditions. We investigate the relationship between HCLFs and synergistic control Lyapunov functions (SCLFs), and show that a family of HCLFs generalizes an SCLF whose synergy gap is bounded away from zero. Furthermore, given an HCLF family, we derive sufficient conditions for the existence of globally asymptotically stabilizing hybrid feedbacks. Lastly, we provide a constructive optimization-based design procedure for such stabilizing hybrid feedbacks.

The last chapter of this thesis presents a generalization of synergistic Lyapunov function and feedback (SLFF) pairs, which in turn are a generalization of the aforementioned synergistic functions. In particular, we allow the logic variable paramount to traditional synergistic control to possess flow dynamics, thereby translating SLFF pairs into SLFF triples. The generalized logic state is referred to as a synergy variable, for which we introduce the two modified jumping strategies optional jumping and independently triggered jumping. Moreover, it is shown that SLFF triples, like SLFF pairs, are amenable to integrator backstepping. We demonstrate the usefulness of the proposed framework by constructing a globally stabilizing synergistic maneuvering control law for surface vessels that allows optional jumps of the path parameter.

Contents

List of Symbols

$\mathbb{R}$	The set or real numbers.
$\mathbb{R}_{\geq 0}$	The set of nonnegative real numbers.
$\mathbb{C}$	The set of complex numbers.
$\mathbb{Z}_{\geq 0}$	Set of nonnegative integers.
$\mathbb{R}^n$	n-dimensional Euclidean space.
$\mathbb{C}^n$	n-dimensional space of complex numbers.
$\mathbb{R}^{n\times n}$	Space of $n \times n$ matrices with real entries.
$\mathbb{C}^{n\times n}$	Space of $n \times n$ matrices with complex entries.
C^r	r-times continuously differentiable.
$r\mathbb{B}$	The closed ball of radius r in $\mathbb{R}^n$.
$\operatorname{col} A$	Column space of the matrix $A \in \mathbb{R}^{m\times n}$.
$\overline{\operatorname{con}}\, S$	Closed convex hull of the set S.
$\mathbb{S}^n$	The unit n-sphere embedded in $\mathbb{R}^{n+1}$.
$\subset$	Subset.
$\overline{S}$	The closure of the set S.
S°	The interior of the set S.
∂S	The boundary of the set S.
$S_1 \setminus S_2$	The relative complement of S_2 in S_1.
$\pi_i(S)$	The projection of $S \subset X = X_1 \times X_2 \times \cdots \times X_n$ onto the set $X_i, 1 \leq i \leq n$.
(x, y)	Equivalent notation for the vector $(x^\mathsf{T}\ y^\mathsf{T})^\mathsf{T}$.
$\langle x, y\rangle$	The Euclidean inner product of two vectors $x, y \in \mathbb{R}^n$.
$\lvert x\rvert$	The Euclidean norm of a vector $x \in \mathbb{R}^n$.
$\lvert A\rvert$	Induced norm of a matrix $A \in \mathbb{R}^{n\times n}$.
$\lvert x\rvert_{\mathcal{A}}$	The distance from a point $x \in \mathbb{R}^n$ to a set $\mathcal{A} \subset \mathbb{R}^n$, which is given by $\inf_{y\in\mathcal{A}}\lvert x - y\rvert$.
$\lVert A\rVert$	The Frobenius norm $\sqrt{\operatorname{tr}(A^\mathsf{T}A)}$ of a matrix $A \in \mathbb{R}^{n\times n}$.
$\nabla V(x)$	The gradient of a function $V : \mathbb{R}^n \to \mathbb{R}$ at $x \in \mathbb{R}^n$.
∇^M	The bilinear map $\nabla^M : \mathbb{R}^k \times \mathbb{R}^k \to \mathbb{R}^k$ induced by a left-invariant metric $M \in \mathbb{R}^{k\times k}$.
$\mathrm{D}f(x)$	The derivative of $f : \mathbb{R}^n \to \mathbb{R}^m$ at $x \in \mathbb{R}^n$.
$\mathrm{d}f(g)$	The trivialized derivative of $f : \mathcal{G} \to \mathbb{R}^m$ at $g \in \mathcal{G}$, where $\mathcal{G}$ is a matrix Lie group.
$f'(x)$	The derivative of a function $f : \mathbb{R} \to \mathbb{R}^n$ at $x \in \mathbb{R}$.

$(e_1, e_2, \ldots, e_n)$	The standard basis for $\mathbb{R}^n$.
$\mathrm{E}(n)$	The Euclidean group of dimension n.
$\mathfrak{e}(n)$	Lie algebra of $\mathrm{E}(n)$.
$f : \mathbb{R}^n \to \mathbb{R}^m$	A single-valued mapping from $\mathbb{R}^n$ to $\mathbb{R}^m$.
$F : \mathbb{R}^n \rightrightarrows \mathbb{R}^m$	A set-valued mapping from $\mathbb{R}^n$ to $\mathbb{R}^m$.
$\operatorname{rge} f$	The range of a mapping $f : \mathbb{R}^n \to \mathbb{R}^m$.
$\operatorname{gph} f$	The graph of the mapping f.
$\mathcal{G}$	A matrix Lie group.
$\mathfrak{g}$	Lie algebra of a Lie group $\mathcal{G}$.
$x \otimes y$	Outer product of two vectors $x \in \mathbb{R}^n$ and $y \in \mathbb{R}^m$.
$\mathrm{O}(n)$	The orthogonal group of dimension n.
$\mathfrak{o}(n)$	Vector space of skew-symmetric $n \times n$ matrices, and the Lie algebra of $\mathrm{O}(n)$.
$\mathrm{SE}(n)$	The special Euclidean group of dimension n.
$\mathfrak{se}(n)$	Lie algebra of $\mathrm{SE}(n)$.
$\widetilde{\mathrm{SE}}(3)$	The universal covering group of $\mathrm{SE}(3)$.
$\widetilde{\mathfrak{se}}(3)$	Lie algebra of $\widetilde{\mathrm{SE}}(3)$.
$\mathrm{SO}(n)$	The special orthogonal group of dimension n.
$\mathfrak{so}(n)$	Vector space of skew-symmetric $n \times n$ matrices, and the Lie algebra of $\mathrm{SO}(n)$.
$\mathrm{SU}(2)$	The special unitary group of dimension 2.
$\mathfrak{su}(2)$	Lie algebra of $\mathrm{SU}(2)$.
$\widehat{\cdot}$	Isomorphism between $\mathbb{R}^m$ and an m-dimensional Lie algebra $\mathfrak{g}$.
$T_S(x)$	The tangent cone to the set $S \subset \mathbb{R}^n$ at $x \in \overline{S}$.
$\operatorname{tr} A$	The trace of a matrix $A \in \mathbb{R}^{n \times n}$.
Z	The group of unit quaternions.
$\mathfrak{z}$	Lie algebra of Z.

Preface

This thesis is submitted in partial fulfillment of the requirements for the degree of philosophiae doctor (PhD) at the Norwegian University of Science and Technology (NTNU), Trondheim. The work presented in this thesis has been carried out at the Centre for Autonomous Marine Operations and Systems (AMOS) and the Department of Marine Technology under the supervision of Professor Asgeir J. Sørensen (Dept. Marine Technology, NTNU) and co-supervision of Professor Kristin Y. Pettersen (Dept. Engineering Cybernetics, NTNU). The work was supported by the Research Council of Norway (grant no. 223254) at AMOS.

Acknowledgments

I would first like to thank my supervisor Professor Asgeir J. Sørensen. He has been immensely supportive and understanding throughout my academic career, and has helped me through several difficult times. Asgeir is not only an exceptional motivator, but also a positive, thoughtful, and empathetic leader.

I am deeply grateful to my co-supervisor Professor Kristin Y. Pettersen for supporting me academically throughout my doctoral work. Her calm and rational disposition has been a blessing during stressful times. I am also grateful to her for providing me with the opportunity to lecture her course, TTK4150 - Nonlinear Control Systems, during the fall semester of 2021.

I would like to thank Professor Roger Skjetne at the Department of Marine Technology for giving me the opportunity to be a teaching assistant for his course TMR4243 - Marine Control Systems II. I found the experience of working closely with his students in the dynamic positioning lab very rewarding.

This work would not have been possible without the contributions of my close friend Erlend A. Basso. While Erlend has a large number talents, it is primarily his efficiency and great ability to isolate the most important aspects of a given problem that synergized very well with my much slower and detail-oriented approach to research. I am very proud of our joint achievements.

I would like to thank all my friends and colleagues at the Department of Marine Technology for their support, and in particular Emil Smilden, Pål Takle Bore, Einar Ueland, and Mathias Marley. I am also grateful to several people I got acquainted with at the Department of Engineering Cybernetics after migrating there, in particular Trym Tengesdal, Eirik Foseid, Erlend Lundby, and Amer Orucevic.

Lastly, I would like to thank my family for their continuing encouragement and support.

Henrik M. Schmidt-Didlaukies
Trondheim, February 2023

Publications

The results presented in this thesis are based on the following conference and journal papers:

Journal Papers

1. E. A. Basso[#], H. M. Schmidt-Didlaukies[#], K. Y. Pettersen and A. J. Sørensen, "Global Asymptotic Tracking for Marine Vehicles using Adaptive Hybrid Feedback", *IEEE Transactions on Automatic Control*, 2022.
2. H. M. Schmidt-Didlaukies, E. A. Basso, A. J. Sørensen and K. Y. Pettersen, "Modeling of Underwater Vehicles: Dissipativity and Symmetry", submitted to the *IEEE Transactions on Robotics*, 2023.

Conference Papers

1. E. A. Basso[#], H. M. Schmidt-Didlaukies[#], K. Y. Pettersen and J. T. Gravdahl, "Synergistic PID and Output Feedback Control on Matrix Lie Groups ", *Proc. 12th IFAC Symposium on Nonlinear Control Systems (NOLCOS)*, Canberra, Australia, Jan. 4-6, 2023.
2. H. M. Schmidt-Didlaukies[#], E. A. Basso[#], A. J. Sørensen and K. Y. Pettersen, "A Generalization of Synergistic Hybrid Feedback Control with Application to Maneuvering Control of Ships", *Proc. 61st Conference on Decision and Control (CDC)*, Cancún, Mexico, Dec. 6-9, 2022.
3. E. A. Basso[#], H. M. Schmidt-Didlaukies[#], K. Y. Pettersen and A. J. Sørensen, "Global Asymptotic Tracking for Marine Surface Vehicles using Hybrid Feedback in the Presence of Parametric Uncertainties," *Proc. 2021 American Control Conference (ACC)*, Online/New Orleans, LA, USA, May 25-28, 2021.
4. E. A. Basso[#], H. M. Schmidt-Didlaukies[#] and K. Y. Pettersen, "Hysteretic Control Lyapunov Functions with Application to Global Asymptotic Tracking for Underwater Vehicles," *Proc. 59th Conference on Decision and Control (CDC)*, Online/Jeju island, Republic of Korea, Dec. 8-11, 2020.
5. H. M. Schmidt-Didlaukies, A. J. Sørensen, K. Y. Pettersen, Modeling of Articulated Underwater Robots for Simulation and Control, *Proc. 2018 IEEE/OES Autonomous Underwater Vehicle Workshop*, Porto, Portugal, Nov 6–9, 2018.

Other Publications

The following publications were written during the PhD, but are not included in this thesis.

1. E. A. Basso[#], H. M. Schmidt-Didlaukies[#] and K. Y. Pettersen, "Global Asymptotic Position and Heading Tracking for Multirotors using Tuning Function-based Adaptive Hybrid Feedback", *IEEE Control Systems Letters*, 2022
2. T. Tengesdal, S. V. Rothmund, E. A. Basso, T. A. Johansen and H. M. Schmidt-Didlaukies, "Obstacle Intention Aware Collision Avoidance in Confined Waters: Full Scale Experiments", *Submitted to Field Robotics*, 2022.

[#]E. A. Basso and H. M. Schmidt-Didlaukies contributed equally to these articles and should be considered co-first authors.

Chapter 1

Introduction

In this thesis, we present contributions to the mathematical modeling of underwater vehicles and hybrid feedback control of nonlinear systems. While all presented results on hybrid feedback control can be directly applied to the control of underwater vehicles, they are much more general in their area of application. The thesis is therefore divided into two parts, the first treating modeling of underwater vehicles, and the second treating hybrid feedback control. The usefulness of the devised hybrid feedback control approaches to the design of underwater vehicle control systems is illustrated with simulation studies and experiments.

1.1 Modeling of Underwater Vehicles

The first part of this thesis considers the mathematical modeling of underwater vehicles. A mathematical model of an underwater vehicle is a system of ordinary differential equations that describes the response of the vehicle, represented by its configuration and its velocity, to an input, represented by a force-moment pair applied to the vehicle or by a control signal sent to the thrusters and control surfaces of the vehicle. Most models of this type are either devised to serve as simulation models, or to be used in the stability analysis and design of feedback control laws and observers. While these two objectives are not mutually exclusive, certain modeling aspects that are relevant to simulation models are typically neglected in models used for the design and stability analysis of feedback control systems. Examples of such unmodeled features are thruster dynamics and saturation, the detailed modeling of the effect of ocean currents, and, if present, the influence of an umbilical cable.

Simulation models of underwater vehicles typically constitute one part of a larger simulation suite with the purpose of simulating full operations. Such simulation suites also comprise, for instance, sensor models, models to describe the intricacies of underwater communication, and contact models for manipulation. Although experimental verification of the control systems of underwater vehicles is necessary, it can be a laborious and costly task. This is especially so when the experiments are conducted in the field. Simulations, on the other hand, can establish a measure of confidence in the vehicle control system with minimal risk to equipment and personnel. The ability to thoroughly test the vehicle control system through simulations before moving on to laboratory or field experiments is therefore of great value.

Model properties derived from physical principles are frequently taken advantage of in the stability analysis and design of nonlinear feedback control laws and observers for underwater vehicles. These are often considerations related to the evolution of the underwater vehicle's energy. In particular, Lyapunov functions inspired by the total energy of the vehicle can simplify the overall stability analysis, and the dissipativity of the hydrodynamic forces acting on the vehicle can be directly exploited in the design of feedback control laws and observers.

1.1.1 Modeling of Rigid Underwater Vehicles

The theoretical investigation into the general motion of a rigid body through an inviscid and irrotational fluid of constant density and infinite extent was pioneered by Kirchhoff and Thomson [1, 2] in the 1870s. In these works, a Cartesian reference frame is attached to the body, and subsequently its equations of motion expressed in this this frame derived through energy considerations [3]. It is shown that the hydrodynamic force and moment exerted by the fluid on the body are described solely in terms of the body velocity, the body acceleration, and at most 21 coefficients that depend on the fluid density and body shape. This result is surprising, because the fluid, even though assumed ideal, nonetheless constitutes an infinite-dimensional system. It is therefore not at all obvious that its effects on the body can be completely described in terms of variables pertaining to the body motion and a finite number of coefficients. The works [1, 2] thereby introduce the modern theoretical concept of rigid body hydrodynamic inertia, also referred to as added mass.

The theoretical endeavor of determining the force and moment acting on a rigid body undergoing general motion is much more difficult if a more realistic fluid model is utilized. The case of a rotational and linearly viscous fluid of constant density and infinite extent is treated in [4], building on important contributions from the earlier works [5–7]. The acting hydrodynamic force and moment depend in an intricate manner on the specifics of the flow field, and the aforementioned reduction of variables describing them is no longer possible. Nonetheless, the hydrodynamic inertia effects as conceived by Kirchhoff and Thomson can still be cleanly separated from other contributions to the force and moment, such as free vorticity and skin friction. Numerical simulations also indicate that the added mass effect can be properly defined in constant density linearly viscous flow [8]. It must in this case be defined in terms of the instantaneous change of hydrodynamic force and moment produced by a corresponding change in body acceleration.

An early effort to produce a low-dimensional modeling framework for the general motion of rigid underwater vehicles, specifically submarines, is found in [9]. The model combines added mass and hydrostatic effects with memoryless nonlinear modeling of hydrodynamic damping. The mathematical expressions for the hydrodynamic damping force and moment are a combination of second-order polynomial functions and second-order modulus functions of the submarine velocities. Such expressions were previously utilized to devise maneuvering models of ships in [10, 11]. The model presented in [9] undergoes minor modifications in [12] to more accurately describe the motion of an autonomous underwater vehicle (AUV), and is utilized as the basis for AUV-autopilot design. The model of [12] also forms the basis for the sliding-mode AUV-autopilot design reported in [13]. A complete modeling framework for remotely

operated underwater vehicles is provided in [14, 15]. The hydrodynamic damping force and moment are modeled as a third-order polynomial function of the velocities.

Inspired by modeling work on robot manipulators as presented for instance in [16], the works [17–19] introduce a matrix-form of the equations of motion for rigid underwater and surface vehicles. The matrix-form of the equations is mathematically equivalent to the earlier models in component-form, but allows easier exploitation of physical system properties in the control design process. Additionally, the novel model structure allows the direct application of control algorithms devised for robot manipulators, such as the celebrated adaptive control law of Slotine and Li [20], to underwater vehicles. One early example of such an adaptive control law for underwater vehicles is presented in [21]. Further refinements of the modeling paradigm are introduced [22]. This class of models forms the basis for the textbooks on ocean vehicle modeling and control [23, 24], and consequently, for the modern approach to the subject.

The mathematical models that describe underwater vehicle motion involve a large number of hydrodynamic parameters that must be determined through experiments or computational hydrodynamic analysis. Consequently, any principle that allows for the reduction of model parameters and subsequent simplification of the equations of motion is of great value. One way to reduce model complexity is to exploit the fact that underwater vehicles usually have regular shapes, and consequently possess symmetries of reflection or proper rotation. For instance, the majority of ocean vehicles possess port-starboard reflection symmetry. Certain types of underwater vehicles may also possess fore-aft reflection symmetry, or may at least approximately be a solid of revolution. The fact that symmetries of body shape can provide simplifications of the hydrodynamic inertia coefficients is already recognized in the work [1] for the case of a rigid body moving in an ideal fluid of infinite extent. The most comprehensive description of the effects of symmetries on the hydrodynamic inertia forces and moments is to the authors' best knowledge found in [25]. These results are also stated in Lamb's renowned work on hydrodynamics [26, Article 126]. Here, results are presented for bodies that are regular polyhedra (for instance a platonic solid), for bodies whose cross-section is any regular polygon, and for bodies with helicoidal symmetry (for instance a propeller). In [11], port-starboard symmetry is used to reduce the number of added mass parameters and hydrodynamic damping parameters for maneuvering models of ships. Similar considerations for remotely operated underwater vehicles are reported in [14].

1.1.2 Modeling of Multibody Underwater Vehicles

Mathematical models describing the motion of underwater vehicles that can be considered systems of several constrained rigid bodies are of interest mainly due to their applicability to underwater vehicle-manipulator systems (UVMSs). Conventional UVMSs comprise a clearly distinguished base on which one or two manipulator arms are mounted. The arm dimensions and mass in relationship to the base vary, and with them the dynamic influence that the manipulator has on the base. In cases where the manipulator is relatively large, as is the case for instance for the Girona AUV [27] or the Trident AUV [28], the manipulator and base system must be considered coupled. An extreme example is the highly unconventional Eelume underwater vehicle [29], which does not have a distinguishable base.

Due to the considerable difference in shape between the base and manipulator, different hydrodynamic modeling approaches are typically used for these components. The base is modeled following the principles briefly outlined in the preceding section. Since most manipulator arms comprise relatively slender links, it is customary to model the acting hydrodynamic forces and moments by integrating cross-sectional contributions along the link. Such approaches have a long history in the modeling of slender-body hydrodynamics, exemplified by the work of Morison, O'Brien, Johnson, and Schaaf for piles in waves ("Morison's equation") based mostly on empirical considerations [30], and the work of Salvesen, Tuck, and Faltinsen for ships at forward speed in waves based on the theory of potential flow [31]. For submerged robot manipulators, this modeling approach is used in a very similar manner in a large number of works [32–37]. In [38], the sectional hydrodynamic inertia and damping coefficients are taken to depend on the travel distance of the section to better model the effect of shed vorticity. Experiments for a single degree-of-freedom manipulator are conducted and show good agreement between theory and observation. However, it is not clear how the model can be modified to describe the acting forces and moments for more general motions.

The study of UVMSs as multibody systems has received considerable attention. In [35], a complete forward dynamics algorithm for single-arm UVMSs based on the articulated rigid body algorithm [39, 40] is presented. The algorithm complexity grows linearly with the number of manipulator degrees of freedom. Consequently, it is particularly efficient for manipulators comprising many links. The work incorporates directly the hydrodynamic and hydrostatic forces and moments acting on the base and manipulator. It also considers the effect of a spatially uniform and unsteady ocean current. Several works [32, 34, 41] present very similar inverse dynamics algorithms based on the Newton-Euler formulation. In particular, the algorithms incorporate hydrodynamic inertia, hydrodynamic damping, and hydrostatic effects directly in the recursive inverse dynamics. Interestingly, [32, 34] also include the effect of oscillating lift forces due to vortex shedding in their analysis. These are typically neglected because they are, at least in an ideal setting, of relatively high frequency and have a mean value of zero.

A matrix-form of the equations of motion, similar to the one introduced in [17–19] for rigid underwater vehicles, is presented in [34, 42]. This approach to the equations of motion is refined in [43], drawing on earlier work on free-flying robotic systems presented in [44]. The matrix-form is of particular value for control design, where it allows for easy exploitation of system properties. It forms the basis for most modern textbooks that cover the control of UVMSs, in particular [45, 46]. Other derivations of the matrix-form of the equations of motion are found in [36], which is based on Kane's method [47, 48], and in [49], which is based on the quasi-Lagrangian formulation of Meirovitch [50]. The quasi-Lagrangian formulation of analytical dynamics is very similar to a reformulation of the Lagrangian equations of motion attributed to Hamel [51, 52]. See [53, Section 3.8] for a clear and modern exposition.

1.2 Hybrid Feedback Control

The basin of attraction of an asymptotically stable equilibrium point of a time-invariant continuous-time system defined on a smooth manifold is diffeomorphic to

Euclidean space [54, 55]. This result demonstrates that there is a fundamental topological obstruction to global asymptotic point stabilization with continuous state-feedback control laws on any manifold that can not be identified with Euclidean space. While discontinuous state-feedback control laws can provide global asymptotic stability on such manifolds, the resulting global attractivity property is not robust to arbitrarily small measurement noise. It follows that there exist topological obstructions to robust global stabilization for any mechanical system with rotational degrees of freedom, such as underwater vehicles.

The topological obstructions to robust global asymptotic stabilization can be effectively overcome by employing a hybrid feedback control law [56]. A hybrid feedback control law typically comprises a collection of continuous state feedback control laws and a state-based switching logic that decides which feedback control law from the collection is to be used. Examples of such control strategies are furnished by hybrid patchy feedback control [57–59], the geometric approach proposed in [60] where the switching logic is devised from an atlas of the manifold, and synergistic control. Synergistic control is a hybrid feedback control formalism that encodes the switching logic directly in the value of a Lyapunov-like function [61, 62].

Synergistic potential functions are utilized to derive proportional-derivative (PD) control laws for global asymptotic stabilization of rigid body orientation on the special orthogonal group in [63]. The work also proposes a procedure for the construction of synergistic potential functions by applying an angular warping transformation to modified trace functions [64]. The synergistic control laws are extended to solve the global asymptotic tracking problem for rigid body orientation in [65]. A smoothing approach for the devised control laws is presented, which removes jumps in the control signal resulting from switching. The work also presents a procedure to construct synergistic potential functions on the special orthogonal group through translation, scaling, and biasing of modified trace functions. Results on synergistic tracking control of rigid body orientation without angular velocity measurements are presented in [66]. Additionally, further results on the construction of synergistic potential functions with angular warping applied to modified trace functions are established.

Global exponential synergistic control laws for the tracking problem on the special orthogonal group are presented in [67]. The synergistic potential functions are constructed by applying an angular warping transformation to a class of local potential functions first utilized for orientation control in [68]. A control law with integral action that ensures global exponential tracking control of rigid body orientation in the presence of a constant and matched disturbance is presented in [69]. While not referred to as such, the introduced potential functions are synergistic, and in fact closely related to the ones proposed in [63]. The introduced switching mechanism is different than in the aforementioned references as it depends explicitly on the value of the integral state. Lastly, a generalized synergistic control strategy and an associated class of potential functions is introduced in [70]. In particular, the logic variable that traditionally only changes across jumps is also allowed to change along flows. The result is applied to global tracking control of rigid body orientation and rigid body pose.

The synergistic control paradigm is applied to orientation tracking control for rigid bodies utilizing unit quaternions in [71], where a globally asymptotically stabilizing PD control law is derived. The work also introduces an output feedback modification of this control law, as well as a modification utilizing biased angular velocity measurements. The global output feedback quaternion tracking-problem for a rigid

body is also addressed in [72], where a synergistic observer-controller scheme is presented. The aforementioned quaternion strategies have been refined and applied to solve the global asymptotic tracking problem for translation-underactuated vehicles such as AUVs and quad-rotors in [73].

The global stabilization problem on spheres of arbitrary dimension is addressed within the synergistic framework in [74], generalizing results for the circle presented in [75]. A PD control law ensuring global reduced orientation tracking for a rigid body is derived. Moreover, a smoothing modification for the control law is devised that removes the jumps in the control signal resulting from switching. The work also presents a constructive procedure for synergistic potential functions on the sphere based on scaling and biasing of local potential functions. Further results for the sphere are presented in [76], where a new class of synergistic potential functions is introduced. These potential functions are utilized in the design of novel global synergistic tracking control laws for quad-rotors.

Synergistic potential functions are generalized to synergistic Lyapunov functions and feedback (SLFF) pairs in [77]. It is proven that SLFF pairs are amenable to integrator backstepping. Furthermore, a general smoothing modification for the resulting control laws is presented. Several further refinements of the SLFF concept are introduced in [78]. Utilizing converse hybrid Lyapunov theory [79, 80], it is also shown that a wide class of systems can be stabilized by feedback derived from SLFF pairs. Parameter-adaptive control within the SLFF framework is introduced in [81] for systems with matched uncertainties.

1.3 Outline and Contributions

This thesis is organized into two parts and eight chapters. Chapter 2 covers briefly some mathematical concepts that are utilized frequently throughout this work. We summarize in the following the topic and contributions of each chapter in this thesis.

1.3.1 Part I: Modeling of Underwater Vehicles

Modeling of Rigid Underwater Vehicles (Chapter 3)

Chapter 3 introduces a matrix Lie group formulation of the standard Fossen-Sagatun model for underwater vehicles [24, Chapter 8]. We include the effect of an unsteady and uniform ocean current, and show that the presented model can be derived from a variational principle. Various properties of this model that are of importance for control design are derived utilizing principles from matrix Lie theory. We introduce a stronger notion of dissipativity, monotone dissipativity, and shed light on a fundamental relationship between monotonically dissipative mappings and convex Rayleigh dissipation functions. Lastly, we introduce a hydrodynamic symmetry principle based on matrix Lie theory and provide several examples of its application. The chapter also introduces a control model where unit quaternions are used to represent the vehicle's orientation.

The contributions of this chapter are threefold. Firstly, we present a Lagrangian derivation of the equation of motion for an underwater vehicle in the presence of unsteady ocean currents. In particular, we utilize a global and non-minimal representation of the Euclidean group to derive the equation of motion from the Lagrange-

d'Alembert principle. Secondly, we introduce a stronger notion of dissipativity, namely monotone dissipativity. We show that damping models which admit Rayleigh dissipation functions are monotonically dissipative if and only if their Rayleigh dissipation functions are convex and have a minimum at the origin. Finally, the third contribution is the introduction of a hydrodynamic symmetry principle stated in terms of matrix Lie theory, which makes possible a systematic exploitation of vehicle symmetries to simplify the modeling of hydrodynamic inertia and damping effects. This symmetry principle allows us to drastically reduce the number of model parameters by exploiting the symmetries of the vehicle geometry. Consequently, the possibility of overfitting is reduced, and less experimental data may be needed to achieve an acceptable fit.

This chapter is based on the following work:

- H. M. Schmidt-Didlaukies, E. A. Basso, and K. Y. Pettersen, "Modeling of Underwater Vehicles: Dissipativity and Symmetry", submitted to the *IEEE Transactions on Robotics*, 2023.

Modeling of Multibody Underwater Vehicles (Chapter 4)

Chapter 4 introduces a modeling framework based on matrix Lie theory for multibody underwater vehicles with kinematic tree-structure. We derive the equations of motion in a global matrix-form, and outline some of their properties that are of particular importance for control design. We also present two recursive formulations of the equations of motion based on well-known multibody dynamics algorithms. In particular, a generalized Newton-Euler algorithm for inverse dynamics and controller implementation, and a composite-rigid-body algorithm for forward dynamics.

The main contribution of this chapter is a modeling framework for multibody underwater vehicles which possess a kinematic tree structure, the equations in matrix-form, and the aforementioned recursive algorithms. The devised equations of motion in matrix-form are based on Lie theory, and therefore global and singularity-free. Furthermore, the generalized Newton-Euler algorithm is to the extent of our knowledge novel. The forward dynamics algorithm includes the most important hydromechanical effects, and serves as a base for simulators of multibody underwater vehicles.

Some of the presented results appeared in the following publication:

[82] H. M. Schmidt-Didlaukies, A. J. Sørensen and K. Y. Pettersen, Modeling of Articulated Underwater Robots for Simulation and Control, *Proc. 2018 IEEE/OES Autonomous Underwater Vehicle Workshop*, Porto, Portugal, Nov 6–9, 2018.

1.3.2 Part II: Hybrid Feedback Control

Synergistic PID and Output Feedback Control on Matrix Lie Groups (Chapter 5)

Chapter 5 introduces multiple synergistic hybrid feedback control laws for mechanical systems on matrix Lie groups with left-invariant metrics. With the goal of globally asymptotically tracking a desired reference trajectory, we propose a full-state feedback hybrid proportional-derivative (PD) type control law and a hybrid output feedback type control law which only utilizes configuration measurements. We also show that these controllers can be modified to not cancel certain potential forces appearing in the system. Lastly, to ensure global asymptotic tracking in the presence of a constant and

unknown disturbance in the system dynamics, we introduce two novel proportional-integral-derivative (PID) type control laws with slightly different integral action. The theoretical developments are validated through numerical simulation of an underwater vehicle.

This chapter has three main contributions. First, we propose a baseline synergistic PD control law ensuring global asymptotic tracking for mechanical systems on matrix Lie groups with a left-invariant Riemannian metric. The second contribution is a generalization of the synergistic output feedback control law proposed for orientation control in [71] to any system whose configuration space can be identified with a matrix Lie group. Finally, we present two novel synergistic PID type control laws, both of which ensure global asymptotic tracking in the presence of unknown constant disturbances.

This chapter is based on the following publication:

[83] E. A. Basso[#], H. M. Schmidt-Didlaukies[#], K. Y. Pettersen and J. T. Gravdahl, "Synergistic PID and Output Feedback Control on Matrix Lie Groups ", *Proc. 12th IFAC Symposium on Nonlinear Control Systems (NOLCOS)*, Canberra, Australia, Jan. 4-6, 2023.

Global Asymptotic Tracking for Marine Vehicles (Chapter 6)

Chapter 6 presents an adaptive hybrid feedback control law for global asymptotic tracking of a hybrid reference system for marine vehicles in the presence of parametric modeling errors. The reference system is constructed from a parametrized loop and a speed assignment specifying the motion along the path, which decouples the geometry of the path from the motion along the path. During flows, the hybrid feedback consists of a PD-action and an adaptive feedforward term, while a hysteretic switching mechanism that is independent of the vehicle velocities determines jumps. The effectiveness of the proposed control law is demonstrated through experiments.

The main contribution of this chapter is the development of an adaptive hybrid feedback controller for global asymptotic tracking of a hybrid reference system for marine vehicles subject to parametric uncertainties. In contrast to backstepping-based hybrid adaptive control [81], the proposed approach permits estimation of the inertia matrix, and the switching mechanism is independent of the system velocities. As our approach is based on traditional Euler-Lagrange system models, the adaptive hybrid control law is applicable to other mechanical systems as well. In particular, it can easily be extended to robot manipulators or, more generally, vehicle-manipulator systems. The hybrid reference system is constructed from a parametrized loop and a speed assignment for the motion along the loop. The main benefit of this formulation is that it decouples the design of the path from the motion along the path, allowing us to globally asymptotically track a given parametrized loop at a desired and time-varying speed. The proposed reference system can be considered an adaptation of the maneuvering problem [84, 85] to a hybrid dynamical systems setting. Preliminary results were presented in [86], and in this chapter we extend the hybrid feedback control law from surface vehicles to a more general class of Euler-Lagrange systems on SE(2) or SE(3) satisfying a set of general conditions on the switching mechanism and the potential functions. Moreover, we show that the potential functions and switching mechanisms introduced in [86] and [71] satisfy these conditions, and these

potential functions and switching mechanisms are subsequently employed to design hybrid adaptive control laws for surface and underwater vehicles. Finally, we validate the theoretical developments for surface and underwater vehicle applications through experiments.

This chapter is based on the following publications:

[87] E. A. Basso#, H. M. Schmidt-Didlaukies#, K. Y. Pettersen and A. J. Sørensen, "Global Asymptotic Tracking for Marine Vehicles using Adaptive Hybrid Feedback", *IEEE Transactions on Automatic Control*, 2022.

[86] E. A. Basso#, H. M. Schmidt-Didlaukies#, K. Y. Pettersen and A. J. Sørensen, "Global Asymptotic Tracking for Marine Surface Vehicles using Hybrid Feedback in the Presence of Parametric Uncertainties," *Proc. 2021 American Control Conference (ACC)*, Online/New Orleans, LA, USA, May 25-28, 2021.

Hysteretic Control Lyapunov Functions (Chapter 7)

Chapter 7 introduces hysteretic control Lyapunov functions (HCLFs) for hybrid feedback control of a class of continuous-time systems. A family of HCLFs consists of local control Lyapunov functions defined on a finite cover of the state space which satisfy certain decrease conditions. We present sufficient conditions for the existence of a stabilizing hybrid feedback and show how such hybrid feedbacks can be constructed from an HCLF family through an optimization-based procedure.

The main contribution of this chapter is the concept of a hysteretic control Lyapunov function and its application to hybrid feedback control with global asymptotic stability properties for nonlinear continuous-time systems. In particular, we show that the existence of a family of HCLFs satisfying the small control property implies global stabilizability of a compact set. We also prove that optimization-based hybrid feedback laws, an extension of the pointwise minimum-norm control laws covered for instance in [88, 89], can be constructed under minor assumptions on the objective functions. The collection of optimization-based feedback laws are continuous, implying that the hybrid basic conditions hold such that the stability is robust in the sense of [90]. As a case study, we construct an HCLF family for tracking control of an underwater vehicle through a backstepping approach. In contrast to traditional backstepping, we find the control input that pointwise minimizes a strictly convex objective function from the set of stabilizing control inputs defined by the HCLFs. The HCLF construction is reminiscent of the backstepping-based synergistic Lyapunov functions constructed for set-point regulation in [91]. However, we extend the work in [91] to the tracking problem in terms of HCLFs, and exploit inherent stabilizing nonlinear terms through online optimization.

This chapter is based on the following publication:

[92] E. A. Basso#, H. M. Schmidt-Didlaukies# and K. Y. Pettersen, "Hysteretic Control Lyapunov Functions with Application to Global Asymptotic Tracking for Underwater Vehicles," *Proc. 59th Conference on Decision and Control (CDC)*, Online/Jeju island, Republic of Korea, Dec. 8-11, 2020.

Synergistic Lyapunov Functions and Feedback Triples (Chapter 8)

Chapter 8 generalizes results on synergistic hybrid feedback control. Specifically, we propose a generalization of synergistic Lyapunov functions and feedback (SLFF) pairs, in which the logic variable in traditional synergistic control is allowed to change along flows. This flowing logic variable is called the synergy variable, and an SLFF triple comprises an SLFF pair in addition to the flow map of the synergy variable. We introduce synergy gaps relative to components of product sets, which enable us to define modified synergistic jump conditions for different components of the synergy variable. Furthermore, we show that SLFF triples are amenable to backstepping. Finally, we give an example of how our generalized theory can be used to combine traditional synergistic control with ship maneuvering control by introducing optional jumps in the path parameter.

The main contribution of this chapter is the extension of the SLFF definition introduced in [77, 78]. The generalized notion of synergy and the modified jumping conditions allow us to show that the quaternion output feedback control law for rigid-body orientation presented in [71] is synergistic. The proposed generalization also encompasses the results for SO(3) and SE(3) in [70], in which the logic variable is also allowed to change during flows. However, our proposed framework also includes path-following control scenarios in which the path variable exhibits jump dynamics, such as instantaneously moving the desired state closer to the actual state. As a result, ship maneuvering control as outlined in [84] and [85] can be augmented with a jumping path parameter and a traditional synergistic control approach to solve the maneuvering problem.

This chapter is based on the following publication:

[93] H. M. Schmidt-Didlaukies[#], E. A. Basso[#], A. J. Sørensen and K. Y. Pettersen, "A Generalization of Synergistic Hybrid Feedback Control with Application to Maneuvering Control of Ships", *Proc. 61st Conference on Decision and Control (CDC)*, Cancún, Mexico, Dec. 6-9, 2022.

Chapter 2

Mathematical Preliminaries

This chapter introduces mathematical preliminaries and notation relevant to the rest of this thesis.

2.1 Analysis in $\mathbb{R}^n$

We here introduce several fundamental properties of mappings between subsets of Euclidean spaces. Furthermore, we introduce manifolds and matrix Lie groups.

2.1.1 Mappings

Let $X \subset \mathbb{R}^n$ and $Y \subset \mathbb{R}^m$. We write $f : X \to Y$ to denote a mapping that associates with every $x \in X$ an element $y \in Y$. The set X is called the domain of f, and we write $\operatorname{dom} f = X$. The set Y is called the codomain. The range of f, denoted $\operatorname{rge} f$, is defined as the set of all $y \in Y$ for which there exists $x \in X$ such that $f(x) = y$, that is,

$$\operatorname{rge} f \coloneqq \{y \in Y : \exists x \in X \text{ s.t. } f(x) = y\}. \tag{2.1}$$

The codomain can be used to convey information about the mapping. For instance, a non-negative function $f : X \to \mathbb{R}$ can be written as $f : X \mapsto \mathbb{R}_{\geq 0}$, and a positive function $f : X \to \mathbb{R}$ as $f : X \mapsto \mathbb{R}_{>0}$. Some important properties of mappings utilized often in this thesis follow.

Definition 2.1 (Continuous mapping)**.** *Let $X \subset \mathbb{R}^n$ and $f : X \to \mathbb{R}^m$. The mapping f is continuous at $x \in X$ if for every $\varepsilon > 0$, there exists $\delta > 0$ such that for every $z \in X$ satisfying $|z - x| \leq \delta$, it holds that $|f(z) - f(x)| \leq \varepsilon$. The mapping f is continuous if it is continuous at every $x \in X$.*

Definition 2.2 (Proper mapping)**.** *Let $X \subset \mathbb{R}^n$, $Y \subset \mathbb{R}^m$, and $f : X \to Y$. The mapping f is proper if it is continuous and $f^{-1}(K)$ is compact for every compact set $K \subset Y$.*

We remark that a set $K \subset \mathbb{R}^n$ is compact if and only if it is closed and bounded.

Definition 2.3 (Continuously differentiable mapping)**.** *Let $X \subset \mathbb{R}^n$ be open and $f : X \to \mathbb{R}^m$. The mapping f is continuously differentiable if there exists a continuous mapping $\mathrm{D}f : X \to \mathbb{R}^{m\times n}$ such that for every $x \in X$ and every $v \in \mathbb{R}^n$,*

$$\mathrm{D}f(x)v = \lim_{s\to 0} \frac{f(x+sv) - f(x)}{s} \tag{2.2}$$

If X is not open, then we say that $f : X \to \mathbb{R}^m$ is continuously differentiable if there exists an open set $O \subset \mathbb{R}^n$ containing X and a continuously differentiable mapping $g : O \to \mathbb{R}^m$ such that $g(x) = f(x)$ for every $x \in X$. We then define $\mathrm{D}f : X \to \mathbb{R}^{m\times n}$ by the restriction $\mathrm{D}f \coloneqq \mathrm{D}g|_X$.

For a continuously differentiable function $f : X \to \mathbb{R}$, we use the gradient vector $\nabla f : X \to \mathbb{R}^n$ defined by $\nabla f(x) \coloneqq \mathrm{D}f(x)^\mathsf{T}$. A consequence of Definition 2.3 is that the derivative is not necessarily uniquely defined if X is not open (consider for instance the case $f : \{0\} \to \{0\}$). When conditions are placed on $\mathrm{D}f$ in this case, there must exist a single extension g of f such that $\mathrm{D}f = \mathrm{D}g|_X$ satisfies all conditions. For mappings whose argument is a matrix, that is, $f : X \to \mathbb{R}^m$ where $X \subset \mathbb{R}^{n\times n}$, we write $\mathrm{D}f(x, v)$ to mean the derivative of f along $v \in \mathbb{R}^{n\times n}$.

2.1.2 Manifolds in $\mathbb{R}^n$

For our purposes, it suffices to think of manifolds as smooth surfaces in $\mathbb{R}^n$ [94, 95]. An introduction to the abstract theory of manifolds is found in [96].

Definition 2.4 (Manifold)**.** *A set $\mathcal{M} \subset \mathbb{R}^n$ is a k-manifold, where $0 \le k \le n$, if the following equivalent conditions hold:*

1. *For each $x \in \mathcal{M}$, there exists an open neighborhood U of x, an open set $V \subset \mathbb{R}^k$, and a smooth immersion $\varphi : V \to \mathbb{R}^n$ such that $\varphi : V \to \mathcal{M} \cap U$ is a homeomorphism.*
2. *For each $x \in \mathcal{M}$, there exists an open neighborhood U of x and a smooth submersion $\vartheta : U \to \mathbb{R}^{n-k}$ such that $\{x \in U : \vartheta(x) = 0\} = \mathcal{M} \cap U$.*

Definition 2.4 presents two equivalent characterizations of a k-manifold in $\mathbb{R}^n$. In particular, item 1 characterizes the manifold in terms of local parametrizations, and item 2 in terms of local defining mappings. A manifold $\mathcal{M} \subset \mathbb{R}^n$ is said to be properly embedded if it is a closed set.

Definition 2.5 (Tangent space)**.** *Let $\mathcal{M} \subset \mathbb{R}^n$ be a k-manifold. The tangent space to $\mathcal{M}$ at x is a k-dimensional vector subspace of $\mathbb{R}^n$. The following characterizations are equivalent:*

1. *The tangent space to $\mathcal{M}$ at x is the set of vectors $v \in \mathbb{R}^n$ for which there exists a smooth curve $c : \mathbb{R} \to \mathcal{M}$ such that $c(0) = x$ and $c'(0) = v$, that is,*

$$T_{\mathcal{M}}(x) = \{v \in \mathbb{R}^n : \exists c : \mathbb{R} \to \mathcal{M} \text{ smooth, s.t. } c(0) = x, c'(0) = v\}.$$

2. *For (U, φ) as in item 1 in Definition 2.4 and $x \in \mathcal{M} \cap U$,*

$$T_{\mathcal{M}}(x) = \{v \in \mathbb{R}^n : w \in \mathbb{R}^k, v = \mathrm{D}\varphi(\varphi^{-1}(x))w\}.$$

3. *For (U, ϑ) as in item 2 in Definition 2.4 and $x \in \mathcal{M} \cap U$,*

$$T_{\mathcal{M}}(x) = \{v \in \mathbb{R}^n : \mathrm{D}\vartheta(x)v = 0\}.$$

2.1.3 Matrix Lie Groups

This section gives a very brief overview of the theory of matrix Lie groups. The material is mostly based on [96, 97]. A matrix group is a subset of

$$\mathrm{GL}(n) \coloneqq \{g \in \mathbb{R}^{n\times n} : \det g \neq 0\} \tag{2.3}$$

that is closed under matrix inversion and multiplication. Since $\mathrm{GL}(n)$ is open in $\mathbb{R}^{n\times n}$, it may be regarded as an n^2-dimensional manifold in $\mathbb{R}^{n\times n}$. A matrix Lie group is a matrix group that is also a submanifold of $\mathrm{GL}(n)$.

Definition 2.6 (Matrix Lie group)**.** *A matrix group is a set $\mathcal{G} \subset \mathrm{GL}(n)$ satisfying*

1. *if $g \in \mathcal{G}$, then $g^{-1} \in \mathcal{G}$;*
2. *if $g \in \mathcal{G}$ and $h \in \mathcal{G}$, then $gh \in \mathcal{G}$.*

A matrix Lie group is a matrix group that is a submanifold of $\mathrm{GL}(n)$.

A very useful result is the following: A matrix group $\mathcal{G} \subset \mathrm{GL}(n)$ is a submanifold of $\mathrm{GL}(n)$ if and only if it is a relatively closed subset of $\mathrm{GL}(n)$ [96, Theorem 7.21 and Theorem 20.12].

With every matrix Lie group, one can associate a particular algebra, known as the Lie algebra of the matrix Lie group.

Definition 2.7 (Lie algebra of a matrix Lie group)**.** *Let $\mathcal{G} \subset \mathrm{GL}(n)$ be a matrix Lie group. The Lie algebra $\mathfrak{g}$ of $\mathcal{G}$ is the tangent space to $\mathcal{G}$ at the identity equipped with the matrix commutator $[\,\cdot\,,\cdot\,] : \mathfrak{g}\times\mathfrak{g} \to \mathfrak{g}$ defined by*

$$[X, Y] \coloneqq XY - YX. \tag{2.4}$$

It follows from the properties of the tangent space of a manifold that the Lie algebra $\mathfrak{g}$ is a vector space in $\mathbb{R}^{n\times n}$ with dimension k equal to the dimension of $\mathcal{G}$ as a manifold. In the robotics literature, e.g. [98–100], it has become commonplace to work in $\mathbb{R}^k$ instead of $\mathfrak{g}$. This is accomplished by choosing a basis $(X_1, \ldots, X_k)$ for $\mathfrak{g}$ and defining the vector space isomorphism $\widehat{\cdot} : \mathbb{R}^k \to \mathfrak{g}$ by

$$\widehat{\nu} \coloneqq \sum_{i=1}^{k} X_i \nu_i. \tag{2.5}$$

We write $\widehat{\nu}^{\mathfrak{g}}$ instead of $\widehat{\nu}$ if it is not clear from context which Lie algebra isomorphism is meant. For each $g \in \mathcal{G}$ and $\nu \in \mathbb{R}^k$, we define the adjoint mappings $\mathrm{Ad}_g \in \mathbb{R}^{k\times k}$ and $\mathrm{ad}_\nu \in \mathbb{R}^{k\times k}$ by

$$\begin{aligned} \widehat{\mathrm{Ad}_g \mu} &\coloneqq g\widehat{\mu}g^{-1}, \\ \widehat{\mathrm{ad}_\nu \mu} &\coloneqq [\widehat{\nu}, \widehat{\mu}]. \end{aligned} \tag{2.6}$$

It can be shown that for each $g \in \mathcal{G}$, there exists an open set $V \subset \mathbb{R}^k$ such that the mapping $\varphi : V \to \mathrm{GL}(n)$ defined by $\varphi(x) \coloneqq g\exp\widehat{x}$, where $\exp : \mathbb{R}^{n\times n} \to \mathrm{GL}(n)$ is the matrix exponential, is a local parametrization of a neighborhood of g, as utilized in item 1 of Definition 2.4.

Definition 2.8 (Continuously differentiable mapping, matrix Lie group)**.** *Let $\mathcal{G} \subset \mathrm{GL}(n)$ be a matrix Lie group of dimension k and $f : \mathcal{G} \to \mathbb{R}^m$. The mapping f is continuously differentiable if there exists a continuous mapping $\mathrm{d}f : \mathcal{G} \to \mathbb{R}^{m\times k}$ such that for every $g \in \mathcal{G}$ and every $\nu \in \mathbb{R}^k$,*

$$\mathrm{d}f(g)\nu = \lim_{s\to 0} \frac{f(g\exp(s\widehat{\nu})) - f(g)}{s}. \tag{2.7}$$

A mapping $f : \mathcal{G} \to \mathbb{R}^m$ is continuously differentiable in the sense of Definition 2.8 if and only if it is continuously differentiable in the sense of Definition 2.3, and $\mathrm{d}f(g)\nu = \mathrm{D}f(g, g\widehat{\nu})$ for all $(g, \nu) \in \mathcal{G} \times \mathbb{R}^k$. We remark that we throughout this thesis use the operator d as a Lie group analogue to both D and ∇. It will be clear from context which one is meant.

A Lie group homomorphism is a smooth mapping from one Lie group to another that preserves the group structure. If a homomorphism is also diffeomorphism, that is, a bijection with a smooth inverse, then it is called an Lie group isomorphism, and the two Lie groups are called isomorphic.

Definition 2.9 (Lie group homomorphism, isomorphism)**.** *Let $\mathcal{G}$ and $\mathcal{H}$ be matrix Lie groups. A Lie group homomoprhism is a smooth mapping $\varphi : \mathcal{G} \to \mathcal{H}$ such that for all $g_1, g_2 \in \mathcal{G}$, it holds that $\varphi(g_1)\varphi(g_2) = \varphi(g_1 g_2)$. If φ is also a diffeomorphism, then φ is a Lie group isomorphism.*

Finally, the bilinear map $\nabla^M \colon \mathbb{R}^k \times \mathbb{R}^k \to \mathbb{R}^k$ induced by the symmetric and positive definite matrix $M \in \mathbb{R}^{k\times k}$ is defined by [101, Theorem 5.40 (iii)]

$$\nabla^M_\nu \mu \coloneqq \tfrac{1}{2}\operatorname{ad}_\nu \mu - \tfrac{1}{2}M^{-1}[\operatorname{ad}^{\mathsf{T}}_\nu M\mu + \operatorname{ad}^{\mathsf{T}}_\mu M\nu]. \tag{2.8}$$

Observe that $M\nabla^M_\nu \nu = -\operatorname{ad}^{\mathsf{T}}_\nu M\nu$. Furthermore, ∇^M has the following skew-property.

Lemma 2.1. For all $(\nu, \mu) \in \mathbb{R}^k \times \mathbb{R}^k$, it holds that

$$\langle M\nabla^M_\nu \mu, \mu\rangle = 0. \tag{2.9}$$

Proof. It follows from (2.8) that

$$\begin{aligned}\langle M\nabla^M_\nu \mu, \mu\rangle &= \tfrac{1}{2}\langle M\operatorname{ad}_\nu \mu - \operatorname{ad}^{\mathsf{T}}_\nu M\mu - \operatorname{ad}^{\mathsf{T}}_\mu M\nu, \mu\rangle \\ &= \tfrac{1}{2}\langle M\operatorname{ad}_\nu \mu, \mu\rangle - \tfrac{1}{2}\langle M\operatorname{ad}_\nu \mu, \mu\rangle - \tfrac{1}{2}\langle M\operatorname{ad}_\mu \mu, \nu\rangle \\ &= 0,\end{aligned} \tag{2.10}$$

where it was used that $\operatorname{ad}_\mu \mu = 0$ for all $\mu \in \mathbb{R}^k$. □

2.2 Set-Valued Analysis in $\mathbb{R}^n$

This section provides a brief introduction to basic aspects of set-valued analysis. It is mostly based on [102, 103].

2.2.1 Tangent Cone

We already encountered tangent vectors in the context of smooth manifolds. It is possible to generalize tangents to arbitrary subsets of $\mathbb{R}^n$. The set of tangents at a point are then not guaranteed to be a vector space. Instead, they will form a closed cone. A cone is a set $C \subset \mathbb{R}^n$ such that $v \in C$ implies that $\alpha v \in C$ for every $\alpha \geq 0$.

Definition 2.10 (Tangent cone)**.** *The tangent cone to a set $X \subset \mathbb{R}^n$ at a point $x \in \mathbb{R}^n$, denoted $T_X(x)$, is the set of all vectors $v \in \mathbb{R}^n$ for which there exist $x_i \in X, \tau_i > 0$ with $x_i \to x, \tau_i \searrow 0$, and*

$$v = \lim_{i \to \infty} \frac{x_i - x}{\tau_i}. \tag{2.11}$$

If the set X is a manifold, then the tangent cone to X at x coincides with the tangent space to X at x, as illustrated in [102, Example 6.8].

2.2.2 Set-Valued Mappings

A set-valued mapping is denoted by a double arrow, $S : \mathbb{R}^n \rightrightarrows \mathbb{R}^m$. We define the domain, range and graph of a set-valued mapping S by

$$\operatorname{dom} S \coloneqq \{x \in \mathbb{R}^n : S(x) \neq \emptyset\}, \tag{2.12}$$

$$\operatorname{rge} S \coloneqq \{y \in \mathbb{R}^m : \exists x \in \mathbb{R}^n \text{ such that } y \in S(x)\}, \tag{2.13}$$

$$\operatorname{gph} S \coloneqq \{(x, y) \in \mathbb{R}^n \times \mathbb{R}^m : y \in S(x)\}. \tag{2.14}$$

The inverse mapping of S, $S^{-1} : \mathbb{R}^m \rightrightarrows \mathbb{R}^n$, is defined by

$$S^{-1}(y) \coloneqq \{x \in \mathbb{R}^n : y \in S(x)\}. \tag{2.15}$$

Moreover, we define the image of a set $X \subset \mathbb{R}^n$ under S and the inverse image of a set $Y \subset \mathbb{R}^m$ under S, respectively, by

$$S(X) \coloneqq \bigcup_{x \in X} S(x) = \{y \in \mathbb{R}^m : S^{-1}(y) \cap X \neq \emptyset\}, \tag{2.16}$$

$$S^{-1}(Y) \coloneqq \bigcup_{y \in Y} S^{-1}(y) = \{x \in \mathbb{R}^n : S(x) \cap Y \neq \emptyset\}. \tag{2.17}$$

2.2.3 Semicontinuity and Local Boundedness

Continuity properties of set-valued mappings are described in terms of the following concepts.

Definition 2.11 (Outer and inner semicontinuous set-valued mapping)**.** *Let $S : \mathbb{R}^n \rightrightarrows \mathbb{R}^m$ and $X \subset \mathbb{R}^n$.*

1. *S is outer semicontinuous relative to X at $x \in X$ if for every $y \notin S(x)$ there are neighborhoods U of x and V of y such that $X \cap U \cap S^{-1}(V) = \emptyset$.*
2. *S is inner semicontinuous relative to X at $x \in X$ if for every $y \in S(x)$ and every neighborhood V of y there exists a neighborhood U of x such that $X \cap U \subset S^{-1}(V)$.*

S is outer (inner) semicontinuous relative to X if it is outer (inner) semicontinuous relative to X at every $x \in X$. S is continuous relative to X at $x \in X$ if it is both outer semicontinuous and inner semicontinuous relative to X at x. S is continuous relative to X if it is continuous relative to X at every $x \in X$.

Inner semicontinuity is also known as lower semicontinuity in the literature, e.g. in [103]. Outer semicontinuity of a set-valued mapping can be characterized in terms of the graph of the mapping.

Lemma 2.2 ([90, Lemma 5.10])**.** A set-valued mapping $S : \mathbb{R}^n \rightrightarrows \mathbb{R}^m$ is outer semicontinuous relative to $X \subset \mathbb{R}^n$ if and only if $\operatorname{gph} S \cap (X \times \mathbb{R}^m)$ is relatively closed in $X \times \mathbb{R}^m$.

Another widely used notion of continuity in the set-valued analysis literature is upper semicontinuity [103].

Definition 2.12 (Upper semicontinuous set-valued mapping)**.** *Let $S : \mathbb{R}^n \rightrightarrows \mathbb{R}^m$ and $X \subset \mathbb{R}^n$. S is upper semicontinuous relative to X at $x \in X$ if for every open set $O \subset \mathbb{R}^m$ such that $S(x) \subset O$, there exists a neighborhood U of x such that $F(X \cap U) \subset O$. S is upper semicontinuous relative to X if it is upper semicontinuous relative to X at every $x \in X$.*

We also require a notion of local boundedness for set-valued mappings.

Definition 2.13 (Locally bounded set-valued mapping)**.** *Let $S : \mathbb{R}^n \rightrightarrows \mathbb{R}^m$ and $X \subset \mathbb{R}^n$. S is locally bounded relative to X at $x \in X$ if there exists a neighborhood U of x such that $S(X \cap U)$ is bounded. S is locally bounded relative to X if it is locally bounded relative to X at every $x \in X$.*

An equivalent characterization of local boundedness of $S : \mathbb{R}^n \rightrightarrows \mathbb{R}^m$ relative to $X \subset \mathbb{R}^n$ is that for every compact set $K \subset X$, the image $S(K)$ is bounded. The notion of local boundedness allows us to formulate a relation between outer semicontinuity and upper semicontinuity of set-valued mappings. If $S : \mathbb{R}^n \rightrightarrows \mathbb{R}^m$ is upper semicontinuous relative to $X \subset \mathbb{R}^n$ and bounded-valued on X, then S is locally bounded relative to X. This follows directly from Definition 2.12 because O now can be chosen as a bounded set. Furthermore, if S is upper semicontinuous relative to X and closed-valued on X, then S is outer semicontinuous relative to X (see for instance [104, Proposition 5.2.18] or [89, Proposition 2.5]). It follows that if S is upper semicontinuous relative to X and compact-valued on X, then S is outer semicontinuous relative to X and locally bounded relative to X. The converse to this statement also holds (see for instance [102, Theorem 5.19] which can be invoked relative to a set $X \subset \mathbb{R}^n$).

2.2.4 Selections

Lastly, we shall introduce results from the theory of selections. Given a set-valued mapping $S : \mathbb{R}^n \rightrightarrows \mathbb{R}^m$, a selection s of S is a single-valued mapping $s : \operatorname{dom} S \to \mathbb{R}^m$ such that $s(x) \in S(x)$ for every $x \in \operatorname{dom} S$. The following famous theorem states sufficient conditions for the existence of a continuous selection of a given set-valued mapping S.

Theorem 2.14 ([105, Theorem 3.2'']). *Let $S : \mathbb{R}^n \rightrightarrows \mathbb{R}^m$. If S is inner semicontinuous relative to* $\operatorname{dom} S$*, and S is closed-convex-valued, then S admits a continuous selection.*

Remark 2.15. The stated theorem is more specialized than the cited one. Here we have used that $X \subset \mathbb{R}^n$ with the subspace topology is a metric space, and therefore $\mathcal{T}_1$ and paracompact. The set-valued mapping S maps into $\mathbb{R}^m$, which is a Banach space.

2.3 Hybrid Systems

In this section, we introduce the notion of a hybrid dynamical system. This introduction is by no means complete, and the reader is referred to the excellent resources [61, 90, 106] for more details.

2.3.1 Data of a Hybrid System

A hybrid dynamical system, or hybrid system, allows for both continuous-time and discrete-time evolution of the state. In this thesis, we employ the hybrid systems framework of [61, 90, 106]. In those works, a hybrid system $\mathcal{H}$ is defined by four objects (C, F, D, G), the data of the hybrid system, and represented by

$$\mathcal{H} : \begin{cases} \dot{x} \in F(x), & x \in C \\ x^+ \in G(x), & x \in D \end{cases} \tag{2.18}$$

where $x \in \mathbb{R}^n$ is the state, the set-valued mapping $F : \mathbb{R}^n \rightrightarrows \mathbb{R}^n$ is the flow map, the set-valued mapping $G : \mathbb{R}^n \rightrightarrows \mathbb{R}^n$ is the jump map, the set $C \subset \mathbb{R}^n$ is the flow set, and the set $D \subset \mathbb{R}^n$ is the jump set.

We will typically consider hybrid systems for which the data satisfies the following three basic assumptions [90, Assumption 6.5].

Assumption 2.16 (Hybrid basic conditions)**.**

(A1) C and D are closed subsets of $\mathbb{R}^n$;
(A2) $F : \mathbb{R}^n \rightrightarrows \mathbb{R}^n$ is outer semicontinuous and locally bounded relative to C, $C \subset \operatorname{dom} F$, and F is convex-valued on C;
(A3) $G : \mathbb{R}^n \rightrightarrows \mathbb{R}^n$ is outer semicontinuous and locally bounded relative to D, and $D \subset \operatorname{dom} G$.

It should be emphasized that when F is a single-valued and continuous mapping, the differential equation $\dot{z} = F(z)$ corresponds to a hybrid system satisfying the hybrid basic conditions.

2.3.2 Solution Concept

A solution ϕ to $\mathcal{H}$ is called a hybrid arc and is parametrized by the elapsed time $t \in \mathbb{R}_{\geq 0}$ and the number of jumps $j \in \mathbb{Z}_{\geq 0}$ that have occurred. To formally define a hybrid arc, we require the notion of a hybrid time domain [90, Definition 2.3].

Definition 2.17 (Hybrid time domain)**.** *A subset $E \subset \mathbb{R}_{\geq 0} \times \mathbb{Z}_{\geq 0}$ is a compact hybrid time domain if*

$$E = \bigcup_{j=0}^{J-1} ([t_j, t_{j+1}], j) \tag{2.19}$$

for some finite sequence of times $0 = t_0 \leq t_1 \leq \cdots \leq t_J$. It is a hybrid time domain if for all $(T, J) \in E$, $E \cap ([0, T] \times \{0, 1, \ldots, J\})$ is a compact hybrid time domain.

If E is a hybrid time domain, we define $\mathrm{I}_j(E) \coloneqq \{t \in \mathbb{R}_{\geq 0} : (t, j) \in E\}$. $\mathrm{I}_j(E)$ can be thought of as the largest time interval that can be associated with the jump j for the hybrid time domain E. It should be noted that $\mathrm{I}_j(E)$ can be a singleton or empty.

The notion of a hybrid arc is introduced in the following definition [90, Definition 2.4].

Definition 2.18 (Hybrid arc)**.** *A mapping $\phi : \operatorname{dom}\phi \to \mathbb{R}^n$ is a hybrid arc if $\operatorname{dom}\phi$ is a hybrid time domain and if for each $j \in \mathbb{Z}_{\geq 0}$, the mapping $t \mapsto \phi(t, j)$ is locally absolutely continuous on $\mathrm{I}_j(\operatorname{dom}\phi)$.*

If ϕ is a hybrid arc, then, for every $j \in \mathbb{Z}_{\geq 0}$, the derivative $\dot{\phi}(t, j)$ exists at every $t \in \mathrm{I}_j(\operatorname{dom}\phi)$ except on a set of Lebesgue measure zero (that is, it is differentiable at *almost* every $t \in \mathrm{I}_j(\operatorname{dom}\phi)$). The solution to a hybrid system is defined as follows.

Definition 2.19 (Solution to a hybrid system)**.** *A hybrid arc ϕ is a solution to the hybrid system $\mathcal{H}$ if $\phi(0, 0) \in \overline{C} \cup D$, and*

(S1) *for every $j \in \mathbb{Z}_{\geq 0}$ such that $\mathrm{I}_j(\operatorname{dom}\phi)$ has nonempty interior,*

$$\begin{aligned} &\phi(t, j) \in C && \text{for every } t \in \mathrm{I}_j(\operatorname{dom}\phi)^\circ, \\ &\dot{\phi}(t, j) \in F(\phi(t, j)) && \text{for almost every } t \in \mathrm{I}_j(\operatorname{dom}\phi), \end{aligned} \tag{2.20}$$

(S2) *for all $(t, j) \in \operatorname{dom}\phi$ such that $(t, j + 1) \in \operatorname{dom}\phi$,*

$$\begin{aligned} &\phi(t, j) \in D, \\ &\phi(t, j + 1) \in G(\phi(t, j)). \end{aligned} \tag{2.21}$$

A solution ϕ to $\mathcal{H}$ is said to be complete if $\operatorname{dom}\phi$ is unbounded and maximal if ϕ is not the truncation of another solution.

Conditions for the existence of solutions for a hybrid system satisfying the hybrid basic conditions can be stated as follows [90, Proposition 6.10].

Proposition 2.20 (Basic existence of solutions)**.** *Let the hybrid system $\mathcal{H}$ satisfy Assumption 2.16. If $F(x) \cap T_C(x) \neq \emptyset$ for every $x \in C \setminus D$, then there exists a nontrivial solution to $\mathcal{H}$ from every initial point in $C \cup D$, and every maximal solution to $\mathcal{H}$ satisfies exactly one of the following conditions:*

(a) *ϕ is complete;*
(b) *$\operatorname{dom}\phi$ is bounded and the interval $\mathrm{I}_J(\operatorname{dom}\phi)$, where $J = \sup_j \operatorname{dom}\phi$, has nonempty interior and $t \mapsto \phi(t, J)$ is a maximal solution to $\dot{z} \in F(z)$, in fact $\lim_{t \to T} |\phi(t, J)| = \infty$, where $T = \sup_t \operatorname{dom}\phi$;*
(c) *$\phi(T, J) \notin C \cup D$, where $(T, J) = \sup \operatorname{dom}\phi$.*

Furthermore, if $G(D) \subset C \cup D$, then (c) above does not occur.

2.3.3 Stability of Sets

This section introduces stability concepts for a closed set $\mathcal{A} \subset \mathbb{R}^n$. We will require two classes of comparison functions.

Definition 2.21 (Comparison functions)**.**

- *A function $\alpha : \mathbb{R}_{\geq 0} \to \mathbb{R}_{\geq 0}$ is a class-$\mathcal{K}_\infty$ function, also written $\alpha \in \mathcal{K}_\infty$, if α is zero at zero, continuous, strictly increasing, and unbounded.*
- *A function $\beta : \mathbb{R}_{\geq 0} \times \mathbb{R}_{\geq 0} \to \mathbb{R}_{\geq 0}$ is a class-$\mathcal{KL}$ function, also written $\beta \in \mathcal{KL}$, if it is nondecreasing in its first argument, nonincreasing in its second argument, $\lim_{r \searrow 0} \beta(r, s) = 0$ for each $s \in \mathbb{R}_{\geq 0}$, and $\lim_{s \to \infty} \beta(r, s) = 0$ for each $r \in \mathbb{R}_{\geq 0}$.*

Uniform global pre-asymptotic stability of a closed set $\mathcal{A} \subset \mathbb{R}^n$ for a hybrid system is defined following [90, Definition 3.6].

Definition 2.22 (Uniform global pre-asymptotic stability)**.** *A closed set $\mathcal{A} \subset \mathbb{R}^n$ is said to be*

- *uniformly globally stable for $\mathcal{H}$ if there exists a class $\mathcal{K}_\infty$ function α such that any solution ϕ to $\mathcal{H}$ satisfies $|\phi(t, j)|_{\mathcal{A}} \leq \alpha(\phi(0, 0))$ for all $(t, j) \in \operatorname{dom} \phi$;*
- *uniformly globally pre-attractive for $\mathcal{H}$ if for each $\epsilon > 0$ and $r > 0$ there exists $T > 0$ such that, for any solution ϕ to $\mathcal{H}$ with $|\phi(0, 0)|_{\mathcal{A}} \leq r$, $(t, j) \in \operatorname{dom} \phi$ and $t + j \geq T$ implies $|\phi(t, j)|_{\mathcal{A}} \leq \epsilon$;*
- *uniformly globally pre-asymptotically stable for $\mathcal{H}$ if it is both uniformly globally stable and uniformly globally pre-attractive.*

The prefix *pre* is employed to emphasize the fact that maximal solutions are not required to be complete.

Uniform global pre-asymptotic stability according to Definition 2.22 is equivalent to a stability characterization in terms of a $\mathcal{KL}$-bound [90, Theorem 3.40].

Theorem 2.23. *A closed set $\mathcal{A} \subset \mathbb{R}^n$ is uniformly globally pre-asymptotically stable for $\mathcal{H}$ if and only if there exists $\beta \in \mathcal{KL}$ such that any solution ϕ to $\mathcal{H}$ satisfies*

$$|\phi(t, j)|_{\mathcal{A}} \leq \beta(|\phi(0, 0)|_{\mathcal{A}}, t + j) \tag{2.22}$$

for all $(t, j) \in \operatorname{dom} \phi$.

If $\mathcal{A}$ is compact and the hybrid system satisfies the hybrid basic conditions, then uniform global pre-asymptotic stability is equivalent to global pre-asymptotic stability [90, Theorem 7.12] defined as

Definition 2.24 (Global pre-asymptotic stability)**.** *Let $\mathcal{H}$ be a hybrid system satisfying Assumption 2.16. A compact set $\mathcal{A} \subset \mathbb{R}^n$ is said to be*

- *stable for $\mathcal{H}$ if for every $\varepsilon > 0$ there exists $\delta > 0$ such that every solution ϕ to $\mathcal{H}$ with $|\phi(0, 0)|_{\mathcal{A}} \leq \delta$ satisfies $|\phi(t, j)|_{\mathcal{A}} \leq \varepsilon$ for all $(t, j) \in \operatorname{dom} \phi$;*
- *globally pre-attractive for $\mathcal{H}$ if every solution ϕ to $\mathcal{H}$ is bounded and, if ϕ is complete, then $\lim_{t+j \to \infty} |\phi(t, j)|_{\mathcal{A}} = 0$;*
- *globally pre-asymptotically stable for $\mathcal{H}$ if it is both stable and globally pre-attractive for $\mathcal{H}$.*

2.3.4 Hybrid Systems with Input

A hybrid system with input $\mathcal{H}$ is also defined by four objects (C, F, D, G),

$$\mathcal{H} : \begin{cases} \dot{x} \in F(x,u), & (x,u) \in C \\ x^+ \in G(x,u), & (x,u) \in D \end{cases} \tag{2.23}$$

where $x \in \mathbb{R}^n$ is the state of the system, $u \in \mathbb{R}^m$ is the input to the system, the set-valued mapping $F : \mathbb{R}^n \times \mathbb{R}^m \rightrightarrows \mathbb{R}^n$ is the flow map, $G : \mathbb{R}^n \times \mathbb{R}^m \rightrightarrows \mathbb{R}^n$ is the jump map, and $C \subset \mathbb{R}^n \times \mathbb{R}^m$ and $D \subset \mathbb{R}^n \times \mathbb{R}^m$ are the flow and jump sets, respectively.

We will typically consider hybrid systems with input that satisfy the following three basic assumptions [61, Definition 2.20].

Assumption 2.25 (Input hybrid basic conditions)**.**

(A1) C and D are closed subsets of $\mathbb{R}^n \times \mathbb{R}^m$;
(A2) $F : \mathbb{R}^n \times \mathbb{R}^m \rightrightarrows \mathbb{R}^n$ is outer semicontinuous and locally bounded relative to C, $C \subset \operatorname{dom} F$, and F is convex-valued on C;
(A3) $G : \mathbb{R}^n \times \mathbb{R}^m \rightrightarrows \mathbb{R}^n$ is outer semicontinuous and locally bounded relative to D, and $D \subset \operatorname{dom} G$.

It should be remarked that the conditions $(x,u) \in C$ and $(x,u) \in D$ as they appear (2.23) can be recast as explicit input constraints such as in the modeling framework of [89]. In particular, define the set $X_C := \pi_1(C)$ and the set-valued mapping $U_C(x) := \{u \in \mathbb{R}^m : (x,u) \in C\}$. Then $\operatorname{dom} U_C = X_C$ and $\operatorname{gph} U_C = C$. It now follows that $(x,u) \in C$ if and only if $x \in X_C$ and $u \in U_C(x)$. The condition (A1) in Assumption 2.25 stating that C is closed then amounts to U_C being outer semicontinuous by Lemma 2.2. Similar results are found for the jump set D.

The definition of a hybrid input is as follows [61, Definition 2.27].

Definition 2.26 (Hybrid input)**.** *A mapping $\psi : \operatorname{dom}\psi \to \mathbb{R}^m$ is a hybrid input if $\operatorname{dom}\psi$ is a hybrid time domain and for each $j \in \mathbb{Z}_{\geq 0}$, the mapping $t \mapsto \psi(t,j)$ is Lebesgue measurable and locally essentially bounded on $\mathrm{I}_j(\operatorname{dom}\psi)$.*

A mapping is locally essentially bounded if it is equal to a locally bounded mapping except on a set of Lebesgue measure zero. Consequently, an essentially locally bounded mapping is locally bounded almost everywhere in this sense. We are now equipped to introduce the solution concept for hybrid systems with input.

Definition 2.27 (Solution to a hybrid system with input)**.** *A pair (ϕ, ψ), where ϕ is a hybrid arc and ψ is a hybrid input, is a solution to the hybrid system $\mathcal{H}$ if $\phi(0,0) \in \overline{C} \cup D$, $\operatorname{dom}\phi = \operatorname{dom}\psi$, and*

(S1) *for every $j \in \mathbb{Z}_{\geq 0}$ such that $\mathrm{I}_j(\operatorname{dom}\phi)$ has nonempty interior,*

$$\begin{aligned} &(\phi(t,j), \psi(t,j)) \in C && \text{for every } t \in \mathrm{I}_j(\operatorname{dom}\phi)^\circ, \\ &\dot{\phi}(t,j) \in F(\phi(t,j), \psi(t,j)) && \text{for almost every } t \in \mathrm{I}_j(\operatorname{dom}\phi), \end{aligned} \tag{2.24}$$

(S2) *for all $(t,j) \in \operatorname{dom}\phi$ such that $(t, j+1) \in \operatorname{dom}\phi$,*

$$\begin{aligned} &(\phi(t,j), \psi(t,j)) \in D, \\ &\phi(t, j+1) \in G(\phi(t,j), \psi(t,j)). \end{aligned} \tag{2.25}$$

Part I

Modeling of Underwater Vehicles

Chapter 3

Modeling of Rigid Underwater Vehicles

In this chapter, we present a modeling framework for rigid underwater vehicles utilizing matrix Lie theory. The fundamental kinematic relations for the vehicle are derived directly on the Euclidean group and its Lie algebra. We subsequently derive the vehicle dynamics, where we incorporate hydrodynamic inertia effects, hydrodynamic damping effects, and the hydrostatic wrenches. Additionally, the effect of a uniform and unsteady ocean current is considered. We then introduce the novel concept of monotone dissipativity that has applications when designing model-based feedback control laws for underwater vehicles. Finally, a hydrodynamic symmetry principle is introduced which can be utilized to reduce the number of hydrodynamic parameters in the model.

3.1 Introduction

The mathematical modeling of underwater vehicles is of tremendous importance in the design and stability analysis of underwater vehicle feedback control laws, and for verification of underwater vehicle control systems. Unfortunately, the formulation of sufficiently accurate and mathematically tractable models is severely impeded by the complexity of the hydrodynamic forces and moments acting on the vehicle. Out of this challenge a fairly standardized modeling approach has arisen, which is well described in [24, Chapter 8]. It is in general necessary to neglect the infinite degrees of freedom that the fluid possesses, and to model the acting hydrodynamic wrenches in terms of variables describing the motion of the vehicle only. Such modeling approaches attempt to capture the mean effect that the fluid has on the vehicle over a wide range of operating conditions.

The remainder of this chapter is organized as follows. In Section 3.2, we present a kinematic analysis of rigid underwater vehicles on the Euclidean group. In particular, the kinematic quantities of interest and their transformation rules under a change of reference frame are introduced. We then present the equations of motion in Section 3.3. Dissipativity, monotone dissipativity, and Rayleigh dissipation functions are treated in Section 3.4. Then, Section 3.5 covers vehicle symmetry and the hydrodynamic symmetry principle. Lastly, a control model utilizing a quaternion attitude representation

is introduced in Section 3.6.

3.2 Vehicle Kinematics

To effectively describe the kinematics of a rigid underwater vehicle, we will first introduce a few matrix Lie groups and their properties. The three-dimensional orthogonal group, O(3), is defined by

$$\mathrm{O}(3) \coloneqq \{R \in \mathbb{R}^{3\times 3} : R^{\mathsf{T}} = R^{-1}\} \subset \mathrm{GL}(3). \tag{3.1}$$

The elements of this group are called rotation matrices. A rotation matrix $R \in \mathrm{O}(3)$ is called proper if $\det R = 1$, and improper if $\det R = -1$. The difference between them lies in the fact that improper rotations contain a reflection through some plane. It is usually not necessary to consider improper rotations in the field of robotics, and most references therefore only consider the three-dimensional special orthogonal group,

$$\mathrm{SO}(3) \coloneqq \{R \in \mathrm{O}(3) : \det R = 1\} \subset \mathrm{GL}(3), \tag{3.2}$$

which is the Lie subgroup of O(3) comprising all proper rotations. However, improper rotations are necessary when describing reflection symmetries of underwater vehicles, which we must consider when formulating the hydrodynamic symmetry principle in Section 3.5.

The Lie algebra of O(3) is denoted $\mathfrak{o}(3)$, and comprises all skew symmetric matrices in $\mathbb{R}^{3\times 3}$,

$$\mathfrak{o}(3) \coloneqq \{\Omega \in \mathbb{R}^{3\times 3} : \Omega^{\mathsf{T}} = -\Omega\}. \tag{3.3}$$

We identify $\mathfrak{o}(3)$ with $\mathbb{R}^3$ through the vector space isomorphism $(\,\cdot\,)^{\times} : \mathbb{R}^3 \to \mathfrak{o}(3)$ defined by

$$\omega^{\times} \coloneqq \begin{pmatrix} 0 & -\omega_3 & \omega_2 \\ \omega_3 & 0 & -\omega_1 \\ -\omega_2 & \omega_1 & 0 \end{pmatrix}. \tag{3.4}$$

The adjoint operators formulated relative to the isomorphism (3.4) can then be shown to be

$$\mathrm{Ad}_R^{\mathrm{O}(3)} \coloneqq \det(R) R, \tag{3.5}$$

$$\mathrm{ad}_{\omega}^{\mathfrak{o}(3)} \coloneqq \omega^{\times}. \tag{3.6}$$

We note that the special orthogonal group and the orthogonal group have the same Lie algebra, that is $\mathfrak{so}(3) = \mathfrak{o}(3)$.

The three-dimensional Euclidean group is the semidirect product $\mathbb{R}^3 \rtimes \mathrm{O}(3)$,

$$\mathrm{E}(3) \coloneqq \left\{ \begin{pmatrix} R & p \\ 0 & 1 \end{pmatrix} : p \in \mathbb{R}^3, R \in \mathrm{O}(3) \right\} \subset \mathrm{GL}(4). \tag{3.7}$$

This group comprises all translations and rotations in three dimensions. The representation (3.7) is somewhat cumbersome, and we therefore often write an element

$g \in \mathrm{E}(3)$ as a pair $g = (p, R)$. The Euclidean group acts on $\mathbb{R}^3$ via rotation and translation, which we for $r \in \mathbb{R}^3$ write as $g \cdot r \coloneqq p + Rr$. The mapping $g\cdot\ : \mathbb{R}^3 \to \mathbb{R}^3$ is easily shown to be a smooth diffeomorphism. In the robotics literature, one usually only encounters the three-dimensional special Euclidean group,

$$\mathrm{SE}(3) \coloneqq \left\{ \begin{pmatrix} R & p \\ 0 & 1 \end{pmatrix} : p \in \mathbb{R}^3, R \in \mathrm{SO}(3) \right\} \subset \mathrm{GL}(4). \tag{3.8}$$

This is the matrix Lie subgroup of E(3) where the rotations are restricted to be proper.

The Lie algebra of E(3) is denoted $\mathfrak{e}(3)$, and defined by

$$\mathfrak{e}(3) \coloneqq \left\{ \begin{pmatrix} \Omega & v \\ 0 & 0 \end{pmatrix} : v \in \mathbb{R}^3, \Omega \in \mathfrak{o}(3) \right\}. \tag{3.9}$$

We identify $\mathfrak{e}(3)$ with $\mathbb{R}^6$ by utilizing the vector space isomorphism $\widehat{\cdot} : \mathbb{R}^6 \to \mathfrak{e}(3)$ defined by

$$\widehat{\nu} \coloneqq \begin{pmatrix} \omega^\times & v \\ 0 & 0 \end{pmatrix} \text{ where } \nu = \begin{pmatrix} v \\ \omega \end{pmatrix} \tag{3.10}$$

The following proposition establishes the adjoint operators on E(3) and $\mathfrak{e}(3)$ relative to this isomorphism.

Proposition 3.1. *The adjoint operators on* E(3) *and* $\mathfrak{e}(3)$ *relative to the isomorphism* (3.10) *are given by*

$$\mathrm{Ad}_g \coloneqq \begin{pmatrix} R & \det(R)\, p^\times R \\ 0 & \det(R)\, R \end{pmatrix}, \tag{3.11}$$

$$\mathrm{ad}_\nu \coloneqq \begin{pmatrix} \omega^\times & v^\times \\ 0 & \omega^\times \end{pmatrix}, \tag{3.12}$$

respectively.

Proof. To characterize Ad_g, we first compute,

$$\begin{aligned} g\widehat{\nu}g^{-1} &= \begin{pmatrix} R & p \\ 0 & 1 \end{pmatrix} \begin{pmatrix} \omega^\times & v \\ 0 & 0 \end{pmatrix} \begin{pmatrix} R & p \\ 0 & 1 \end{pmatrix}^{-1} \\ &= \begin{pmatrix} R\omega^\times R^\mathsf{T} & Rv - R\omega^\times R^\mathsf{T} p \\ 0 & 0 \end{pmatrix}. \end{aligned} \tag{3.13}$$

The skew operator satisfies

$$R\omega^\times R^\mathsf{T} = (\det(R) R\omega)^\times \tag{3.14}$$

for all $(R, \omega) \in \mathrm{O}(3) \times \mathbb{R}^3$. Consequently,

$$-R\omega^\times R^\mathsf{T} p = \det(R) p^\times R\omega. \tag{3.15}$$

The operator Ad_g is therefore characterized by

$$\mathrm{Ad}_g : \begin{pmatrix} v \\ \omega \end{pmatrix} \mapsto \begin{pmatrix} Rv + \det(R) p^\times R\omega \\ \det(R) R\omega \end{pmatrix}, \tag{3.16}$$

which admits the matrix representation in (3.11). To characterize ad_ν, we first compute the Lie bracket,

$$\begin{aligned}[\widehat{\nu}_1, \widehat{\nu}_2] &= \begin{pmatrix} \omega_1^\times & v_1 \\ 0 & 0 \end{pmatrix} \begin{pmatrix} \omega_2^\times & v_2 \\ 0 & 0 \end{pmatrix} - \begin{pmatrix} \omega_2^\times & v_2 \\ 0 & 0 \end{pmatrix} \begin{pmatrix} \omega_1^\times & v_1 \\ 0 & 0 \end{pmatrix} \\ &= \begin{pmatrix} \omega_1^\times \omega_2^\times - \omega_2^\times \omega_1^\times & \omega_1^\times v_2 - \omega_2^\times v_1 \\ 0 & 0 \end{pmatrix}. \end{aligned} \tag{3.17}$$

It follows from the Jacobi-identity of the skew operator that

$$\omega_1^\times \omega_2^\times - \omega_2^\times \omega_1^\times = (\omega_1^\times \omega_2)^\times. \tag{3.18}$$

Since $-\omega_2^\times v_1 = v_1^\times \omega_2$, we find that

$$[\widehat{\nu}_1, \widehat{\nu}_2] = \begin{pmatrix} (\omega_1^\times \omega_2)^\times & v_1^\times \omega_2 + \omega_1^\times v_2 \\ 0 & 0 \end{pmatrix}. \tag{3.19}$$

Consequently, the operator ad_{ν_1} is characterized by

$$\mathrm{ad}_{\nu_1} : \begin{pmatrix} v_2 \\ \omega_2 \end{pmatrix} \mapsto \begin{pmatrix} v_1^\times \omega_2 + \omega_1^\times v_2 \\ \omega_1^\times \omega_2 \end{pmatrix} \tag{3.20}$$

which admits the matrix representation in (3.12). □

The special Euclidean group and the Euclidean group have the same Lie algebra, $\mathfrak{se}(3) = \mathfrak{e}(3)$.

By introducing a world-fixed Cartesian reference frame and a vehicle-fixed Cartesian reference frame, the configuration of an underwater vehicle can be identified with $\mathrm{E}(3)$. In particular, $g = (p, R) \in \mathrm{E}(3)$ relates the vehicle coordinate $r \in \mathbb{R}^3$ and the world coordinate $x \in \mathbb{R}^3$ of an arbitrary point via $x = g \cdot r$, as illustrated in Figure 3.1. Consequently, denoting by $\mathcal{R} \subset \mathbb{R}^3$ the set of vehicle coordinates that describe the

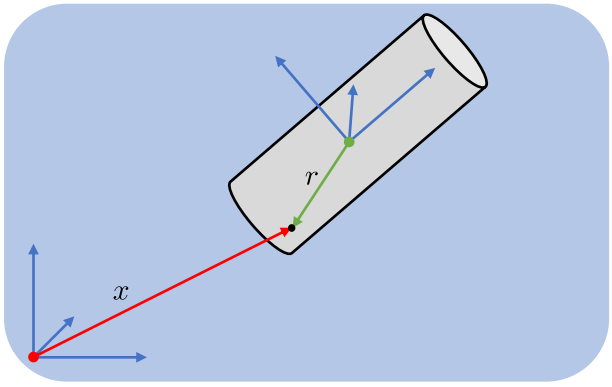

Figure 3.1: The world coordinate x and vehicle coordinate r of a point.

physical points comprising the vehicle, $g \cdot \mathcal{R} = \{Rr + p : r \in \mathcal{R}\}$ describes the corresponding set of world coordinates. In this context, $p \in \mathbb{R}^3$ is the vehicle position, and $R \in \mathrm{O}(3)$ the vehicle orientation. The position p should be understood as the vector

from the world frame origin to the vehicle frame origin expressed in the world frame. The orientation R describes the axes of the vehicle frame expressed in the world frame. Moreover, R is a proper rotation ($\det R = 1$) if the world frame and vehicle frame have the same handedness, and R is an improper rotation ($\det R = -1$) otherwise.

We denote by $v \in \mathbb{R}^3$ and $\omega \in \mathbb{R}^3$ the linear and angular velocity, respectively, of the vehicle frame relative to the world frame expressed in the vehicle frame. These are sometimes referred to as body velocities, e.g. in [98, Chapter 2, Section 4], or convective velocities, e.g. in [107, Chapter 15, Section 2]. Furthermore, we denote by $a \in \mathbb{R}^3$ and $\varpi \in \mathbb{R}^3$ the linear and angular vehicle accelerations, respectively. The differential second-order kinematics are then described by

$$\left.\begin{aligned} \dot{p} &= Rv \\ \dot{R} &= R\omega^{\times} \\ \dot{v} &= a \\ \dot{\omega} &= \varpi \end{aligned}\right\} (p, R, v, \omega, a, \varpi) \in \mathbb{R}^3 \times \mathrm{O}(3) \times \mathbb{R}^3 \times \mathbb{R}^3 \times \mathbb{R}^3 \times \mathbb{R}^3, \tag{3.21}$$

where a and ϖ are considered inputs. By introducing the vehicle velocity $\nu = (v, \omega) \in \mathbb{R}^6$ and the vehicle acceleration $\alpha = (a, \varpi) \in \mathbb{R}^6$, the kinematic system (3.21) can be equivalently stated as

$$\left.\begin{aligned} \dot{g} &= g\widehat{\nu} \\ \dot{\nu} &= \alpha \end{aligned}\right\} (g, \nu, \alpha) \in \mathrm{E}(3) \times \mathbb{R}^6 \times \mathbb{R}^6, \tag{3.22}$$

where α is considered an input.

A generalized force acting on a rigid underwater vehicle comprises a linear component, a pure linear force $l \in \mathbb{R}^3$, and an angular component, a pure moment $\kappa \in \mathbb{R}^3$. Such a force-moment pair is typically referred to as a wrench, and represented as a vector $f = (l, \kappa) \in \mathbb{R}^6$. We consider wrenches to be expressed in the vehicle frame. In particular, a wrench f contracts naturally with the vehicle velocity ν to form the instantaneous work done by the wrench, $W = \langle f, \nu \rangle = \langle l, v \rangle + \langle \kappa, \omega \rangle$.

A change of world frame can be encoded in a rigid transformation $h = (b, S) \in \mathrm{E}(3)$ that describes the configuration of the old world frame relative to the new world frame. In particular, $b \in \mathbb{R}^3$ describes the origin of the old world frame expressed in the new world frame. Furthermore, $S \in \mathrm{O}(3)$ describes the axes of the old world frame expressed in the new world frame. The introduced kinematic quantities then transform as

$$\begin{aligned} g^* &= hg, \\ \nu^* &= \nu, \\ \alpha^* &= \alpha, \\ f^* &= f. \end{aligned} \tag{3.23}$$

In particular, g^* is the configuration of the vehicle frame relative to the new world frame, ν^* and α^* are the vehicle frame velocity and acceleration relative to the new world frame expressed in the vehicle frame, respectively, and f^* is the transformed vehicle wrench. Evidently, the latter three quantities are independent of the world frame placement.

A change of vehicle frame is in turn facilitated by a transformation $h = (b, S) \in \mathrm{E}(3)$ that describes the configuration of the new vehicle frame relative to the old vehicle frame. Here, $b \in \mathbb{R}^3$ is the origin of the new vehicle frame expressed in the old vehicle frame. The rotation matrix $S \in \mathrm{O}(3)$ describes the axes of the new vehicle frame expressed in the old vehicle frame. The introduced kinematic quantities transform as

$$\begin{aligned} g^* &= gh, \\ \nu^* &= \mathrm{Ad}_h^{-1}\, \nu, \\ \alpha^* &= \mathrm{Ad}_h^{-1}\, \alpha, \\ f^* &= \mathrm{Ad}_h^{\mathsf{T}}\, f. \end{aligned} \tag{3.24}$$

Here, g^* is the configuration of the new vehicle frame relative to the world frame, ν^* and α^* are the velocity and acceleration of the new vehicle frame relative to the world frame expressed in the new vehicle frame, respectively, and f^* is the wrench expressed in the new vehicle frame.

3.3 Vehicle Dynamics

We will in this section derive the equations that describe the motion of the underwater vehicle. To this end, the following assumptions are made.

Assumption 3.2.

1. The world frame is an inertial reference frame.
2. $\mathcal{R}$ is a nonempty compact regular domain in $\mathbb{R}^3$ [96, Page 120].

The first assumption is from an empirical standpoint necessary to ensure that the derived equations of motion describe the vehicle motion. The second assumption ensures that the vehicle has a smooth surface and nonzero volume, such that we can guarantee the existence of certain hydrodynamic quantities.

In the following, we start out with a brief treatment of rigid body dynamics before turning our attention to the modeling of the acting hydromechanical wrenches. It is customary to separate the contributions to the hydromechanical wrench that act on an underwater vehicle into three basic components,

1. the hydrodynamic inertia wrench;
2. the hydrodynamic damping wrench;
3. the hydrostatic wrench.

We remark that the hydrodynamic wrench acting on a submerged rigid body undergoing general motion is extremely challenging to model accurately. The fluid is a highly complicated infinite-dimensional dynamical system coupled with the finite dimensional underwater vehicle. Consequently, the acting wrench would realistically depend on the motion history of the vehicle. To derive a manageable set of governing equations for the rigid body, this aspect of the hydrodynamic wrench is typically neglected in modeling practice. In particular, the hydrodynamic wrench acting on the body at an instant in time is taken to depend solely on the configuration, velocity, and acceleration of the body at that instant in time. Such hydrodynamic models are referred to as memoryless, and are the sole focus of this chapter.

3.3.1 Rigid Body Dynamics

The tendency of a body to resist a change of its velocity is commonly referred to as inertia. The central principles of analytical mechanics relate the inertial properties of a rigid body to its kinetic energy. Let us consider an arbitrary material point with vehicle coordinate $r \in \mathcal{R}$. The corresponding world coordinate is given by $x = g \cdot r$. Consequently, the velocity of the material point as seen from the world frame is

$$\begin{aligned} \dot{x} &= \dot{g} \cdot r \\ &= Rv + R\omega^{\times} r \\ &= R \begin{pmatrix} I & -r^{\times} \end{pmatrix} \nu. \end{aligned} \tag{3.25}$$

The underwater vehicle is taken to have a density measure $\rho d^3 r$ with support equal to $\mathcal{R}$. It follows that the kinetic energy of the underwater vehicle, $T_R : \mathbb{R}^6 \to \mathbb{R}$, can be computed by

$$\begin{aligned} T_R(\nu) &\coloneqq \frac{1}{2} \int_{r \in \mathcal{R}} |\dot{g} \cdot r|^2 \, \rho(r) d^3 r \\ &= \frac{1}{2} \int_{r \in \mathcal{R}} \left\langle \begin{pmatrix} I & -r^{\times} \\ r^{\times} & -r^{\times} r^{\times} \end{pmatrix} \nu, \nu \right\rangle \rho(r) d^3 r \\ &= \frac{1}{2} \langle M_R \nu, \nu \rangle. \end{aligned} \tag{3.26}$$

The vehicle inertia matrix M_R can be written as

$$M_R \coloneqq \begin{pmatrix} mI & -r_m^{\times} \\ r_m^{\times} & J_R \end{pmatrix}, \tag{3.27}$$

where the vehicle mass m, the vehicle center of mass r_m, and the vehicle rotational inertia matrix J_R, are defined by

$$m \coloneqq \int_{r \in \mathcal{R}} \rho(r) d^3 r, \tag{3.28}$$

$$r_m \coloneqq \frac{1}{m} \int_{r \in \mathcal{R}} r \, \rho(r) d^3 r, \tag{3.29}$$

$$J_R \coloneqq \int_{r \in \mathcal{R}} (|r|^2 I - r \otimes r) \, \rho(r) d^3 r. \tag{3.30}$$

We here used the fact that $r^{\times} r^{\times} = r \otimes r - |r|^2 I$ for every $r \in \mathbb{R}^3$ to define J_R. The vehicle inertia matrix M_R is symmetric and positive definite.

The rigid body equation of motion for the vehicle is given by

$$M_R \alpha - \mathrm{ad}_{\nu}^{\mathsf{T}} M_R \nu = f, \tag{3.31}$$

where f is a placeholder for other wrenches acting on the vehicle. In fact, (3.31) can be derived directly from the kinetic energy (3.26) in a variational setting, as done for instance in [101, Section 5.3.3] and [107, Chapter 15]. It is also possible to arrive at (3.31) with Newtonian mechanics, as done for instance in [98, Section 4.2.4] and [24, Section 3.3].

3.3.2 Hydrodynamic Inertia

A moving submerged body disturbs the surrounding water, and in this manner sets mass into motion. Consequently, the submerged body has different inertial properties in water than it would have in vacuum. While this is also true for a rigid body submerged in a fluid such as air, it is the high density of water that makes it particularly important to consider this additional hydrodynamic inertia in the modeling process. From a theoretical perspective, the hydrodynamic inertia wrench is typically derived under the following additional assumptions.

Assumption 3.3.

1. The underwater vehicle is the only bounding surface of the fluid.
2. The fluid motion is globally described by a potential.
3. The fluid density, $\varrho > 0$, is constant.
4. The fluid is at rest far away from the vehicle.

The fluid motion induced by the vehicle can then be described by a collection of harmonic functions introduced by Kirchhoff in [1].

Definition 3.4. *A classical Kirchhoff potential for $\mathcal{R}$ is a mapping $\varphi : \overline{\mathbb{R}^3 \setminus \mathcal{R}} \to \mathbb{R}^6$ satisfying the following three conditions:*

1. *φ is continuously differentiable on $\overline{\mathbb{R}^3 \setminus \mathcal{R}}$ and each component of φ is harmonic on $\mathbb{R}^3 \setminus \mathcal{R}$;*
2. *φ satisfies the Neumann boundary condition*

$$\mathrm{D}\varphi(r)n(r) = \begin{pmatrix} n(r) \\ r \times n(r) \end{pmatrix} \tag{3.32}$$

   on $\partial\mathcal{R}$, where $n : \partial\mathcal{R} \to \mathbb{S}^2$ is the outwards-pointing unit normal of $\mathcal{R}$;
3. *$|\varphi(r)| \to 0$ as $|r|_{\mathcal{R}} \to \infty$.*

Since $\mathcal{R}$ is assumed to be a compact regular domain, it follows from [108, Theorem 6.10.6] that there exists a unique classical Kirchhoff potential φ for $\mathcal{R}$. Furthermore, it follows from [108, Proposition 2.17.3] that the decay of $|\varphi|$ is $\mathcal{O}(|r|_{\mathcal{R}}^{-1})$, and the decay of $\|\mathrm{D}\varphi\|$ is $\mathcal{O}(|r|_{\mathcal{R}}^{-2})$.

A Kirchhoff potential encodes the velocity of every material particle in the fluid. In particular, the fluid particle that at some instant in time has the vehicle coordinate $r \in \mathbb{R}^3 \setminus \mathcal{R}$ and world coordinate $x = g \cdot r$, has at that instant in time the world frame velocity

$$\dot{x} = R\,\mathrm{D}\varphi(r)^{\mathsf{T}}\nu, \tag{3.33}$$

which can be viewed as an analogue to the expression (3.25). It follows that the kinetic energy of the fluid is given by

$$\begin{aligned} T_H(\nu) &\coloneqq \frac{1}{2}\int_{r\in\mathbb{R}^3\setminus\mathcal{R}} |R\,\mathrm{D}\varphi(r)^{\mathsf{T}}\nu|^2\,\varrho d^3r \\ &= \frac{1}{2}\int_{r\in\mathbb{R}^3\setminus\mathcal{R}} \langle \mathrm{D}\varphi(r)\,\mathrm{D}\varphi(r)^{\mathsf{T}}\nu, \nu\rangle\,\varrho d^3r \\ &= \frac{1}{2}\langle M_H\nu, \nu\rangle, \end{aligned} \tag{3.34}$$

where the hydrodynamic inertia matrix is defined by

$$M_H \coloneqq \int_{r\in\mathbb{R}^3\setminus\mathcal{R}} \mathrm{D}\varphi(r)\,\mathrm{D}\varphi(r)^\mathsf{T}\,\varrho d^3 r. \tag{3.35}$$

Due to the aforementioned rapid decay of $\|\mathrm{D}\varphi\|$ at large distances from the body, the integral (3.35) is guaranteed to converge. It should be remarked that several references define the hydrodynamic inertia matrix as

$$M_H = -\int_{r\in\partial\mathcal{R}} \varphi(r)\otimes\begin{pmatrix} n(r) \\ r\times n(r)\end{pmatrix}\varrho d^2 r. \tag{3.36}$$

The expression (3.36) is equivalent to (3.35) under Assumption 3.3. A proof of this fact can be found in [109, Section 4.14].

It is seen directly from the development (3.34) that the hydrodynamic inertia matrix is symmetric and positive semidefinite. While the rigid body inertia matrix M_R is determined by 10 independent coefficients, the hydrodynamic inertia matrix is determined by the maximum number of 21. Fortunately, symmetry of the vehicle shape can be used to bring this number down substantially. We will investigate this topic further in Section 3.5.

The acting hydrodynamic inertia wrench is denoted $f_H : \mathbb{R}^6\times\mathbb{R}^6\to\mathbb{R}^6$, and defined by

$$f_H(\nu,\alpha) \coloneqq -M_H\alpha + \mathrm{ad}_\nu^\mathsf{T} M_H\nu. \tag{3.37}$$

This can be proven by utilizing T_H directly in a variational principle, as was done originally in [1]. Furthermore, it can also be shown that direct integration of the dynamic pressure induced by the Kirchhoff potentials over the vehicle surface yields the same result [109, Chapter 4, equations (115-116)]. Consequently, the stated form (3.37) of the hydrodynamic inertia wrench is uncontroversial provided that Assumption 3.3 is satisfied.

We shall now state the necessary changes to (3.37) when the vehicle is in the presence of a spatially uniform and unsteady ocean current, thereby alleviating the fourth item in Assumption 3.3. The fluid velocity and acceleration associated with the current are denoted $v_c\in\mathbb{R}^3$ and $a_c \coloneqq \dot{v}_c\in\mathbb{R}^3$, respectively. These quantities are expressed in the world frame. Furthermore, we define

$$\begin{aligned}\nu_c &\coloneqq \mathrm{Ad}_g^{-1}\begin{pmatrix} v_c \\ 0\end{pmatrix} = \begin{pmatrix} R^\mathsf{T} v_c \\ 0\end{pmatrix}, \\ \alpha_c &\coloneqq \dot{\nu}_c = \mathrm{Ad}_g^{-1}\begin{pmatrix} a_c \\ 0\end{pmatrix} - \mathrm{ad}_\nu\,\nu_c = \begin{pmatrix} R^\mathsf{T} a_c - \omega^\times R^\mathsf{T} v_c \\ 0\end{pmatrix}.\end{aligned} \tag{3.38}$$

It is seen that ν_c is the current velocity treated as a vector in $\mathbb{R}^6$ and expressed in the vehicle frame. Furthermore, α_c is the derivative of ν_c and therefore contains not only the current acceleration rotated into the vehicle frame, but also a coupling term involving the vehicle angular velocity resulting from the motion of the vehicle frame.

The current wrench acting on the vehicle in potential flow is derived in [110, 111], and found to be given by the mapping $f_C : \mathrm{E}(3)\times\mathbb{R}^6\times\mathbb{R}^3\times\mathbb{R}^3\to\mathbb{R}^6$ defined by

$$\begin{aligned} f_C(g,\nu,v_c,a_c) \coloneqq{}& M_H\alpha_c + \mathrm{ad}_{\nu_c}^\mathsf{T} M_H\nu_c - \mathrm{ad}_\nu^\mathsf{T} M_H\nu_c \\ &- \mathrm{ad}_{\nu_c}^\mathsf{T} M_H\nu + \begin{pmatrix} \varrho\upsilon I \\ \varrho\upsilon r_\upsilon^\times\end{pmatrix} R^\mathsf{T} a_c.\end{aligned} \tag{3.39}$$

The last term present in (3.39) is referred to as the acceleration-reaction wrench. It can be identified as the wrench acting on the vehicle in a uniform and unsteady flow field that is undisturbed by the vehicle. The sum of (3.37) and (3.39) constitutes the hydrodynamic potential flow force $f_P : \mathrm{E}(3) \times \mathbb{R}^6 \times \mathbb{R}^6 \times \mathbb{R}^3 \times \mathbb{R}^3 \to \mathbb{R}^6$, defined by

$$\begin{aligned} f_P(g, \nu, \alpha, v_c, a_c) &\coloneqq f_H(\nu, \alpha) + f_C(g, \nu, v_c, a_c) \\ &= -M_H \alpha_r + \mathrm{ad}_{\nu_r}^{\mathsf{T}} M_H \nu_r + \begin{pmatrix} \varrho \upsilon I \\ \varrho \upsilon r_{\upsilon}^{\times} \end{pmatrix} R^{\mathsf{T}} a_c, \end{aligned} \tag{3.40}$$

where we for readability have introduced the vehicle-current relative velocity and acceleration $\nu_r \coloneqq \nu - \nu_c$ and $\alpha_r \coloneqq \alpha - \alpha_c$, respectively.

It should be remarked that experimentally determined hydrodynamic inertia parameters may differ significantly from the ideal values computed from the Kirchhoff potential with (3.35) or (3.36). Since a memoryless model can not describe the hydrodynamic wrenches exerted on the vehicle by a viscous and rotational fluid exactly, unmodeled effects will inevitably be captured in the hydrodynamic inertia parameters when the memoryless model is fitted to experimental data.

3.3.3 Hydrodynamic Damping

In a viscous and rotational fluid, additional physical effects such as viscous shear stresses and free vorticity must be considered. The simplified memoryless approximation to these effects is typically referred to as the hydrodynamic damping wrench, e.g. [24, Section 6.4], due to their empirically observable tendency to dampen out the motion of the underwater vehicle. The damping wrench is modeled as a continuous mapping $d : \mathbb{R}^6 \to \mathbb{R}^6$, dependent solely on the vehicle velocity.

The particular expressions chosen for d can be considered semi-empirical at best. An example from the literature is given by the second-order modulus damping model

$$d(\nu) \coloneqq -\sum_{i=1}^{6} |\nu_i| D_i \nu, \tag{3.41}$$

where ν_i denotes component i of the vehicle velocity ν, and $D_i \in \mathbb{R}^{6\times 6}$ is a matrix of damping coefficients for every $i \in \{1, \ldots, 6\}$. This damping model is found in the literature rather frequently. For instance, it is referred to in [24] as a possible choice for describing the hydrodynamic damping wrench acting on an underwater vehicle during general maneuvers.

Viscous current effects are usually taken into account by reformulating the hydrodynamic damping wrench relative to the current. In particular, $d(\nu)$ is replaced by $d(\nu_r)$. This is certainly reasonable when v_c is constant due to the Galilean invariance of the underlying hydrodynamic equations. When the current is unsteady, it might be necessary to use a different set of hydrodynamic coefficients in d than in the steady case. It is for instance well known that the averaged drag coefficients of piles in oscillatory flow depend on the frequency of oscillation, which is captured by the so-called Keulegan-Carpenter number. A more detailed discussion of this phenomenon can be found in [112, Chapter 7] and [113, Chapter 3].

3.3.4 Hydrostatics

The hydrostatic wrench comprises in the context of ocean vehicles both weight and buoyancy, and we start by treating the former. The vehicle weight, considered as a wrench, can be computed by integrating gravitational contributions expressed in the vehicle frame over $\mathcal{R}$. Denoting by $a_\gamma \in \mathbb{R}^3$ the gravitational acceleration in the world frame, taken to point downwards, we find

$$\begin{aligned} f_W(g) &\coloneqq \int_{r\in\mathcal{R}} \begin{pmatrix} I \\ r^\times \end{pmatrix} R^\mathsf{T} a_\gamma \, \rho(r) d^3 r \\ &= \begin{pmatrix} mI \\ mr_m^\times \end{pmatrix} R^\mathsf{T} a_\gamma. \end{aligned} \tag{3.42}$$

The buoyancy wrench takes the same form in all commonly used constant-density fluid models. It results from integrating the hydrostatic pressure contributions over the surface of the vehicle. In particular,

$$f_B(g) \coloneqq -\int_{r\in\partial\mathcal{R}} \langle R^\mathsf{T} a_\gamma, r\rangle \begin{pmatrix} n(r) \\ r \times n(r) \end{pmatrix} \varrho d^2 r. \tag{3.43}$$

For a fluid with constant density in a uniform gravitational field, this surface integral can be transformed into a volume integral over the body, and can further be shown to have an expression similar to the gravitational wrench (3.42). In particular,

$$f_B(g) = -\begin{pmatrix} \varrho\upsilon I \\ \varrho\upsilon r_\upsilon^\times \end{pmatrix} R^\mathsf{T} a_\gamma \tag{3.44}$$

for every $g \in \mathrm{E}(3)$, where the vehicle volume υ and center of volume r_υ are defined by

$$\upsilon \coloneqq \int_{r\in\mathcal{R}} d^3 r, \qquad r_\upsilon \coloneqq \frac{1}{\upsilon}\int_{r\in\mathcal{R}} r \, d^3 r, \tag{3.45}$$

respectively. The quantity $\varrho\upsilon$ is the mass of the fluid displaced by the vehicle. The hydrostatic wrench is the sum of (3.42) and (3.44), $\chi : \mathrm{E}(3) \to \mathbb{R}^6$,

$$\chi(g) \coloneqq \begin{pmatrix} (m-\varrho\upsilon)I \\ (mr_m^\times - \varrho\upsilon r_\upsilon^\times) \end{pmatrix} R^\mathsf{T} a_\gamma. \tag{3.46}$$

It is readily seen that (3.46) can be derived from the potential $U_\chi : \mathrm{E}(3) \to \mathbb{R}$ defined by

$$U_\chi(g) \coloneqq -\langle a_\gamma, (m-\varrho\upsilon)p + R(mr_m - \varrho\upsilon r_\upsilon)\rangle, \tag{3.47}$$

that is, $\chi(g) = -\,\mathrm{d}U_\chi(g)$ for every $g \in \mathrm{E}(3)$.

We end this section with a proof of the fact that (3.43) and (3.44) are indeed equivalent.

Proposition 3.5. *The expressions* (3.43) *and* (3.44) *are equivalent.*

Proof. The proof is easiest in component-notation. Defining $a^* \coloneqq R^\mathsf{T} a_\gamma$, the linear force components of the buoyancy wrench (3.43) are

$$l_i = -\int_{r\in\partial\mathcal{R}} a_j^* r_j n_i \, \varrho d^2 r, \tag{3.48}$$

where summation over repeated indices is implied. Applying the divergence theorem yields

$$l_i = -\int_{r\in\mathcal{R}} a_j^* \delta_{ij}\, \varrho d^3 r = -\varrho \int_{r\in\mathcal{R}} d^3 r\, a_i^* = -\varrho \upsilon a_i^* \tag{3.49}$$

where δ_{ij} is the Kronecker-delta. Denoting by ϵ_{ijk} Levi-Civita symbol, the moment components of the buoyancy wrench are

$$\begin{aligned}
\kappa_i &= -\int_{r\in\partial\mathcal{R}} a_s^* r_s \epsilon_{ijk} r_j n_k\, \varrho d^2 r \\
&= -\int_{r\in\mathcal{R}} a_s^* (\delta_{ks}\epsilon_{ijk} r_j + r_s \epsilon_{ijk}\delta_{jk}) \varrho d^3 r \\
&= -\varrho \epsilon_{ijk} \int_{r\in\mathcal{R}} r_j d^3 r\, a_k^* \\
&= -\varrho \upsilon \epsilon_{ijk} r_{v,j} a_k^*,
\end{aligned} \tag{3.50}$$

where the divergence theorem and the fact that $\delta_{ij}\epsilon_{ijk} = 0$ were used. This establishes that f_B is indeed given by the volume integral (3.44). □

3.3.5 Equation of Motion

We will now combine the expressions presented in the previous sections to form the equation of motion for the underwater vehicle. Denoting the wrenches generated by the vehicle's thrusters and control surfaces by τ, we have

$$\begin{aligned}
M_R\alpha - \mathrm{ad}_\nu^\mathsf{T} M_R \nu = f_P(g,\nu,\alpha,v_c,a_c) \\
+ d(\nu-\nu_c) + \chi(g) + \tau,
\end{aligned} \tag{3.51}$$

or equivalently,

$$\begin{aligned}
M\alpha - \mathrm{ad}_\nu^\mathsf{T} M \nu = f_C(g,\nu,v_c,a_c) \\
+ d(\nu-\nu_c) + \chi(g) + \tau,
\end{aligned} \tag{3.52}$$

where we defined the total inertia matrix

$$M \coloneqq M_R + M_H. \tag{3.53}$$

It is possible to simplify (3.52) further by rewriting it in terms of the relative velocity ν_r and relative acceleration α_r. To this end, we require the following lemma which can be viewed as a minor generalization of [114, Property 2] to the case of unsteady ocean currents.

Lemma 3.1. It holds that

$$M_R\alpha_r - \mathrm{ad}_{\nu_r}^\mathsf{T} M_R \nu_r = M_R\alpha - \mathrm{ad}_\nu^\mathsf{T} M_R \nu - \begin{pmatrix} mI \\ mr_m^\times \end{pmatrix} R^\mathsf{T} a_c. \tag{3.54}$$

Proof. Using the linearity of ad, we find

$$\begin{aligned} M_R\alpha_r - \operatorname{ad}_{\nu_r}^{\mathsf{T}} M_R\nu_r = M_R\alpha - \operatorname{ad}_{\nu}^{\mathsf{T}} M_R\nu - M_R\alpha_c \\ + M_R \operatorname{ad}_{\nu} \nu_c + \operatorname{ad}_{\nu_c}^{\mathsf{T}} M_R\nu + \operatorname{ad}_{\nu}^{\mathsf{T}} M_R\nu_c \\ - \operatorname{ad}_{\nu_c}^{\mathsf{T}} M_R\nu_c \end{aligned} \tag{3.55}$$

The last term in the first line of (3.55) is found to be equal to the last term in (3.54). We now investigate the terms appearing in the second line of (3.55). Straightforward computations yield

$$\begin{aligned} M_R \operatorname{ad}_{\nu} \nu_c &= m \begin{pmatrix} \omega^{\times} R^{\mathsf{T}} v_c \\ r_m^{\times} \omega^{\times} R^{\mathsf{T}} v_c \end{pmatrix}, \\ \operatorname{ad}_{\nu_c}^{\mathsf{T}} M_R\nu &= m \begin{pmatrix} 0 \\ -(R^{\mathsf{T}} v_c)^{\times} v + (R^{\mathsf{T}} v_c)^{\times} r_m^{\times} \omega \end{pmatrix}, \\ \operatorname{ad}_{\nu}^{\mathsf{T}} M_R\nu_c &= -m \begin{pmatrix} \omega^{\times} R^{\mathsf{T}} v_c \\ v^{\times} R^{\mathsf{T}} v_c + \omega^{\times} r_m^{\times} R^{\mathsf{T}} v_c \end{pmatrix}. \end{aligned} \tag{3.56}$$

The sum of the expressions presented in (3.56) is

$$m \begin{pmatrix} 0 \\ -v^{\times} R^{\mathsf{T}} v_c - (R^{\mathsf{T}} v_c)^{\times} v + r_m^{\times} \omega^{\times} R^{\mathsf{T}} v_c + (R^{\mathsf{T}} v_c)^{\times} r_m^{\times} \omega - \omega^{\times} r_m^{\times} R^{\mathsf{T}} v_c \end{pmatrix},$$

and the terms containing v are readily seen to cancel due to the anti-symmetry of the cross product. Furthermore, the terms containing ω cancel due to the Jacobi identity. It remains to show that the last term in (3.55) vanishes. We find that

$$- \operatorname{ad}_{\nu_c}^{\mathsf{T}} M_R\nu_c = m \begin{pmatrix} 0 \\ (R^{\mathsf{T}} v_c)^{\times} R^{\mathsf{T}} v_c \end{pmatrix}, \tag{3.57}$$

which vanishes due to anti-symmetry of the cross product. □

In light of Lemma 3.1 and the expression (3.40) for the hydrodynamic potential wrench, it is possible to write the full equation of motion for the underwater vehicle as

$$M\alpha_r - \operatorname{ad}_{\nu_r}^{\mathsf{T}} M\nu_r = d(\nu_r) + \overline{\chi}(g, a_c) + \tau, \tag{3.58}$$

where $\overline{\chi} : \mathrm{E}(3) \times \mathbb{R}^3 \to \mathbb{R}^6$ comprises hydrostatic contributions, the acceleration-reaction wrench, and the last term appearing in (3.54),

$$\overline{\chi}(g, a_c) \coloneqq \begin{pmatrix} (m - \varrho v) I \\ m r_m^{\times} - \varrho v r_v^{\times} \end{pmatrix} R^{\mathsf{T}} (a_\gamma - a_c). \tag{3.59}$$

The form of the equation (3.58) when a uniform and unsteady current is present is to the authors' knowledge novel. When the current is steady, $\overline{\chi}$ reduces to the hydrostatic wrench χ, and (3.58) to the standard model found in [24, Equation (8.2)]. It follows that the complete system describing the motion of the underwater vehicle can be

stated as

$$\underbrace{\begin{aligned}\dot{g} &= g(\widehat{\nu}_r + \widehat{\nu}_c)\\ \dot{\nu}_r &= M^{-1}[\mathrm{ad}^{\mathsf{T}}_{\nu_r} M\nu_r + d(\nu_r) + \overline{\chi}(g, a_c) + \tau]\\ \dot{v}_c &= a_c\end{aligned}}_{(g,\nu_r,\tau,v_c,a_c)\in \mathrm{E}(3)\times\mathbb{R}^6\times\mathbb{R}^6\times\mathbb{R}^3\times\mathbb{R}^3,} \tag{3.60}$$

where $\tau \in \mathbb{R}^6$ and $a_c \in \mathbb{R}^3$ are considered inputs.

We finalize this section by showing that the equation of motion (3.58) can be derived from the Lagrange-d'Alembert principle (see for instance [107, Section 7.8], [53, Section 5.2], and [101, Section 4.4.3] for details). Our result shows that the inertial and hydrostatic terms present in (3.58), including those resulting from unsteady ocean currents, can be directly derived from a Lagrangian function.

Theorem 3.6. *The equation of motion (3.58) can be derived from the Lagrange-d'Alembert principle by utilizing the Lagrangian* $L : \mathrm{E}(3)\times\mathbb{R}^6\times\mathbb{R}^3\times\mathbb{R}^3 \to \mathbb{R}$,

$$L(g, \nu_r, a_c) \coloneqq \frac{1}{2}\langle M\nu_r, \nu_r\rangle - U(g, a_c), \tag{3.61}$$

where $U : \mathrm{E}(3)\times\mathbb{R}^3 \to \mathbb{R}$ *is defined by*

$$U(g, a_c) \coloneqq -\langle a_\gamma - a_c, (m - \varrho\upsilon)p + R(mr_m - \varrho\upsilon r_\upsilon)\rangle, \tag{3.62}$$

and including d *and* τ *in the external wrenches.*

Proof. Let $T \geq 0$, and consider curves $g : [0, T] \to \mathrm{E}(3)$ and $v_c : [0, T] \to \mathbb{R}^3$ such that $\dot{g}$ and v_c are absolutely continuous. Given a smooth curve $\xi : [0, T] \to \mathbb{R}^6$, we write a variation of g as $g_\xi : [0, T]\times\mathbb{R} \to \mathrm{E}(3)$,

$$g_\xi(t, s) \coloneqq g(t)\exp(s\widehat{\xi}(t)). \tag{3.63}$$

From g_ξ, we can define the variation ν_ξ of the corresponding velocity $t \mapsto \nu(t)$ defined such that $\widehat{\nu}(t) = g(t)^{-1}\dot{g}(t)$. In particular,

$$\widehat{\nu}_\xi(t, s) \coloneqq g_\xi(t, s)^{-1}\dot{g}_\xi(t, s). \tag{3.64}$$

The variation of ν_c is denoted $\nu_{c,\xi}$ and defined by

$$\begin{aligned}\nu_{c,\xi}(t, s) &\coloneqq \mathrm{Ad}^{-1}_{g_\xi(t,s)}\begin{pmatrix} v_c(t)\\ 0\end{pmatrix}\\ &= \mathrm{Ad}^{-1}_{\exp(s\widehat{\xi}(t))}\nu_c(t)\end{aligned} \tag{3.65}$$

The variation of ν_r is then $\nu_{r,\xi}(t, s) \coloneqq \nu_\xi(t, s) - \nu_{c,\xi}(t, s)$.

The corresponding infinitesimal variation of the configuration is now defined as

$$\begin{aligned}\delta g_\xi(t) &\coloneqq \frac{d}{ds}\bigg|_{s=0} g_\xi(t, s)\\ &= g(t)\frac{d}{ds}\bigg|_{s=0}(I + s\widehat{\xi}(t) + \ldots)\\ &= g(t)\widehat{\xi}(t).\end{aligned} \tag{3.66}$$

The infinitesimal variation of the velocity is defined analogously,

$$\begin{aligned}\widehat{\delta\nu}_\xi(t) &\coloneqq \frac{d}{ds}\Big|_{s=0} \widehat{\nu}_\xi(t,s) \\ &= -\frac{d}{ds}\Big|_{s=0} (I + s\widehat{\xi}(t) + \ldots)\widehat{\nu}(t) + \widehat{\nu}(t)\frac{d}{ds}\Big|_{s=0} (I + s\widehat{\xi}(t) + \ldots) + \dot{\widehat{\xi}}(t) \\ &= \dot{\widehat{\xi}}(t) + [\widehat{\nu}(t), \widehat{\xi}(t)]. \end{aligned} \tag{3.67}$$

Consequently, $\delta\nu_\xi(t) = \dot{\xi}(t) + \operatorname{ad}_{\nu(t)} \xi(t)$. Lastly, the infinitesimal variation of $\nu_{c,\xi}$ is

$$\begin{aligned}\delta\nu_{c,\xi}(t) &\coloneqq \frac{d}{ds}\Big|_{s=0} \nu_{c,\xi}(t,s) \\ &= \frac{d}{ds}\Big|_{s=0} (I - s\operatorname{ad}_{\xi(t)} + \ldots)\nu_c(t) \\ &= -\operatorname{ad}_{\xi(t)} \nu_c(t), \end{aligned} \tag{3.68}$$

where we used the general fact that $\operatorname{Ad}_{\exp\widehat{\nu}} = \exp\operatorname{ad}_\nu$ for every $\nu \in \mathbb{R}^6$. Consequently, the infinitesimal variation of ν_r is $\delta\nu_{r,\xi}(t,s) \coloneqq \delta\nu_\xi(t) - \delta\nu_{c,\xi}(t) = \dot{\xi}(t) + \operatorname{ad}_{\nu_r(t)} \xi(t)$.

The Lagrange-d'Alembert principle states that the motion of the underwater vehicle, $g : [0,T] \to \mathrm{E}(3)$, should satisfy

$$\frac{d}{ds}\Big|_{s=0} \int_0^T L(g_\xi(t,s), \nu_{r,\xi}(t,s), a_c(t))\, dt + \int_0^T \langle f(t), \xi(t)\rangle\, dt = 0 \tag{3.69}$$

for every smooth curve $\xi : [0,T] \to \mathbb{R}^6$ such that $\xi(0) = \xi(T) = 0$. We focus on the left-hand side of (3.69). Due to the independence of t and s, the differentiation with respect to s can be moved inside the integral. It follows from the definition of the infinitesimal variations that

$$\begin{aligned}\frac{d}{ds}\Big|_{s=0} L(g_\xi(t,s), \nu_{r,\xi}(t,s), a_c(t)) &= \langle \mathrm{d}_1 L(g(t), \nu_r(t), a_c(t)), \xi(t)\rangle \\ &\quad + \langle \nabla_2 L(g(t), \nu_r(t), a_c(t)), \dot{\xi}(t) + \operatorname{ad}_{\nu_r(t)} \xi(t)\rangle. \end{aligned} \tag{3.70}$$

Let us now isolate the term containing $\dot{\xi}$. Utilizing integration by parts gives

$$\begin{aligned}\int_0^T \langle \nabla_2 L(g(t), \nu_r(t), a_c(t)), \dot{\xi}(t)\rangle\, dt &= \langle \nabla_2 L(g(t), \nu_r(t), a_c(t)), \xi(t)\rangle\Big|_{t=0}^{t=T} \\ &\quad - \int_0^T \langle \tfrac{d}{dt}[\nabla_2 L(g(t), \nu_r(t), a_c(t))], \xi(t)\rangle\, dt. \end{aligned} \tag{3.71}$$

Since $\xi(0) = \xi(T) = 0$ by assumption, the boundary term in (3.71) vanishes. Since (3.69) should hold for all smooth curves $\xi : [0,T] \to \mathbb{R}^6$ vanishing at the domain endpoints, the Lagrange d'Alembert principle is satisfied if and only if the curve g satisfies

$$\begin{aligned}\frac{d}{dt}\nabla_2 L(g(t), \nu_r(t), a_c(t)) - \operatorname{ad}^{\mathsf{T}}_{\nu_r(t)} \nabla_2 L(g(t), \nu_r(t), a_c(t)) \\ - \mathrm{d}_1 L(g(t), \nu_r(t), a_c(t)) = f(t) \end{aligned} \tag{3.72}$$

almost everywhere in $[0,T]$. Substituting the Lagrangian (3.61) into (3.72) and setting $f(t) \coloneqq d(\nu_r(t)) + \tau(t)$ yields (3.58). □

3.4 Dissipativity

We introduce in this section the notions of dissipative and monotonically dissipative damping models, and investigate some of their properties. We remark that all results remain valid if the damping model d maps from and to $\mathbb{R}^n$ instead of $\mathbb{R}^6$, that is, if $d : \mathbb{R}^n \to \mathbb{R}^n$.

3.4.1 Dissipative Damping Models

We say that a hydrodynamic damping model d is dissipative if the instantaneous work done by d is nonpositive at any velocity, and strictly dissipative if the instantaneous work done by d is negative at any nonzero velocity.

Definition 3.7. *A mapping $d : \mathbb{R}^6 \to \mathbb{R}^6$ is dissipative if it is continuous and*

$$\langle d(\nu), \nu \rangle \leq 0 \tag{3.73}$$

for every $\nu \in \mathbb{R}^6$. It is strictly dissipative if it is continuous and

$$\langle d(\nu), \nu \rangle < 0 \tag{3.74}$$

for every $\nu \in \mathbb{R}^6 \setminus \{0\}$.

Our definition of dissipativity is the same as [101, Definition 4.65]. Some works, e.g. [107, Definition 7.8.7], refer to dissipativity in the sense of Definition 3.7 as weak dissipativity, and strict dissipativity in the sense of Definition 3.7 as dissipativity. For linear damping models, the situation is particularly simple.

Example 3.8. Let $D \in \mathbb{R}^{6\times 6}$ and $d(\nu) \coloneqq -D\nu$. Then d is dissipative if and only if D is positive semidefinite, that is, if all eigenvalues of $D + D^\mathsf{T}$ are nonnegative. Furthermore, d is strictly dissipative if and only if D is positive definite, that is, if all eigenvalues of $D + D^\mathsf{T}$ are positive.

The following lemma demonstrates that a dissipative damping model always vanishes at the origin, and that its derivative at the origin is a negative semidefinite matrix.

Lemma 3.2. If $d : \mathbb{R}^6 \to \mathbb{R}^6$ is a dissipative mapping, then $d(0) = 0$. If d is also differentiable at the origin, then $\mathrm{D}d(0)$ is negative semidefinite.

Proof. Let $c \coloneqq d(0)$. Utilizing (3.73) and the Cauchy-Schwarz inequality,

$$\begin{aligned} 0 &\geq \langle d(\nu), \nu \rangle \\ &= \langle c, \nu \rangle + \langle d(\nu) - c, \nu \rangle \\ &\geq \langle c, \nu \rangle - |d(\nu) - c||\nu|. \end{aligned} \tag{3.75}$$

By continuity of d, for every $\varepsilon > 0$ there exists $\delta > 0$ such that

$$|\nu| \leq \delta \implies |d(\nu) - c| \leq \varepsilon. \tag{3.76}$$

Assume now that $c \neq 0$. We may then set $\varepsilon = |c|/2$ and $\nu = \delta\, c/|c|$. From (3.75), we find that

$$0 \geq \frac{\delta|c|}{2}, \tag{3.77}$$

which is a contradiction. Consequently, $c = 0$, and the first claim is proven. From (3.73), it now follows that

$$\frac{\langle d(s\nu) - d(0), \nu \rangle}{s} \leq 0, \tag{3.78}$$

for every $\nu \in \mathbb{R}^6$ and every $s > 0$. If d is continuously differentiable, then taking the limit $s \searrow 0$ gives

$$\langle \mathrm{D}d(0)\nu, \nu \rangle \leq 0, \tag{3.79}$$

which proves the second claim. □

3.4.2 Monotonically Dissipative Damping Models

We shall now investigate a stronger notion of dissipativity that is useful for stability analysis and design of feedback control laws for underwater vehicles. This dissipativity notion will be referred to as monotone dissipativity, and damping models with this property will be referred to as monotonically dissipative damping models. The idea of a monotonically dissipative damping model utilized in this chapter comes from the concept of a monotone mapping, that is, a mapping $f : \mathbb{R}^n \to \mathbb{R}^n$ that satisfies

$$\langle f(\nu) - f(\mu), \nu - \mu \rangle \geq 0, \tag{3.80}$$

for all $\nu, \mu \in \mathbb{R}^n$. This class of mappings has numerous applications in control theory, for instance global tracking control on matrix Lie groups [83], and nonlinear observer design [115, 116].

Definition 3.9. *A mapping $d : \mathbb{R}^6 \to \mathbb{R}^6$ is monotonically dissipative if it is continuous, $d(0) = 0$, and*

$$\langle d(\nu) - d(\mu), \nu - \mu \rangle \leq 0 \tag{3.81}$$

for all $\nu, \mu \in \mathbb{R}^6$. It is strictly monotonically dissipative if it is continuous, $d(0) = 0$, and

$$\langle d(\nu) - d(\mu), \nu - \mu \rangle < 0 \tag{3.82}$$

for all $\nu, \mu \in \mathbb{R}^6$ such that $\nu \neq \mu$. Given $K \in \mathbb{R}^{6\times 6}$, we say that d is (strictly) monotonically dissipative modulo K if the mapping $\nu \mapsto d(\nu) - K\nu$ is (strictly) monotonically dissipative.

The purpose of the requirement $d(0) = 0$ is to ensure that monotone dissipativity implies dissipativity. Indeed, the monotone dissipation inequalities (3.81) and (3.82) are completely independent of the value $d(0)$. It should be emphasized that monotone dissipativity modulo $K \in \mathbb{R}^{6\times 6}$ only depends on the symmetric part of K.

Evidently, (3.81) holding for all $\nu, \mu \in \mathbb{R}^6$ is equivalent to the mapping $\nu \mapsto -d(\nu)$ being monotone. Monotonicity of a differentiable mapping can be equivalently stated in terms of its derivative. In particular, [102, Proposition 12.3] establishes that f is monotone if and only if $\mathrm{D}f$ takes positive semidefinite values. The following proposition builds on this result and constitutes a tool to verify that a damping model satisfies one of the monotone dissipation inequalities (3.81) and (3.82) modulo $K \in \mathbb{R}^{6\times 6}$.

Proposition 3.10. *Let $K \in \mathbb{R}^{6\times 6}$. If $d : \mathbb{R}^6 \to \mathbb{R}^6$ is continuously differentiable, then*

$$\langle d(\nu) - d(\mu), \nu - \mu \rangle \leq \langle K(\nu - \mu), \nu - \mu \rangle \tag{3.83}$$

for all $\nu, \mu \in \mathbb{R}^6$ if and only if $\mathrm{D}d(\nu) - K$ is negative semidefinite for every $\nu \in \mathbb{R}^6$. Furthermore,

$$\langle d(\nu) - d(\mu), \nu - \mu \rangle < \langle K(\nu - \mu), \nu - \mu \rangle \tag{3.84}$$

for all $\nu, \mu \in \mathbb{R}^6$ such that $\nu \neq \mu$ if $\mathrm{D}d(\nu) - K$ is negative definite for every $\nu \in \mathbb{R}^6 \setminus S$, where $S \subset \mathbb{R}^6$ is a discrete set.

Proof. The first claim follows immediately by applying [102, Proposition 12.3] to the mapping $\varphi(\nu) \coloneqq -d(\nu) + K\nu$.

We now prove the claim related to the strict monotone dissipation inequality (3.84). Since the mapping $(\nu, \mu) \mapsto \langle \mathrm{D}\varphi(\nu)\mu, \mu \rangle$ is continuous on $\mathbb{R}^6 \times \mathbb{R}^6$, it follows that the set

$$\{(\nu, \mu) \in \mathbb{R}^6 \times \mathbb{R}^6 : \langle \mathrm{D}\varphi(\nu)\mu, \mu \rangle \geq 0\} \tag{3.85}$$

is closed. By assumption, it holds that $\langle \mathrm{D}\varphi(\nu)\mu, \mu \rangle > 0$ for all $(\nu, \mu) \in (\mathbb{R}^6 \setminus S) \times \mathbb{R}^6$. Consequently, $\langle \mathrm{D}\varphi(\nu)\mu, \mu \rangle \geq 0$ for all $(\nu, \mu) \in \overline{(\mathbb{R}^6 \setminus S) \times \mathbb{R}^6}$. Furthermore,

$$\begin{aligned} \overline{(\mathbb{R}^6 \setminus S) \times \mathbb{R}^6} &= \overline{\mathbb{R}^6 \setminus S} \times \mathbb{R}^6 \\ &= \mathbb{R}^6 \times \mathbb{R}^6, \end{aligned} \tag{3.86}$$

where the first equality follows from the fact that the closure of a Cartesian product is the product of the closures of the factors, and the last equality follows from the fact that S is discrete and therefore contains only isolated points. It follows that $\mathrm{D}\varphi(\nu)$ is positive semidefinite for every $\nu \in \mathbb{R}^6$. Now, fix $\nu, \mu \in \mathbb{R}^6$ such that $\nu \neq \mu$. Define $\xi : [0, 1] \to \mathbb{R}^6$ and $\zeta : [0, 1] \to \mathbb{R}$ by

$$\begin{aligned} \xi(s) &\coloneqq s\nu + (1 - s)\mu, \\ \zeta(s) &\coloneqq \langle \varphi(\xi(s)) - \varphi(\mu), \nu - \mu \rangle. \end{aligned} \tag{3.87}$$

Then, $\zeta(0) = 0$ and $\zeta(1) = \langle \varphi(\nu) - \varphi(\mu), \nu - \mu \rangle$. Furthermore, $\zeta'(s) = \langle \mathrm{D}\varphi(\xi(s))(\nu - \mu), \nu - \mu \rangle$. It then holds that

$$\begin{aligned} \zeta(1) &= \int_0^1 \zeta'(s)\, ds \\ &= \int_0^1 \langle \mathrm{D}\varphi(\xi(s))(\nu - \mu), \nu - \mu \rangle\, ds. \end{aligned} \tag{3.88}$$

To prove that $\zeta(1)$ is in fact strictly positive, we will show that there exists a compact subinterval $[s_1, s_2]$ of $[0,1]$, where $s_2 > s_1$, such that $\mathrm{D}\varphi(\xi(s))$ is positive definite for every $s \in [s_1, s_2]$. It then follows that

$$\begin{aligned}\zeta(1) &= \int_0^1 \zeta'(s)\,ds \\ &= \int_0^{s_1} \zeta'(s)\,ds + \int_{s_1}^{s_2} \zeta'(s)\,ds + \int_{s_2}^1 \zeta'(s)\,ds \\ &\geq \int_{s_1}^{s_2} \langle \mathrm{D}\varphi(\xi(s))(\nu-\mu), \nu-\mu\rangle\,ds > 0,\end{aligned} \tag{3.89}$$

where it was used that $\mathrm{D}\varphi(\xi(s))$ is positive semidefinite for every $s \in [0,1]$. It is seen that (3.89) is equivalent to (3.84) for the chosen ν, μ. To show that the interval $[s_1, s_2]$ exists, assume that $\langle \mathrm{D}\varphi(\xi(s_0))(\nu-\mu), \nu-\mu\rangle = 0$ for some $s_0 \in [0,1]$. This necessitates $\xi(s_0) \in S$, since $\mathrm{D}\varphi$ takes positive definite values everywhere else by assumption. Since S is discrete, there exists an open neighborhood U of $\xi(s_0)$ such that $U \cap S = \xi(s_0)$. It follows that $U \setminus \xi(s_0)$ is an open set on which $\mathrm{D}\varphi$ takes positive definite values. By continuity of ξ, it holds that $V \coloneqq \xi^{-1}(U \setminus \xi(s_0))$ is relatively open in $[0,1]$. Furthermore, since $\xi([0,1])$ is a line-segment that passes through $\xi(s_0)$ and U is open, there must be other points in $U \cap \xi([0,1])$ than $\xi(s_0)$. It follows that V is also nonempty. Since V is relatively open in $[0,1]$ and nonempty, it must contain a subinterval $[s_1, s_2]$ of $[0,1]$ such that $s_2 > s_1$. It follows that (3.84) holds for the chosen ν, μ. Since ν, μ are arbitrary except for $\nu \neq \mu$, it follows that (3.84) in fact holds for all $\nu, \mu \in \mathbb{R}^6$ such that $\nu \neq \mu$. □

We now treat as an example the diagonal modulus damping model, which has found ample applications in the literature. It is for instance used in [117] in a control design model for an autonomous underwater vehicle.

Example 3.11. Consider the diagonal modulus hydrodynamic damping model $d : \mathbb{R}^6 \to \mathbb{R}^6$ defined by

$$d(\nu) \coloneqq -\begin{pmatrix} \delta_1|\nu_1|\nu_1 \\ \vdots \\ \delta_6|\nu_6|\nu_6 \end{pmatrix}, \tag{3.90}$$

where $\delta_i \geq 0$ for every $i \in \{1, \ldots, 6\}$. The model (3.90) is precisely (3.41) with $D_i = \delta_i\, e_i \otimes e_i$. Certainly $d(0) = 0$, and

$$\mathrm{D}d(\nu) = -2\,\mathrm{diag}(\delta_1|\nu_1|, \ldots, \delta_6|\nu_6|) \tag{3.91}$$

is continuous and negative semidefinite for every $\nu \in \mathbb{R}^6$. Consequently, d is monotonically dissipative by Proposition 3.10. Furthermore, if every $\delta_i > 0$, then $\mathrm{D}d(\nu)$ is negative definite for every $\nu \in \mathbb{R}^6 \setminus \{0\}$. Since the set $\{0\}$ is discrete, it follows from Proposition 3.10 that d is strictly monotonically dissipative.

It turns out that d has strong monotone dissipativity properties that can not be readily concluded from Proposition 3.10. In particular, it holds that

$$\begin{aligned}\langle d(\nu) - d(\mu), \nu - \mu \rangle &\leq -\frac{1}{2}\sum_{i=1}^{6} \delta_i |\nu_i - \mu_i|^3 \\ &\leq -\frac{\min\{\delta_1, \ldots, \delta_6\}}{2\sqrt{6}} |\nu - \mu|^3.\end{aligned} \tag{3.92}$$

To show this, let $\nu_i \geq 0$ and $\mu_i \geq 0$. Then,

$$\begin{aligned}(|\nu_i|\nu_i - |\mu_i|\mu_i)(\nu_i - \mu_i) &= (\nu_i^2 - \mu_i^2)(\nu_i - \mu_i) \\ &= (\nu_i + \mu_i)(\nu_i - \mu_i)^2 \\ &\geq |\nu_i - \mu_i|^3.\end{aligned}$$

Equality holds if $\nu_i = \mu_i$, or if either $\nu_i = 0$ or $\mu_i = 0$. Let now $\nu_i \geq 0$ and $\mu_i \leq 0$. Then

$$\begin{aligned}(|\nu_i|\nu_i - |\mu_i|\mu_i)(\nu_i - \mu_i) &= (\nu_i^2 + \mu_i^2)(\nu_i - \mu_i) \\ &= \tfrac{1}{2}(\nu_i - \mu_i)^3 \\ &\quad + \tfrac{1}{2}(\nu_i + \mu_i)^2(\nu_i - \mu_i) \\ &\geq \tfrac{1}{2}|\nu_i - \mu_i|^3.\end{aligned}$$

Equality holds if $\nu_i = -\mu_i$. The remaining cases can be handled in the same manner as the two shown, and the first inequality in (3.92) is readily established. The second inequality in (3.92) can be shown by noting that $|\nu|_3^3 \geq |\nu|^3/\sqrt{6}$ for every $\nu \in \mathbb{R}^6$.

3.4.3 Rayleigh Dissipation Functions

Rayleigh dissipation functions are scalar functions that can be used to describe dissipative mappings. They are named after John William Strutt, 3rd Baron Rayleigh, who introduced them in 1871 [118]. Rayleigh only considered quadratic functions, which he used to encode linear damping in the Euler-Lagrange equations of motion. We here impose no such restriction, and base our definition on a more general form utilized for instance in [107, Definition 7.8.9].

Definition 3.12. *A Rayleigh dissipation function is a continuously differentiable function $D : \mathbb{R}^6 \to \mathbb{R}$ such that $-\nabla D$ is a dissipative mapping.*

We shall say that a dissipative mapping $d : \mathbb{R}^6 \to \mathbb{R}^6$ admits a Rayleigh dissipation function if there exists a function D such that $d = -\nabla D$. The following lemma shows how to compute the Rayleigh dissipation function from the dissipative mapping, if possible.

Lemma 3.3. If $d : \mathbb{R}^6 \to \mathbb{R}^6$ admits a Rayleigh dissipation function, then it is defined uniquely up to an additive constant by the expression

$$D(\nu) \coloneqq -\int_0^1 \langle d(s\nu), \nu \rangle \, ds. \tag{3.93}$$

Proof. Assume that E is a Rayleigh dissipation function for d. Then, from (3.93),

$$\begin{aligned} D(\nu) &= \int_0^1 \langle \nabla E(s\nu), \nu \rangle \, ds \\ &= \int_0^1 \frac{d}{ds} E(s\nu) \, ds \\ &= E(\nu) - E(0), \end{aligned} \tag{3.94}$$

is also a Rayleigh dissipation function for d. Moreover, D and E differ by a constant. □

If $d : \mathbb{R}^6 \to \mathbb{R}^6$ is a continuously differentiable dissipative mapping, then the existence of a Rayleigh dissipation function is equivalent to the symmetry of the derivative of d.

Proposition 3.13. *If d is continuously differentiable, then d admits a Rayleigh dissipation function if and only if $\mathrm{D}d(\nu)$ is symmetric for every $\nu \in \mathbb{R}^6$.*

Proof. If d is continuously differentiable, then the associated Rayleigh dissipation function must be twice continuously differentiable. Since second partial derivatives commute in this case, having $\mathrm{D}d(\nu)$ symmetric for each $\nu \in \mathbb{R}^6$ is necessary for the existence of the Rayleigh dissipation function. If d admits a Rayleigh dissipation function, then it is given uniquely up to an additive constant by (3.93). Differentiating this expression and integrating by parts gives

$$\begin{aligned} \nabla D(\nu) &= -\int_0^1 [\mathrm{D}d(s\nu)^\mathsf{T} s\nu + d(s\nu)] \, ds \\ &= \int_0^1 [\mathrm{D}d(s\nu) - \mathrm{D}d(s\nu)^\mathsf{T}] s\nu \, ds - \Big[s d(s\nu) \Big]_{s=0}^{s=1} \\ &= \int_0^1 [\mathrm{D}d(s\nu) - \mathrm{D}d(s\nu)^\mathsf{T}] s\nu \, ds - d(\nu), \end{aligned} \tag{3.95}$$

which shows that a symmetric-valued $\mathrm{D}d$ is also sufficient. □

It turns out that a Rayleigh dissipation function can be used to characterize monotone dissipativity of the associated mapping. The following result is based on [102, Theorem 2.14].

Proposition 3.14. *Let $K \in \mathbb{R}^{6\times 6}$. If $d : \mathbb{R}^6 \to \mathbb{R}^6$ admits the Rayleigh dissipation function D, then*

$$\langle d(\nu) - d(\mu), \nu - \mu \rangle \leq \langle K(\nu - \mu), \nu - \mu \rangle \tag{3.96}$$

for all $\nu, \mu \in \mathbb{R}^6$ if and only if

$$\begin{aligned} D(s\nu + (1-s)\mu) \leq{}& sD(\nu) + (1-s)D(\mu) \\ &+ \frac{s(1-s)}{2} \langle K(\nu - \mu), \nu - \mu \rangle \end{aligned} \tag{3.97}$$

for all $s \in [0,1]$ *and all* $\nu, \mu \in \mathbb{R}^6$. *Furthermore,*

$$\langle d(\nu) - d(\mu), \nu - \mu \rangle < \langle K(\nu - \mu), \nu - \mu \rangle \tag{3.98}$$

for all $\nu, \mu \in \mathbb{R}^6$ *if and only if*

$$\begin{aligned} D(s\nu + (1-s)\mu) < sD(\nu) + (1-s)D(\mu) \\ + \frac{s(1-s)}{2}\langle K(\nu - \mu), \nu - \mu \rangle \end{aligned} \tag{3.99}$$

for all $s \in (0,1)$ *and all* $\nu, \mu \in \mathbb{R}^6$ *such that* $\nu \neq \mu$.

Proof. Let $A \coloneqq \frac{1}{2}(K + K^\mathsf{T})$ and $\varphi(\nu) \coloneqq -d(\nu) + A\nu$. Then, (3.96) is equivalent to φ being a monotone mapping. Moreover, $\varphi = \nabla \Phi$, where $\Phi(\nu) \coloneqq D(\nu) + \frac{1}{2}\langle A\nu, \nu \rangle$. It follows from [102, Theorem 2.14] that φ is monotone if and only if Φ is convex, that is,

$$\Phi(s\nu + (1-s)\mu) \leq s\Phi(\nu) + (1-s)\Phi(\mu) \tag{3.100}$$

for all $s \in [0,1]$ and all $\nu, \mu \in \mathbb{R}^6$. Substituting Φ into (3.100) and noting that $\langle A\nu, \nu \rangle = \langle K\nu, \nu \rangle$ for all $\nu \in \mathbb{R}^6$ gives the desired expression (3.97). The strict case is similar. □

In the case where $K = 0$, the condition (3.97) holding for all $s \in [0,1]$ and all $\nu, \mu \in \mathbb{R}^6$, characterizes D as convex. Similarly, the condition (3.99) holding for all $s \in (0,1)$ and all $\nu, \mu \in \mathbb{R}^6$ such that $\nu \neq \mu$, characterizes D as strictly convex. Consequently, if $D : \mathbb{R}^6 \to \mathbb{R}$ is a continuously differentiable (strictly) convex function such that the origin is a minimum of D, then $-\nabla D$ is a (strictly) monotonically dissipative mapping. Conversely, if d is a (strictly) monotonically dissipative mapping that admits a Rayleigh dissipation function, then this Rayleigh dissipation function is (strictly) convex and the origin is a minimum.

Example 3.15. Consider again the diagonal modulus damping model defined by (3.90). We have that $\mathrm{D}d$ is continuous and symmetric-valued, and therefore by Proposition 3.13 that d admits a Rayleigh dissipation function. In this case, we find that

$$D(\nu) \coloneqq \sum_{i=1}^{6} \int_0^1 s^2 \delta_i |\nu_i|^3 \, ds = \frac{1}{3} \sum_{i=1}^{6} \delta_i |\nu_i|^3. \tag{3.101}$$

If $\delta_i \geq 0$ for $i \in \{1, 2, \ldots, 6\}$, then D is convex and the origin is a minimum of D. Furthermore, if If $\delta_i > 0$ for $i \in \{1, 2, \ldots, 6\}$, then D is strictly convex and the origin is a global minimum of D

3.5 Hydrodynamic Symmetry Principle

This section will cover simplifications of the hydrodynamic inertia matrix M_H and the damping wrench d by exploiting symmetries of the underwater vehicle. A symmetry should in this context be understood as a change of vehicle frame that leaves the vehicle looking identical. In particular, given a change of vehicle frame $h \in \mathrm{E}(3)$, we denote the set of coordinates of the points comprising the vehicle in the new frame by $\mathcal{R}^* \subset \mathbb{R}^3$. The relationship between $\mathcal{R}$ and $\mathcal{R}^*$ is then $\mathcal{R} = h \cdot \mathcal{R}^*$. By a symmetry of $\mathcal{R}$, we mean a change of frame h such that $\mathcal{R} = \mathcal{R}^*$, that is, such that $\mathcal{R} = h \cdot \mathcal{R}$.

Definition 3.16. *A rigid transformation $h \in \mathrm{E}(3)$ is a symmetry of the vehicle if $\mathcal{R} = h \cdot \mathcal{R}$.*

An equivalent definition provided that $\mathcal{R}$ is compact is the following: A rigid transformation $h \subset \mathrm{E}(3)$ is a symmetry of $\mathcal{R}$ if $r \in \mathcal{R}$ implies $h \cdot r \in \mathcal{R}$. It is readily seen that the set of symmetries of $\mathcal{R}$, denoted $\mathcal{H}$, is a matrix group. In particular,

1. if $\mathcal{R} = h \cdot \mathcal{R}$, then $\mathcal{R} = h^{-1} \cdot \mathcal{R}$, and
2. if $\mathcal{R} = h_1 \cdot \mathcal{R}$ and $\mathcal{R} = h_2 \cdot \mathcal{R}$, then $\mathcal{R} = (h_1 h_2) \cdot \mathcal{R}$.

We refer to $\mathcal{H}$ as the symmetry group of $\mathcal{R}$. It can furthermore be shown that $\mathcal{H}$ is closed in $\mathbb{R}^{4\times 4}$, and consequently relatively closed in $\mathrm{GL}(4)$. It then follows by the closed subgroup theorem that $\mathcal{H}$ is a matrix Lie group.

Lemma 3.4. If $\mathcal{H} \subset \mathrm{E}(3)$ is the symmetry group of $\mathcal{R}$, then $\mathcal{H}$ is closed.

Proof. Let $h = (b, S) \in \overline{\mathcal{H}}$. Then there exists a sequence $h_k \in \mathcal{H}$ converging to h. Furthermore, for every $r \in \mathcal{R}$, the sequence $x_k = h_k \cdot r$ converges to $x = h \cdot r$. This can be seen by writing

$$\begin{aligned} |x - x_k| &= |b - b_k + (S - S_k)r| \\ &\leq |b - b_k| + |S - S_k||r| \\ &\leq (1 + |r|)\|h - h_k\|. \end{aligned} \tag{3.102}$$

Since $x_k \in \mathcal{R}$ is a convergent sequence and $\mathcal{R}$ is closed, it follows that $x \in \mathcal{R}$. Consequently, $r \in \mathcal{R}$ implies $h \cdot r \in \mathcal{R}$. By definition, $h \in \mathcal{H}$. Since h is arbitrary, it follows that $\mathcal{H} = \overline{\mathcal{H}}$. □

It is easy to show that the vehicle center of volume is invariant under a symmetry transformation.

Lemma 3.5. If h is a symmetry of $\mathcal{R}$, then $h \cdot r_\upsilon = r_\upsilon$.

Proof. We have that

$$h \cdot r_\upsilon = \frac{1}{\upsilon} \int_{\mathcal{R}} h \cdot r \, d^3 r = \frac{1}{\upsilon} \int_{h \cdot \mathcal{R}} z \, d^3 z = \frac{1}{\upsilon} \int_{\mathcal{R}} z \, d^3 z = r_\upsilon,$$

where we used the substitution $z = h \cdot r$ and the fact that $h \cdot \mathcal{R} = \mathcal{R}$. □

Consequently, if the vehicle frame is chosen such that its origin lies in the center of volume, then all vehicle symmetries must be pure rotations. This is seen as follows: If $h = (b, S)$ is a symmetry, then $S r_\upsilon + b = r_\upsilon$ by Lemma 3.5. If the frame origin is in the center of volume, then $r_\upsilon = 0$, and hence $b = 0$. Consequently, $h = (0, S)$. For this reason, we only consider pure rotations in the examples presented later. It should nonetheless be remarked that the existence of symmetries does not depend on the particular vehicle frame chosen.

3.5.1 Hydrodynamic Inertia Symmetry

Every vehicle inertia matrix M transforms as $M^* = \mathrm{Ad}_h^{\mathsf{T}} M \mathrm{Ad}_h$ under a change of vehicle frame h. Since the hydrodynamic inertia matrix M_H depends solely on the shape of the vehicle and the fluid density, it is reasonable to assume that if $\mathcal{R} = \mathcal{R}^*$, then $M_H = M_H^* = \mathrm{Ad}_h^{\mathsf{T}} M_H \mathrm{Ad}_h$. Roughly speaking, we are claiming that a change of frame that leaves the vehicle looking the same should leave the hydrodynamic inertia matrix unchanged. This consideration forms the basis of hydrodynamic inertia symmetry.

Symmetry Principle for Hydrodynamic Inertia. If h is a symmetry of $\mathcal{R}$, then $M_H = \mathrm{Ad}_h^{\mathsf{T}} M_H \mathrm{Ad}_h$.

To prove this result under Assumption 3.3, we must first establish a symmetry property of the unit outward normal n of $\mathcal{R}$.

Lemma 3.6. If $h = (b, S) \in \mathrm{E}(3)$ is a symmetry of $\mathcal{R}$, then $Sn(r) = n(h \cdot r)$ for every $r \in \partial\mathcal{R}$.

Proof. Let (U, ψ) be a local chart for $\mathcal{R}$ such that

$$n(r) = -\frac{\nabla\psi_3(r)}{|\nabla\psi_3(r)|} \tag{3.103}$$

for all $r \in U \cap \partial\mathcal{R}$. It then follows that $(h \cdot U, \beta)$, where $\beta(r) \coloneqq \psi(h^{-1} \cdot r)$ for all $r \in h \cdot U$, is a local chart for $h \cdot \mathcal{R} = \mathcal{R}$. Furthermore, since h is a diffeomorphism and a symmetry of $\mathcal{R}$, it follows that $h \cdot (U \cap \partial\mathcal{R}) = (h \cdot U) \cap \partial(h \cdot \mathcal{R}) = (h \cdot U) \cap \partial\mathcal{R}$.

Now,

$$n(r) = -\frac{\nabla\beta_3(r)}{|\nabla\beta_3(r)|} \tag{3.104}$$

for all $r \in (h \cdot U) \cap \partial\mathcal{R}$. Since $\psi(r) = \beta(h \cdot r)$ for all $r \in U \cap \mathcal{R}$, we find from the chain rule that

$$\nabla\psi_3(r) = S^{\mathsf{T}} \nabla\beta_3(h \cdot r) \tag{3.105}$$

for all $r \in U \cap \mathcal{R}$, which in light of the expressions (3.103) and (3.104) gives the desired result. □

An illustration of Lemma 3.6 is presented in Figure 3.2. We are now ready to proceed with the main result of this section.

Theorem 3.17. *If h is a symmetry of $\mathcal{R}$, then the classical Kirchhoff potential for $\mathcal{R}$ satisfies $\varphi(r) = \mathrm{Ad}_h^{\mathsf{T}} \varphi(h \cdot r)$ for every $r \in \overline{\mathbb{R}^3 \setminus \mathcal{R}}$.*

Proof. The result is proven by showing that the transformed Kirchhoff potential $\varphi^*(r) \coloneqq \mathrm{Ad}_h^{\mathsf{T}} \varphi(h \cdot r)$ is also a classical Kirchhoff potential for $\mathcal{R}$ as per Definition 3.4. The desired result then follows from the uniqueness of the potential.

Since the domain of φ is $\overline{\mathbb{R}^3 \setminus \mathcal{R}}$, it follows that the domain of φ^* must be $h^{-1} \cdot \left(\overline{\mathbb{R}^3 \setminus \mathcal{R}}\right)$. Since $h \cdot \, : \mathbb{R}^3 \to \mathbb{R}^3$ is a diffeomorphism, it holds that $h^{-1} \cdot \left(\overline{\mathbb{R}^3 \setminus \mathcal{R}}\right) = \overline{(h^{-1} \cdot \mathbb{R}^3) \setminus (h^{-1} \cdot \mathcal{R})}$. We have that $h^{-1} \cdot \mathbb{R}^3 = \mathbb{R}^3$, and, since h is a symmetry of

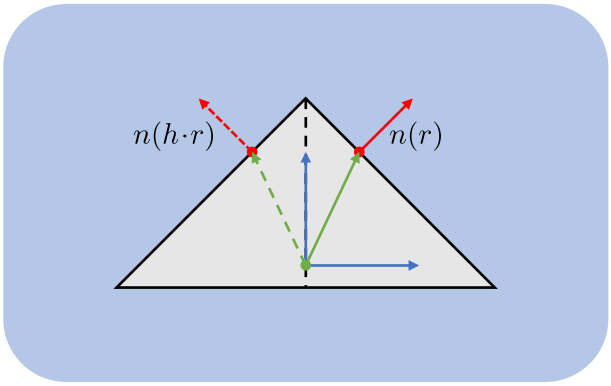

Figure 3.2: Reflection of the normal vector n for a triangle.

$\mathcal{R}$, that $h^{-1}\cdot\mathcal{R}=\mathcal{R}$. Consequently, the domain of φ^* is $\overline{\mathbb{R}^3\setminus\mathcal{R}}$. Furthermore, φ^* is seen to be continuously differentiable on $\overline{\mathbb{R}^3\setminus\mathcal{R}}$. Since rigid transformations preserve harmonic functions (see [108, Lemma 2.1.2]) and linear combinations of harmonic functions are harmonic functions, each component of φ^* is harmonic on $h^{-1}\cdot(\mathbb{R}^3\setminus\mathcal{R})=(h^{-1}\cdot\mathbb{R}^3)\setminus(h^{-1}\cdot\mathcal{R})=\mathbb{R}^3\setminus\mathcal{R}$. Consequently, φ^* satisfies item 1 in Definition 3.4.

Let $h=(b,S)$. Utilizing the chain rule, Lemma 3.6, and the boundary condition satisfied by φ, we find

$$\begin{aligned}\mathrm{D}\varphi^*(r)n(r)&=\mathrm{Ad}_h^{\mathsf{T}}\,\mathrm{D}\varphi(h\cdot r)Sn(r)\\&=\mathrm{Ad}_h^{\mathsf{T}}\,\mathrm{D}\varphi(h\cdot r)n(h\cdot r)\\&=\mathrm{Ad}_h^{\mathsf{T}}\begin{pmatrix}n(h\cdot r)\\(h\cdot r)\times n(h\cdot r)\end{pmatrix}.\end{aligned}\tag{3.106}$$

Continuing, it follows from Lemma 3.6 and properties of the cross product that the matrix appearing in the last line of (3.106) can be rewritten as

$$\begin{aligned}\begin{pmatrix}n(h\cdot r)\\(h\cdot r)\times n(h\cdot r)\end{pmatrix}&=\begin{pmatrix}Sn(r)\\(b+Sr)\times(Sn(r))\end{pmatrix}\\&=\begin{pmatrix}Sn(r)\\b^{\times}Sn(r)+\det(S)S(r\times n(r))\end{pmatrix}\\&=\begin{pmatrix}S&0\\b^{\times}S&\det(S)S\end{pmatrix}\begin{pmatrix}n(r)\\r\times n(r)\end{pmatrix}\\&=\mathrm{Ad}_h^{-\mathsf{T}}\begin{pmatrix}n(r)\\r\times n(r)\end{pmatrix}.\end{aligned}\tag{3.107}$$

In light of (3.106), it follows from (3.107) that φ^* satisfies the same Neumann boundary condition as φ. Consequently, φ^* satisfies item 2 in Definition 3.4.

Lastly, $|\varphi^*(r)|\leq|\mathrm{Ad}_h||\varphi(h\cdot r)|$, and $|h\cdot r|_{\mathcal{R}}\leq|r|_{\mathcal{R}}+|b|_{\mathcal{R}}$. Since $|r|_{\mathcal{R}}\to\infty$ therefore implies $|h\cdot r|_{\mathcal{R}}\to\infty$, and since $|\varphi(r)|\to 0$ as $|r|_{\mathcal{R}}\to\infty$, it follows that $|\varphi^*(r)|\to 0$ as $|r|_{\mathcal{R}}\to\infty$. Consequently, φ^* satisfies item 3 in Definition 3.4. It follows that φ^* is a classical Kirchhoff potential for $\mathcal{R}$. Since this potential is unique, it must hold that $\varphi^*=\varphi$. □

With Theorem 3.17 in place, it is straightforward to show the symmetry principle for hydrodynamic inertia.

Corollary 3.18. *If h is a symmetry of $\mathcal{R}$, then $M_H = \mathrm{Ad}_h^{\mathsf{T}} M_H \mathrm{Ad}_h$.*

Proof. Let $h = (b, S)$. It follows from Theorem 3.17 and the chain rule that

$$\mathrm{D}\varphi(r) = \mathrm{Ad}_h^{\mathsf{T}} \mathrm{D}\varphi(h \cdot r) S \tag{3.108}$$

for every $r \in \overline{\mathbb{R}^3 \setminus \mathcal{R}}$. Utilizing the definition of the hydrodynamic inertia matrix (3.35) and the relationship (3.108), we find

$$\begin{aligned} M_H &= \int_{r \in \mathbb{R}^3 \setminus \mathcal{R}} \mathrm{D}\varphi(r)\, \mathrm{D}\varphi(r)^{\mathsf{T}}\, \varrho d^3 r \\ &= \int_{r \in \mathbb{R}^3 \setminus \mathcal{R}} \mathrm{Ad}_h^{\mathsf{T}}\, \mathrm{D}\varphi(h \cdot r)\, \mathrm{D}\varphi(h \cdot r)^{\mathsf{T}}\, \mathrm{Ad}_h\ \varrho d^3 r. \end{aligned} \tag{3.109}$$

We then perform the substitution $z = h \cdot r$ and utilize the fact that $h \cdot (\mathbb{R}^3 \setminus \mathcal{R}) = (h \cdot \mathbb{R}^3) \setminus (h \cdot \mathcal{R}) = \mathbb{R}^3 \setminus \mathcal{R}$. This gives

$$\begin{aligned} M_H &= \int_{z \in h \cdot (\mathbb{R}^3 \setminus \mathcal{R})} \mathrm{Ad}_h^{\mathsf{T}}\, \mathrm{D}\varphi(z)\, \mathrm{D}\varphi(z)^{\mathsf{T}}\, \mathrm{Ad}_h\ \varrho d^3 z \\ &= \int_{z \in \mathbb{R}^3 \setminus \mathcal{R}} \mathrm{Ad}_h^{\mathsf{T}}\, \mathrm{D}\varphi(z)\, \mathrm{D}\varphi(z)^{\mathsf{T}}\, \mathrm{Ad}_h\ \varrho d^3 z \\ &= \mathrm{Ad}_h^{\mathsf{T}}\, M_H\, \mathrm{Ad}_h\,. \end{aligned} \tag{3.110}$$

□

It is important to note that if a vehicle $\mathcal{R}$ has symmetry group $\mathcal{H}$, then it is not necessary to check that M_H satisfies the symmetry principle for every element in $\mathcal{H}$. It suffices to check a subset of $\mathcal{H}$ called a generating set. A generating set for $\mathcal{H}$ is a set $S \subset \mathcal{H}$ such that every element in $\mathcal{H}$ can be written as a composition of finitely many elements in S and inverses of elements in S. To see why this is possible, let $h \in \mathcal{H}$, and suppose that $M_H = \mathrm{Ad}_h^{\mathsf{T}} M_H \mathrm{Ad}_h$. Since generally $\mathrm{Ad}_h^{-1} = \mathrm{Ad}_{h^{-1}}$, it follows that $M_H = \mathrm{Ad}_{h^{-1}}^{\mathsf{T}} M_H \mathrm{Ad}_{h^{-1}}$, such that M_H automatically has the required invariance with respect to h^{-1}. Similarly, if $h_1, h_2 \in \mathcal{H}$, and also $M_H = \mathrm{Ad}_{h_1}^{\mathsf{T}} M_H \mathrm{Ad}_{h_1}$ and $M_H = \mathrm{Ad}_{h_2}^{\mathsf{T}} M_H \mathrm{Ad}_{h_2}$, then it follows that $M_H = \mathrm{Ad}_{h_2}^{\mathsf{T}} \mathrm{Ad}_{h_1}^{\mathsf{T}} M_H \mathrm{Ad}_{h_1} \mathrm{Ad}_{h_2}$. Since generally $\mathrm{Ad}_{h_1} \mathrm{Ad}_{h_2} = \mathrm{Ad}_{h_1 h_2}$, it follows that $M_H = \mathrm{Ad}_{h_1 h_2}^{\mathsf{T}} M_H \mathrm{Ad}_{h_1 h_2}$. Consequently, M_H automatically has the required invariance with respect to the product $h_1 h_2$.

We finally remark that symmetry considerations for the added inertia matrix are similar to those for linear damping models, which are covered in Example 3.19.

3.5.2 Hydrodynamic Damping Symmetry

This section introduces a symmetry principle for the hydrodynamic damping wrench. While the main idea behind this symmetry principle and the symmetry principle for hydrodynamic inertia is precisely the same, it is not possible to formulate any formal proof for damping symmetry. This is because the hydrodynamic damping wrench is not based on mathematical hydrodynamics, and there really is no underlying theory from which its properties can be derived. Nonetheless, we argue that the symmetry

principle is reasonable in the context of memoryless hydrodynamic damping models. In particular, the principle states that a change of vehicle frame that leaves the vehicle looking the same, should leave the damping wrench unchanged. We recall from (3.23) that the vehicle velocity and vehicle wrench transform as $\nu^* = \mathrm{Ad}_h^{-1}\,\nu$ and $f^* = \mathrm{Ad}_h^{\mathsf{T}}\,f$, respectively, under a change of vehicle frame h. The damping wrench therefore transforms such that $d^*(\mathrm{Ad}_h^{-1}\,\nu) = \mathrm{Ad}_h^{\mathsf{T}}\,d(\nu)$ for every $\nu \in \mathbb{R}^6$, or equivalently, $d^*(\nu^*) \coloneqq \mathrm{Ad}_h^{\mathsf{T}}\,d(\mathrm{Ad}_h\,\nu^*)$. The symmetry principle for hydrodynamic damping now states that if $\mathcal{R} = \mathcal{R}^*$, then $d(\nu) = d^*(\nu)$ for every $\nu \in \mathbb{R}^6$. Consequently, if $\mathcal{R} = \mathcal{R}^*$, then $d(\nu) = \mathrm{Ad}_h^{\mathsf{T}}\,d(\mathrm{Ad}_h\,\nu)$ for every $\nu \in \mathbb{R}^6$.

Symmetry Principle for Hydrodynamic Damping. If h is a symmetry of $\mathcal{R}$, then $d(\nu) = \mathrm{Ad}_h^{\mathsf{T}}\,d(\mathrm{Ad}_h\,\nu)$ for every $\nu \in \mathbb{R}^6$.

It should be remarked that it also here is not necessary to consider symmetry with respect to all elements of the symmetry group $\mathcal{H}$ of $\mathcal{R}$. A generating set for $\mathcal{H}$ suffices. We now illustrate the simplification of linear damping models by symmetry. These results are also applicable to symmetry considerations for hydrodynamic inertia.

Example 3.19. Linear damping models take the general form $d(\nu) \coloneqq -D\nu$, where $D \in \mathbb{R}^{6\times 6}$. The symmetry principle for hydrodynamic damping then dictates that if h is a symmetry of $\mathcal{R}$, then $D = \mathrm{Ad}_h^{\mathsf{T}}\,D\,\mathrm{Ad}_h$. We recall from Lemma 3.5 that we without loss of generality can assume that h is a pure rotation. We therefore only consider symmetries of the form $h = (0, S)$, where $S \in \mathrm{O}(3)$, in which case

$$\mathrm{Ad}_h \coloneqq \mathrm{blkdiag}(S, (\det S)S). \tag{3.111}$$

If we partition D as

$$D = \begin{pmatrix} D_1 & D_3 \\ D_2 & D_4 \end{pmatrix}, \tag{3.112}$$

where $D_i \in \mathbb{R}^{3\times 3}$ for $i \in \{1, \ldots, 4\}$, then the symmetry principle for linear damping requires that

$$\begin{aligned} D_i &= S^{\mathsf{T}} D_i S && \text{if } i \in \{1, 4\}, \\ D_i &= (\det S) S^{\mathsf{T}} D_i S && \text{if } i \in \{2, 3\}. \end{aligned} \tag{3.113}$$

Let us compute how the damping matrix D can be simplified if we demand invariance with respect to a reflection through the 2-3-plane. This is done by considering (3.113) with $S = \mathrm{diag}(-1, 1, 1)$. Straightforward computations yield

$$S^{\mathsf{T}} D_i S = \begin{pmatrix} D_{i,11} & -D_{i,12} & -D_{i,13} \\ -D_{i,21} & D_{i,22} & D_{i,23} \\ -D_{i,31} & D_{i,32} & D_{i,33} \end{pmatrix}, \tag{3.114}$$

and, since $\det S = -1$, (3.113) gives

$$D = \begin{pmatrix} D_{11} & 0 & 0 & 0 & D_{15} & D_{16} \\ 0 & D_{22} & D_{23} & D_{24} & 0 & 0 \\ 0 & D_{32} & D_{33} & D_{34} & 0 & 0 \\ 0 & D_{42} & D_{43} & D_{44} & 0 & 0 \\ D_{51} & 0 & 0 & 0 & D_{55} & D_{56} \\ D_{61} & 0 & 0 & 0 & D_{65} & D_{66} \end{pmatrix}. \tag{3.115}$$

If $\mathcal{R}$ describes an underwater vehicle with vehicle frame chosen such that the 1-axis points from aft to fore, the 2-axis from port to starboard, and the 3-axis from top to bottom of the vehicle, as is convention, then this particular symmetry is referred to as *fore-aft symmetry*. Similar computations then yield for $S = \operatorname{diag}(1, -1, 1)$ (*starboard-port symmetry*),

$$D = \begin{pmatrix} D_{11} & 0 & D_{13} & 0 & D_{15} & 0 \\ 0 & D_{22} & 0 & D_{24} & 0 & D_{26} \\ D_{31} & 0 & D_{33} & 0 & D_{35} & 0 \\ 0 & D_{42} & 0 & D_{44} & 0 & D_{46} \\ D_{51} & 0 & D_{53} & 0 & D_{55} & 0 \\ 0 & D_{62} & 0 & D_{64} & 0 & D_{66} \end{pmatrix}, \tag{3.116}$$

and for $S = \operatorname{diag}(1, 1 - 1)$ (*bottom-top symmetry*),

$$D = \begin{pmatrix} D_{11} & D_{12} & 0 & 0 & 0 & D_{16} \\ D_{21} & D_{22} & 0 & 0 & 0 & D_{26} \\ 0 & 0 & D_{33} & D_{34} & D_{35} & 0 \\ 0 & 0 & D_{43} & D_{44} & D_{36} & 0 \\ 0 & 0 & D_{53} & D_{54} & D_{55} & 0 \\ D_{61} & D_{62} & 0 & 0 & 0 & D_{66} \end{pmatrix}. \tag{3.117}$$

For a vehicle with a rectangular cross-section, we combine port-starboard and bottom-top symmetries. This gives

$$D = \begin{pmatrix} D_{11} & 0 & 0 & 0 & 0 & 0 \\ 0 & D_{22} & 0 & 0 & 0 & D_{26} \\ 0 & 0 & D_{33} & 0 & D_{35} & 0 \\ 0 & 0 & 0 & D_{44} & 0 & 0 \\ 0 & 0 & D_{53} & 0 & D_{55} & 0 \\ 0 & D_{62} & 0 & 0 & 0 & D_{66} \end{pmatrix}. \tag{3.118}$$

Let us consider a vehicle with a square cross section. We take our first symmetry to be a 90°-rotation around the 1-axis,

$$S_1 \coloneqq \begin{pmatrix} 1 & 0 & 0 \\ 0 & 0 & -1 \\ 0 & 1 & 0 \end{pmatrix}. \tag{3.119}$$

Straightforward computations yield

$$S_1^{\mathsf{T}} D_i S_1 = \begin{pmatrix} D_{i,11} & D_{i,13} & -D_{i,12} \\ D_{i,31} & D_{i,33} & -D_{i,32} \\ -D_{i,21} & -D_{i,23} & D_{i,22} \end{pmatrix}. \tag{3.120}$$

Since $\det S_1 = 1$, the relations (3.113) state that $D_{i,12} = D_{i,13}$, $D_{i,13} = -D_{i,12}$, $D_{i,21} = D_{i,31}$, $D_{i,31} = -D_{i,21}$, $D_{i,32} = -D_{i,23}$, and $D_{i,22} = D_{i,33}$. Evidently, this requires $D_{i,12} = D_{i,13} = D_{i,21} = D_{i,31} = 0$. Consequently, the damping matrix taking

into account the symmetry S_1 has the form

$$D = \begin{pmatrix} D_{11} & 0 & 0 & D_{14} & 0 & 0 \\ 0 & D_{22} & D_{23} & 0 & D_{25} & D_{26} \\ 0 & -D_{23} & D_{22} & 0 & -D_{26} & D_{25} \\ D_{41} & 0 & 0 & D_{44} & 0 & 0 \\ 0 & D_{52} & D_{53} & 0 & D_{55} & D_{56} \\ 0 & -D_{53} & D_{52} & 0 & -D_{56} & D_{55} \end{pmatrix} \tag{3.121}$$

As our second symmetry, we take a reflection through the 1-3-plane, that is, $S_2 = \operatorname{diag}(1, -1, 1)$. The simplifications are in this case already stated in (3.116). The damping matrix taking into account both symmetries S_1 and S_2 is therefore

$$D = \begin{pmatrix} D_{11} & 0 & 0 & 0 & 0 & 0 \\ 0 & D_{22} & 0 & 0 & 0 & D_{26} \\ 0 & 0 & D_{22} & 0 & -D_{26} & 0 \\ 0 & 0 & 0 & D_{44} & 0 & 0 \\ 0 & 0 & D_{53} & 0 & D_{55} & 0 \\ 0 & -D_{53} & 0 & 0 & 0 & D_{55} \end{pmatrix}. \tag{3.122}$$

If the vehicle has a square cross section, then it also has bottom-top symmetry. However, it is seen from (3.117) that taking $S_3 = \operatorname{diag}(1, 1, -1)$ yields no further simplifications of D in (3.122). This is because S_3 can be stated in terms of S_1 and S_2. In particular, $S_3 = S_1 S_1 S_2$.

We will now apply the symmetry principle to a class of nonlinear hydrodynamic damping models of the form

$$d(\nu) \coloneqq -\sum_{i=1}^{k} \sigma_i(\nu) D_i \nu, \tag{3.123}$$

where $\sigma : \mathbb{R}^6 \to \mathbb{R}^k$ is a continuous mapping and $D_i \in \mathbb{R}^{6\times 6}$ is a constant matrix of coefficients for every $i \in \{1, \dots k\}$. The second-order modulus damping model (3.41) is seen to be a special case of (3.123) with $k = 6$ and σ chosen as the entrywise absolute value. These models admit a representation in terms of a nonlinear damping matrix $D : \mathbb{R}^6 \to \mathbb{R}^{6\times 6}$,

$$D(\nu) = \sum_{i=1}^{k} \sigma_i(\nu) D_i, \tag{3.124}$$

such that $d(\nu) = -D(\nu)\nu$. Of course, there exist other choices for D than (3.124) that result in the damping wrench (3.123). The following theorem establishes symmetry for the class of models (3.123) under the assumption that σ is invariant under the symmetry.

Theorem 3.20. *Let h be a symmetry of $\mathcal{R}$ and d be defined by (3.123). If $\sigma(\nu) = \sigma(\operatorname{Ad}_h \nu)$ for every $\nu \in \mathbb{R}^6$, then d satisfies the symmetry principle for hydrodynamic damping if and only if $\langle A_j \nu, \sigma(\nu)\rangle = 0$ for every $\nu \in \mathbb{R}^6$ and every $j \in \{1, \dots, 6\}$,*

where

$$A_j \coloneqq \begin{pmatrix} e_j^\mathsf{T}(D_1 - \operatorname{Ad}_h^\mathsf{T} D_1 \operatorname{Ad}_h) \\ \vdots \\ e_j^\mathsf{T}(D_k - \operatorname{Ad}_h^\mathsf{T} D_k \operatorname{Ad}_h) \end{pmatrix}. \tag{3.125}$$

Proof. The symmetry principle demands that $d(\nu) = \operatorname{Ad}_h^\mathsf{T} d(\operatorname{Ad}_h \nu)$ for every $\nu \in \mathbb{R}^6$. Due to the invariance of σ, we find that

$$\begin{aligned} \delta(\nu) &\coloneqq d(\nu) - \operatorname{Ad}_h^\mathsf{T} d(\operatorname{Ad}_h \nu) \\ &= \sum_{i=1}^{k} \sigma_i(\nu)(D_i - \operatorname{Ad}_h^\mathsf{T} D_i \operatorname{Ad}_h)\nu. \end{aligned} \tag{3.126}$$

Denoting by δ_j the jth component of δ, we find that

$$\begin{aligned} \delta_j(\nu) &= \sum_{i=1}^{k} \sigma_i(\nu)\langle e_j, (D_i - \operatorname{Ad}_h^\mathsf{T} D_i \operatorname{Ad}_h)\nu\rangle \\ &= \langle A_j\nu, \sigma(\nu)\rangle. \end{aligned} \tag{3.127}$$

Consequently, damping symmetry holds if and only if $\langle A_j\nu, \sigma(\nu)\rangle = 0$ for every $\nu \in \mathbb{R}^6$ and every $j \in \{1, \dots, 6\}$. □

It follows from Theorem 3.20 that a sufficient condition for the damping model (3.123) to satisfy the symmetry principle with respect to a symmetry h of $\mathcal{R}$ is that $D_i = \operatorname{Ad}_h^\mathsf{T} D_i \operatorname{Ad}_h$ for every $i \in \{1, \dots, k\}$. If σ satisfies a certain independence property, then this condition is also necessary.

Corollary 3.21. *Let the conditions of Theorem 3.20 hold and let $A \in \mathbb{R}^{k\times 6}$. If $\langle A\nu, \sigma(\nu)\rangle = 0$ for every $\nu \in \mathbb{R}^6$ implies that $A = 0$, then (3.123) satisfies the symmetry principle if and only if $D_i = \operatorname{Ad}_h^\mathsf{T} D_i \operatorname{Ad}_h$ for every $i \in \{1, \dots, k\}$.*

Proof. The independence property of σ ensures that the requirement $\langle A_j\nu, \sigma(\nu)\rangle = 0$ for every $\nu \in \mathbb{R}^6$ and every $j \in \{1, \dots, 6\}$ presented in Theorem 3.20 is satisfied only if every $A_j = 0$. In light of (3.125), this is true only if $D_i = \operatorname{Ad}_h^\mathsf{T} D_i \operatorname{Ad}_h$ for every $i \in \{1, \dots, k\}$. Sufficiency of the requirement $D_i = \operatorname{Ad}_h^\mathsf{T} D_i \operatorname{Ad}_h$ for every $i \in \{1, \dots, k\}$ is straightforward in light of Theorem 3.20. □

Theorem 3.20 and Corollary 3.21 suggest an approach to the design of damping models for vehicles with certain symmetries. In particular, one first identifies a generating set of the symmetry group $\mathcal{H}$ of the vehicle. Then, one looks for a mapping σ that is invariant under the elements of the generating set (and therefore under $\mathcal{H}$), ideally with the independence property of Corollary 3.21. Finally, one forms the model (3.123), where every D_i satisfies $D_i = \operatorname{Ad}_h^\mathsf{T} D_i \operatorname{Ad}_h$, a property which is established as outlined in Example 3.19. We now present an example in which we show that this approach leads to the second-order modulus damping model if a vehicle has three planes of symmetry.

Example 3.22. The second-order modulus damping model, also stated in (3.41), is given by

$$d(\nu) \coloneqq -\sum_{i=1}^{6} |\nu_i| D_i \nu. \tag{3.128}$$

If the vehicle frame is placed in the center of volume with its axes directed along the intersections of the symmetry planes, then the symmetries of $\mathcal{R}$ can be written as $h_i = (0, S_i)$ for $i \in \{1, 2, 3\}$, where $S_1 = \operatorname{diag}(-1, 1, 1)$, $S_2 = \operatorname{diag}(1, -1, 1)$, and $S_3 = \operatorname{diag}(1, 1, -1)$. It is readily seen that

$$\operatorname{Ad}_{h_1} \nu = \begin{pmatrix} -\nu_1 \\ \nu_2 \\ \nu_3 \\ \nu_4 \\ -\nu_5 \\ -\nu_6 \end{pmatrix}, \operatorname{Ad}_{h_2} \nu = \begin{pmatrix} \nu_1 \\ -\nu_2 \\ \nu_3 \\ -\nu_4 \\ \nu_5 \\ -\nu_6 \end{pmatrix}, \operatorname{Ad}_{h_3} \nu = \begin{pmatrix} \nu_1 \\ \nu_2 \\ -\nu_3 \\ -\nu_4 \\ -\nu_5 \\ \nu_6 \end{pmatrix}. \tag{3.129}$$

It is therefore reasonable to select σ as a mapping that is independent of the sign of the entries of its argument. There are of course many such mappings. For example, $k = 1$ and $\sigma(\nu) \coloneqq |\nu|$, or $k = 2$ and $\sigma(\nu) \coloneqq (|v|, |\omega|)$. However, both of these mappings are invariant under a much larger group than what we consider here. In particular, both of them satisfy $\sigma(\nu) = \sigma(\operatorname{Ad}_h \nu)$ for every $\nu \in \mathbb{R}^6$ and every $h = (0, S)$ where $S \in \mathrm{O}(3)$. These choices of σ would therefore also be candidates for a spherical underwater vehicle. Indeed, reasoning along these lines very quickly leads to $k = 6$ and $\sigma(\nu) = \operatorname{abs} \nu$ for the present case if one wishes the entries of d to be of second order. It can also be established that abs has the independence property, as shown below in Lemma 3.7. It then follows by Corollary 3.21 and considerations presented in Example 3.19 that every D_i should be a diagonal matrix. This constitutes a reduction from 216 parameters to 36 parameters.

Lemma 3.7. Let $A \in \mathbb{R}^{6\times 6}$. Then

$$\langle A\nu, \operatorname{abs} \nu \rangle = 0 \tag{3.130}$$

for every $\nu \in \mathbb{R}^6$ if and only if $A = 0$.

Proof. Let $i, j \in \{1, \ldots, 6\}$. Set all entries of ν except ν_i and ν_j to zero. Consider first the case where $i = j$. Then, (3.130) simplifies to $A_{ii}|\nu_i|\nu_i = 0$. Since this must hold for all ν_i, it can be concluded that $A_{ii} = 0$. Since i is arbitrary, it follows that A has only zeros on its diagonal. Consider now the case where $i \neq j$. From what has been established, it can be concluded that (3.130) simplifies to $A_{ij}|\nu_i|\nu_j + A_{ji}|\nu_j|\nu_i = 0$. This must hold for all ν_i and ν_j. In particular, the cases $(\nu_i, \nu_j) = (1, 1)$ and $(\nu_i, \nu_j) = (1, -1)$ yield the equation

$$\begin{pmatrix} 1 & 1 \\ -1 & 1 \end{pmatrix} \begin{pmatrix} A_{ij} \\ A_{ji} \end{pmatrix} = 0, \tag{3.131}$$

with the unique solution $A_{ij} = A_{ji} = 0$. Since (i, j) are arbitrary apart from $i \neq j$, this proves that $A = 0$. □

Lastly, we will highlight the connection between vehicle symmetry and Rayleigh dissipation functions. If a hydrodynamic damping wrench d admits a Rayleigh dissipation function D, as introduced in Definition 3.12, then the symmetry properties of d can be completely characterized in terms of D. The following proposition makes this statement precise.

Proposition 3.23. *Let $h \in \mathrm{E}(3)$ be a symmetry of $\mathcal{R}$. If d admits the Rayleigh dissipation function D, then d satisfies the symmetry principle for hydrodynamic damping if and only if $D(\nu) = D(\mathrm{Ad}_h\, \nu)$ for every $\nu \in \mathbb{R}^6$.*

Proof. Assume that $d(\nu) = \mathrm{Ad}_h^{\mathsf{T}}\, d(\mathrm{Ad}_h\, \nu)$ for every $\nu \in \mathbb{R}^6$. From Lemma 3.3, we have that

$$\begin{aligned} D(\nu) &= -\int_0^1 \langle d(s\nu), \nu \rangle\, ds + D_0 \\ &= -\int_0^1 \langle \mathrm{Ad}_h^{\mathsf{T}}\, d(s\, \mathrm{Ad}_h\, \nu), \nu \rangle\, ds + D_0 \\ &= -\int_0^1 \langle d(s\, \mathrm{Ad}_h\, \nu), \mathrm{Ad}_h\, \nu \rangle\, ds + D_0 \\ &= D(\mathrm{Ad}_h\, \nu), \end{aligned} \tag{3.132}$$

where $D_0 \in \mathbb{R}$ is a free parameter specifying $D(0)$. This shows necessity.

Let now $D(\nu) = D(\mathrm{Ad}_h\, \nu)$ for every $\nu \in \mathbb{R}^6$. It then follows from the chain rule that

$$\nabla D(\nu) = \mathrm{Ad}_h^{\mathsf{T}}\, \nabla D(\mathrm{Ad}_h\, \nu) \tag{3.133}$$

for every $\nu \in \mathbb{R}^6$. Consequently, $d(\nu) = \mathrm{Ad}_h^{\mathsf{T}}\, d(\mathrm{Ad}_h\, \nu)$ for every $\nu \in \mathbb{R}^6$. This shows sufficiency. □

3.6 Control Model with Quaternion Attitude Representation

It is convenient for control design purposes to employ unit quaternions to describe the orientation of the underwater vehicle. The group of unit quaternions can be represented as the matrix Lie group

$$\mathrm{Z} \coloneqq \left\{ z = \begin{pmatrix} \eta & -\epsilon^{\mathsf{T}} \\ \epsilon & \eta I + \epsilon^{\times} \end{pmatrix} : (\eta, \epsilon) \in \mathbb{S}^3 \right\} \subset \mathrm{GL}(4), \tag{3.134}$$

where η is the real part of the unit quaternion and ϵ is the imaginary part of the unit quaternion. The underlying manifold of Z is seen to be $\mathbb{S}^3$. Let us now characterize the basic group operations. Skipping some tedious but straightforward computations, the inverse of $z \in \mathrm{Z}$ is found to be

$$z^{-1} = \begin{pmatrix} \eta & -\epsilon^{\mathsf{T}} \\ \epsilon & \eta I + \epsilon^{\times} \end{pmatrix}^{-1} = \begin{pmatrix} \eta & -\epsilon^{\mathsf{T}} \\ \epsilon & \eta I + \epsilon^{\times} \end{pmatrix}^{\mathsf{T}} = \begin{pmatrix} \eta & \epsilon^{\mathsf{T}} \\ -\epsilon & \eta I - \epsilon^{\times} \end{pmatrix}. \tag{3.135}$$

Furthermore, the product of $z_1 \in \mathrm{Z}$ and $z_2 \in \mathrm{Z}$ is

$$\begin{aligned} z_1 z_2 &= \begin{pmatrix} \eta_1 & -\epsilon_1^\mathsf{T} \\ \epsilon_1 & \eta_1 I + \epsilon_1^\times \end{pmatrix} \begin{pmatrix} \eta_2 & -\epsilon_2^\mathsf{T} \\ \epsilon_2 & \eta_2 I + \epsilon_2^\times \end{pmatrix} \\ &= \begin{pmatrix} \eta_1\eta_2 - \langle \epsilon_1, \epsilon_2 \rangle & -(\eta_1\epsilon_2 + \eta_2\epsilon_1 + \epsilon_1 \times \epsilon_2)^\mathsf{T} \\ \eta_1\epsilon_2 + \eta_2\epsilon_1 + \epsilon_1 \times \epsilon_2 & (\eta_1\eta_2 - \langle \epsilon_1, \epsilon_2 \rangle) I + (\eta_1\epsilon_2 + \eta_2\epsilon_1 + \epsilon_1 \times \epsilon_2)^\times \end{pmatrix}. \end{aligned} \tag{3.136}$$

Unit quaternions are connected to proper rotations via the mapping $\mathrm{rot} : \mathrm{Z} \to \mathrm{SO}(3)$, defined by

$$\mathrm{rot}(z) \coloneqq I + 2\eta\epsilon^\times + 2\epsilon^\times\epsilon^\times. \tag{3.137}$$

The mapping rot establishes Z as a double covering group of SO(3). In particular, it can be shown that rot is surjective and that for every $R \in \mathrm{SO}(3)$, there exists an open neighborhood U of R and two disjoint open sets V_1 and V_2 in Z such that $\mathrm{rot}^{-1}(U) = V_1 \cup V_2$ and the restriction $\mathrm{rot}|_{V_i} \colon V_i \to U$ is a homeomorphism for $i \in \{1, 2\}$. The neighborhoods V_1 and V_2 have the the property that $z \in V_1$ if and only if $-z \in V_2$. Furthermore, it can be shown that for all $z_1, z_2 \in \mathrm{Z}$, it holds that $\mathrm{rot}(z_1)\,\mathrm{rot}(z_2) = \mathrm{rot}(z_1 z_2)$. Consequently, rot is also a Lie group homomorphism. Since Z is simply connected, it is in fact the universal covering group of SO(3).

We now seek to characterize the Lie algebra of Z, denoted $\mathfrak{z}$. The tangent space to Z at $z \in \mathrm{Z}$ is

$$T_\mathrm{Z}(z) \coloneqq \left\{ \begin{pmatrix} \varsigma & -\sigma^\mathsf{T} \\ \sigma & \varsigma I + \sigma^\times \end{pmatrix} : \varsigma \in \mathbb{R}, \sigma \in \mathbb{R}^3, \eta\varsigma + \langle \epsilon, \sigma \rangle = 0 \right\}. \tag{3.138}$$

The Lie algebra to Z, as introduced in Definition 2.7, is the tangent space to Z at the identity equipped with the matrix commutator. It follows that

$$\mathfrak{z} \coloneqq T_\mathrm{Z}(I) = \left\{ \begin{pmatrix} 0 & -\sigma^\mathsf{T} \\ \sigma & \sigma^\times \end{pmatrix} : \sigma \in \mathbb{R}^3 \right\}. \tag{3.139}$$

We identify $\mathfrak{z}$ with $\mathbb{R}^3$ by utilizing the vector space isomorphism $\widehat{\cdot}^{\mathfrak{z}} : \mathbb{R}^3 \to \mathfrak{z}$, is defined by

$$\widehat{\sigma}^{\mathfrak{z}} \coloneqq \frac{1}{2} \begin{pmatrix} 0 & -\sigma^\mathsf{T} \\ \sigma & \sigma^\times \end{pmatrix}. \tag{3.140}$$

The factor $1/2$ is included to ensure that the derivative of rot satisfies

$$\mathrm{Drot}(z, z\widehat{\omega}^{\mathfrak{z}}) = \mathrm{rot}(z)\omega^\times \tag{3.141}$$

for all $(z, \omega) \in \mathrm{Z} \times \mathbb{R}^3$. Equivalently, every solution $t \mapsto (z(t), \omega(t))$ to the differential equation with input

$$\dot{z} = z\widehat{\omega}^{\mathfrak{z}}, \quad (z, \omega) \in \mathrm{Z} \times \mathbb{R}^3 \tag{3.142}$$

satisfies the kinematic relation on SO(3),

$$\frac{d}{dt}\,\mathrm{rot}(z(t)) = \mathrm{rot}(z(t))\omega(t)^\times \tag{3.143}$$

for almost all $t \in \operatorname{dom} z$.

We now consider the counterpart to SE(3) when the orientation is described by a unit quaternion. We refer to this matrix Lie group as $\widetilde{\mathrm{SE}}(3)$, and define it by

$$\widetilde{\mathrm{SE}}(3) \coloneqq \left\{ \begin{pmatrix} \operatorname{rot}(z) & 0 & p \\ 0 & z & 0 \\ 0 & 0 & 1 \end{pmatrix} : p \in \mathbb{R}^3, z \in \mathrm{Z} \right\} \subset \mathrm{GL}(8). \tag{3.144}$$

For every $g \in \widetilde{\mathrm{SE}}(3)$, it holds that

$$g^{-1} = \begin{pmatrix} \operatorname{rot}(z) & 0 & p \\ 0 & z & 0 \\ 0 & 0 & 1 \end{pmatrix}^{-1} = \begin{pmatrix} \operatorname{rot}(z)^{\mathsf{T}} & 0 & -\operatorname{rot}(z)^{\mathsf{T}} p \\ 0 & z^{\mathsf{T}} & 0 \\ 0 & 0 & 1 \end{pmatrix}, \tag{3.145}$$

and for every $g_1 \in \widetilde{\mathrm{SE}}(3)$ and $g_2 \in \widetilde{\mathrm{SE}}(3)$,

$$\begin{aligned} g_1 g_2 &= \begin{pmatrix} \operatorname{rot}(z_1) & 0 & p_1 \\ 0 & z_1 & 0 \\ 0 & 0 & 1 \end{pmatrix} \begin{pmatrix} \operatorname{rot}(z_2) & 0 & p_2 \\ 0 & z_2 & 0 \\ 0 & 0 & 1 \end{pmatrix} \\ &= \begin{pmatrix} \operatorname{rot}(z_1 z_2) & 0 & \operatorname{rot}(z_1) p_2 + p_1 \\ 0 & z_1 z_2 & 0 \\ 0 & 0 & 1 \end{pmatrix}. \end{aligned} \tag{3.146}$$

The configuration of a rigid body is described in terms of $\widetilde{\mathrm{SE}}(3)$ with the mapping $\operatorname{cnf} : \widetilde{\mathrm{SE}}(3) \to \mathrm{SE}(3)$ defined by

$$\operatorname{cnf}(g) \coloneqq \begin{pmatrix} \operatorname{rot}(z) & p \\ 0 & 1 \end{pmatrix}. \tag{3.147}$$

Just as rot established Z as a double covering group of SO(3), the mapping cnf establishes $\widetilde{\mathrm{SE}}(3)$ as a double covering group of SE(3). Since the product of simply connected spaces is simply connected, it follows that $\widetilde{\mathrm{SE}}(3)$ is simply connected. Consequently, it is the universal covering group of SE(3). The Lie algebra to $\widetilde{\mathrm{SE}}(3)$, denoted $\widetilde{\mathfrak{se}}(3)$, is found to be

$$\widetilde{\mathfrak{se}}(3) \coloneqq \left\{ \begin{pmatrix} \omega^{\times} & 0 & v \\ 0 & \widehat{\omega}^{\mathfrak{z}} & 0 \\ 0 & 0 & 0 \end{pmatrix} : v \in \mathbb{R}^3, \omega \in \mathbb{R}^3 \right\}. \tag{3.148}$$

We identify $\widetilde{\mathfrak{se}}(3)$ with $\mathbb{R}^6$ through the vector space isomorphism $\widehat{\cdot} : \mathbb{R}^6 \to \widetilde{\mathfrak{se}}(3)$,

$$\widehat{\cdot} : \begin{pmatrix} v \\ \omega \end{pmatrix} \mapsto \begin{pmatrix} \omega^{\times} & 0 & v \\ 0 & \widehat{\omega}^{\mathfrak{z}} & 0 \\ 0 & 0 & 0 \end{pmatrix}. \tag{3.149}$$

The adjoint operators on $\widetilde{\mathrm{SE}}(3)$ and $\widetilde{\mathfrak{se}}(3)$ can then for $g \in \widetilde{\mathrm{SE}}(3)$ and $\nu \in \mathbb{R}^6$ be defined as

$$\begin{aligned} \operatorname{Ad}_g &\coloneqq \begin{pmatrix} \operatorname{rot}(z) & p^{\times} \operatorname{rot}(z) \\ 0 & \operatorname{rot}(z) \end{pmatrix}, \\ \operatorname{ad}_\nu &\coloneqq \begin{pmatrix} \omega^{\times} & v^{\times} \\ 0 & \omega^{\times} \end{pmatrix}, \end{aligned} \tag{3.150}$$

respectively. Using the Lie group structure of the configuration space, the equations of motion for a fully actuated underwater vehicle are given by

$$\left.\begin{aligned} \dot{g} &= g\widehat{\nu}, \\ M\dot{\nu} - \operatorname{ad}_{\nu}^{\mathsf{T}} M\nu &= d(\nu) + \widetilde{\chi}(g) + b + \tau \end{aligned}\right\} (g, \nu, \tau) \in \widetilde{\mathrm{SE}}(3) \times \mathbb{R}^6 \times \mathbb{R}^6. \tag{3.151}$$

The mapping $\widetilde{\chi} : \widetilde{\mathrm{SE}}(3) \to \mathbb{R}^6$ describes the hydrostatic wrench acting on the vehicle, and is defined as $\widetilde{\chi}(g) \coloneqq \chi(\mathrm{cnf}(g))$. The effect of the ocean current has here been captured by a constant bias $b \in \mathbb{R}^6$.

Chapter 4

Modeling of Multibody Underwater Vehicles

This chapter presents a framework for the mathematical modeling of multibody underwater vehicles possessing a kinematic tree structure. Under the assumption of hydrodynamical decoupling of the bodies composing the vehicle, the kinematics and dynamics are presented in a global and singularity-free matrix-form. We present a generalized inverse dynamics algorithm that allows efficient implementation of model-based control laws for this structurally complex class of vehicles. Lastly, we present an efficient forward dynamics algorithm which greatly simplifies simulation of multibody underwater vehicle motion.

The material in this chapter is based on [82].

4.1 Introduction

Control design models for general multibody underwater vehicles are, in the absence of other simplifying assumptions, unwieldy dynamical systems evolving on a state space of high dimension. For control strategies based on such general models, the implementation is usually not treated in detail, and overly simplified examples are used to show their effectiveness. Similarly, when it comes to models for simulation of multibody underwater vehicles, the presented numerical algorithms, although highly efficient, can in many cases not be used directly in the computation of the control effort [32, 35, 36]. This is because the controllers exploit properties of certain matrix forms of the equations of motion which are not respected by the recursive algorithms used in simulators. The main objective of this chapter is to outline a unified treatment of mathematical modeling for a broad class of multibody underwater vehicles, which can serve as the basis for simulators and model-based controllers.

The remainder of this chapter is organized as follows. Section 4.2 introduces the necessary concepts from Lie theory and multibody kinematics, in particular the notion of kinematic tree systems and the most important kinematic relations in recursive and matrix-form. In Section 4.3 we derive the general equations of motion in matrix-form. Lastly, Section 4.4 introduces algorithms for generalized inverse dynamics and forward dynamics.

4.2 Vehicle Kinematics

We consider in this chapter the modeling of rigid underwater vehicles with tree topology comprising n rigid bodies. To effectively describe the kinematics of such multibody underwater vehicles, we first introduce a few concepts from matrix Lie theory. For matrix Lie groups $\mathcal{G}_i$, where $i \in \{1, 2, \ldots, n\}$, the product group $\mathcal{G} = \mathcal{G}_1 \times \mathcal{G}_2 \times \cdots \times \mathcal{G}_n$ is the matrix Lie group

$$\mathcal{G} \coloneqq \{\operatorname{blkdiag}(g_1, g_2, \ldots, g_n) : g_i \in \mathcal{G}_i\}. \tag{4.1}$$

For convenience, we write elements of $\mathcal{G}$ as $g = (g_1, g_2, \ldots, g_n) \in \mathcal{G}$. Evidently, if each matrix Lie group $\mathcal{G}_i$ has dimension m_i as a manifold, then $\mathcal{G}$ has dimension $m = \sum_{i=1}^{n} m_i$. Denoting by $\mathfrak{g}_i$ the Lie algebra of $\mathcal{G}_i$, the Lie algebra of $\mathcal{G}$ is

$$\mathfrak{g} \coloneqq \{\operatorname{blkdiag}(V_1, V_2, \ldots, V_n) : V_i \in \mathfrak{g}_i\}. \tag{4.2}$$

Furthermore, there exists for each $i \in \{1, 2, \ldots, n\}$ a vector space isomorphism $\widehat{\cdot}^{\mathfrak{g}_i} : \mathbb{R}^{m_i} \to \mathfrak{g}_i$. Consequently, we can define

$$\widehat{\nu}^{\mathfrak{g}} \coloneqq \operatorname{blkdiag}(\widehat{\nu}_1^{\mathfrak{g}_1}, \widehat{\nu}_2^{\mathfrak{g}_2}, \ldots, \widehat{\nu}_n^{\mathfrak{g}_n}), \tag{4.3}$$

where $\nu = (\nu_1, \nu_2, \ldots, \nu_n) \in \mathbb{R}^m$ and each $\nu_i \in \mathbb{R}^{m_i}$. Continuing, each $\mathcal{G}_i$ and $\mathfrak{g}_i$ have adjoint operators $\operatorname{Ad}^{\mathcal{G}_i}$ and $\operatorname{ad}^{\mathfrak{g}_i}$, respectively, defined relative to the vector space isomorphism $\widehat{\cdot}_i^{\mathfrak{g}_i}$. Consequently, we define the adjoint operators

$$\begin{aligned} \operatorname{Ad}_g^{\mathcal{G}} &\coloneqq \operatorname{blkdiag}(\operatorname{Ad}_{g_1}^{\mathcal{G}_1}, \operatorname{Ad}_{g_2}^{\mathcal{G}_2}, \ldots, \operatorname{Ad}_{g_n}^{\mathcal{G}_n}) \in \mathbb{R}^{m \times m}, \\ \operatorname{ad}_\nu^{\mathfrak{g}} &\coloneqq \operatorname{blkdiag}(\operatorname{ad}_{\nu_1}^{\mathfrak{g}_1}, \operatorname{ad}_{\nu_2}^{\mathfrak{g}_2}, \ldots, \operatorname{ad}_{\nu_n}^{\mathfrak{g}_n}) \in \mathbb{R}^{m \times m}, \end{aligned} \tag{4.4}$$

where $g = (g_1, g_2, \ldots g_n) \in \mathcal{G}$ and $\nu = (\nu_1, \nu_2, \ldots, \nu_n) \in \mathbb{R}^m$ such that every $\nu_i \in \mathbb{R}^{m_i}$.

Recall that if $\mathcal{G}$ is a matrix Lie group, then a matrix Lie subgroup of $\mathcal{G}$ is a matrix Lie group $\mathcal{H}$ such that $\mathcal{H} \subset \mathcal{G}$. Furthermore, if $\mathcal{H}$ is a matrix Lie subgroup of $\mathcal{G}$, then the Lie algebra $\mathfrak{h}$ of $\mathcal{H}$ is a vector subspace of $\mathfrak{g}$. Denoting the dimension of $\mathcal{H}$ as a manifold by k, there exists a vector space isomorphism $\widehat{\cdot}^{\mathfrak{h}} : \mathbb{R}^k \to \mathfrak{h}$ that allows us to identify $\mathfrak{h}$ with $\mathbb{R}^k$. It then follows from the fact that $\mathfrak{h}$ is a vector subspace of $\mathfrak{g}$ that there exists a matrix $\Phi \in \mathbb{R}^{m \times k}$ such that

$$\widehat{\mu}^{\mathfrak{h}} = \widehat{\Phi \mu}^{\mathfrak{g}} \tag{4.5}$$

for every $\mu \in \mathbb{R}^k$. The matrix Φ describes the subspace $\mathfrak{h}$ of $\mathfrak{g}$ relative to the isomorphisms $\widehat{\cdot}^{\mathfrak{h}}$ and $\widehat{\cdot}^{\mathfrak{g}}$. Utilizing the definition (2.6) of the adjoint operators, it holds that

$$\begin{aligned} \Phi \operatorname{Ad}_h^{\mathcal{H}} &= \operatorname{Ad}_h^{\mathcal{G}} \Phi, \\ \Phi \operatorname{ad}_\mu^{\mathfrak{h}} &= \operatorname{ad}_{\Phi\mu}^{\mathfrak{g}} \Phi \end{aligned} \tag{4.6}$$

for every $h \in \mathcal{H}$ and every $\mu \in \mathbb{R}^k$. Here, $\operatorname{Ad}^{\mathfrak{h}}$ and $\operatorname{ad}^{\mathfrak{h}}$ are formulated relative to $\widehat{\cdot}^{\mathfrak{h}}$, and $\operatorname{Ad}^{\mathfrak{g}}$ and $\operatorname{ad}^{\mathfrak{g}}$ are formulated relative to $\widehat{\cdot}^{\mathfrak{g}}$.

4.2.1 Unconstrained Motion

By introducing a Cartesian world-fixed reference frame and n Cartesian body-fixed reference frames, the configuration of each rigid body composing the vehicle can be identified with $\mathrm{E}(3)$. In particular, we denote by $g_i = (p_i, R_i) \in \mathrm{E}(3)$ the configuration of the ith body frame expressed relative to the world frame for $i \in \{1, 2 \ldots, n\}$, as illustrated in Figure 4.1. The position p_i should be understood as the vector from the world frame origin to the origin of body frame i expressed in the world frame. The orientation R_i describes the axes of body frame i expressed in the world frame. It can be verified that R_i is a proper rotation if the world frame and body frame i have the same handedness, and an improper rotation otherwise.

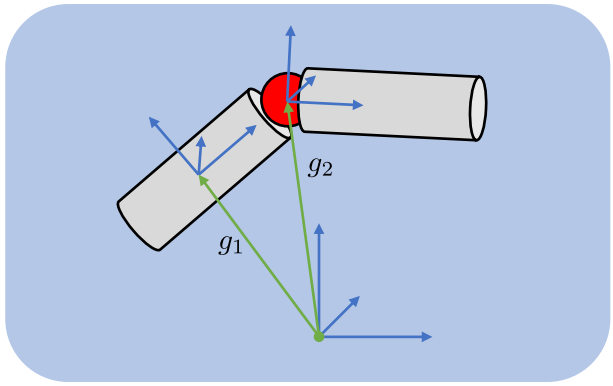

Figure 4.1: A multibody underwater vehicle comprising two rigid bodies interconnected by a joint.

The Lie algebra $\mathfrak{e}(3)$ of $\mathrm{E}(3)$ is identified with $\mathbb{R}^6$ by utilizing the vector space isomorphism $\widehat{\cdot}: \mathbb{R}^6 \to \mathfrak{e}(3)$ defined by (3.10). Furthermore, we use the adjoint operators Ad and ad as defined in (3.11) and (3.12), respectively. We denote by $v_i \in \mathbb{R}^3$ and $\omega_i \in \mathbb{R}^3$ the linear and angular velocity, respectively, of body frame i relative to the world frame, both expressed in body frame i. Furthermore, we denote by $a_i = \dot{v}_i \in \mathbb{R}^3$ and $\varpi_i = \dot{\omega}_i \in \mathbb{R}^3$ the linear and angular accelerations of body i, respectively. The velocity of body i is denoted by $\nu_i = (v_i, \omega_i) \in \mathbb{R}^6$, and the acceleration of body i by $\alpha_i = (a_i, \varpi_i) \in \mathbb{R}^6$.

The configuration of the rigid bodies composing the multibody underwater vehicle is denoted $g \in \mathrm{E}(3)^n$, where $\mathrm{E}(3)^n$ denotes the direct product of n copies of $\mathrm{E}(3)$. The velocity and acceleration of the multibody underwater vehicle are written $\nu := (\nu_1, \nu_2, \ldots, \nu_n) \in \mathbb{R}^{6n}$ and $\alpha := (\alpha_1, \alpha_2, \ldots, \alpha_n) \in \mathbb{R}^{6n}$, respectively. We also utilize the symbol $\widehat{\cdot}$ to denote the vector space isomorphism $\widehat{\cdot}^{\mathfrak{e}(3)^n} : \mathbb{R}^{6n} \to \mathfrak{e}(3)^n$, and write Ad and ad instead of $\mathrm{Ad}^{\mathrm{E}(3)^n}$ and $\mathrm{ad}^{\mathfrak{e}(3)^n}$, respectively. Consequently, the unconstrained motion of the vehicle is described by the system

$$\left.\begin{aligned} \dot{g} &= g\widehat{\nu} \\ \dot{\nu} &= \alpha \end{aligned}\right\} (g, \nu, \alpha) \in \mathrm{E}(3)^n \times \mathbb{R}^{6n} \times \mathbb{R}^{6n}, \tag{4.7}$$

where α is considered an input.

We denote by $f_i \in \mathbb{R}^6$ a wrench acting on body i, which we take to be expressed in body frame i. The wrenches acting on all bodies in the system are collected and

expressed as $f = (f_1, f_2, \ldots, f_n) \in \mathbb{R}^{6n}$. A deeper treatment of the topics briefly examined here is found in [98, Chapter 2] and [119, Chapter 1], the latter being more mathematically rigorous.

4.2.2 Constrained Motion

The rigid bodies composing the underwater vehicle can in general not move freely relative to each other. They are interconnected by joints which permit relative motion only in certain directions. A description of how the rigid bodies in the multibody system are connected together by joints is referred to as its topology or connectivity. We will in this chapter represent the topology of the multibody system as a so-called connectivity graph. In particular, we follow the approach presented in the standard reference [40, Chapter 4].

The connectivity graph comprises $n+1$ vertices, each of which describes a reference frame. The root vertex 0 is assigned to the world frame, and the remaining n vertices are assigned to the body-fixed frames. Every edge in the graph represents a joint. The conception of a joint must here be understood in a slightly generalized sense. In particular, for the graph-description to be applicable to free-floating mechanisms such as underwater vehicles, we must accept the existence of "free joints" that describe unconstrained relative motion between rigid bodies and the world.

We will restrict our attention to underwater vehicles whose connectivity graph is a rooted tree. This means that there is a unique path between any two vertices in the graph, or equivalently, that it is connected and possesses no cycles. Since a tree always has one less edge than it has vertices, the underwater vehicles in question possess exactly n (generalized) joints. An edge connects from a vertex referred to as the parent to a vertex referred to as the child, and inherits the number of the child. We employ a regular numbering scheme, where the number assigned to a vertex is always lower than the number assigned to its children.

The graph can be represented numerically by its parent mapping $\lambda : \{1, 2, \ldots n\} \to \{0, 1, \ldots, n\}$, which takes as input a non-zero vertex and gives as output the number of its parent. The children of a given vertex i are consequently the elements of the set $\lambda^{-1}(i)$. Regular numbering for vertices can be stated in terms of the parent mapping as $\lambda(i) < i$. It is clear that for every $k \in \{1, \ldots, n\}$, there exists $r \leq n$ such that $\lambda^r(k) = 0$. Another important quantity is the set-valued mapping $\kappa : \{1, 2, \ldots, n\} \rightrightarrows \{1, 2, \ldots, n\}$ which returns the set of vertices in the path from the root vertex up to and including its argument. Let us illustrate the introduced concepts with an example.

Example 4.1. The connectivity graph, λ, and κ of the very simple mechanism depicted in Figure 4.1 is presented in Figure 4.2. In particular, joint 1 is seen to be a

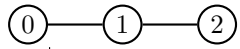

i	1	2
$\lambda(i)$	0	1
$\kappa(i)$	$\{1\}$	$\{1, 2\}$

Figure 4.2: The connectivity graph, λ, and κ for the vehicle depicted in Figure 4.1.

free joint. For a slightly more interesting example, consider the underwater vehicle

with a dual arm configuration illustrated in Figure 4.3. Assigning the number 1 to the distinguishable base, the numbers 2 through 4 to one arm, and 5 through 7 to the other, results in the connectivity graph and associated λ and κ depicted in Figure 4.4. Since this is a floating base mechanism, joint 1 is again a free joint.

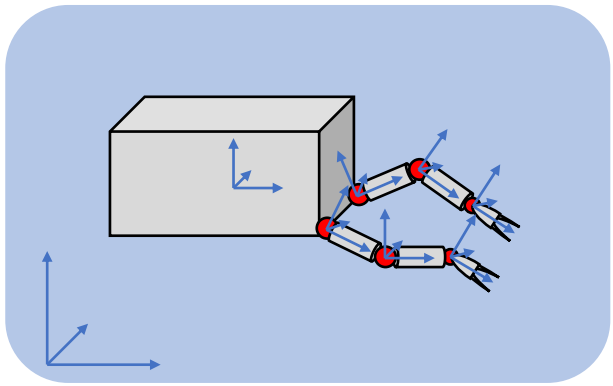

Figure 4.3: A multibody underwater vehicle comprising a distinguished base and two manipulator arms.

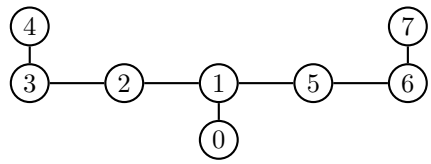

i	1	2	3	4	5	6	7
$\lambda(i)$	0	1	2	3	1	5	6
$\kappa(i)$	$\{1\}$	$\{1,2\}$	$\{1,2,3\}$	$\{1,2,3,4\}$	$\{1,5\}$	$\{1,5,6\}$	$\{1,5,6,7\}$

Figure 4.4: A possible connectivity graph with the associated λ and κ for the vehicle depicted in Figure 4.3.

A joint model describes the possible relative motion between the two rigid bodies it connects. We will here assume that the configuration space of each joint in the underwater vehicle can be described by a matrix Lie subgroup of E(3). The particular subgroup describing the motion of joint i, and therefore the relative motion of bodies $\lambda(i)$ and i, will be denoted $\mathcal{X}_i$ for every $i \in \{1, 2, \ldots, n\}$. It follows that the configuration space of the multibody underwater vehicle is the product group $\mathcal{X} = \mathcal{X}_1 \times \mathcal{X}_2 \times \cdots \times \mathcal{X}_n$. We take the dimension of each Lie group $\mathcal{X}_i$ as a manifold to be $m_i > 0$, and the dimension of $\mathcal{X}$ to be $m \coloneqq \sum_{i=1}^{n} m_i$. Furthermore, we denote by $\mathfrak{x}_i \subset \mathbb{R}^{m_i \times m_i}$ the Lie algebra of $\mathcal{X}_i$, and by $\mathfrak{x} \subset \mathbb{R}^{m \times m}$ the Lie algebra of $\mathcal{X}$. Each Lie algebra $\mathfrak{x}_i$ comes equipped with a vector space isomorphism $\widehat{\cdot}^{\mathfrak{x}_i} : \mathbb{R}^{m_i} \to \mathfrak{x}_i$, from which we construct the vector space isomorphism $\widehat{\cdot}^{\mathfrak{x}} : \mathbb{R}^m \to \mathfrak{x}$ for $\mathfrak{x}$. Note also that there for each $i \in \{1, 2, \ldots n\}$ exists a matrix $\Phi_i \in \mathbb{R}^{6 \times m_i}$ such that $\widehat{\mu_i}^{\mathfrak{x}_i} = \widehat{\Phi_i \mu_i}$ for every $\mu_i \in \mathbb{R}^{m_i}$. It then follows that $\widehat{\mu}^{\mathfrak{x}} = \widehat{\Phi \mu}$ for every $\mu \in \mathbb{R}^m$, where the matrix $\Phi \coloneqq \operatorname{blkdiag}(\Phi_1, \Phi_2, \ldots, \Phi_n) \in \mathbb{R}^{6n \times m}$. We denote the joint configuration, joint

velocity, and joint acceleration of joint i by $x_i \in \mathcal{X}_i$, $\mu_i \in \mathbb{R}^{m_i}$, and $\sigma_i \in \mathbb{R}^{m_i}$, respectively. Furthermore, we denote the global joint configuration, joint velocity, and joint acceleration by $x \coloneqq (x_1, x_2, \dots, x_n) \in \mathcal{X}$, $\mu \coloneqq (\mu_1, \mu_2, \dots, \mu_n) \in \mathbb{R}^m$, and $\sigma \coloneqq (\sigma_1, \sigma_2, \dots, \sigma_n) \in \mathbb{R}^m$, respectively. Consequently, the kinematics of joint i are described by the system

$$\left.\begin{aligned} \dot{x}_i &= x_i \widehat{\mu}_i^{\mathfrak{r}_i} \\ &= x_i \widehat{\Phi_i \mu_i} \\ \dot{\mu}_i &= \sigma_i \end{aligned}\right\} (x_i, \mu_i, \sigma_i) \in \mathcal{X}_i \times \mathbb{R}^{m_i} \times \mathbb{R}^{m_i}, \tag{4.8}$$

where σ_i is considered an input. Similarly, the overall joint kinematics are described by the system

$$\left.\begin{aligned} \dot{x} &= x \widehat{\mu}^{\mathfrak{r}} \\ &= x \widehat{\Phi \mu} \\ \dot{\mu} &= \sigma \end{aligned}\right\} (x, \mu, \sigma) \in \mathcal{X} \times \mathbb{R}^m \times \mathbb{R}^m, \tag{4.9}$$

where σ is considered an input.

We present all nontrivial connected subgroups of E(3) up to conjugacy in Table 4.1. These are the most attractive candidates for the subgroups $\mathcal{X}_i$. The first column states the dimension m_i of the group, the second column shows which often-encountered group it is isomorphic to, the third column shows the overall structure of the elements x_i of the group, and the last column shows the associated matrix Φ_i. A derivation of these subgroups is found in [99, Chapter 3].

The configuration of the reference frame $i > 0$ expressed relative to the reference frame $\lambda(i)$ is written $h_i \in \mathrm{E}(3)$, and decomposed as

$$h_i \coloneqq c_i x_i, \tag{4.10}$$

where $c_i \in \mathrm{E}(3)$ describes how joint i is situated in the frame $\lambda(i)$. In particular, we see that if joint i is at its identity configuration, that is $x_i = I$, then the configuration of frame i expressed in frame $\lambda(i)$ is given by c_i. For this decomposition to be possible, the reference frame i must be placed in joint i, as illustrated in Figures 4.1 and 4.3. If joint i is a free joint, then c_i can always be taken as the identity. We emphasize that h_i is technically a function of x_i, and that every c_i is considered a constant parameter that describes the geometry of the vehicle. There is then the following result.

Proposition 4.2. *Let $g_0 = I$, $\nu_0 = 0$, and $\alpha_0 = 0$. The configuration, velocity, and acceleration of frame $i > 0$ relative to the world frame 0 satisfy the recursions*

$$\begin{aligned} g_i &= g_{\lambda(i)} h_i, \\ \nu_i &= \mathrm{Ad}_{h_i}^{-1} \nu_{\lambda(i)} + \Phi_i \mu_i, \\ \alpha_i &= \mathrm{Ad}_{h_i}^{-1} \alpha_{\lambda(i)} + \mathrm{ad}_{\nu_i} \Phi_i \mu_i + \Phi_i \sigma_i. \end{aligned} \tag{4.11}$$

Proof. The fact that $g_i = g_{\lambda(i)} h_i$ for every $i > 0$ follows by definition of h_i. Differentiating this expression gives

$$\begin{aligned} g_i \widehat{\nu}_i &= g_{\lambda(i)} \widehat{\nu}_{\lambda(i)} h_i + g_{\lambda(i)} h_i \widehat{\Phi_i \mu_i} \\ &= g_i [h_i^{-1} \widehat{\nu}_{\lambda(i)} h_i + \widehat{\Phi_i \mu_i}] \end{aligned} \tag{4.12}$$

m	$\mathcal{X} \cong$	x	Φ
6	SE(3)	$\begin{pmatrix} R_{11} & R_{12} & R_{13} & p_1 \\ R_{21} & R_{22} & R_{23} & p_2 \\ R_{31} & R_{32} & R_{33} & p_3 \\ 0 & 0 & 0 & 1 \end{pmatrix}$	$\begin{pmatrix} 1 & 0 & 0 & 0 & 0 & 0 \\ 0 & 1 & 0 & 0 & 0 & 0 \\ 0 & 0 & 1 & 0 & 0 & 0 \\ 0 & 0 & 0 & 1 & 0 & 0 \\ 0 & 0 & 0 & 0 & 1 & 0 \\ 0 & 0 & 0 & 0 & 0 & 1 \end{pmatrix}$
4	$\mathbb{R} \times$ SE(2)	$\begin{pmatrix} R_{11} & R_{12} & 0 & p_1 \\ R_{21} & R_{22} & 0 & p_2 \\ 0 & 0 & 1 & p_3 \\ 0 & 0 & 0 & 1 \end{pmatrix}$	$\begin{pmatrix} 1 & 0 & 0 & 0 \\ 0 & 1 & 0 & 0 \\ 0 & 0 & 1 & 0 \\ 0 & 0 & 0 & 0 \\ 0 & 0 & 0 & 0 \\ 0 & 0 & 0 & 1 \end{pmatrix}$
3	SE(2)	$\begin{pmatrix} R_{11} & R_{12} & 0 & p_1 \\ R_{21} & R_{22} & 0 & p_2 \\ 0 & 0 & 1 & 0 \\ 0 & 0 & 0 & 1 \end{pmatrix}$	$\begin{pmatrix} 1 & 0 & 0 \\ 0 & 1 & 0 \\ 0 & 0 & 0 \\ 0 & 0 & 0 \\ 0 & 0 & 0 \\ 0 & 0 & 1 \end{pmatrix}$
3	SO(3)	$\begin{pmatrix} R_{11} & R_{12} & R_{13} & 0 \\ R_{21} & R_{22} & R_{23} & 0 \\ R_{31} & R_{32} & R_{33} & 0 \\ 0 & 0 & 0 & 1 \end{pmatrix}$	$\begin{pmatrix} 0 & 0 & 0 \\ 0 & 0 & 0 \\ 0 & 0 & 0 \\ 1 & 0 & 0 \\ 0 & 1 & 0 \\ 0 & 0 & 1 \end{pmatrix}$
3	$\mathbb{R}^3$	$\begin{pmatrix} 1 & 0 & 0 & p_1 \\ 0 & 1 & 0 & p_2 \\ 0 & 0 & 1 & p_3 \\ 0 & 0 & 0 & 1 \end{pmatrix}$	$\begin{pmatrix} 1 & 0 & 0 \\ 0 & 1 & 0 \\ 0 & 0 & 1 \\ 0 & 0 & 0 \\ 0 & 0 & 0 \\ 0 & 0 & 0 \end{pmatrix}$
3	$\mathbb{R}^3$	$\begin{pmatrix} \cos\theta & -\sin\theta & 0 & p_1 \\ \sin\theta & \cos\theta & 0 & p_2 \\ 0 & 0 & 1 & k\theta/2\pi \\ 0 & 0 & 0 & 1 \end{pmatrix}$	$\begin{pmatrix} 1 & 0 & 0 \\ 0 & 1 & 0 \\ 0 & 0 & k/2\pi \\ 0 & 0 & 0 \\ 0 & 0 & 0 \\ 0 & 0 & 1 \end{pmatrix}$
2	$\mathbb{R} \times$ SO(2)	$\begin{pmatrix} R_{11} & R_{12} & 0 & 0 \\ R_{21} & R_{22} & 0 & 0 \\ 0 & 0 & 1 & p_3 \\ 0 & 0 & 0 & 1 \end{pmatrix}$	$\begin{pmatrix} 0 & 0 \\ 0 & 0 \\ 1 & 0 \\ 0 & 0 \\ 0 & 0 \\ 0 & 1 \end{pmatrix}$
2	$\mathbb{R}^2$	$\begin{pmatrix} 1 & 0 & 0 & p_1 \\ 0 & 1 & 0 & p_2 \\ 0 & 0 & 1 & 0 \\ 0 & 0 & 0 & 1 \end{pmatrix}$	$\begin{pmatrix} 1 & 0 \\ 0 & 1 \\ 0 & 0 \\ 0 & 0 \\ 0 & 0 \\ 0 & 0 \end{pmatrix}$
1	SO(2)	$\begin{pmatrix} R_{11} & R_{12} & 0 & 0 \\ R_{21} & R_{22} & 0 & 0 \\ 0 & 0 & 1 & 0 \\ 0 & 0 & 0 & 1 \end{pmatrix}$	$\begin{pmatrix} 0 \\ 0 \\ 0 \\ 0 \\ 0 \\ 1 \end{pmatrix}$
1	$\mathbb{R}$	$\begin{pmatrix} 1 & 0 & 0 & 0 \\ 0 & 1 & 0 & 0 \\ 0 & 0 & 1 & p_3 \\ 0 & 0 & 0 & 1 \end{pmatrix}$	$\begin{pmatrix} 0 \\ 0 \\ 1 \\ 0 \\ 0 \\ 0 \end{pmatrix}$
1	$\mathbb{R}$	$\begin{pmatrix} \cos\theta & -\sin\theta & 0 & 0 \\ \sin\theta & \cos\theta & 0 & 0 \\ 0 & 0 & 1 & k\theta/2\pi \\ 0 & 0 & 0 & 1 \end{pmatrix}$	$\begin{pmatrix} 0 \\ 0 \\ k/2\pi \\ 0 \\ 0 \\ 1 \end{pmatrix}$

Table 4.1: The nontrivial connected subgroups of E(3) up to conjugacy.

from which the velocity-recursion in (4.11) immediately follows. Differentiation of the expression for the velocity in (4.11) yields

$$\alpha_i = \mathrm{Ad}_{h_i}^{-1}\,\alpha_{\lambda(i)} - \mathrm{ad}_{\Phi_i\mu_i}\,\mathrm{Ad}_{h_i}^{-1}\,\nu_{\lambda(i)} + \Phi_i\sigma_i. \tag{4.13}$$

Substituting $\mathrm{Ad}_{h_i}^{-1}\,\nu_{\lambda(i)} = \nu_i - \Phi_i\mu_i$ into (4.13) and utilizing the anti-symmetry of the ad operator then gives the desired result. □

While the recursive relations presented in (4.11) are utilized in efficient multibody dynamics algorithms, we would also like a global formulation of the vehicle kinematic relations in terms of the joint configurations $x \in \mathcal{X}$, the joint velocities $\mu \in \mathbb{R}^m$, and the joint accelerations $\sigma \in \mathbb{R}^m$. To this end, define the adjacency block matrix $\Lambda \in \mathbb{R}^{6n\times 6n}$ in terms of the blocks $\Lambda_{ij} \in \mathbb{R}^{6\times 6}$ by

$$\Lambda_{ij} = \begin{cases} I & \text{if } \lambda(i) = j, \\ 0 & \text{otherwise.} \end{cases} \tag{4.14}$$

The adjacency block matrix relates objects to their parents in the following sense: If $\nu = (\nu_1, \nu_2, \ldots, \nu_n) \in \mathbb{R}^{6n}$ and $\nu_\lambda = (\nu_{\lambda(1)}, \nu_{\lambda(2)}, \ldots, \nu_{\lambda(n)}) \in \mathbb{R}^{6n}$ such that $\nu_0 = 0$, then $\Lambda\nu = \nu_\lambda$. It is seen from (4.14) that Λ is strictly lower triangular due to the regular numbering scheme we have adopted. Consequently, Λ is a nilpotent matrix of degree n, i.e. $\Lambda^n = 0$. A matrix closely related to Λ is $K \in \mathbb{R}^{6n\times 6n}$, defined such that its blocks $K_{ij} \in \mathbb{R}^{6\times 6}$ satisfy

$$K_{ij} = \begin{cases} I & \text{if } j \in \kappa(i), \\ 0 & \text{if } j \notin \kappa(i). \end{cases} \tag{4.15}$$

Due to regular numbering, K is lower triangular. Furthermore, it can be shown that $K = (I - \Lambda)^{-1} = I + \Lambda + \Lambda^2 + \cdots + \Lambda^{n-1}$ [120, Chapter 5].

We will also require the matrix $\Theta : \mathcal{X} \to \mathbb{R}^{6n\times 6n}$, defined by

$$\Theta(x) \coloneqq (I - \mathrm{Ad}_h^{-1}\,\Lambda)^{-1}, \tag{4.16}$$

where $h \coloneqq (h_1, h_2, \ldots, h_n) \in \mathrm{E}(3)^n$. We remark that since Λ is strictly lower triangular and Ad_h is block diagonal, it follows that $I - \mathrm{Ad}_h^{-1}\,\Lambda$ is lower triangular with ones on its diagonal. Such a matrix is always invertible, and Θ is therefore always well-defined. The following result establishes some properties of Θ.

Proposition 4.3. *It holds that*

$$\Theta(x) = \mathrm{Ad}_g^{-1}\,K\,\mathrm{Ad}_g\,. \tag{4.17}$$

Furthermore, denoting by $\mathrm{d}\Theta : \mathcal{X}\times\mathbb{R}^m \to \mathbb{R}^{6n\times 6n}$ *the derivative of* Θ*, it holds that*

$$\mathrm{d}\Theta(x,\mu) \coloneqq \Theta(x)\,\mathrm{ad}_{\Phi\mu} - \Theta(x)\,\mathrm{ad}_{\Phi\mu}\,\Theta(x). \tag{4.18}$$

Proof. We first show that $\mathrm{Ad}_{g_\lambda}\,\Lambda = \Lambda\,\mathrm{Ad}_g$, where $g_\lambda = (g_{\lambda(1)}, g_{\lambda(2)}, \ldots, g_{\lambda(n)}) \in \mathrm{E}(3)^n$ with $g_0 = I$. Letting $\nu = (\nu_1, \nu_2, \ldots, \nu_n) \in \mathbb{R}^{6n}$ be arbitrary, it holds that $\Lambda\nu = \nu_\lambda$. Since Ad_g is a block diagonal matrix, it also holds that $\Lambda\,\mathrm{Ad}_g\,\nu = \mathrm{Ad}_{g_\lambda}\,\nu_\lambda$.

Consequently, $\Lambda \operatorname{Ad}_g \nu = \operatorname{Ad}_{g_\lambda} \Lambda\nu$ for every $\nu \in \mathbb{R}^{6n}$. It follows that $\Lambda \operatorname{Ad}_g = \operatorname{Ad}_{g_\lambda} \Lambda$. Since $g = g_\lambda h$, we find the relation $\operatorname{Ad}_h^{-1} \Lambda = \operatorname{Ad}_g^{-1} \operatorname{Ad}_{g_\lambda} \Lambda = \operatorname{Ad}_g^{-1} \Lambda \operatorname{Ad}_g$, and finally

$$\begin{aligned} \Theta(x) &= (I - \operatorname{Ad}_h^{-1} \Lambda)^{-1} \\ &= (I - \operatorname{Ad}_g^{-1} \Lambda \operatorname{Ad}_g)^{-1} \\ &= \operatorname{Ad}_g^{-1} (I - \Lambda)^{-1} \operatorname{Ad}_g, \end{aligned} \tag{4.19}$$

which is the desired expression.

We compute the time derivative of Θ along $\dot{x} = x\widehat{\Phi\mu}$, which gives

$$\begin{aligned} \mathrm{d}\Theta(x,\mu) &= -\Theta(x) \operatorname{ad}_{\Phi\mu} \operatorname{Ad}_h^{-1} \Theta(x) \\ &= -\Theta(x) \operatorname{ad}_{\Phi\mu} (\operatorname{Ad}_h^{-1} - I + I)\Theta(x) \\ &= \Theta(x) \operatorname{ad}_{\Phi\mu} - \Theta(x) \operatorname{ad}_{\Phi\mu} \Theta(x) \end{aligned} \tag{4.20}$$

where we used the fact that $\mathrm{d}\{A^{-1}\}(x,\mu) = -A(x)^{-1}\, \mathrm{d}A(x,\mu)\, A(x)^{-1}$ for a differentiable function $A : \mathcal{X} \to \mathbb{R}^{n\times n}$ such that $A(x)$ is invertible for every $x \in \mathcal{X}$. □

With these properties of Θ in place, it is possible to establish the global formulation of the underwater vehicle kinematics.

Theorem 4.4. *If $g_0 = I$, $\nu_0 = 0$, and $\alpha_0 = 0$, then the recursive relations (4.11) are equivalent to*

$$\begin{aligned} g &= F(x), \\ \nu &= \Theta(x)\Phi\mu, \\ \alpha &= -\Theta(x) \operatorname{ad}_{\Phi\mu} \Theta(x)\Phi\mu + \Theta(x)\Phi\sigma, \end{aligned} \tag{4.21}$$

where $F = (F_1, F_2, \ldots, F_n) : \mathcal{X} \to \mathrm{E}(3)^n$ is defined by

$$F_i(x) \coloneqq \prod_{j \in \kappa(i)} h_j. \tag{4.22}$$

Proof. The fact that g can be defined in terms of F as stated in (4.22) is easily seen by inspecting the recursive relations for g_i in (4.11). To show the expression for ν in (4.21), we note that the velocity-recursion in (4.11) can be stated as

$$\begin{aligned} \nu &= \operatorname{Ad}_h^{-1} \nu_\lambda + \Phi\mu \\ &= \operatorname{Ad}_h^{-1} \Lambda\nu + \Phi\mu \end{aligned} \tag{4.23}$$

which can readily be solved for the desired expression. To find the expression for the acceleration, we differentiate the velocity in (4.21) with respect to time. This gives

$$\begin{aligned} \alpha &= \mathrm{d}\Theta(x,\mu)\Phi\mu + \Theta(x)\Phi\sigma \\ &= \Theta(x) \operatorname{ad}_{\Phi\mu} \Phi\mu - \Theta(x) \operatorname{ad}_{\Phi\mu} \Theta(x)\Phi\mu + \Theta(x)\Phi\sigma \\ &= -\Theta(x) \operatorname{ad}_{\Phi\mu} \Theta(x)\Phi\mu + \Theta(x)\Phi\sigma \end{aligned} \tag{4.24}$$

where the expression for $\mathrm{d}\Theta$ derived in Proposition 4.3 and the anti-symmetry of the ad-operator were used. □

It follows from Theorem 4.4 that the body Jacobian $J : \mathcal{X} \to \mathbb{R}^{6n\times m}$ which relates ν and μ through $\nu = J(x)\mu$ can be defined as $J(x) \coloneqq \Theta(x)\Phi$. Furthermore, it follows from Proposition 4.3 that its derivative $\mathrm{d}J : \mathcal{X} \times \mathbb{R}^m \to \mathbb{R}^{6n\times m}$ can be expressed as

$$\mathrm{d}J(x,\mu) \coloneqq \Theta(x)\,\mathrm{ad}_{\Phi\mu}[\Phi - J(x)]. \tag{4.25}$$

The global expressions (4.21) can be equivalently restated in terms of the Jacobian J as

$$\begin{aligned} g &= F(x), \\ \nu &= J(x)\mu, \\ \alpha &= \mathrm{d}J(x,\mu)\mu + J(x)\sigma. \end{aligned} \tag{4.26}$$

We end this section by briefly covering generalized joint forces and their relationship with wrenches applied to the multibody underwater vehicle. The generalized joint forces are denoted $\zeta_i \in \mathbb{R}^{m_i}$. They contract naturally with the joint velocities μ_i to form instantaneous work produced by the force, $W = \langle \zeta_i, \mu_i \rangle$. If a collection of wrenches $f = (f_1, f_2, \ldots, f_n)$ is applied to the vehicle, with f_i acting on body i, then the resulting generalized joint forces required to counteract f can be computed by the recursion

$$\begin{aligned} w_i &= -f_i + \sum_{j\in\lambda^{-1}(i)} \mathrm{Ad}_{h_j}^{-\mathsf{T}}\, w_j, \\ \zeta_i &= \Phi_i^{\mathsf{T}} w_i. \end{aligned} \tag{4.27}$$

where w_i denotes the wrench transmitted from body $\lambda(i)$ to body i across joint i. It should be emphasized that (4.27) is a backwards recursion from $i = n$ to $i = 1$. Globally, the recursion computes $\zeta = -J(x)^{\mathsf{T}} f$, where $\zeta = (\zeta_1, \zeta_2, \ldots, \zeta_n)$. More details can be found in [40, Chapter 5].

4.3 Vehicle Dynamics in Global Matrix-Form

In this section, we derive the equations of motion for multibody underwater vehicles in a global matrix-form, and state their most important properties for control design purposes. We shall require the following assumptions.

Assumption 4.5.

1. The world frame is an inertial frame.
2. The bodies composing the vehicle are hydrodynamically decoupled.

Hydrodynamic decoupling in essence means that the hydrodynamic influence that the bodies have on each other is neglected. In particular, each body in the system is modeled hydrodynamically as if the other bodies were not present. This assumption is so common in the underwater vehicle literature that it usually is not explicitly stated as an assumption. It is nonetheless very important to understand that this is technically incorrect even in the context of memoryless models. Indeed, more mathematical works that focus on potential flow theory do sometimes take hydrodynamic coupling into account. Examples include [121] where the equation of motion of an articulated

swimmer immersed in potential flow is derived, and [122] where the equations of motion of several deformable bodies immersed in potential flow are derived.

Hydrodynamic decoupling allows us to model the wrenches acting on each body in the vehicle utilizing results from Chapter 3. The equation of motion of body i can then, in the absence of ocean currents, be stated as

$$M_i\alpha_i - \operatorname{ad}_{\nu_i}^{\mathsf{T}} M_i\nu_i = d_i(\nu_i) + \chi_i(g_i) + \tau_i + \overline{w}_i \tag{4.28}$$

where $M_i \coloneqq M_{R,i} + M_{H,i}$ is the total inertia matrix of body i, $d_i : \mathbb{R}^6 \to \mathbb{R}^6$ is the damping wrench of body i, $\chi_i : \mathrm{E}(3) \to \mathbb{R}^6$ is the hydrostatic wrench acting on body i, τ_i is the wrench due to thrusters and control surfaces attached to body i, and

$$\overline{w}_i \coloneqq w_i - \sum_{j \in \lambda^{-1}(i)} \operatorname{Ad}_{h_j}^{-\mathsf{T}} w_j \tag{4.29}$$

is the net wrench transmitted to body i from all joints connected to it. It is clear that (4.28) can be restated globally as

$$M\alpha - \operatorname{ad}_{\nu}^{\mathsf{T}} M\nu = d(\nu) + \chi(g) + \tau + \overline{w} \tag{4.30}$$

where $M \in \mathbb{R}^{6n\times 6n}$, $d : \mathbb{R}^{6n} \to \mathbb{R}^{6n}$, $\chi : \mathrm{E}(3)^n \to \mathbb{R}^{6n}$, $\tau \in \mathbb{R}^{6n}$, and $\overline{w} \in \mathbb{R}^{6n}$ are defined by

$$\begin{aligned} M &\coloneqq \operatorname{blkdiag}(M_1, M_2, \dots, M_n), \\ d(\nu) &\coloneqq (d_1(\nu_1), d_2(\nu_2), \dots, d_n(\nu_n)), \\ \chi(g) &\coloneqq (\chi_1(g_1), \chi_2(g_2), \dots, \chi_n(g_n)), \\ \tau &\coloneqq (\tau_1, \tau_2, \dots, \tau_n), \\ \overline{w} &\coloneqq (\overline{w}_1, \overline{w}_2, \dots, \overline{w}_n). \end{aligned} \tag{4.31}$$

The constraint forces present in $\overline{w}$ can be eliminated by premultiplying (4.30) by $J(x)^{\mathsf{T}}$. In particular, $J(x)^{\mathsf{T}}\overline{w} = \eta$, where $\eta \coloneqq (\eta_1, \eta_2, \dots, \eta_n) \in \mathbb{R}^m$ denotes the active generalized joint forces. These include for instance generalized motor forces and joint friction, and will subsequently be treated as an input. Substituting the global kinematic expressions (4.26) into (4.30) then yields the equation of motion

$$M_\circ(x)\sigma + C_\circ(x,\mu)\mu = d_\circ(x,\mu) + \chi_\circ(x) + J(x)^{\mathsf{T}}\tau + \eta, \tag{4.32}$$

where $M_\circ : \mathcal{X} \to \mathbb{R}^{m\times m}$ is the vehicle inertia matrix, $C_\circ : \mathcal{X} \times \mathbb{R}^m \to \mathbb{R}^{m\times m}$ describes velocity-dependent inertia terms, $d_\circ : \mathcal{X} \times \mathbb{R}^m \to \mathbb{R}^m$ is the generalized damping force, and $\chi_\circ : \mathcal{X} \to \mathbb{R}^m$ the generalized hydrostatic force. These objects are defined by

$$\begin{aligned} M_\circ(x) &\coloneqq J(x)^{\mathsf{T}} M J(x), \\ C_\circ(x,\mu) &\coloneqq J(x)^{\mathsf{T}} M\, \mathrm{d}J(x,\mu) - J(x)^{\mathsf{T}} \operatorname{ad}_{J(x)(\,\cdot\,)}^{\mathsf{T}} MJ(x)\mu, \\ d_\circ(x,\mu) &\coloneqq J(x)^{\mathsf{T}} d(J(x)\mu), \\ \chi_\circ(x) &\coloneqq J(x)^{\mathsf{T}} \chi(F(x)). \end{aligned} \tag{4.33}$$

The quantities (4.33) that appear in (4.32) are, unlike equations of motion derived with local coordinates, well-defined for all $(x,\mu) \in \mathcal{X} \times \mathbb{R}^m$. The equation of motion (4.32) can be viewed as an extension of similar expressions presented in [123, Chapter 7] to account for a more general mechanism topology and more general joint types.

We now state the most important properties of the quantities in (4.33).

Theorem 4.6. *The following hold:*

1. *If each M_i is symmetric and positive definite, then $M_\circ(x)$ is symmetric and positive definite for every $x \in \mathcal{X}$.*
2. *If each M_i is symmetric, then $\mathrm{d}M_\circ(x,\mu) - 2C_\circ(x,\mu)$ is skew-symmetric for all $(x,\mu) \in \mathcal{X} \times \mathbb{R}^m$.*
3. *If each d_i is dissipative, then $\langle d(x,\mu),\mu\rangle \leq 0$ for all $(x,\mu) \in \mathcal{X} \times \mathbb{R}^m$.*
4. *If each d_i is monotonically dissipative, then $\langle d(x,\mu) - d(x,\overline{\mu}), \mu - \overline{\mu}\rangle \leq 0$ for all $(x,\mu,\overline{\mu}) \in \mathcal{X} \times \mathbb{R}^m \times \mathbb{R}^m$.*

Proof. The fact that $M_\circ(x)$ is symmetric for every $x \in \mathcal{X}$ if M is symmetric is clear. The matrix $\Theta(x)$ has full rank for every $x \in \mathcal{X}$. Furthermore, since each $\Phi_i \in \mathbb{R}^{6\times m_i}$ is defined to span an m_i-dimensional subspace of $\mathbb{R}^6$, it must have rank m_i. Consequently, $\Phi = \mathrm{blkdiag}(\Phi_1, \Phi_2, \ldots, \Phi_n)$ has rank m. It follows that $J(x)$ has rank m for very $x \in \mathcal{X}$, and therefore, that $\nu = J(x)\mu$ is nonzero for every nonzero μ. Since $\langle M_\circ(x)\mu,\mu\rangle = \langle M\nu,\nu\rangle$ for all $(x,\mu) \in \mathcal{X} \times \mathbb{R}^m$ and M is positive definite, it follows that $M_\circ(x)$ is positive definite for every $x \in \mathcal{X}$.

To prove the second claim, we compute the derivative of $M_\circ$ as

$$\mathrm{d}M_\circ(x,\mu) = \mathrm{d}J(x,\mu)^\mathsf{T} M J(x) + J(x)^\mathsf{T} M\, \mathrm{d}J(x,\mu). \tag{4.34}$$

Then, for all $(x,\mu,\overline{\mu}) \in \mathcal{X} \times \mathbb{R}^m \times \mathbb{R}^m$, we find

$$\begin{aligned}\langle [\mathrm{d}M_\circ(x,\mu) - 2C_\circ(x,\mu)]\overline{\mu},\overline{\mu}\rangle &= \langle [\mathrm{d}J(x,\mu)^\mathsf{T} M J(x) - J(x)^\mathsf{T} M\, \mathrm{d}J(x,\mu)]\overline{\mu},\overline{\mu}\rangle \\ &\quad + 2\langle J(x)^\mathsf{T}\, \mathrm{ad}^\mathsf{T}_{J(x)\overline{\mu}}\, M J(x)\mu, \overline{\mu}\rangle \\ &= 0 \end{aligned} \tag{4.35}$$

where the symmetry of M and the anti-symmetry of the ad-operator were used. Consequently, $\mathrm{d}M_\circ(x,\mu) - 2C_\circ(x,\mu)$ is skew-symmetric for all $(x,\mu) \in \mathcal{X} \times \mathbb{R}^m$.

To prove the third property, let $\nu = J(x)\mu$. Then,

$$\langle d(x,\mu),\mu\rangle = \sum_{i=1}^n \langle d_i(\nu_i),\nu_i\rangle \leq 0 \tag{4.36}$$

due to dissipativity of each d_i.

To show the last property, let $\nu = J(x)\mu$ and $\overline{\nu} = J(x)\overline{\mu}$. Then

$$\langle d(x,\mu) - d(x,\overline{\mu}), \mu - \overline{\mu}\rangle = \sum_{i=1}^n \langle d_i(\nu_i) - d_i(\overline{\nu}_i), \nu_i - \overline{\nu}_i\rangle \leq 0 \tag{4.37}$$

due to monotone dissipativity of each d_i. □

It should be remarked that the second property in Theorem 4.6 can be equivalently stated as

$$\mathrm{d}M_\circ(x,\mu) = C_\circ(x,\mu) + C_\circ(x,\mu)^\mathsf{T} \tag{4.38}$$

for all $(x,\mu) \in \mathcal{X} \times \mathbb{R}^m$. This is done for a less general class of models in [45]. Furthermore, strict versions of the third and fourth property in Theorem 4.6 can be shown by similar means.

We now extend (4.32) to include the effect of a uniform and unsteady ocean current. The resulting formulations are to the author's best knowledge novel. To this end, let $v_c \in \mathbb{R}^3$ and $a_c \in \mathbb{R}^3$ denote the current velocity and acceleration expressed in the world frame, respectively. Furthermore, define the current velocities $\nu_{c,i} \in \mathbb{R}^6$ and current accelerations $\alpha_{c,i} \in \mathbb{R}^6$ by

$$\begin{aligned} \nu_{c,i} &\coloneqq \mathrm{Ad}_{g_i}^{-1} \begin{pmatrix} v_c \\ 0 \end{pmatrix} = \begin{pmatrix} R_i^\mathsf{T} v_c \\ 0 \end{pmatrix}, \\ \alpha_{c,i} &\coloneqq \mathrm{Ad}_{g_i}^{-1} \begin{pmatrix} a_c \\ 0 \end{pmatrix} - \mathrm{ad}_{\nu_i} \nu_{c,i} = \begin{pmatrix} R_i^\mathsf{T} a_c - \omega_i^\times R_i^\mathsf{T} v_c \\ 0 \end{pmatrix}, \end{aligned} \tag{4.39}$$

and the body-current relative velocities and accelerations by

$$\begin{aligned} \nu_{r,i} &\coloneqq \nu_i - \nu_{c,i}, \\ \alpha_{r,i} &\coloneqq \alpha_i - \alpha_{c,i}, \end{aligned} \tag{4.40}$$

respectively. Lastly, define the global counterparts to the above quantities,

$$\begin{aligned} \nu_c &\coloneqq (\nu_{c,1}, \nu_{c,2}, \dots, \nu_{c,n}), \\ \nu_r &\coloneqq (\nu_{r,1}, \nu_{r,2}, \dots, \nu_{r,n}), \\ \alpha_c &\coloneqq (\alpha_{c,1}, \alpha_{c,2}, \dots, \alpha_{c,n}), \\ \alpha_r &\coloneqq (\alpha_{r,1}, \alpha_{r,2}, \dots, \alpha_{r,n}). \end{aligned} \tag{4.41}$$

Following results presented in [110, 111], the inertial current wrench exerted on body i is a mapping $f_{C,i} : \mathrm{E}(3) \times \mathbb{R}^6 \times \mathbb{R}^3 \times \mathbb{R}^3 \to \mathbb{R}^6$ defined by

$$\begin{aligned} f_{C,i}(g_i, \nu_i, v_c, a_c) \coloneqq M_{H,i}\alpha_{c,i} + \mathrm{ad}_{\nu_{c,i}}^\mathsf{T} M_{H,i}\nu_{c,i} - \mathrm{ad}_{\nu,i}^\mathsf{T} M_{H,i}\nu_{c,i} \\ - \mathrm{ad}_{\nu_{c,i}}^\mathsf{T} M_{H,i}\nu_i + \begin{pmatrix} \varrho v_i I \\ \varrho v_i r_{v,i}^\times \end{pmatrix} R_i^\mathsf{T} a_c, \end{aligned} \tag{4.42}$$

where $\varrho > 0$ denotes the fluid density, $v_i \geq 0$ the effective volume of body i, and $r_{v,i} \in \mathbb{R}^3$ the effective center of volume of body i. Collecting the current wrenches in the mapping $f_C : \mathrm{E}(3)^n \times \mathbb{R}^{6n} \times \mathbb{R}^3 \times \mathbb{R}^3 \to \mathbb{R}^{6n}$ defined by $f_C(g, \nu, v_c, a_c) \coloneqq (f_{C,1}(g_1, \nu_1, v_c, a_c), f_{C,2}(g_2, \nu_2, v_c, a_c), \dots, f_{C,n}(g_n, \nu_n, v_c, a_c))$, the generalized current force $\zeta_C : \mathcal{X} \times \mathbb{R}^m \times \mathbb{R}^3 \times \mathbb{R}^3 \to \mathbb{R}^m$ can be defined by

$$\zeta_C(x, \mu, v_c, a_c) \coloneqq J(x)^\mathsf{T} f_C(F(x), J(x)\mu, v_c, a_c). \tag{4.43}$$

Furthermore, the viscous current loads are accounted for by reformulating d with the body-current relative velocity. To this end, let $d_{\circ,C} : \mathcal{X} \times \mathbb{R}^m \times \mathbb{R}^3 \to \mathbb{R}^m$ be defined by

$$d_{\circ,C}(x, \mu, v_c) \coloneqq J(x)^\mathsf{T} d(J(x)\mu - \nu_c). \tag{4.44}$$

Consequently, the equation of motion in the presence of a uniform and unsteady ocean current becomes

$$\begin{aligned} M_\circ(x)\sigma + C_\circ(x, \mu)\mu = d_{\circ,C}(x, \mu, v_c) + \zeta_C(x, \mu, v_c, a_c) \\ + \chi_\circ(x) + J(x)^\mathsf{T}\tau + \eta. \end{aligned} \tag{4.45}$$

As shown in (3.58), the equation of motion of a rigid underwater vehicle permits an attractive reformulation in terms of the vehicle-current relative velocity. It turns out that such a reformulation is also possible for multibody underwater vehicles if the allowed motion of all joints connecting from the world frame is sufficiently general. We state this precisely in the following result.

Lemma 4.1. For every $x \in \mathcal{X}$ and every $v_c \in \mathbb{R}^3$, there exists $\mu_c \in \mathbb{R}^m$ such that $J(x)\mu_c = \nu_c$ if and only if $\operatorname{span}\{e_1, e_2, e_3\} \subset \operatorname{col} \Phi_i$ for every $i \in \lambda^{-1}(0)$. In this case, it holds that $\mathrm{d}J(x, \mu_c) = 0$.

Proof. We seek to solve the system

$$J(x)\mu_c = \nu_c \tag{4.46}$$

for μ_c. In light of Proposition 4.3, we can rewrite (4.46) as

$$\Phi\mu_c = \operatorname{Ad}_g^{-1}(I - \Lambda) \operatorname{Ad}_g \nu_c \tag{4.47}$$

The above is readily shown to be equivalent to

$$\Phi_i\mu_{c,i} = \begin{cases} \nu_{c,i} & \text{if } i \in \lambda^{-1}(0) \\ 0 & \text{otherwise} \end{cases} \tag{4.48}$$

for each $i \in \{1, 2, \ldots, n\}$. Isolating the case where $i \in \lambda^{-1}(0)$, we find

$$\Phi_i\mu_{c,i} = \begin{pmatrix} R_i^{\mathsf{T}} v_c \\ 0 \end{pmatrix}, \tag{4.49}$$

which has a solution for every $v_c \in \mathbb{R}^3$ if and only if $\operatorname{span}\{e_1, e_2, e_3\} \subset \operatorname{col} \Phi_i$. In this case, it can be computed by

$$\mu_{c,i} = (\Phi_i^{\mathsf{T}}\Phi_i)^{-1}\Phi_i^{\mathsf{T}}\nu_{c,i}. \tag{4.50}$$

If $i \notin \lambda^{-1}(0)$, then the only possible solution is $\mu_{c,i} = 0$.

We will now prove that $\mathrm{d}J(x, \mu_c) = 0$ if μ_c is well-defined. It follows from (4.25) that $\mathrm{d}J(x, \mu_c) = 0$ if and only if

$$\operatorname{ad}_{\Phi\mu_c}[\Phi - J(x)]\mu = 0 \tag{4.51}$$

for every $\mu \in \mathbb{R}^m$. If $\nu = J(x)\mu$, then $\nu_i = \Phi_i\mu_i$ for every $i \in \lambda^{-1}(0)$. If $i \notin \lambda^{-1}(0)$, then $\mu_{c,i} = 0$. Since (4.51) can be restated as

$$\operatorname{ad}_{\Phi_i\mu_{c,i}}[\Phi_i\mu_i - \nu_i] = 0 \tag{4.52}$$

for every $i \in \{1, 2, \ldots, n\}$, it follows that (4.51) holds. □

If the conditions of Lemma 4.1 are satisfied, it is possible to define $\mu_r \coloneqq \mu - \mu_c$, and subsequently write $\nu_r = J(x)\mu_r$. Furthermore, letting $\sigma_c \coloneqq \dot{\mu}_c$ and $\sigma_r \coloneqq \dot{\mu}_r$, it holds that $\alpha_r = \mathrm{d}J(x, \mu)\mu_r + J(x)\sigma_r = \mathrm{d}J(x, \mu_r)\mu_r + J(x)\sigma_r$ since $\mathrm{d}J(x, \mu_c) = 0$.

The analogue of (3.58) for body i in the multibody underwater vehicle is

$$M_i\alpha_{r,i} - \operatorname{ad}_{\nu_{r,i}}^{\mathsf{T}} M_i\nu_{r,i} = d_i(\nu_{r,i}) + \overline{\chi}_i(g_i, a_c) + \tau_i + \overline{w}_i, \tag{4.53}$$

where $\overline{\chi}_i : \mathrm{E}(3) \to \mathbb{R}^6$ is a wrench of the form (3.59) that contains the hydrostatic and current acceleration-reaction wrenches. A global formulation of (4.53) is

$$M\alpha_r - \mathrm{ad}_{\nu_r}^{\mathsf{T}} M\nu_r = d(\nu_r) + \overline{\chi}(g, a_c) + \tau + \overline{w}, \tag{4.54}$$

where $\chi : \mathrm{E}(3)^n \times \mathbb{R}^3 \to \mathbb{R}^6$ is defined by

$$\overline{\chi}(g, a_c) \coloneqq (\overline{\chi}_1(g_1, a_c), \overline{\chi}_2(g_2, a_c), \ldots, \overline{\chi}_n(g_n, a_c)). \tag{4.55}$$

Premultiplying (4.54) by $J(x)^{\mathsf{T}}$ and expressing (g, ν_r, α_r) in terms of (x, μ_r, σ_r) then results in

$$M_\circ(x)\sigma_r + C_\circ(x, \mu_r)\mu_r = d_\circ(x, \mu_r) + \overline{\chi}_\circ(x, a_c) + J(x)^{\mathsf{T}}\tau + \eta, \tag{4.56}$$

where $\overline{\chi}_\circ : \mathcal{X} \times \mathbb{R}^3 \to \mathbb{R}^m$ is defined by

$$\overline{\chi}_\circ(x, a_c) \coloneqq J(x)^{\mathsf{T}}\overline{\chi}(F(x), a_c). \tag{4.57}$$

The formulation (4.56) is usable for all floating-base multibody underwater vehicles. There are however cases of interest that do not satisfy Lemma 4.1. One example is a manipulator arm attached to a subsea structure by means of a common revolute or prismatic joint. For these applications, the more general formulation (4.45) should be used.

4.4 Recursive Dynamics Algorithms

The global matrix formulations presented in Section 4.3 are well-suited for stability analysis. However, implementing this form of the equations directly can be cumbersome for vehicles comprising a large number of bodies. We therefore present a generalized inverse dynamics algorithm suitable for implementing feedback control laws, and a forward dynamics algorithm for use in simulation studies.

4.4.1 Generalized Newton-Euler Algorithm

In this section, we present a recursive inverse dynamics algorithm that computes the quantity

$$\zeta = M_\circ(x)\overline{\sigma} + C_\circ(x, \mu)\overline{\mu} - J(x)^{\mathsf{T}} f - \eta. \tag{4.58}$$

Model-based feedback control laws for underwater vehicle-manipulator systems often involve an expression of the form (4.58). However, actually implementing these expressions can be a daunting task. Indeed, typically no methods are provided to compute the involved quantities. Our approach, presented in Algorithm 1, is based on the standard Newton-Euler algorithm.

The algorithm has three stages. First, a few kinematic quantities are initialized. Second, a forward pass computes the involved configurations, velocities, accelerations, and the wrenches acting on each body. Lastly, a backward pass, readily seen to be equivalent to (4.27), propagates these wrenches through the multibody system and computes the generalized forces acting on the joints. It should be remarked that if $\overline{\mu} = \mu$, then Algorithm 1 reduces to the standard Newton-Euler algorithm presented in for instance [40, Chapter 5]. We now establish that Algorithm 1 does in fact compute (4.58).

Algorithm 1 Generalized Newton-Euler Algorithm

$g_0 = I$,
$\nu_0 = 0$
$\overline{\nu}_0 = 0$
$\overline{\alpha}_0 = 0$
for $i = 1$ to n **do**
  $h_i = c_i x_i$
  $g_i = g_{\lambda(i)} h_i$
  $\nu_i = \mathrm{Ad}_{h_i}^{-1} \nu_{\lambda(i)} + \Phi_i \mu_i$
  $\overline{\nu}_i = \mathrm{Ad}_{h_i}^{-1} \overline{\nu}_{\lambda(i)} + \Phi_i \overline{\mu}_i$
  $\overline{\alpha}_i = \mathrm{Ad}_{h_i}^{-1} \overline{\alpha}_{\lambda(i)} + \mathrm{ad}_{\overline{\nu}_i} \Phi_i \mu_i + \Phi_i(\overline{\sigma}_i + \mathrm{ad}_{\mu_i}^{\mathfrak{r}_i} \overline{\mu}_i)$
  $w_i = M_i \overline{\alpha}_i - \mathrm{ad}_{\overline{\nu}_i}^{\mathsf{T}} M_i \nu_i - f_i$
end for
for $i = n$ to 1 **do**
  $\zeta_i = \Phi_i^{\mathsf{T}} w_i - \eta_i$
  if $\lambda(i) \neq 0$ **then**
    $w_{\lambda(i)} = w_{\lambda(i)} + \mathrm{Ad}_{h_i}^{-\mathsf{T}} w_i$
  end if
end for
return ζ

Theorem 4.7. *Algorithm 1 computes* (4.58).

Proof. It is evident that Algorithm 1 computes

$$\zeta = J(x)^{\mathsf{T}}[M\overline{\alpha} - \mathrm{ad}_{\overline{\nu}}^{\mathsf{T}} M\nu - f] - \eta. \tag{4.59}$$

Furthermore, it is seen that

$$\begin{aligned} \nu &= J(x)\mu, \\ \overline{\nu} &= J(x)\overline{\mu}. \end{aligned} \tag{4.60}$$

Writing the recursion relation for $\overline{\alpha}$ globally yields

$$(I - \mathrm{Ad}_h^{-1} \Lambda)\overline{\alpha} = \mathrm{ad}_{\overline{\nu}} \Phi\mu + \Phi(\overline{\sigma} + \mathrm{ad}_{\mu}^{\mathfrak{r}} \overline{\mu}), \tag{4.61}$$

and consequently,

$$\begin{aligned} \overline{\alpha} &= \Theta(x)\, \mathrm{ad}_{\overline{\nu}} \Phi\mu + \Theta(x)\Phi(\overline{\sigma} + \mathrm{ad}_{\mu}^{\mathfrak{r}} \overline{\mu}) \\ &= -\Theta(x)\, \mathrm{ad}_{\Phi\mu}\, \overline{\nu} + J(x)\overline{\sigma} + \Theta(x)\Phi\, \mathrm{ad}_{\mu}^{\mathfrak{r}}\, \overline{\mu} \\ &= -\Theta(x)\, \mathrm{ad}_{\Phi\mu}\, J(x)\overline{\mu} + J(x)\overline{\sigma} + \Theta(x)\, \mathrm{ad}_{\Phi\mu}\, \Phi\overline{\mu} \\ &= \Theta(x)\, \mathrm{ad}_{\Phi\mu}[\Phi - J(x)]\overline{\mu} + J(x)\overline{\sigma} \\ &= \mathrm{d}J(x,\mu)\overline{\mu} + J(x)\overline{\sigma}. \end{aligned} \tag{4.62}$$

Substituting the derived expressions for ν, $\overline{\nu}$, and $\overline{\alpha}$ into (4.59) yields

$$\zeta = J(x)^{\mathsf{T}}[MJ(x)\overline{\sigma} + M\, \mathrm{d}J(x,\mu)\overline{\mu} - \mathrm{ad}_{J(x)\overline{\mu}}^{\mathsf{T}} MJ(x)\mu - f] - \eta, \tag{4.63}$$

which in light of (4.33) constitutes the desired result. □

4.4.2 Composite-Rigid-Body Algorithm

In this section, we present a forward dynamics algorithm for multibody underwater vehicles that computes the accelerations σ predicted by the general equation of motion (4.45). It is based on the composite-rigid-body algorithm found in [40, Chapter 6]. We first use a modified Newton-Euler algorithm, presented as Algorithm 2, to compute the generalized joint forces modulo the term $M_\circ(x)\sigma$, which we denote ζ. Then, we use a composite-rigid-body algorithm, stated as Algorithm 3, to compute $M_\circ(x)$. The joint acceleration can then be computed with the relation $\sigma = -M_\circ(x)^{-1}\zeta$.

Algorithm 2 Modified Newton-Euler Algorithm

$\nu_{r,0} = -(v_c, 0)$
$\alpha_{r,0} = -(a_c, 0)$
$a_{e,0} = a_g - a_c$
for $i = 1$ to n **do**
    $h_i = c_i x_i$
    $\nu_{r,i} = \mathrm{Ad}_{h_i}^{-1}\, \nu_{r,\lambda(i)} + \Phi_i \mu_i$
    $\alpha_{r,i} = \mathrm{Ad}_{h_i}^{-1}\, \alpha_{r,\lambda(i)} + \mathrm{ad}_{\nu_{r,i}}\, \Phi_i \mu_i$
    $a_{e,i} = S_i^{\mathsf{T}}\, a_{e,\lambda(i)}$, where S_i is the rotation associated with h_i
    $w_i = M_i \alpha_{r,i} - \mathrm{ad}_{\nu_{r,i}}^{\mathsf{T}}\, M_i \nu_{r,i} - d_i(\nu_{r,i}) - \overline{\chi}_i(g_i, a_c) - \tau_i$
end for
for $i = n$ to 1 **do**
    $\zeta_i = \Phi_i^{\mathsf{T}} w_i - \eta_i$
    if $\lambda(i) \neq 0$ **then**
        $w_{\lambda(i)} = w_{\lambda(i)} + \mathrm{Ad}_{h_i}^{-\mathsf{T}}\, w_i$
    end if
end for
return ζ

Algorithm 2 has three stages. First, the relative velocity, relative acceleration, and effective acceleration are initialized. In the forward pass, the current-relative kinematic quantities that enter the equations of motion are computed recursively, an approach inspired by [35]. Since the quantity $\overline{\chi}_i$ depends solely on constant parameters and the effective acceleration $a_{e,i}$, it is not necessary to compute every configuration g_i. The last step in the forward pass computes the wrenches acting on each body. Lastly, a backward pass propagates the computed wrenches through the multibody system and computes the generalized forces acting in the joints.

The composite-rigid-body algorithm, here presented as Algorithm 3, is essentially unmodified from [40, Table 6.2]. It must be emphasized that $M_{\circ,ij} \in \mathbb{R}^{m_i \times m_j}$ here denotes the (i, j) block of the matrix $M_\circ$.

Algorithm 3 Composite-Rigid-Body Algorithm

$M_\circ = 0$
for $i = 1$ to n **do**
    $M_i^c = M_i$
end for
for $i = n$ to 1 **do**
    if $\lambda(i) \neq 0$ **then**
        $M_{\lambda(i)}^c = M_{\lambda(i)}^c + \mathrm{Ad}_{h_i}^{-\mathsf{T}} M_i^c \mathrm{Ad}_{h_i}^{-1}$
    end if
    $X = M_i^c \Phi_i$
    $M_{\circ,ii} = \Phi_i^\mathsf{T} X$
    $j = i$
    while $\lambda(j) \neq 0$ **do**
        $X = \mathrm{Ad}_{h_j}^{-\mathsf{T}} X$
        $j = \lambda(j)$
        $M_{\circ,ij} = X^\mathsf{T} \Phi_j$
        $M_{\circ,ji} = M_{\circ,ij}^\mathsf{T}$
    end while
end for
return $M_\circ$

Part II

Hybrid Feedback Control

Chapter 5

Synergistic PID and Output Feedback Control on Matrix Lie Groups

In this chapter, we present several novel synergistic trajectory tracking controllers for mechanical systems defined on matrix Lie groups with left-invariant metrics. In particular, we propose synergistic PD and output feedback control laws ensuring global asymptotic tracking. Furthermore, we propose two synergistic PID control laws that ensure global asymptotic tracking in the presence of an unknown constant disturbance in the system dynamics. Finally, a simulation study with a small underwater vehicle is conducted.

The material in this chapter is based on [83].

5.1 Introduction

While several hybrid feedback control laws that guarantee global asymptotic tracking on $\mathbb{R}^n$, SO(3), and SE(3) exist, much less work has been done on global hybrid tracking controllers with integral action. One example is the work [69], where a hybrid control law with integral action ensuring global asymptotic tracking on SO(3) is presented. The switching logic employed here depends explicitly on the integral state due to cross-terms that are employed in the Lyapunov analysis.

A continuous-time intrinsic controller with integral action on compact Lie groups is presented in [124]. The integral action stems from integration of the P-action in the controller. The controller ensures bounded tracking error in the presence of uncertainty, and almost global asymptotic stability in the absence of uncertainty. Several similar controllers with integral action are presented in [125]. Here, the integral action stems from integrating the PD-action in the controller. This controller achieves almost global asymptotic stability in the presence of a constant disturbance.

The remainder of this chapter is organized as follows. In Section 5.2, we present the class of mechanical systems and reference trajectories considered in this chapter, and derive the associated tracking error system. We then treat synergistic functions in Section 5.3. In Section 5.4, we present a synergistic PD control law that ensures global asymptotic tracking, and in Section 5.5 an output feedback modification of this control law. Section 5.6 introduces two novel synergistic control laws with integral action, both of which ensure global asymptotic tracking of a given bounded reference

trajectory in the presence of a constant and unknown disturbance. Finally, Section 5.7 presents simulation results for the integral control of a small underwater vehicle.

5.2 Modeling

Consider a fully actuated simple mechanical system with left-invariant metric on a matrix Lie group $\mathcal{G} \subset \mathrm{GL}(n)$ of dimension m,

$$\left.\begin{aligned} \dot{g} &= g\widehat{\nu} \\ M\dot{\nu} - \mathrm{ad}_{\nu}^{\mathsf{T}} M\nu &= d(\nu) + \chi(g) + b + \tau \end{aligned}\right\} (g, \nu, \tau) \in \mathcal{G} \times \mathbb{R}^m \times \mathbb{R}^m. \tag{5.1}$$

In accordance with the modeling theory for rigid underwater vehicles outlined in Chapter 3, $g \in \mathcal{G}$ is the configuration of the mechanical system, $\nu \in \mathbb{R}^m$ is the system velocity, $M \in \mathbb{R}^{m \times m}$ is the symmetric and positive definite inertia matrix associated with the left-invariant metric on $\mathcal{G}$, $d : \mathbb{R}^m \to \mathbb{R}^m$ is a continuous velocity-dependent force, $\chi : \mathcal{G} \to \mathbb{R}^m$ is a continuous configuration-dependent force, $b \in \mathbb{R}^m$ is a constant disturbance, and $\tau \in \mathbb{R}^m$ is an idealized input force.

The desired configuration, desired velocity, and desired acceleration are assumed to form a solution to the constrained differential equation with input

$$\left.\begin{aligned} \dot{g}_d &= g_d\widehat{\nu}_d \\ \dot{\nu}_d &= \alpha_d \end{aligned}\right\} (g_d, \nu_d, \alpha_d) \in \Omega \times c\mathbb{B} \times l\mathbb{B}, \tag{5.2}$$

where $\Omega \subset \mathcal{G}$ is a compact set, $c > 0$ and $l > 0$. We remark that we consider (5.2) as a special case of a hybrid system with input, such that solutions to (5.2) are characterized by Definition 2.27. Consequently, a solution to (5.2) may with some abuse of notion be regarded as a mapping $t \mapsto (g_d(t), \nu_d(t), \alpha_d(t))$ defined on some subinterval E of $\mathbb{R}_{\geq 0}$ containing the origin such that the following three properties hold.

1. $\operatorname{rge} g_d \subset \mathcal{G}$, g_d is continuously differentiable, bounded, and has determinant bounded away from zero. Furthermore, $\dot{g}_d(t) = g_d(t)\widehat{\nu}_d(t)$ for every $t \in E$.
2. $\operatorname{rge} \nu_d \subset \mathbb{R}^m$, ν_d is Lipschitz continuous and bounded. Furthermore $\dot{\nu}_d(t) = \alpha_d(t)$ for almost every $t \in E$.
3. $\operatorname{rge} \alpha_d \subset \mathbb{R}^m$, α_d is measurable and bounded.

Conversely, every mapping $t \mapsto (g_d(t), \nu_d(t), \alpha_d(t))$ defined on some subinterval E of $\mathbb{R}_{\geq 0}$ containing the origin that satisfies the above three properties is a solution to (5.2) for an appropriate choice of compact set $\Omega \subset \mathcal{G}$, $c > 0$, and $l > 0$.

For a matrix Lie group $\mathcal{G}$ that is not a properly embedded submanifold of $\mathbb{R}^{n \times n}$, that is, a matrix Lie group that is not closed in $\mathbb{R}^{n \times n}$, boundedness of a desired trajectory g_d in $\mathcal{G}$ does not imply that there exists a compact set $\Omega \subset \mathcal{G}$ such that $\operatorname{rge} g_d \subset \Omega$. This is because g_d in this case can coverge to a point outside of $\mathcal{G}$. The following example shows that the requirement on the trajectory determinant is necessary if $\mathcal{G}$ is not properly embedded.

Example 5.1. Consider the matrix Lie group $\mathrm{GL}(1) = \mathbb{R} \setminus \{0\}$, which is not properly embedded in $\mathbb{R}$. The trajectory $g_d : [0, \infty) \to \mathrm{GL}(1)$ defined by

$$g_d(t) \coloneqq \frac{1}{1+t} \tag{5.3}$$

is smooth and bounded in $\mathbb{R}$, but leaves every compact subset of GL(1).

Given a configuration $g \in \mathcal{G}$ and a desired configuration $g_d \in \mathcal{G}$, we define the configuration error

$$g_e \coloneqq g_d^{-1} g. \tag{5.4}$$

Clearly, $g_e = I$ if and only if $g = g_d$. Furthermore, g_e is left-invariant in the sense that $g_d^{-1} g = (h g_d)^{-1}(hg)$ for every $h \in \mathcal{G}$. With the left-invariant error g_e, we associate the error velocity

$$\nu_e \coloneqq \nu - \operatorname{Ad}_{g_e}^{-1} \nu_d. \tag{5.5}$$

It is convenient for notation to also define the body reference velocity $\nu_r \coloneqq \operatorname{Ad}_{g_e}^{-1} \nu_d$ such that $\nu_e = \nu - \nu_r$. Lastly, let

$$\alpha_r \coloneqq \operatorname{Ad}_{g_e}^{-1} \alpha_d \tag{5.6}$$

denote the reference acceleration. It is emphasized that α_r is not the time-derivative of ν_r, which is found to be $\dot{\nu}_r = \alpha_r - \operatorname{ad}_{\nu_e} \nu_r$. We then perform the change of variables $(g, \nu, \tau, g_d, \nu_d, \alpha_d) \mapsto (g_e, \nu_e, \tau, g_d, \nu_d, \alpha_d)$, and restrict the desired coniguration, desired velocity, and desired acceleration as done in (5.2). This results in the tracking error system

$$\begin{aligned}
\dot{g}_e &= g_e \widehat{\nu}_e \\
\dot{\nu}_e &= M^{-1}[\operatorname{ad}_\nu^\mathsf{T} M\nu + d(\nu) + \chi(g) + b + \tau] - \dot{\nu}_r \\
\dot{g}_d &= g_d \widehat{\nu}_d \\
\dot{\nu}_d &= \alpha_d \\
&\underbrace{\qquad\qquad\qquad\qquad\qquad\qquad\qquad\qquad\qquad\qquad}_{(g_e, \nu_e, \tau, g_d, \nu_d, \alpha_d) \in \mathcal{G} \times \mathbb{R}^m \times \mathbb{R}^m \times \Omega \times c\mathbb{B} \times l\mathbb{B}.}
\end{aligned} \tag{5.7}$$

Throughout this chapter, we will make heavy use of the feedforward control $\kappa_{ff} : \mathcal{G} \times \mathbb{R}^m \times \mathbb{R}^m \to \mathbb{R}^m$ defined by

$$\kappa_{ff}(g, \nu, \alpha) \coloneqq M\alpha - \operatorname{ad}_\nu^\mathsf{T} M\nu - d(\nu) + \chi(g). \tag{5.8}$$

The following lemma introduces two characterizations of the velocity error dynamics in terms of (5.8).

Lemma 5.1. The velocity error dynamics in (5.7) can be restated as

$$\begin{aligned}
\dot{\nu}_e &= -\nabla^M_{\nu+\nu_r} \nu_e + M^{-1}[d(\nu) - d(\nu_r) + b + \tau - \kappa_{ff}(g, \nu_r, \alpha_r)] \\
&= M^{-1}[b + \tau - \kappa_{ff}(g, \nu, \dot{\nu}_r)],
\end{aligned} \tag{5.9}$$

where κ_{ff} is defined by (5.8).

Proof. Since $M^{-1} \operatorname{ad}_\nu^\mathsf{T} M\nu = -\nabla^M_\nu \nu$, we find that

$$\begin{aligned}
\dot{\nu}_e = &-\nabla^M_\nu \nu + \nabla^M_{\nu_r} \nu_r + \operatorname{ad}_{\nu_e} \nu_r \\
&+ M^{-1}[d(\nu) - d(\nu_r) + b + \tau - \kappa_{ff}(g, \nu_r, \alpha_r)].
\end{aligned} \tag{5.10}$$

Furthermore,

$$\begin{aligned}\nabla^M_\nu \nu &= \nabla^M_\nu \nu_e + \nabla^M_\nu \nu_r \\ &= \nabla^M_\nu \nu_e + \nabla^M_{\nu_r} \nu_r + \nabla^M_{\nu_e} \nu_r \\ &= \nabla^M_{\nu+\nu_r} \nu_e + \nabla^M_{\nu_r} \nu_r + \nabla^M_{\nu_e} \nu_r - \nabla^M_{\nu_r} \nu_e \\ &= \nabla^M_{\nu+\nu_r} \nu_e + \nabla^M_{\nu_r} \nu_r + \operatorname{ad}_{\nu_e} \nu_r,\end{aligned}$$

where the bilinearity of ∇^M and the fact that $\operatorname{ad}_\mu \nu = \nabla^M_\mu \nu - \nabla^M_\nu \mu$ for every $\nu \in \mathbb{R}^m$ and $\mu \in \mathbb{R}^m$ were used. Substituting this expression for $\nabla^M_\nu \nu$ into (5.10) gives the first equality in (5.9). The second equality in (5.9) is straightforward to verify. □

5.3 Synergistic Functions

In this section, we extend the concept of a synergistic function as defined in [65] for SO(3) to general matrix Lie groups, and present some general properties of these functions.

Definition 5.2. *Let $\mathcal{G} \subset \mathrm{GL}(n)$ be a matrix Lie group, $\mathcal{A} \subset \mathcal{G}$ be a compact set, and $Q \subset \mathbb{Z}$ be a finite set. A proper and continuously differentiable function $U : \mathcal{G} \times Q \to \mathbb{R}_{\geq 0}$ is synergistic on $\mathcal{G}$ relative to $\mathcal{A}$ with gap exceeding $\delta > 0$ if*

1. *the zero set of U,*

$$\operatorname{Zero} U \coloneqq \{(g, q) \in \mathcal{G} \times Q : U(g, q) = 0\}, \tag{5.11}$$

   satisfies $\pi_1(\operatorname{Zero} U) = \mathcal{A}$;
2. *there exists $\delta > 0$ such that the synergy gap*

$$\mu_U(g, q) \coloneqq U(g, q) - \min_{s \in Q} U(g, s), \tag{5.12}$$

   satisfies $\mu_U(g, q) > \delta$ for all $(g, q) \in (\operatorname{Crit} U \cup (\mathcal{A} \times Q)) \setminus \operatorname{Zero} U$, where

$$\operatorname{Crit} U \coloneqq \{(g, q) \in \mathcal{G} \times Q : \mathrm{d}U(g, q) = 0\}, \tag{5.13}$$

   denotes the set of critical points of U.

Item 1 in Definition 5.2 states that $g \in \mathcal{A}$ if and only if there exists at least one $q \in Q$ such that $U(g, q) = 0$. Item 2 in Definition 5.2 may be easier to understand when restated as two separate conditions without direct reference to the synergy gap μ_U. This may be done as follows: There exists $\delta > 0$ such that for every $(g, q) \in \mathcal{G} \times Q$,

1. if $g \in \mathcal{A}$, then either $U(g, q) = 0$ or $U(g, q) > \delta$;
2. if $\mathrm{d}U(g, q) = 0$, then either $U(g, q) = 0$ or $U(g, q) > U(g, s) + \delta$ for some $s \in Q$.

To arrive at the first claim, note that $\mu_U(g, q) = U(g, q)$ for every $(g, q) \in \mathcal{A} \times Q$ because, by item 1 in Definition 5.2, there exists $s \in Q$ such that $(g, s) \in \operatorname{Zero} U$. The following proposition characterizes some general properties of functions defined on $\mathcal{G} \times Q$.

Proposition 5.3. *Let $\mathcal{G} \subset \mathrm{GL}(n)$ be a matrix Lie group, $Q \subset \mathbb{Z}$ be finite, and $U : \mathcal{G} \times Q \to \mathbb{R}_{\geq 0}$. Then the following hold:*

1. *If U is continuous, then the synergy gap $\mu_U : \mathcal{G} \times Q \to \mathbb{R}_{\geq 0}$ is continuous.*
2. *If U is continuously differentiable, then* $\operatorname{Zero} U \subset \operatorname{Crit} U$.

Proof. We prove the first claim. Since $g \mapsto U(g, q)$ is continuous and Q is finite, the mapping $g \mapsto \min_{q \in Q} U(g, q)$ is the minimum of a finite number of continuous functions, and is therefore continuous. The synergy gap μ_U is then the difference between two continuous functions and is therefore continuous. We prove the second claim. It is clear that every element of $\operatorname{Zero} U$ constitutes a global minimum of U. Consequently, if $(g, q) \in \operatorname{Zero} U$, then for every $\nu \in \mathbb{R}^m$ and $s > 0$, it holds that

$$\frac{U(g \exp(s\widehat{\nu}), q)}{s} = \frac{U(g \exp(s\widehat{\nu}), q) - U(g, q)}{s} \geq 0. \tag{5.14}$$

Taking the limit $s \searrow 0$ shows that $\langle \mathrm{d}U(g, q), \nu \rangle \geq 0$ for every $\nu \in \mathbb{R}^m$. Therefore, it must hold that $(g, q) \in \operatorname{Crit} U$. Consequently, $\operatorname{Zero} U \subset \operatorname{Crit} U$. □

A synergistic function induces the following kinematic hybrid control law

$$\begin{cases} \dot{q} = 0 & (g, q) \in C_U \\ q^+ \in G_U(g) & (g, q) \in D_U \\ \nu = -\,\mathrm{d}U(g, q) \end{cases} \tag{5.15}$$

with state $q \in Q$, input $g \in \mathcal{G}$ and output ν, where the flow set $C_U \subset \mathcal{G} \times Q$, jump set $D_U \subset \mathcal{G} \times Q$ and jump map $G_U : \mathcal{G} \rightrightarrows Q$ are defined according to

$$\begin{aligned} C_U &\coloneqq \{(g, q) \in \mathcal{G} \times Q : \mu_U(g, q) \leq \delta\}, \\ D_U &\coloneqq \{(g, q) \in \mathcal{G} \times Q : \mu_U(g, q) \geq \delta\}, \\ G_U(g) &\coloneqq \{q \in Q : \mu_U(g, q) = 0\}. \end{aligned} \tag{5.16}$$

The data (5.16) satisfies the following properties, reminiscent of the input hybrid basic conditions presented as Assumption 2.25.

Proposition 5.4. *Let $\mathcal{G} \subset \mathrm{GL}(n)$ be a matrix Lie group, $Q \subset \mathbb{Z}$ be finite, and $U : \mathcal{G} \times Q \to \mathbb{R}_{\geq 0}$ be synergistic with gap exceeding $\delta > 0$. Then the following hold:*

1. *The sets C_U and D_U defined in (5.16) are relatively closed in $\mathrm{GL}(n) \times \mathbb{R}$. If $\mathcal{G}$ is properly embedded, then C_U and D_U are closed in $\mathbb{R}^{n \times n} \times \mathbb{R}$.*
2. *The set-valued mapping G_U defined in (5.16) is outer semicontinuous and locally bounded relative to $\mathcal{G}$.*

Proof. We prove the first claim. Since μ_U is continuous by item 2 in Proposition 5.3, and sublevel sets and superlevel sets of continuous functions are relatively closed in the domain of the function, it follows that C_U and D_U are relatively closed in $\mathcal{G} \times Q$. $\mathcal{G}$ is relatively closed in $\mathrm{GL}(n)$ by definition, and Q is closed in $\mathbb{R}$ because it is finite. Since the product of two closed sets is closed in the product topology, $\mathcal{G} \times Q$ is in turn relatively closed in $\mathrm{GL}(n) \times \mathbb{R}$. It follows that C_U and D_U are relatively closed in $\mathrm{GL}(n) \times \mathbb{R}$. Recall that $\mathcal{G}$ is properly embedded if and only if it is relatively closed in $\mathbb{R}^{n \times n}$. The preceding argument can then be repeated to show that C_U and D_U are closed in $\mathbb{R}^{n \times n} \times \mathbb{R}$.

We prove the second claim. The graph of G_U is found to be

$$\operatorname{gph} G_U = \{(g, q) \in \mathcal{G} \times Q : \mu_U(g, q) = 0\},$$

which is a level set of the continuous function μ_U. It follows that $\operatorname{gph} G_U$ is relatively closed in $\mathcal{G} \times Q$, and therefore relatively closed in $\mathcal{G} \times \mathbb{R}$. By Lemma 2.2, G_U is outer semicontinuous relative to $\mathcal{G}$. G_U is locally bounded relative to $\mathcal{G}$ because $G_U(g) \subset Q$ for every $g \in \mathcal{G}$ and Q is bounded. □

We end this section with an example of a synergistic potential function on $\widetilde{\mathrm{SE}}(3)$ which is inspired by the work [71].

Example 5.5. Let $\mathcal{G} = \widetilde{\mathrm{SE}}(3)$, $Q = \{-1, 1\}$, and consider the function $U : \widetilde{\mathrm{SE}}(3) \times Q \to \mathbb{R}_{\geq 0}$ defined by

$$U(g, q) \coloneqq \frac{k_1}{2}|p|^2 + 2k_2(1 - q\eta), \tag{5.17}$$

where $k_1, k_2 > 0$ are gains. We aim to show that U is synergistic with gap exceeding $\delta > 0$ relative to $\mathcal{A} = \{g \in \widetilde{\mathrm{SE}}(3) : p = 0, \eta = \pm 1\}$. It is clear that U is proper and continuously differentiable. Furthermore,

$$\operatorname{Zero} U = \{(g, q) \in \widetilde{\mathrm{SE}}(3) \times Q : p = 0, q\eta = 1\}, \tag{5.18}$$

and it therefore holds that $\pi_1(\operatorname{Zero} U) = \mathcal{A}$. Consequently, U satisfies item 1 in Definition 5.2. It is straightforward to verify that

$$\mathrm{d}U(g, q) = \begin{pmatrix} k_1 \operatorname{rot}(z)^\mathsf{T} p \\ k_2 q \epsilon \end{pmatrix}, \tag{5.19}$$

and, since $\operatorname{rot}(z)$ has full rank for every $z \in \mathbb{S}^3$ and $\epsilon = 0$ if and only if $\eta = \pm 1$, it holds that $\operatorname{Crit} U = \mathcal{A} \times Q$. Then,

$$\begin{aligned}(\operatorname{Crit} U \cup (\mathcal{A} \times Q)) \setminus \operatorname{Zero} U &= (\mathcal{A} \times Q) \setminus \operatorname{Zero} U \\ &= \{(g, q) \in \widetilde{\mathrm{SE}}(3) \times Q : p = 0, q\eta = -1\}.\end{aligned}$$

Now, $\mu_U(g, q) = 4k_2 > 0$ for every $(g, q) \in (\operatorname{Crit} U \cup (\mathcal{A} \times Q)) \setminus \operatorname{Zero} U$. It follows that U also satisfies item 2 in Definition 5.2. Therefore, U is synergistic on $\widetilde{\mathrm{SE}}(3)$ relative to $\mathcal{A}$ with gap exceeding δ, where $4k_2 > \delta > 0$.

5.4 Synergistic PD Control

In this section, we employ a synergistic function to design a hybrid PD controller for the control model which renders the closed-loop system globally pre-asymptotically stable in the absence of external disturbances, that is $b = 0$.

We propose the following synergistic PD controller

$$\begin{cases} \dot{q} = 0 & (g_e, \nu_e, g_d, \nu_d, \alpha_d, q) \in \widetilde{C} \\ q^+ \in G_U(g_e) & (g_e, \nu_e, g_d, \nu_d, \alpha_d, q) \in \widetilde{D} \\ \tau = \kappa_{ff}(g, \nu_r, \alpha_r) & \\ \qquad - \mathrm{d}U(g_e, q) - K\nu_e & \end{cases} \tag{5.20}$$

where the feedforward control $\kappa_{ff} : \mathcal{G} \times \mathbb{R}^m \times \mathbb{R}^m \to \mathbb{R}^m$ is defined by (5.8) and the controller flow set and jump set are defined by

$$\begin{aligned}\widetilde{C} &\coloneqq \{(g_e, \nu_e, g_d, \nu_d, \alpha_d, q) : (g_e, q) \in C_U, \nu_e \in \mathbb{R}^m, g_d \in \mathcal{G}, \nu_d \in \mathbb{R}^m, \alpha_d \in \mathbb{R}^m\},\\ \widetilde{D} &\coloneqq \{(g_e, \nu_e, g_d, \nu_d, \alpha_d, q) : (g_e, q) \in D_U, \nu_e \in \mathbb{R}^m, g_d \in \mathcal{G}, \nu_d \in \mathbb{R}^m, \alpha_d \in \mathbb{R}^m\}.\end{aligned} \tag{5.21}$$

Observe that the control law (5.20) comprises a proportional action $\mathrm{d}U$ and a derivative action $K\nu_e$. Moreover, the feedforward control as it appears in the control law (5.20) is independent of the velocity.

Using Lemma 5.1 it is straightforward to verify that the control law (5.20) applied to the system (5.1), while restricting the desired trajectories to those generated by (5.2) for some compact set $\Omega \subset \mathcal{G}$, $c > 0$, and $l > 0$, results in the closed loop system

$$\left.\begin{aligned}\dot{g}_e &= g_e \widehat{\nu}_e\\ \dot{\nu}_e &= -\nabla^M_{\nu+\nu_r}\nu_e + M^{-1}(d(\nu) - d(\nu_r))\\ &\quad - M^{-1}(\mathrm{d}U(g_e, q) + K\nu_e)\\ \dot{g}_d &= g_d \widehat{\nu}_d\\ \dot{\nu}_d &\in l\mathbb{B}\end{aligned}\right\} \quad (g_e, \nu_e, g_d, \nu_d, q) \in C$$
$$q^+ \in G_U(g_e) \qquad (g_e, \nu_e, g_d, \nu_d, q) \in D \tag{5.22}$$

where the flow set C and the jump set D are defined by

$$\begin{aligned}C &\coloneqq \{(g_e, \nu_e, g_d, \nu_d, q) : (g_e, q) \in C_U, \nu_e \in \mathbb{R}^m, g_d \in \Omega, \nu_d \in c\mathbb{B}\},\\ D &\coloneqq \{(g_e, \nu_e, g_d, \nu_d, q) : (g_e, q) \in D_U, \nu_e \in \mathbb{R}^m, g_d \in \Omega, \nu_d \in c\mathbb{B}\}.\end{aligned} \tag{5.23}$$

Before we state the main result of this section, we recall from Definition 3.9 that $d : \mathbb{R}^m \to \mathbb{R}^m$ is strictly monotonically dissipative modulo K if $d(0) = 0$, d is continuous, and $\langle d(\nu) - d(\overline{\nu}), \nu - \overline{\nu}\rangle < \langle K(\nu - \overline{\nu}), \nu - \overline{\nu}\rangle$ for every $\nu \in \mathbb{R}^m$ and every $\overline{\nu} \in \mathbb{R}^m$ such that $\nu \neq \overline{\nu}$.

Theorem 5.6. *If U is synergistic on $\mathcal{G}$ relative to $\mathcal{A}$ with gap exceeding $\delta > 0$ and d is strictly monotonically dissipative modulo K, then the compact set*

$$\mathcal{T} \coloneqq \mathcal{A} \times \{0\} \times \Omega \times c\mathbb{B} \times Q \tag{5.24}$$

is globally pre-asymptotically stable for the system (5.22).

Proof. Let

$$X \coloneqq \mathcal{G} \times \mathbb{R}^m \times \Omega \times c\mathbb{B} \times Q, \tag{5.25}$$

and denote by $x \coloneqq (g_e, \nu_e, g_d, \nu_d, q) \in X$ the closed-loop state vector. Define the set-valued mappings

$$\begin{aligned}F(x) &\coloneqq (g_e \widehat{\nu}_e, \alpha_e(x), g_d \widehat{\nu}_d, l\mathbb{B}, 0),\\ G(x) &\coloneqq (g_e, \nu_e, g_d, \nu_d, G_U(g_e)),\end{aligned} \tag{5.26}$$

with α_e denoting the velocity error dynamics. Then the closed-loop system (5.22) is a hybrid system $\mathcal{H} = (C, F, D, G)$. Consider the continuously differentiable function $W : X \to \mathbb{R}_{\geq 0}$ defined by

$$W(x) \coloneqq U(g_e, q) + \frac{1}{2}\langle \nu_e, M\nu_e \rangle. \tag{5.27}$$

Evidently, W is proper and positive definite with respect to the compact set

$$\mathcal{T}_0 \coloneqq \{x \in X : U(g_e, q) = 0, \nu_e = 0\}. \tag{5.28}$$

Utilizing the skew property of ∇^M (see Lemma 2.1), the derivative of W along flows of the closed-loop system (5.22) is $\dot{W}(x) = \langle d(\nu) - d(\nu_r) - K\nu_e, \nu_e \rangle$ for every $x \in C$. It now follows from the strict monotone dissipativity property of d that $\dot{W}(x) \leq 0$ for every $x \in C$, and also that $\dot{W}(x) < 0$ for every $x \in C$ such that $\nu_e \neq 0$. The change of W across jumps of the closed-loop system is $W(s) - W(x) \leq -\delta$ for every $x \in D$ and $s \in G(x)$. Since W is proper and non-increasing along flows and across jumps of the closed loop system, it follows that $\mathcal{T}_0$ is stable and that every solution to the closed-loop system is bounded. In fact, every sublevel set of W is forward pre-invariant, that is, for every $r \geq 0$, every solution starting in the set $W^{-1}([0, r])$ remains in it.

Consider now, for $r \geq 0$, the family of hybrid systems defined by

$$\mathcal{H}_r \coloneqq (C \cap W^{-1}([0, r]), F, D \cap W^{-1}([0, r]), G). \tag{5.29}$$

Every complete solution to $\mathcal{H}$ that starts in the set $W^{-1}([0, r])$ is a complete solution to $\mathcal{H}_r$. Furthermore, for each $r \geq 0$, $\mathcal{H}_r$ satisfies the hybrid basic conditions (Assumption 2.16). In particular, it follows from Proposition 5.4 that C and D are relatively closed in X. Since $W^{-1}([0, r]) \subset X$ is compact for every $r \geq 0$, it holds that $C \cap W^{-1}([0, r])$ and $D \cap W^{-1}([0, r])$ are compact sets, and therefore closed. The required properties of F and G can then be verified by noting the continuity of the velocity error dynamics α_e and the properties of G_U established in Proposition 5.4.

It now follows from Corollary 8.7 (b) in [90] that, for each $r \geq 0$, complete solutions to $\mathcal{H}_r$ converge to the largest weakly invariant subset $\mathcal{W}_r$ contained in $W^{-1}(\gamma) \cap \{x \in C : \nu_e = 0\}$ for some $\gamma \in [0, r]$. A necessary condition for $\mathcal{W}_r$ to be weakly invariant is that there exists a complete solution to $\mathcal{H}_r$ with range contained in $\mathcal{W}_r$. Let ϕ denote a complete solution to $\mathcal{H}_r$, such that $\operatorname{rge} \phi \subset \mathcal{W}_r$. Since ϕ is complete and the decrease of W over jumps of the closed loop system is strict, it must be the case that $\operatorname{dom} \phi = \mathbb{R}_{\geq 0} \times \{0\}$. Continuing, $\nu_e(t, 0) = 0$ for every $t \in \mathbb{R}_{\geq 0}$, and it follows that $\dot{\nu}_e(t, 0) = 0$ for every $t \in \mathbb{R}_{\geq 0}$. Utilizing the velocity error dynamics, it is seen that $\mathrm{d}U(g_e(t, 0), q(t, 0)) = 0$ for every $t \in \mathbb{R}_{\geq 0}$. By construction, the only points in C where $\mathrm{d}U(g_e, q) = 0$ are those for which $U(g_e, q) = 0$. It follows that $\operatorname{rge} \phi \subset \mathcal{T}_0$. Therefore, for every $r \geq 0$, $\mathcal{W}_r \subset \mathcal{T}_0$. Consequently, every complete solution to $\mathcal{H}_r$ converges to $\mathcal{T}_0$. Since every complete solution to $\mathcal{H}$ is a complete solution to $\mathcal{H}_r$ for some $r \geq 0$, every complete solution to $\mathcal{H}$ converges to $\mathcal{T}_0$. Since $\mathcal{T}_0$ is stable, all solutions are bounded, and every complete solution converges to $\mathcal{T}_0$, it follows that $\mathcal{T}_0$ is globally pre-asymptotically stable for $\mathcal{H}$.

Since $\mathcal{T}_0 \subset \mathcal{T}$, it follows that $\mathcal{T}$ is globally pre-attractive. It follows from Lemma 7.8 in [90] that this pre-attractivity is uniform from any compact subset of X. Moreover, $\mathcal{T}$ is forward pre-invariant because $\mathcal{T}_0$ is forward pre-invariant and

$$\mathcal{T} \setminus \mathcal{T}_0 = \{x \in X : (g_e, q) \in (\mathcal{A} \times Q) \setminus \operatorname{Zero} U\} \subset D \setminus C$$

is such that any maximal solution reaching $\mathcal{T} \setminus \mathcal{T}_0$ is immediately mapped to $\mathcal{T}_0$ via a single jump. It then follows from Proposition 7.5 of [90] that $\mathcal{T}$ is stable. Since $\mathcal{T}$ is stable and globally pre-attractive, it is globally pre-asymptotically stable. □

If the force χ appearing in (5.1) and the considered desired configurations satisfy additional conditions, it is possible to use a modified feedforward control that does not cancel χ in its entirety. In particular, let $\chi(g) = \chi_0(g) - \mathrm{d}P(g)$, where $\chi_0 : \mathcal{G} \to \mathbb{R}^m$ is continuous and $P : \mathcal{G} \to \mathbb{R}_{\geq 0}$ is continuously differentiable. Let $\mathcal{H}$ be a matrix Lie subgroup of $\mathcal{G}$ such that the force $-\mathrm{d}P$ is left-invariant with respect to $\mathcal{H}$, that is, $\mathrm{d}P(hg) = \mathrm{d}P(g)$ for every $h \in \mathcal{H}$ and every $g \in \mathcal{G}$. The following lemma shows that $\mathrm{d}P$ is left-invariant with respect to $\mathcal{H}$ if P is left-invariant with respect to $\mathcal{H}$, that is, if $P(hg) = P(g)$ for every $h \in \mathcal{H}$ and every $g \in \mathcal{G}$.

Lemma 5.2. Let $\mathcal{G} \subset \mathrm{GL}(n)$ be a m-dimensional matrix Lie group and $\mathcal{H}$ be a matrix Lie subgroup of $\mathcal{G}$. If a continuously differentiable function $P : \mathcal{G} \to \mathbb{R}$ is left-invariant with respect to $\mathcal{H}$, then $\mathrm{d}P$ is left-invariant with respect to $\mathcal{H}$.

Proof. We have that for every $g \in \mathcal{G}$, $h \in \mathcal{H}$, and $\nu \in \mathbb{R}^m$,

$$\begin{aligned}\langle \mathrm{d}P(hg), \nu \rangle &= \lim_{s \to 0} \frac{P(hg \exp(s\widehat{\nu})) - P(hg)}{s} \\ &= \lim_{s \to 0} \frac{P(g \exp(s\widehat{\nu})) - P(g)}{s} \\ &= \langle \mathrm{d}P(g), \nu \rangle.\end{aligned}$$

Consequently, $\mathrm{d}P(hg) = \mathrm{d}P(g)$ for every $g \in \mathcal{G}$ and $h \in \mathcal{H}$. □

Consider the synergistic PD-controller defined by

$$\begin{cases} \dot{q} = 0 & (g_e, \nu_e, g_d, \nu_d, \alpha_d, q) \in \widetilde{C} \\ q^+ \in G_U(g_e) & (g_e, \nu_e, g_d, \nu_d, \alpha_d, q) \in \widetilde{D} \\ \tau = \overline{\kappa}_{ff}(g, \nu_r, \alpha_r) & \\ \qquad - \mathrm{d}U(g_e, q) - K\nu_e & \end{cases} \tag{5.30}$$

where $\overline{\kappa}_{ff} : \mathcal{G} \times \mathbb{R}^m \times \mathbb{R}^m \to \mathbb{R}^m$ is defined by

$$\overline{\kappa}_{ff}(g, \nu, \alpha) \coloneqq M\alpha - \mathrm{ad}_\nu^{\mathsf{T}} M\nu - d(\nu) - \chi_0(g), \tag{5.31}$$

and $\widetilde{C}$ and $\widetilde{D}$ are defined by (5.21). The resulting closed-loop system becomes

$$\left.\begin{aligned} \dot{g}_e &= g_e \widehat{\nu}_e \\ \dot{\nu}_e &= -\nabla^M_{\nu+\nu_r} \nu_e + M^{-1}(d(\nu) - d(\nu_r)) \\ &\quad - M^{-1}(\mathrm{d}P(g) + \mathrm{d}U(g_e, q) + K\nu_e) \\ \dot{g}_d &= g_d \widehat{\nu}_d \\ \dot{\nu}_d &\in l\mathbb{B} \end{aligned}\right\} \quad (g_e, \nu_e, g_d, \nu_d, q) \in C$$
$$q^+ \in G_U(g_e) \qquad (g_e, \nu_e, g_d, \nu_d, q) \in D \tag{5.32}$$

It can be shown that the compact set (5.24) is globally pre-asymptotically stable for the closed-loop system (5.32) if in addition to the conditions of Theorem 5.6, we require that $\mathrm{d}P$ is left-invariant with respect to $\mathcal{H}$, that desired trajectories be restricted to a compact subset of $\mathcal{H}$, and that $P+U$ is synergistic on $\mathcal{G}$ relative to $\mathcal{A}$ with gap exceeding $\delta > 0$. It must be emphasized that U being synergistic generally does not imply that $P+U$ is synergistic. In general, $\operatorname{Zero}(P+U) \neq \operatorname{Zero} U$, and $\operatorname{Crit}(P+U) \neq \operatorname{Crit} U$. Since P does not depend on the mode q, it does however hold that $\mu_{P+U} = \mu_U$.

Theorem 5.7. *If $\Omega \subset \mathcal{H}$, $\mathrm{d}P$ is left-invariant with respect to $\mathcal{H}$, $P+U$ is synergistic on $\mathcal{G}$ relative to $\mathcal{A}$ with gap exceeding $\delta > 0$, and d is strictly monotonically dissipative modulo K, then $\mathcal{T}$, as defined in (5.24), is globally pre-asymptotically stable for (5.32).*

Proof. Let x and X be defined as in the proof of Theorem 5.6. Consider the continuously differentiable function $W : X \to \mathbb{R}_{\geq 0}$ defined by

$$W(x) \coloneqq P(g_e) + U(g_e, q) + \frac{1}{2}\langle \nu_e, M\nu_e \rangle. \tag{5.33}$$

Evidently, W is proper and positive definite with respect to the compact set

$$\mathcal{T}_0 \coloneqq \{x \in X : P(g_e) + U(g_e, q) = 0, \nu_e = 0\} \tag{5.34}$$

Utilizing the skew property of ∇^M (Lemma 2.1), the derivative of W along flows of the closed-loop system (5.32) is

$$\dot{W}(x) = \langle d(\nu) - d(\nu_r) - K\nu_e, \nu_e \rangle + \langle \mathrm{d}P(g_e) - \mathrm{d}P(g), \nu_e \rangle$$

for every $x \in C$. Since $g_d \in \Omega \subset \mathcal{H}$ and $\mathrm{d}P(g)$ is left-invariant with respect to $\mathcal{H}$, it holds that $\mathrm{d}P(g) = \mathrm{d}P(g_d g_e) = \mathrm{d}P(g_e)$. The strict monotone dissipativity property of d then ensures that $\dot{W}(x) \leq 0$ for every $x \in C$, and also that $\dot{W}(x) < 0$ for every $x \in C$ such that $\nu_e \neq 0$. The remainder of the proof is similar to the proof of Theorem 5.6. □

We end this section with two examples. First, we show that the hydrostatic moment acting on an underwater vehicle can be derived from a potential P with the necessary properties, provided that the axis of the desired rotation is aligned with the direction of gravity. We then show in a quaternion setting that $P+U$, where U is the potential function introduced in Example 5.5, is synergistic.

Example 5.8. Let $\mathcal{G} = \mathrm{SE}(3)$, and consider the underwater robot model derived in Chapter 3. There is a particular class of desired trajectories that allows us to exploit the hydrostatic moments acting on the robot in the control design process. These are the desired trajectories in

$$\mathcal{H} \coloneqq \left\{ h = \begin{pmatrix} S & r \\ 0 & 1 \end{pmatrix} \in \mathrm{SE}(3) : Sa_\gamma = a_\gamma \right\}, \tag{5.35}$$

where $a_\gamma \in \mathbb{R}^3$ is the gravity vector. Elements of $\mathcal{H}$ have the axis of their orientations restricted to be parallel with a_γ. It can be verified that $\mathcal{H}$ is a matrix Lie subgroup of $\mathrm{SE}(3)$.

The hydrostatic moment acting on the underwater robot can be derived from the potential $P : \mathrm{SE}(3) \to \mathbb{R}_{\geq 0}$ defined by

$$P(g) \coloneqq |a_\gamma||mr_m - \varrho v r_v| - \langle a_\gamma, R(mr_m - \varrho v r_v)\rangle \tag{5.36}$$

The fact that P is non-negative is easily verified by the Cauchy-Schwarz inequality. We find that

$$\begin{aligned} \mathrm{d}P(g) &= -\begin{pmatrix} 0 \\ mr_m^\times - \varrho v r_v^\times \end{pmatrix} R^\mathsf{T} a_\gamma && (5.37)\\ &= -\begin{pmatrix} 0 \\ mr_m^\times - \varrho v r_v^\times \end{pmatrix} R^\mathsf{T} S^\mathsf{T} a_\gamma && (5.38)\\ &= \mathrm{d}P(hg), && (5.39) \end{aligned}$$

since by (5.35), $a_\gamma = S^\mathsf{T} a_\gamma$.

Example 5.9. Let $\mathcal{G} = \widetilde{\mathrm{SE}}(3)$. In this example, we continue developments of Example 5.8 with quaternions, and show that the synergistic function introduced in Example 5.5 can be utilized in Theorem 5.7 with P taken to be a quaternion version of P in Example 5.8. We assume without loss of generality that the reference frames are chosen such that $a_\gamma = |a_\gamma| e_3$ and $mr_m - \varrho v r_v = |mr_m - \varrho v r_v| e_3$. Let $c \coloneqq |a_\gamma||mr_m - \varrho v r_v| > 0$ and P be defined by

$$\begin{aligned} P(g) &\coloneqq c(1 - \langle \mathrm{rot}(z) e_3, e_3\rangle) \\ &= 2c\langle (I - e_3 \otimes e_3)\epsilon, \epsilon\rangle \\ &= 2c(\epsilon_1^2 + \epsilon_2^2). \end{aligned} \tag{5.40}$$

An argument similar to the one utilized in Example 5.8 can be used to establish that P is left-invariant with respect to the matrix Lie group

$$\mathcal{H} \coloneqq \{h \in \widetilde{\mathrm{SE}}(3) : \mathrm{rot}(z) e_3 = e_3\}. \tag{5.41}$$

Recall the synergistic function U on $\widetilde{\mathrm{SE}}(3)$ that was defined in (5.17). Let $V(g, q) \coloneqq U(g, q) + P(g)$, that is,

$$V(g, q) = \frac{k_1}{2}|p|^2 + 2k_2(1 - q\eta) + 2c\langle (I - e_3 \otimes e_3)\epsilon, \epsilon\rangle, \tag{5.42}$$

where $k_1, k_2 > 0$ are positive gains. It is straightforward to verify that $\mathrm{Zero}\, V = \mathrm{Zero}\, U = \{g \in \widetilde{\mathrm{SE}}(3) : p = 0, q\eta = 1\}$. Furthermore,

$$\mathrm{d}V(g, q) = \begin{pmatrix} k_1\, \mathrm{rot}(z)^\mathsf{T} p \\ k_2 q\epsilon + 2c(\eta I - \epsilon^\times)(I - e_3 \otimes e_3)\epsilon \end{pmatrix}. \tag{5.43}$$

To find $\mathrm{Crit}\, V$, we require the unit quaternions such that

$$k_2 q\epsilon + 2c(\eta I - \epsilon^\times)(I - e_3 \otimes e_3)\epsilon = 0. \tag{5.44}$$

To this end, we contract (5.44) with e_3. This gives

$$\begin{aligned} 0 &= k_2 q\epsilon_3 + 2c\eta\langle (I - e_3 \otimes e_3)\epsilon, e_3\rangle - 2c\langle \epsilon^\times (I - e_3 \otimes e_3)\epsilon, e_3\rangle \\ &= k_2 q\epsilon_3 + 2c\eta\langle (I - e_3 \otimes e_3) e_3, \epsilon\rangle + 2c\langle e_3^\times (I - e_3 \otimes e_3)\epsilon, \epsilon\rangle \\ &= k_2 q\epsilon_3. \end{aligned} \tag{5.45}$$

Consequently, (5.44) holds only if $\epsilon_3 = 0$. In this case, $(I - e_3 \otimes e_3)\epsilon = \epsilon$, and (5.44) reduces to

$$(k_2 q + 2c\eta)\epsilon = 0. \tag{5.46}$$

It follows that if $k_2 \geq 2c$, then $\operatorname{Crit} V = \operatorname{Crit} U$. If instead $k_2 < 2c$, then

$$\operatorname{Crit} V = \operatorname{Crit} U \cup \{(g, q) \in \widetilde{\mathrm{SE}}(3) \times Q : p = 0, q\eta = -k_2/2c, \epsilon_3 = 0\}. \tag{5.47}$$

We seek to determine if V is synergistic on $\mathcal{G}$ relative to $\mathcal{A} = \{g \in \widetilde{\mathrm{SE}}(3) : p = 0, \eta = \pm 1\}$. Since $\mu_V = \mu_U$ and $\operatorname{Zero} V = \operatorname{Zero} U$, the critical points of V that are also critical points of U have already been treated in Example 5.5. For the additional critical points given in (5.47) for which $q\eta = -k_2/2c$ and $\epsilon_3 = 0$, we find

$$\begin{aligned} \mu_V(g, q) &= 2k_2 \left(1 + \frac{k_2}{2c}\right) - 2k_2 \left(1 - \frac{k_2}{2c}\right) \\ &= \frac{2k_2^2}{c} > 0. \end{aligned} \tag{5.48}$$

It follows that V is synergistic on $\mathcal{G}$ relative to $\mathcal{A}$ with gap exceeding δ, where $\min(4k_2, 2k_2^2/c) > \delta > 0$.

5.5 Synergistic Output Feedback Control

Due to the fact that the feedforward control in (5.8) is independent of the robot velocities, we can utilize it in the design of a Lyapunov-based output feedback tracking control law. It will also be required in this section that there is no disturbance acting on the mechanical system, that is, $b = 0$. Let $V : \mathcal{G} \times \Sigma \to \mathbb{R}_{\geq 0}$ be synergistic on $\mathcal{G}$ relative to a finite set $\mathcal{B}$ with gap exceeding $\rho > 0$ and denote by $\sigma \in \Sigma \subset \mathbb{Z}$ the associated logic variable. Define, analogously to (5.16), the quantities

$$\begin{aligned} C_V &\coloneqq \{(g, \sigma) \in \mathcal{G} \times \Sigma : \mu_V(g, \sigma) \leq \rho\}, \\ D_V &\coloneqq \{(g, \sigma) \in \mathcal{G} \times \Sigma : \mu_V(g, \sigma) \geq \rho\}, \\ G_V(g) &\coloneqq \{\sigma \in \Sigma : \mu_V(g, \sigma) = 0\} \end{aligned} \tag{5.49}$$

where $\mu_V : \mathcal{G} \times \Sigma \to \mathbb{R}_{\geq 0}$ is the synergy gap of V. Consider the output feedback control law

$$\begin{cases} \dot{g}_f = g_f \widehat{\nu}_f & (g_e, g_d, \nu_d, \alpha_d, g_f, q, \sigma) \in \widetilde{C} \\ \left.\begin{aligned} q^+ &\in G_U(g_e) \\ \sigma^+ &\in G_V(g_o) \end{aligned}\right\} & (g_e, g_d, \nu_d, \alpha_d, g_f, q, \sigma) \in \widetilde{D} \\ \tau = \kappa_{ff}(g, \nu_r, \alpha_r) \\ \qquad - \mathrm{d}V(g_o, \sigma) - \mathrm{d}U(g_e, q) \end{cases} \tag{5.50}$$

where $g_f \in \mathcal{G}$ is a filter state, $g_o \coloneqq g_f^{-1} g_e \in \mathcal{G}$ is the filter error, and the filter velocity $\nu_f \in \mathbb{R}^m$ is defined by $\nu_f \coloneqq \operatorname{Ad}_{g_o} K \, \mathrm{d}V(g_o, \sigma)$. Furthermore, we define the controller

flow set and jump set by

$$\begin{aligned}\widetilde{C} &\coloneqq \{(g_e, g_d, \nu_d, \alpha_d, g_f, q, \sigma) : (g_e, q) \in C_U \text{ and } (g_o, \sigma) \in C_V,\\ &\qquad g_d \in \mathcal{G}, \nu_d \in \mathbb{R}^m, \alpha_d \in \mathbb{R}^m\},\\ \widetilde{D} &\coloneqq \{(g_e, g_d, \nu_d, \alpha_d, g_f, q, \sigma) : (g_e, q) \in D_U \text{ or } (g_o, \sigma) \in D_V,\\ &\qquad g_d \in \mathcal{G}, \nu_d \in \mathbb{R}^m, \alpha_d \in \mathbb{R}^m\}.\end{aligned} \tag{5.51}$$

The closed-loop system becomes

$$\left.\begin{aligned}\dot{g}_e &= g_e \widehat{\nu}_e\\ \dot{\nu}_e &= -\nabla^M_{\nu+\nu_r}\nu_e\\ &\quad + M^{-1}(d(\nu) - d(\nu_r))\\ &\quad - M^{-1}(\mathrm{d}U(g_e, q) + \mathrm{d}V(g_o, \sigma))\\ \dot{g}_d &= g_d \widehat{\nu}_d\\ \dot{\nu}_d &\in l\mathbb{B}\\ \dot{g}_o &= g_o \widehat{\nu}_o\end{aligned}\right\} \quad (g_e, \nu_e, g_d, \nu_d, g_o, q, \sigma) \in C$$

$$\left.\begin{aligned}q^+ &\in G_U(g_e)\\ \sigma^+ &\in G_V(g_o)\end{aligned}\right\} \quad (g_e, \nu_e, g_d, \nu_d, g_o, q, h) \in D \tag{5.52}$$

where the filter error velocity $\nu_o \in \mathbb{R}^m$ is defined by

$$\begin{aligned}\nu_o &\coloneqq \nu_e - \mathrm{Ad}^{-1}_{g_o}\nu_f\\ &= \nu_e - K\,\mathrm{d}V(g_o, \sigma),\end{aligned} \tag{5.53}$$

and the flow set C and jump set D are defined by

$$\begin{aligned}C &\coloneqq \{(g_e, \nu_e, g_d, \nu_d, g_o, q, \sigma) : (g_e, q) \in C_U \text{ and } (g_o, \sigma) \in C_V, \nu_e \in \mathbb{R}^m,\\ &\qquad g_d \in \Omega, \nu_d \in c\mathbb{B}\},\\ D &\coloneqq \{(g_e, \nu_e, g_d, \nu_d, g_o, q, \sigma) : (g_e, q) \in D_U \text{ or } (g_o, \sigma) \in D_V, \nu_e \in \mathbb{R}^m,\\ &\qquad g_d \in \Omega, \nu_d \in c\mathbb{B}\}.\end{aligned} \tag{5.54}$$

Before we state the main result of this section, we recall from Definition 3.9 that $d : \mathbb{R}^m \to \mathbb{R}^m$ is monotonically dissipative if $d(0) = 0$, d is continuous, and $\langle d(\nu) - d(\overline{\nu}), \nu - \overline{\nu}\rangle \leq 0$ for every $\nu \in \mathbb{R}^m$ and every $\overline{\nu} \in \mathbb{R}^m$.

Theorem 5.10. *If U is synergistic on $\mathcal{G}$ relative to $\mathcal{A}$ with gap exceeding $\delta > 0$, V is synergistic on $\mathcal{G}$ relative to a finite set $\mathcal{B}$ with gap exceeding $\rho > 0$, K is positive definite, and d is monotonically dissipative, then the compact set*

$$\mathcal{T} \coloneqq \mathcal{A} \times \{0\} \times \Omega \times c\mathbb{B} \times Q \times \mathcal{B} \times \Sigma, \tag{5.55}$$

is globally pre-asymptotically stable for the system (5.52).

Proof. Define the set $X \coloneqq \mathcal{G} \times \mathbb{R}^m \times \Omega \times c\mathbb{B} \times \mathcal{G} \times Q \times \Sigma$, the state vector $x \coloneqq (g_e, \nu_e, g_d, \nu_d, g_o, q, \sigma) \in X$ and the set-valued mappings

$$\begin{aligned}F(x) &\coloneqq (g_e \widehat{\nu}_e, \alpha_e(x), g_d \widehat{\nu}_d, l\mathbb{B}, g_o \widehat{\nu}_o, 0, 0),\\ G(x) &\coloneqq (g_e, \nu_e, g_d, \nu_d, g_o, G_U(g_e), G_V(g_o)),\end{aligned} \tag{5.56}$$

with α_e denoting the velocity error dynamics. Then the closed-loop system (5.52) is a hybrid system $\mathcal{H} = (C, F, D, G)$. Consider the continuously differentiable function $W : X \to \mathbb{R}_{\geq 0}$ defined by

$$W(x) \coloneqq U(g_e, q) + V(g_o, \sigma) + \frac{1}{2}\langle \nu_e, M\nu_e \rangle. \tag{5.57}$$

Evidently, W is proper and positive definite with respect to the compact set

$$\mathcal{T}_0 \coloneqq \{x \in X : U(g_e, q) = 0, V(g_o, \sigma) = 0, \nu_e = 0\}. \tag{5.58}$$

The derivative of W along flows of the closed-loop system (5.52) is

$$\begin{aligned}
\dot{W}(x) &= \langle \mathrm{d}U(g_e, q), \nu_e \rangle + \langle \mathrm{d}V(g_o, \sigma), \nu_e - K\,\mathrm{d}V(g_o, \sigma) \rangle \\
&\quad - \langle M\nabla^M_{\nu+\nu_r}\nu_e, \nu_e \rangle + \langle d(\nu) - d(\nu_r), \nu_e \rangle \\
&\quad - \langle \mathrm{d}U(g_e, q) + \mathrm{d}V(g_o, \sigma), \nu_e \rangle \\
&\leq -\langle K\,\mathrm{d}V(g_o, \sigma), \mathrm{d}V(g_o, \sigma) \rangle
\end{aligned}$$

for all $x \in C$. The change of W across jumps is found to be

$$W(s) - W(x) \leq -\min(\delta, \rho) \tag{5.59}$$

for all $x \in D$ and $s \in G(x)$. By a similar argument as in the proof of Theorem 5.6, it can be shown that $\mathcal{T}_0$ is stable and that all solutions to $\mathcal{H}$ are bounded. Moreover, every complete solution to $\mathcal{H}_r$ converges to the largest weakly invariant subset $\mathcal{W}_r$ of $W^{-1}(\gamma) \cap \{x \in C : \mathrm{d}V(g_o, \sigma) = 0\}$ for some $\gamma \in [0, r]$.

Let ϕ denote a complete solution to $\mathcal{H}_r$, such that $\operatorname{rge}\phi \subset \mathcal{W}_r$. Since ϕ is complete and the decrease of W over jumps of the closed loop system is strict, it must be the case that $\operatorname{dom}\phi = \mathbb{R}_{\geq 0} \times \{0\}$. By construction, the only points in C where $\mathrm{d}V(g_o, \sigma) = 0$ are those for which $V(g_o, \sigma) = 0$. Consequently, $g_o(t, 0) \in \mathcal{B}$ for every $t \in \mathbb{R}_{\geq 0}$. Since $\mathcal{B}$ is a finite set, it must hold that $\dot{g}_o(t, 0) = 0$ for every $t \in \mathbb{R}_{\geq 0}$. It follows that $\nu_e(t, 0) = 0$ for every $t \in \mathbb{R}_{\geq 0}$. By an argument similar to the one employed in the proof of Theorem 5.6, it now follows that $\mathrm{d}U(g_e(t, 0), q(t, 0)) = 0$ for every $t \in \mathbb{R}_{\geq 0}$. It follows that $\mathcal{W}_r \subset \mathcal{T}_0$ and that every complete solution to $\mathcal{H}_r$ converges to $\mathcal{T}_0$. Since every complete solution to $\mathcal{H}$ is a complete solution to $\mathcal{H}_r$ for some $r \geq 0$, every complete solution to $\mathcal{H}$ converges to $\mathcal{T}_0$. Since $\mathcal{T}_0$ is stable, all solutions are bounded, and every complete solution converges to $\mathcal{T}_0$, it follows that $\mathcal{T}_0$ is globally pre-asymptotically stable for $\mathcal{H}$. The remainder of the proof uses an argument similar to the one utilized in the proof of Theorem 5.6. □

We remark briefly that the output feedback controller (5.50) admits an analogue to the controller (5.30). This controller has the form

$$\begin{cases}
\dot{g}_f = g_f \widehat{\nu}_f & (g_e, g_d, \nu_d, \alpha_d, g_f, q, \sigma) \in \widetilde{C} \\
\left.\begin{aligned} q^+ &\in G_U(g_e) \\ \sigma^+ &\in G_V(g_o) \end{aligned}\right\} & (g_e, g_d, \nu_d, \alpha_d, g_f, q, \sigma) \in \widetilde{D} \\
\tau = \overline{\kappa}_{ff}(g, \nu_r, \alpha_r) \\
\qquad - \mathrm{d}V(g_o, \sigma) - \mathrm{d}U(g_e, q)
\end{cases} \tag{5.60}$$

where $\overline{\kappa}_{ff}$ is defined by (5.31), and $\widetilde{C}$ and $\widetilde{D}$ are defined by (5.51), and leads to the closed-loop system

$$\left.\begin{aligned}
\dot{g}_e &= g_e \widehat{\nu}_e \\
\dot{\nu}_e &= -\nabla^M_{\nu+\nu_r} \nu_e \\
&\quad + M^{-1}(d(\nu) - d(\nu_r)) \\
&\quad - M^{-1}(\mathrm{d}U(g_e, q) + \mathrm{d}V(g_o, \sigma)) \\
&\quad - M^{-1}\,\mathrm{d}P(g) \\
\dot{g}_d &= g_d \widehat{\nu}_d \\
\dot{\nu}_d &\in l\mathbb{B} \\
\dot{g}_o &= g_o \widehat{\nu}_o
\end{aligned}\right\} \quad (g_e, \nu_e, g_d, \nu_d, g_o, q, \sigma) \in C$$
$$\left.\begin{aligned}
q^+ &\in G_U(g_e) \\
\sigma^+ &\in G_V(g_o)
\end{aligned}\right\} \quad (g_e, \nu_e, g_d, \nu_d, g_o, q, \sigma) \in D \tag{5.61}$$

where C and D are defined by (5.54). We then have the following theorem, the proof of which we omit due its similarity to the proofs of Theorem 5.7 and Theorem 5.10.

Theorem 5.11. *If $\Omega \subset \mathcal{H}$, $\mathrm{d}P$ is left-invariant with respect to $\mathcal{H}$, $P+U$ is synergistic on $\mathcal{G}$ relative to $\mathcal{A}$ with gap exceeding $\delta > 0$, V is synergistic on $\mathcal{G}$ relative to the finite set $\mathcal{B}$ with gap exceeding $\rho > 0$, K is positive definite, and d is monotonically dissipative, then $\mathcal{T}$, as defined in (5.55), is globally pre-asymptotically stable for (5.61).*

5.6 Synergistic PID Control

We now treat the full system (5.1) with the constant disturbance b present. Consider the following synergistic PID control law

$$\begin{cases}
\dot{\varphi} = \mathrm{d}U(g_e, q) & (g_e, \nu_e, g_d, \nu_d, \alpha_d, \varphi, q) \in \widetilde{C} \\
q^+ \in G_U(g_e) & (g_e, \nu_e, g_d, \nu_d, \alpha_d, \varphi, q) \in \widetilde{D} \\
\tau = \kappa_{ff}(g, \nu, \dot{\nu}_r) & \\
\qquad - \mathrm{d}U(g_e, q) - k\varphi - K\nu_e &
\end{cases} \tag{5.62}$$

where $K \in \mathbb{R}^{m \times m}$ is the derivative gain, $k \in \mathbb{R}$ is the integral gain, and

$$\begin{aligned}
\widetilde{C} \coloneqq \{&(g_e, \nu_e, g_d, \nu_d, \alpha_d, \varphi, q) : (g_e, q) \in C_U, \nu_e \in \mathbb{R}^m, g_d \in \mathcal{G}, \\
&\nu_d \in \mathbb{R}^m, \alpha_d \in \mathbb{R}^m, \varphi \in \mathbb{R}^m\}, \\
\widetilde{D} \coloneqq \{&(g_e, \nu_e, g_d, \nu_d, \alpha_d, \varphi, q) : (g_e, q) \in D_U, \nu_e \in \mathbb{R}^m, g_d \in \mathcal{G}, \\
&\nu_d \in \mathbb{R}^m, \alpha_d \in \mathbb{R}^m, \varphi \in \mathbb{R}^m\}.
\end{aligned} \tag{5.63}$$

Observe that the feedback control law comprises a proportional term $\mathrm{d}U(g_e, q)$, an integral term $k\varphi$ and a derivative term $K\nu_e$. Let $b_e \coloneqq b - k\varphi$ denote the error of the

integrator. The resulting closed-loop system is then given by

$$\left.\begin{aligned}
\dot{g}_e &= g_e \widehat{\nu}_e \\
\dot{\nu}_e &= -M^{-1}(\mathrm{d}U(g_e, q) - b_e + K\nu_e) \\
\dot{g}_d &= g_d \widehat{\nu}_d \\
\dot{\nu}_d &\in l\mathbb{B} \\
\dot{b}_e &= -k\,\mathrm{d}U(g_e, q)
\end{aligned}\right\} \quad (g_e, \nu_e, g_d, \nu_d, b_e, q) \in C$$
$$q^+ \in G_U(g_e) \qquad (g_e, \nu_e, g_d, \nu_d, b_e, q) \in D \tag{5.64}$$

where

$$\begin{aligned}
C &\coloneqq \{(g_e, \nu_e, g_d, \nu_d, b_e, q) : (g_e, q) \in C_U, \nu_e \in \mathbb{R}^m, g_d \in \mathcal{G}, \nu_d \in c\mathbb{B}, b_e \in \mathbb{R}^m\}, \\
D &\coloneqq \{(g_e, \nu_e, g_d, \nu_d, b_e, q) : (g_e, q) \in D_U, \nu_e \in \mathbb{R}^m, g_d \in \mathcal{G}, \nu_d \in c\mathbb{B}, b_e \in \mathbb{R}^m\}.
\end{aligned} \tag{5.65}$$

We then have the following result.

Theorem 5.12. *If $\mathcal{A}$ is finite, U is synergistic on $\mathcal{G}$ relative to $\mathcal{A}$ with gap exceeding $\delta > 0$, $k > 0$, and $K - kM$ is symmetric and positive definite, then the compact set*

$$\mathcal{T} \coloneqq \mathcal{A} \times \{0\} \times \Omega \times c\mathbb{B} \times \{0\} \times Q, \tag{5.66}$$

is globally pre-asymptotically stable for the system (5.64).

Proof. Define the set $X \coloneqq \mathcal{G} \times \mathbb{R}^m \times \Omega \times c\mathbb{B} \times \mathbb{R}^m \times Q$, the state vector $x \coloneqq (g_e, \nu_e, g_d, \nu_d, b_e, q) \in X$ and the set-valued mappings

$$F(x) \coloneqq (g_e \widehat{\nu}_e, \alpha_e(x), g_d \widehat{\nu}_d, l\mathbb{B}, -k\,\mathrm{d}U(g_e, q), 0), \tag{5.67}$$
$$G(x) \coloneqq (g_e, \nu_e, g_d, \nu_d, b_e, G_U(g_e)), \tag{5.68}$$

with α_e denoting the velocity error dynamics. Then the closed-loop system (5.64) is a hybrid system $\mathcal{H} = (C, F, D, G)$. Define also the symmetric positive definite matrix $A \coloneqq (K - kM)^{-1}$. Note that since M is symmetric positive definite, $k > 0$, and $K - kM$ is symmetric positive definite, we must have that K is symmetric positive definite. Consider the continuously differentiable function $W : X \to \mathbb{R}_{\geq 0}$ defined by

$$W(x) \coloneqq U(g_e, q) + \frac{1}{2}\langle M\nu_e, \nu_e\rangle + \frac{1}{2k}\langle A(b_e - kM\nu_e), b_e - kM\nu_e\rangle, \tag{5.69}$$

Evidently, W is proper and positive definite with respect to the compact set

$$\mathcal{T}_0 \coloneqq \{x \in X : U(g_e, q) = 0, \nu_e = 0, b_e = 0\} \tag{5.70}$$

The derivative of W along flows of the closed-loop system (5.64) is

$$\begin{aligned}
\dot{W}(x) &= \langle b_e - K\nu_e, \nu_e\rangle - \langle A(b_e - K\nu_e), b_e - kM\nu_e\rangle \\
&= \langle b_e - K\nu_e, \nu_e\rangle - \langle A(b_e - K\nu_e), b_e - K\nu_e\rangle - \langle A(b_e - K\nu_e), (K - kM)\nu_e\rangle \\
&= -\langle A(b_e - K\nu_e), b_e - K\nu_e\rangle,
\end{aligned}$$

for every $x \in C$. The change of W across jumps is found to be

$$W(s) - W(x) \leq -\delta \tag{5.71}$$

for all $x \in D$ and $s \in G(x)$. By a similar argument as in the proof of Theorem 5.6, it can be shown that $\mathcal{T}_0$ is stable and that all solutions to $\mathcal{H}$ are bounded. Moreover, every complete solution to $\mathcal{H}_r$ converges to the largest weakly invariant subset $\mathcal{W}_r$ of $W^{-1}(\gamma) \cap \{x \in C : b_e = K\nu_e\}$ for some $\gamma \in [0, r]$.

Let ϕ denote a complete solution to $\mathcal{H}_r$, such that $\operatorname{rge} \phi \subset \mathcal{W}_r$. Since ϕ is complete and the decrease of W over jumps of the closed loop system is strict, it must be the case that $\operatorname{dom} \phi = \mathbb{R}_{\geq 0} \times \{0\}$. We must then have that

$$\begin{aligned} \dot{\nu}_e(t,0) &= -M^{-1}\, \mathrm{d}U(g_e(t,0), q(t,0)), \\ \dot{b}_e(t,0) &= -k\, \mathrm{d}U(g_e(t,0), q(t,0)), \end{aligned}$$

for almost every $t \in \mathbb{R}_{\geq 0}$. Since $b_e(t,0) - K\nu_e(t,0) = 0$ for every $t \in \mathbb{R}_{\geq 0}$, it follows that

$$\begin{aligned} \dot{b}_e(t,0) - K\dot{\nu}_e(t,0) &= (KM^{-1} - kI)\, \mathrm{d}U(g_e(t,0), q(t,0)) \\ &= (K - kM)M^{-1}\, \mathrm{d}U(g_e(t,0), q(t,0)) \\ &= 0 \end{aligned}$$

for almost every $t \in \mathbb{R}_{\geq 0}$. Since $K - kM$ and M have full rank, and the mapping $t \mapsto \mathrm{d}U(g_e(t,0), q(t,0))$ is continuous, it follows that $\mathrm{d}U(g_e(t,0), q(t,0)) = 0$ for every $t \in \mathbb{R}_{\geq 0}$. By construction, the only points in C where $\mathrm{d}U(g_e, q) = 0$ are those for which $U(g_e, q) = 0$. Consequently, $g_e(t,0) \in \mathcal{A}$ for every $t \in \mathbb{R}_{\geq 0}$. Since $\mathcal{A}$ is a finite set, it must hold that $\dot{g}_e(t,0) = 0$ for almost every $t \in \mathbb{R}_{\geq 0}$. It follows that $\nu_e(t,0) = 0$ for every $t \in \mathbb{R}_{\geq 0}$, and since $b_e(t,0) = K\nu_e(t,0)$, that $b_e(t,0) = 0$ for every $t \in \mathbb{R}_{\geq 0}$. It follows further that $\mathcal{W}_r \subset \mathcal{T}_0$ and that every complete solution to $\mathcal{H}_r$ converges to $\mathcal{T}_0$. Since every complete solution to $\mathcal{H}$ is a complete solution to $\mathcal{H}_r$ for some $r \geq 0$, every complete solution to $\mathcal{H}$ converges to $\mathcal{T}_0$. Since $\mathcal{T}_0$ is stable, all solutions are bounded, and every complete solution converges to $\mathcal{T}_0$, it follows that $\mathcal{T}_0$ is globally pre-asymptotically stable for $\mathcal{H}$. The remainder of the proof uses an argument similar to the one utilized in the proof of Theorem 5.6. □

We now present a second synergistic PID controller that integrates both the proportional action and the derivative action. Consider the control law

$$\begin{cases} \dot{\varphi} = \mathrm{d}U(g_e, q) + K\nu_e & (g_e, \nu_e, g_d, \nu_d, \alpha_d, \varphi, q) \in \widetilde{C} \\ q^+ \in G_U(g_e) & (g_e, \nu_e, g_d, \nu_d, \alpha_d, \varphi, q) \in \widetilde{D} \\ \tau = \kappa_{ff}(g, \nu, \dot{\nu}_r) & \\ \qquad - \mathrm{d}U(g_e, q) - k\varphi - K\nu_e & \end{cases} \tag{5.72}$$

where $K \in \mathbb{R}^{m \times m}$, $k \in \mathbb{R}$, and $\widetilde{C}$ and $\widetilde{D}$ are defined by (5.63). The controller (5.72)

leads to the closed-loop system

$$\left.\begin{aligned}
\dot{g}_e &= g_e\widehat{\nu}_e \\
\dot{\nu}_e &= -M^{-1}(\mathrm{d}U(g_e,q) - b_e + K\nu_e) \\
\dot{g}_d &= g_d\widehat{\nu}_d \\
\dot{\nu}_d &\in l\mathbb{B} \\
\dot{b}_e &= -k(\mathrm{d}U(g_e,q) + Kv_e)
\end{aligned}\right\} \quad (g_e,\nu_e,g_d,\nu_d,b_e,q) \in C$$
$$q^+ \in G_U(g_e) \qquad (g_e,\nu_e,g_d,\nu_d,b_e,q) \in D \tag{5.73}$$

where C and D are defined by (5.65). Conditions that ensure stability are less restrictive for the controller (5.72) than for the controller (5.63). In particular, the set $\mathcal{A}$ need not be finite, and the matrix K need not be symmetric.

Theorem 5.13. *If U is synergistic on $\mathcal{G}$ relative to $\mathcal{A}$ with gap exceeding $\delta > 0$, $k > 0$, and $K - kM$ is positive definite, then $\mathcal{T}$, as defined in (5.66), is globally pre-asymptotically stable for (5.73).*

Proof. Define the set $X \coloneqq \mathcal{G} \times \mathbb{R}^m \times \Omega \times c\mathbb{B} \times \mathbb{R}^m \times Q$, the state vector $x \coloneqq (g_e,\nu_e,g_d,\nu_d,b_e,q) \in X$, and the set-valued mappings

$$F(x) \coloneqq (g_e\widehat{\nu}_e, \alpha_e(x), g_d\widehat{\nu}_d, l\mathbb{B}, -k(\mathrm{d}U(g_e,q) + Kv_e), 0), \tag{5.74}$$
$$G(x) \coloneqq (g_e,\nu_e,g_d,\nu_d,b_e,G_U(g_e)), \tag{5.75}$$

with α_e denoting the velocity error dynamics. Then the closed-loop system (5.73) is a hybrid system $\mathcal{H} = (C,F,D,G)$. Note that since M is positive definite, $k > 0$, and $K - kM$ is positive definite, we must have that K is positive definite. Consider the continuously differentiable function $W : X \to \mathbb{R}_{\geq 0}$ defined by

$$W(x) \coloneqq U(g_e,q) + \frac{1}{2}\langle \nu_e, M\nu_e\rangle + \frac{1}{2k}\langle M^{-1}(b_e - kM\nu_e), b_e - kM\nu_e\rangle. \tag{5.76}$$

Evidently, W is proper and positive definite with respect to the compact set

$$\mathcal{T}_0 \coloneqq \{x \in X : U(g_e,q) = 0, \nu_e = 0, b_e = 0\} \tag{5.77}$$

The derivative of W along flows of the closed-loop system (5.73) is

$$\begin{aligned}
\dot{W}(x) &= \langle b_e - Kv_e, \nu_e\rangle - \langle M^{-1}b_e, b_e - kM\nu_e\rangle \\
&= -\langle (K - kM)\nu_e, \nu_e\rangle + \langle b_e - kM\nu_e, \nu_e\rangle - \langle M^{-1}b_e, b_e - kM\nu_e\rangle \\
&= -\langle (K - kM)\nu_e, \nu_e\rangle - \langle M^{-1}(b_e - kM\nu_e), b_e - kM\nu_e\rangle
\end{aligned}$$

for every $x \in C$. The change of W across jumps is found to be

$$W(s) - W(x) \leq -\delta \tag{5.78}$$

for all $x \in D$ and $s \in G(x)$. By a similar argument as in the proof of Theorem 5.6, it can be shown that $\mathcal{T}_0$ is stable and that all solutions to $\mathcal{H}$ are bounded. Moreover, every complete solution to $\mathcal{H}_r$ converges to the largest weakly invariant subset $\mathcal{W}_r$ of $W^{-1}(\gamma) \cap \{x \in C : \nu_e = 0, b_e = 0\}$ for some $\gamma \in [0,r]$. The remainder of the proof is similar to the proof of Theorem 5.6. □

5.7 Application to Underwater Vehicle Control

This section presents simulation results for a small fully actuated underwater vehicle. We utilize a quaternion representation of the vehicle orientation such that $\mathcal{G} = \widetilde{\mathrm{SE}}(3)$. In this case, the model (5.1) reduces to the underwater vehicle control model introduced in Section 3.6. Let us present the data of the underwater vehicle used for the simulation. The center of mass is $r_m = (0, 0, 0.02)\mathrm{m}$, the center of buoyancy is $r_v = 0\,\mathrm{m}$, the dry mass is $m = 13.7\,\mathrm{kg}$, and the displaced mass is ϱv is 1% larger than the dry mass. The hydrodynamic inertia matrix M_H is chosen as

$$M_H := \begin{pmatrix} 5.5 & 0 & 0 & 0 & 0 & 0 \\ 0 & 12.7 & 0 & 0 & 0 & 0 \\ 0 & 0 & 14.6 & 0 & 0 & 0 \\ 0 & 0 & 0 & 0.1 & 0 & 0 \\ 0 & 0 & 0 & 0 & 0.1 & 0 \\ 0 & 0 & 0 & 0 & 0 & 0.1 \end{pmatrix}. \tag{5.79}$$

Furthermore, we use a hydrodynamic damping model comprising linear damping and diagonal second-order modulus damping,

$$d(\nu) := -\begin{pmatrix} 4.0\nu_1 + 18.2|\nu_1|\nu_1 \\ 6.2\nu_2 + 21.7|\nu_2|\nu_2 \\ 5.2\nu_3 + 37.0|\nu_3|\nu_3 \\ 0.1\nu_4 + 1.6|\nu_4|\nu_4 \\ 0.1\nu_5 + 1.6|\nu_5|\nu_5 \\ 0.1\nu_6 + 1.6|\nu_6|\nu_6 \end{pmatrix}. \tag{5.80}$$

The constant disturbance is set to

$$b := \begin{pmatrix} 2 \\ 1 \\ -1 \\ -1 \\ -1 \\ 1 \end{pmatrix}. \tag{5.81}$$

The control law (5.72) is implemented with the synergistic potential function introduced in Example 5.5. Furthermore, we have implemented it without the feedforward term that would cancel the acting hydrodynamic and hydrostatic wrenches to achieve a slightly more realistic picture of its performance. The controller parameters are given by

$$\begin{aligned} k_1 &= 5, \\ k_2 &= 1, \\ K &= \begin{pmatrix} 10 & 0 & 0 & 0 & 0 & 0 \\ 0 & 10 & 0 & 0 & 0 & 0 \\ 0 & 0 & 10 & 0 & 0 & 0 \\ 0 & 0 & 0 & 2 & 0 & 0 \\ 0 & 0 & 0 & 0 & 2 & 0 \\ 0 & 0 & 0 & 0 & 0 & 2 \end{pmatrix}, \\ k &= 0.1. \end{aligned} \tag{5.82}$$

Simulation results are presented in Figures 5.1 to 5.3, from which we conclude that acceptable tracking performance is achieved despite this simplification of the control law.

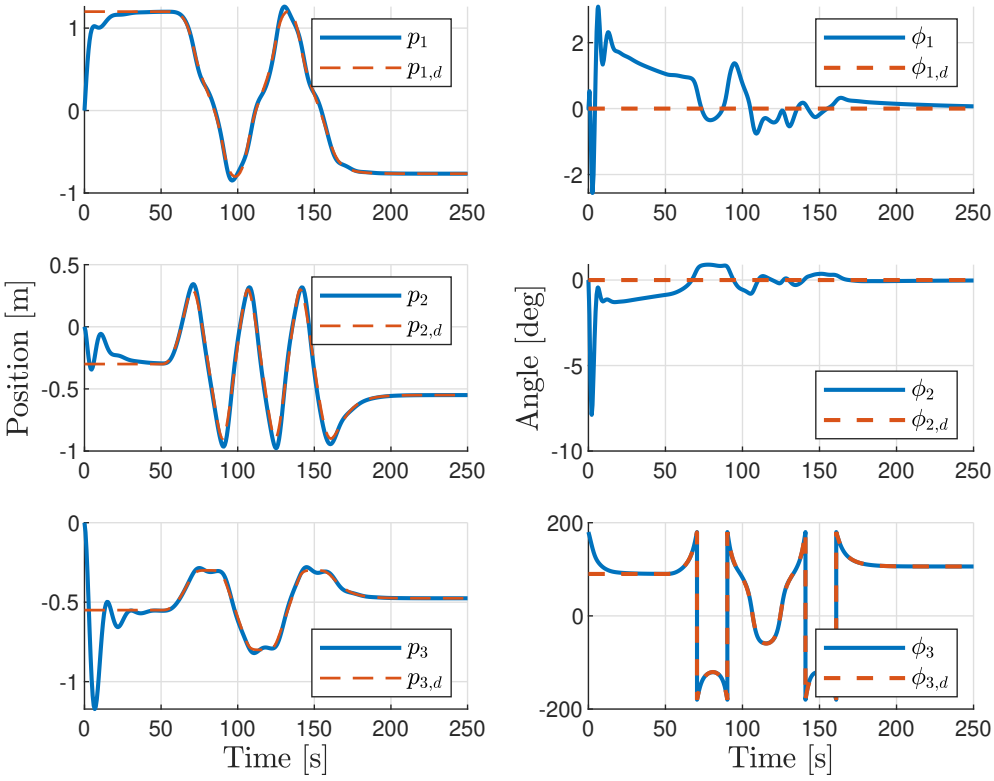

Figure 5.1: The position p, desired position p_d, roll-pitch-yaw angles ϕ and desired roll-pitch-yaw angles ϕ_d.

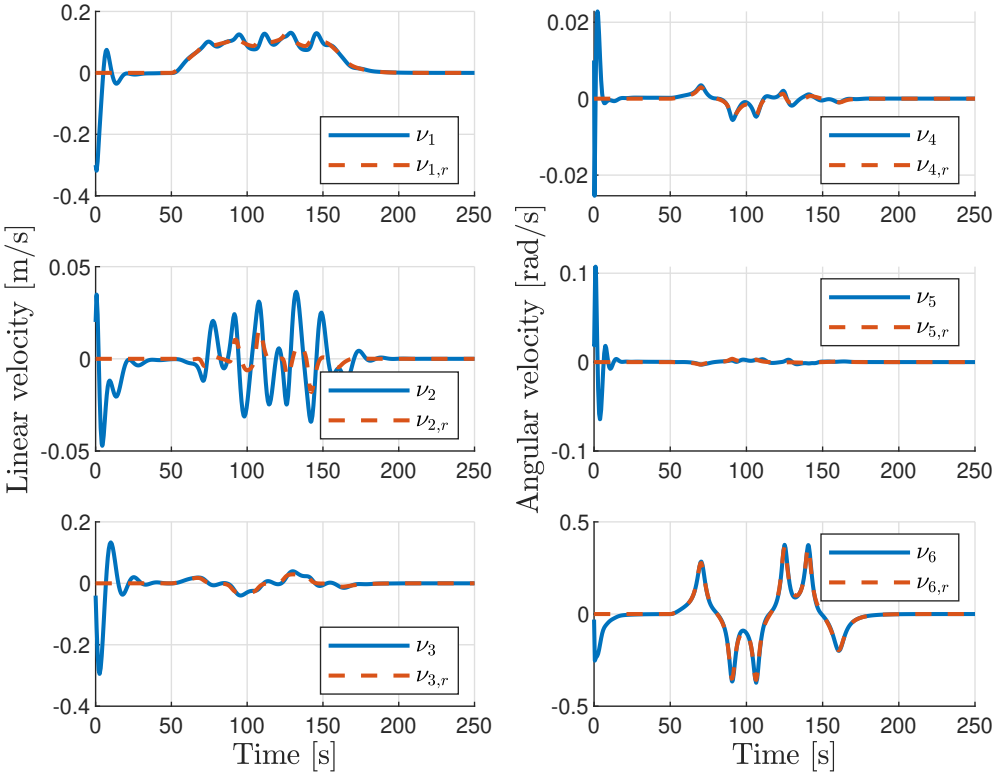

Figure 5.2: The velocity ν and the desired velocity ν_r.

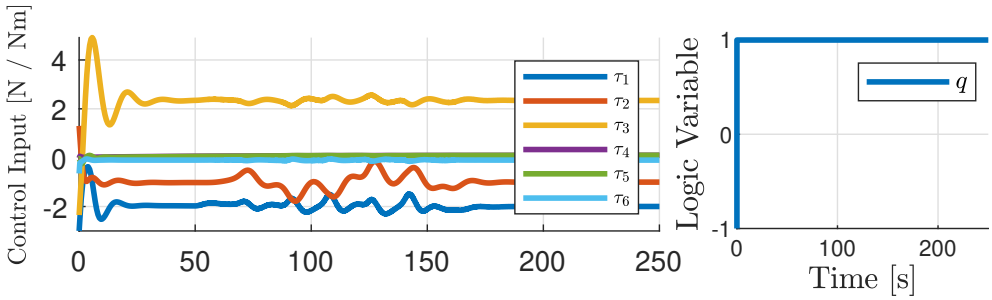

Figure 5.3: The control inputs τ and logic variable q.

Chapter 6

Adaptive Hybrid Feedback Control for Marine Vehicles

This chapter develops an adaptive hybrid feedback controller for global asymptotic tracking of a hybrid reference system for marine vehicles subject to parametric uncertainties. In contrast to backstepping-based hybrid adaptive control [81], the proposed approach permits estimation of the inertia matrix, and the switching mechanism is independent of the system velocities. As our approach is based on traditional Euler-Lagrange system models, the adaptive hybrid control law is applicable to other mechanical systems as well. In particular, it can easily be extended to robot manipulators or, more generally, vehicle-manipulator systems. The hybrid reference system is constructed from a parametrized loop and a speed assignment for the motion along the loop. The main benefit of this formulation is that it decouples the design of the path from the motion along the path, allowing us to globally asymptotically track a given parametrized loop at a desired and time-varying speed. The proposed reference system can be considered an adaptation of the maneuvering problem [84, 85] to a hybrid dynamical systems setting. The theoretical developments are validated experimentally for surface and underwater vehicle applications.

The material in this chapter is based on [86, 87].

6.1 Introduction

Some of the first adaptive control laws proposed for underwater vehicles can be found in [21] and [126], where Euler angle representations were utilized for the vehicle orientation. The first quaternion-based control laws for underwater vehicles were introduced in [127], while adaptive and quaternion-based control approaches for underwater vehicles can be found in [128] and [129]. None of the aforementioned quaternion-based approaches achieve global asymptotic stability results, since they only stabilize one of the equilibrium points corresponding to the desired orientation. Adaptive backstepping designs for tracking control of ships were introduced in [130], [131], and [132]. However, none of these methods permit estimation of the inertia matrix parameters, and all of them lift the vehicle orientation from the circle to the field of real numbers, which leads to unwinding problems.

To the best of our knowledge, experimental validations of globally stabilizing hy-

brid control laws for surface and underwater vehicles are virtually nonexistent in the existing literature. A combined hybrid observer/controller for dynamic positioning of a marine surface vehicle with global exponential stability properties was proposed in [133]. However, this result was achieved by a priori assuming that the angular velocity is bounded and by lifting the vehicle orientation from the circle to the field of real numbers, which leads to unwinding problems.

The remainder of this chapter is organized as follows. Section 6.2 presents kinematic and dynamic models of marine vehicles, a hybrid reference system based on a parametrized loop, and the resulting error system. The hybrid control law developed in Section 6.3 is based on a set of potential functions and a hysteretic switching mechanism. In Section 6.4, we construct potential functions and switching mechanisms to overcome the topological obstructions of SE(2) and SE(3). Moreover, we show that the aforementioned potential functions and switching mechanisms satisfy the assumptions in Section 6.3. In Section 6.5, we present the results of three experiments conducted on marine surface and underwater vehicles.

6.2 Modeling

This section begins by presenting kinematic and dynamic models of marine vehicles. Then, we derive a hybrid reference system generating continuous and bounded configuration, velocity and acceleration references from a parametrized loop. Moreover, the motion along the path can be independently controlled by specifying a desired speed, which takes values within a compact interval. Finally, we derive the error system and formulate the problem statement.

6.2.1 Models for Surface and Underwater Marine Vehicles

The configuration of a marine vehicle can be identified with a matrix Lie group $\mathcal{G} \subset \mathbb{R}^{n\times n}$ of dimension $k \leq 6$, which is typically either $\mathrm{SE}(2), \mathrm{SE}(3)$ or $\widetilde{\mathrm{SE}}(3)$. Let $g \in \mathcal{G}$ denote the configuration and $\nu = (v, \omega) \in \mathbb{R}^k$ denote the body velocity, where v and ω denote the linear and angular velocities of the vehicle. Using the Lie group structure of the configuration space, the equations of motion for fully actuated marine vehicles are given by

$$\dot{g} = g\widehat{\nu}, \tag{6.1a}$$

$$M\dot{\nu} - \mathrm{ad}_\nu^\mathsf{T} M\nu = d(\nu) + f(g) + \tau, \tag{6.1b}$$

where $M \in \mathbb{R}^{k\times k}$ is the inertia matrix, including hydrodynamic added mass, $\mathrm{ad}_\nu^\mathsf{T} M\nu$ describes Coriolis and centrifugal forces, the function $d : \mathbb{R}^k \to \mathbb{R}^k$ describes dissipative forces, $f : \mathcal{G} \to \mathbb{R}^k$ contains potential forces and disturbances, and $\tau \in \mathbb{R}^k$ is the control force.

6.2.2 Hybrid Reference System

We construct a hybrid reference trajectory $g_d : \mathbb{R}_{\geq 0} \times \mathbb{Z}_{\geq 0} \to \mathcal{G}$ by composing a path $\gamma : [0, 1] \to \mathcal{G}$ with a time scaling $s : \mathbb{R}_{\geq 0} \times \mathbb{Z}_{\geq 0} \to [0, 1]$, i.e. $g_d(t, j) = \gamma(s(t, j))$. A key advantage of this formulation is that it decouples the geometric path from the desired motion along the path.

Definition 6.1. *Let $\mathcal{I} = [0,1]$, $\mathrm{H}_2 = \mathrm{SO}(2)$, $\mathrm{H}_3 = \mathrm{SU}(2)$ and $m \in \{2,3\}$. The parametric C^r-path $\gamma\colon \mathcal{I} \to \mathcal{G} \coloneqq \mathbb{R}^m \rtimes \mathrm{H}_m$ defined by*

$$\gamma(s) \coloneqq (\gamma_1(s), \gamma_2(s)), \quad \gamma_1(s) \in \mathbb{R}^m, \gamma_2(s) \in \mathrm{H}_m, \tag{6.2}$$

is a C^r-loop if it satisfies

$$\gamma^{(j)}(0) = \gamma^{(j)}(1), \tag{6.3}$$

for all $0 \leq j \leq r$.

Given a loop γ, the motion along the loop can be controlled through a speed assignment for $\dot{s}$. In particular, by assuming that $|\gamma_1'(s)| \neq 0$ for all $s \in \mathcal{I}$, the desired speed of the vehicle can be controlled through the following speed assignment [84]

$$\dot{s} = \varrho(s, u_d) \coloneqq \frac{u_d}{|\gamma_1'(s)|}, \tag{6.4}$$

where $u_d \in \mathbb{R}$ is a desired input speed. To ensure continuity of the velocity and acceleration references, the desired speed can be obtained from the following set-valued second-order low-pass filter with natural frequency $\omega_n > 0$ and damping factor $\zeta_f > 0$

$$\ddot{u}_d \in \mathcal{U}(u_d, \dot{u}_d) \coloneqq \omega_n^2[0, c] - 2\zeta_f \omega_n \dot{u}_d - \omega_n^2 u_d, \tag{6.5}$$

where the interval $[0, c]$, with $c > 0$, contains the values of the commanded input speed μ.

Let $\Omega_1, \Omega_2 \subset \mathbb{R}$ be compact. The Lie group structure of the desired path γ leads to the following hybrid reference system:

$$\mathcal{R}\colon \begin{cases} \left.\begin{aligned} \dot{s} &= \varrho(s, u_d) \\ \dot{u}_d &= a_d \\ \dot{a}_d &\in \mathcal{U}(u_d, a_d) \end{aligned}\right\} & (s, u_d, a_d) \in \mathcal{I} \times \Omega_1 \times \Omega_2 \\ s^+ = 0 & (s, u_d, a_d) \in \{1\} \times \Omega_1 \times \Omega_2 \\ g_d = \gamma(s) \\ \nu_d = \kappa(s)\varrho(s, u_d) \\ \alpha_d = f_d(s, u_d, a_d) \end{cases}$$

where $\widehat{\kappa}(s) \coloneqq \gamma(s)^{-1}\gamma'(s)$ is the desired tangent vector expressed in the desired frame and the mapping $f_d\colon \mathcal{I} \times \Omega_1 \times \Omega_2 \to \mathbb{R}^k$ is given by

$$f_d(\cdot) = \kappa(s)\left(\frac{\partial \varrho}{\partial s}\varrho(s, u_d) + \frac{\partial \varrho}{\partial u_d}a_d\right) + \kappa'(s)\varrho(s, u_d)^2. \tag{6.6}$$

Conceptually, $\mathcal{R}$ can be considered as a hybrid system with the commanded speed $\mu \in [0, c]$ as the input, and

$$y \coloneqq (g_d, \nu_d, \alpha_d) = (\gamma(s), \kappa(s)\varrho(s, u_d), f_d(s, u_d, a_d)), \tag{6.7}$$

as the output, where $g_d \in \operatorname{rge}\gamma, \nu_d \in \mathbb{R}^k$ and $\alpha_d \in \mathbb{R}^k$ are the desired configuration, velocity and acceleration references, respectively. We remark that the speed assignment

for $\dot{s}$ in (6.4) ensures that the norm of the desired linear velocity v_d is equal to the desired speed u_d. Note that if γ is a C^2-loop, then it follows from $\gamma^{(j)}(0) = \gamma^{(j)}(1)$ for all $0 \leq j \leq 2$ and continuity of u_d, a_d that the output map $y = (g_d, \nu_d, \alpha_d)$ is continuous. We remark that for practical purposes, only a compact path is required. This, in turn, removes the switching component of the reference system. However, the loop assumption helps ensure that every maximal solution is complete.

6.2.3 Error System

The error dynamics are obtained by considering the continuous and invertible transformation $(g, \nu, r) \mapsto (g_e, \nu_e, r)$, using the natural (and left-invariant) error defined by [101]

$$g_e \coloneqq g_d^{-1} g, \tag{6.8}$$

$$\nu_e \coloneqq \nu - \operatorname{Ad}_{g_e}^{-1} \nu_d. \tag{6.9}$$

We observe that g_e expresses the configuration of the vehicle-fixed frame with respect to the desired vehicle-fixed frame, while the term $\nu_r \coloneqq \operatorname{Ad}_{g_e}^{-1} \nu_d$ can be interpreted as ν_d expressed in the vehicle-fixed frame. Moreover, the derivative of ν_r satisfies

$$\dot{\nu}_r = \operatorname{Ad}_{g_e}^{-1} \alpha_d - \operatorname{ad}_{\nu_e} \operatorname{Ad}_{g_e}^{-1} \nu_d. \tag{6.10}$$

The error dynamics can now be stated as

$$\mathcal{N}: \begin{cases} \left.\begin{aligned} \dot{g}_e &= g_e \widehat{\nu}_e \\ \dot{\nu}_e &= f_e(g_e, \nu_e, s, u_d, a_d, \tau) \\ \dot{s} &= \varrho(s, u_d) \\ \dot{u}_d &= a_d \\ \dot{a}_d &\in \mathcal{U}(u_d, a_d) \end{aligned}\right\} & (g_e, \nu_e, s, u_d, a_d) \in \widehat{C} \\ s^+ = 0 & (g_e, \nu_e, s, u_d, a_d) \in \widehat{D} \end{cases}$$

where $\widehat{C} = \mathcal{G} \times \mathbb{R}^k \times \mathcal{I} \times \Omega_1 \times \Omega_2$, $\widehat{D} = \mathcal{G} \times \mathbb{R}^k \times \{1\} \times \Omega_1 \times \Omega_2$ and the mapping $f_e \colon \mathcal{G} \times \mathbb{R}^k \times \mathcal{I} \times \Omega_1 \times \Omega_2 \times \mathbb{R}^k \to \mathbb{R}^k$ is given by

$$\begin{aligned} f_e(\cdot) \coloneqq M^{-1}(\tau - M \nabla_\nu^M \nu + d(\nu) + f(g)) - \operatorname{Ad}_{g_e}^{-1} f_d(s, u_d, a_d) \\ + \operatorname{ad}_{\nu_e} \operatorname{Ad}_{g_e}^{-1} \kappa(s) \varrho(s, u_d). \end{aligned} \tag{6.11}$$

We remark that the matrix representation of the adjoint maps Ad and ad are provided in Section 6.5 for the Lie groups SE(2) and SE(3) and their Lie algebras $\mathfrak{se}(2)$ and $\mathfrak{se}(3)$.

Lemma 6.1. The hybrid system $\mathcal{N}$ satisfies the hybrid basic conditions [90, Assumption 6.5].

Proof. The flow and jump sets $\widehat{C}$ and $\widehat{D}$ are closed since Ω_1 and Ω_2 are closed. Moreover, the jump map is single-valued and continuous. The flow map is single-valued and continuous for every state except a_d. However, since the set-valued mapping $\mathcal{U}$ is outer semicontinuous, convex and locally bounded, the flow map is outer semicontinuous, convex-valued and locally bounded. □

Problem Statement

For a given C^2-loop γ, the speed assignment ϱ defined in (6.4) for $\dot{s}$ and a compact set $\mathcal{A}^\bullet \subset \mathcal{G}$, design a hybrid feedback control law with output $\tau \in \mathbb{R}^k$ such that every solution to $\mathcal{N}$ is bounded and converges to the compact set

$$\mathcal{B} = \{(g_e, \nu_e, s, u_d, a_d) : g_e \in \mathcal{A}^\bullet, \nu_e = 0\}, \tag{6.12}$$

for the system $\mathcal{N}$ under parametric uncertainties.

6.3 Hybrid Control Design

In this section, we propose an adaptive hybrid feedback control law for the system $\mathcal{N}$. The control law is derived from a set of potential functions and a hysteretic switching mechanism encoded by the flow and jump sets and the jump map. The hybrid controller is based on the following assumption.

Assumption 6.2. Given a 5-tuple $(\mathcal{A}, C, D, G, V)$, where $V : \mathcal{O} \to \mathbb{R}$ is defined by $(g, q) \mapsto V(g, q) = V_q(g)$, where $q \in Q$ is a logic variable, $Q \subset \mathbb{R}$ is a finite set and $\mathcal{O}$ is an open set containing $C \subset \mathcal{G} \times Q$.

(A1) $\mathcal{A} \subset C$ is a compact set and $\pi_1(\mathcal{A}) = \mathcal{A}^\bullet$;
(A2) C and D are closed subsets of $\mathcal{G} \times Q$ such that $C \cup D = \mathcal{G} \times Q$ and $\pi_1(C) = \mathcal{G}$;
(A3) The set-valued mapping $G : D \rightrightarrows Q$ is nonempty for all $(g, q) \in D$ and outer semicontinuous and locally bounded relative to D;
(A4) for every $(g, q) \in C \cap D$, it holds that $(g, w) \in C \setminus D$ for each $w \in G(g, q)$;
(A5) there exists $N \in \mathbb{Z}_{\geq 1}$ such that for every $(g, q) \in D$, it holds that $(g, w) \in C \setminus D$ for each $(g, w) \in \overline{G}^K(g, q)$, where $1 \leq K \leq N$, $\overline{G}(g, q) = \{g\} \times G(g, q)$ and $\overline{G}^K := \underbrace{\overline{G} \circ \overline{G} \circ \cdots \circ \overline{G}}_{K\text{times}}$;
(A6) V is continuously differentiable on $\mathcal{O}$ and the restriction of V to C is proper and positive definite with respect to $\mathcal{A}$;
(A7) for all $(g, q) \in C \cap D$ and each $w \in G(g, q)$

$$V_w(g) - V_q(g) \leq 0; \tag{6.13}$$

(A8) for all $(g, q) \in C$, $\mathrm{d}V_q(g) = 0$ if and only if $(g, q) \in \mathcal{A}$.

Assumption 6.2 guarantees that the switching is hysteretic, the hybrid control law satisfies the hybrid basic conditions and is required to ensure that every solution to $\mathcal{N}$ converges to $\mathcal{B}$.

We remark that the conditions of Assumption 6.2 are different from the conditions for synergistic control [61, Definition 7.3]. First, they do not enforce a strict decrease in V across jumps. Second, they are not restricted to a switching mechanism based on the value of the potential functions V_q. Finally, they permit each potential function V_q to be defined locally, i.e., having a domain that is a strict subset of $\mathcal{G}$.

To establish convergence to the set $\mathcal{B}$ when the model parameters are unknown, we define the modified reference velocity $\nu_m \in \mathbb{R}^k$ and the corresponding reference velocity error $\zeta := \nu_m - \nu_r$ through the differential equation

$$\Lambda[\dot{\zeta} + \nabla_\nu^\Lambda \zeta] = -\mathrm{d}V_q(g_e) - \vartheta_q(\zeta), \tag{6.14}$$

where $\vartheta_q : \mathbb{R}^k \to \mathbb{R}^k$ is continuous and satisfies $\langle \vartheta_q(\zeta), \zeta \rangle > 0$ for every $\zeta \in \mathbb{R}^k \setminus \{0\}$ and every $q \in Q$. We remark that ϑ can be chosen independent of q and that the term $\Lambda \nabla^{\Lambda}_{\nu} \zeta$ is optional. The latter is because $\langle \zeta, \Lambda \nabla^{\Lambda}_{\xi} \zeta \rangle = 0$ for any $\xi \in \mathbb{R}^k$, which entails that any velocity can be used in place of ν in the bilinear map ∇^{Λ}. The velocity error is now redefined as

$$\xi \coloneqq \nu - \nu_m = \nu_e - \zeta. \tag{6.15}$$

Since $\zeta = 0$ implies $\xi = \nu_e$, the velocity tracking control objective $\nu_e = 0$ is accomplished when $(\xi, \zeta) = 0$. In practice, this type of velocity error may be advantageous when the configuration error encoded by $\mathrm{d}V$ is significant while the velocity error ν_e is zero.

Before delving into the proposed adaptive controller, we begin by presenting the non-adaptive version. Given a 5-tuple $(\mathcal{A}, C, D, G, V)$ satisfying Assumption 6.2 and if the model parameters in (6.1) are known, we propose the following hybrid control law

$$\begin{cases} \dot{\zeta} = -\nabla^{\Lambda}_{\nu} \zeta - \Lambda^{-1}\big(\mathrm{d}V_q(g_e) + \vartheta_q(\zeta)\big), & (g_e, q) \in C \\ q^+ \in G(g_e, q), & (g_e, q) \in D \\ \tau = M[\dot{\nu}_m + \nabla^{M}_{\nu} \nu_m] - d(\nu) \\ \qquad - f(g) - \mathrm{d}V_q(g_e) - \varphi_q(\xi). \end{cases} \tag{6.16}$$

Observe that the feedback control law (6.16) comprises a proportional action $\mathrm{d}V$ and a derivative action φ, where $\varphi_q \colon \mathbb{R}^k \to \mathbb{R}^k$ is continuous and satisfies $\langle \varphi_q(\xi), \xi \rangle > 0$ for every $\xi \in \mathbb{R}^k \setminus \{0\}$ and every $q \in Q$. In other words, the control law (6.16) is essentially a PD+ control law [134] with desired velocity ν_m and hysteretic switching. We note that the derivative action can be chosen independently of the logic variable q. However, the proportional action can only be chosen independently of q provided that the configuration space is globally diffeomorphic to Euclidean space.

To make the control law (6.16) adaptive, we make the following assumption on the unknown model parameters.

Assumption 6.3. There exists a known matrix-valued function of available data $\Phi \colon \mathcal{G} \times \mathbb{R}^k \times \mathbb{R}^k \times \mathcal{I} \times \Omega_1 \times \Omega_2 \to \mathbb{R}^{k \times l}$ and a vector of unknown model parameters $\theta \in \mathbb{R}^l$ with known lower and upper bounds $\underline{\theta}$ and $\overline{\theta}$ such that

$$M[\dot{\nu}_m + \nabla^{M}_{\nu} \nu_m] - d(\nu) - f(g) = \Phi(g_e, \zeta, \xi, s, u_d, a_d)\theta, \tag{6.17}$$

for all $(g_e, \zeta, \xi, s, u_d, a_d) \in \mathcal{G} \times \mathbb{R}^k \times \mathbb{R}^k \times \mathcal{I} \times \Omega_1 \times \Omega_2$.

The boundedness assumption on the parameters is justified by the fact that the parameters represent real physical quantities that we often have rough estimates of in practice. Assumption 6.3 implies that the parameters are contained in the convex set

$$\mathcal{P} \coloneqq \{\theta \in \mathbb{R}^l : \underline{\theta} \leq \theta \leq \overline{\theta}\}. \tag{6.18}$$

Define the extended tangent cone to $\mathcal{P}$ by

$$T_{\mathbb{R},\mathcal{P}}(\theta) \coloneqq T_{\mathbb{R},[\underline{\theta}_1, \overline{\theta}_1]}(\theta_1) \times T_{\mathbb{R},[\underline{\theta}_2, \overline{\theta}_2]}(\theta_2) \times \cdots \times T_{\mathbb{R},[\underline{\theta}_l, \overline{\theta}_l]}(\theta_l), \tag{6.19}$$

where the extended tangent cone to each interval is given by

$$T_{\mathbb{R},[\underline{\theta}_i,\overline{\theta}_i]}(\theta_i) \coloneqq \begin{cases} [0,\infty) & \text{if } \theta_i \leq \underline{\theta}_i \\ (-\infty,\infty) & \text{if } \theta_i \in (\underline{\theta}_i,\overline{\theta}_i) \\ (-\infty,0] & \text{if } \theta_i \geq \overline{\theta}_i \end{cases} \tag{6.20}$$

Let $\theta_a \in \mathbb{R}^l$ denote the estimate of θ and define the convex set

$$\mathcal{P}_\epsilon \coloneqq \{\theta_a \in \mathbb{R}^l : \underline{\theta} - \epsilon \leq \theta_a \leq \overline{\theta} + \epsilon\}, \tag{6.21}$$

where $\epsilon = (\epsilon_1, \ldots, \epsilon_l) \in \mathbb{R}^l$, defines boundary layers of length $\epsilon_i > 0$ around each interval in (6.18). The goal is to enforce $\theta_a \in \mathcal{P}_\epsilon$ through the adaptive update law. To this end, we define the projection operator $\mathrm{Proj}\colon \mathbb{R}^l \times \mathcal{P}_\epsilon \to \mathbb{R}^l$ by [135]

$$\mathrm{Proj}(\chi, \theta_a) \coloneqq \begin{cases} \chi, & \text{if } \chi \in T_{\mathbb{R},\Omega}(\theta_a) \\ (1 - h(\theta_a))\chi & \text{if } \chi \notin T_{\mathbb{R},\Omega}(\theta_a) \end{cases} \tag{6.22}$$

where the components of $h(\theta_a)$ are given by

$$h_i(\theta_{a,i}) = \begin{cases} 0, & \text{if } \theta_{a,i} \in (\underline{\theta}_i,\overline{\theta}_i) \\ \min\{1, \frac{\underline{\theta}_i - \theta_{a,i}}{\epsilon_i}\}, & \text{if } \theta_{a,i} \leq \underline{\theta}_i \\ \min\{1, \frac{\theta_{a,i} - \overline{\theta}_i}{\epsilon_i}\}, & \text{if } \theta_{a,i} \geq \overline{\theta}_i \end{cases} \tag{6.23}$$

The following lemma can be found in [135, Lemma E.1].

Lemma 6.2. The projection operator (6.22) satisfies

(P1) The mapping $\mathrm{Proj}\colon \mathbb{R}^l \times \mathcal{P}_\epsilon \to \mathbb{R}^l$ is Lipschitz continuous in χ and θ_a.

(P2) The differential equation

$$\dot{\theta}_a = \mathrm{Proj}(\chi, \theta_a), \quad \theta_a(t_0) \in \mathcal{P}_\epsilon, \tag{6.24}$$

satisfies $\theta_a \in \mathcal{P}_\epsilon$ for all $t \geq t_0$.

(P3) Let $\theta_e = \theta - \theta_a$ denote the estimation error, then

$$-\langle \theta_e, \Gamma^{-1}\mathrm{Proj}(\chi, \theta_a)\rangle \leq -\langle \theta_e, \Gamma^{-1}\chi\rangle, \tag{6.25}$$

for all $\theta_a \in \mathcal{P}_\epsilon$ and $\theta \in \mathcal{P}$.

Using (6.17) and the projection operator defined in (6.22), we define an adaptive version of (6.16) by

$$\begin{cases} \left.\begin{aligned} \dot{\zeta} &= -\nabla_\nu^\Lambda \zeta - \Lambda^{-1}\big(\mathrm{d}V_q(g_e) + \vartheta_q(\zeta)\big) \\ \dot{\theta}_a &= \mathrm{Proj}(-\Gamma\Phi(g_e,\zeta,\xi,s,u_d,a_d)^\mathsf{T}\xi, \theta_a) \end{aligned}\right\} (g_e,q) \in C \\ q^+ \in G(g_e,q) \qquad (g_e,q) \in D \\ \tau = \Phi(g_e,\zeta,\xi,s,u_d,a_d)\theta_a - \mathrm{d}V_q(g_e) - \varphi_q(\xi). \end{cases} \tag{6.26}$$

By defining $x \coloneqq (g_e, \xi, s, u_d, a_d, \zeta, \theta_a, q) \in \mathcal{X}$ and the extended state space

$$\mathcal{X} \coloneqq \mathcal{G} \times \mathbb{R}^k \times \mathcal{I} \times \Omega_1 \times \Omega_2 \times \mathbb{R}^k \times \mathcal{P}_\epsilon \times Q, \tag{6.27}$$

the adaptive hybrid control law (6.26) applied to the hybrid system $\mathcal{N}$ leads to the hybrid closed-loop system

$$\mathcal{H}: \begin{cases} \left.\begin{aligned} \dot{g}_e &= g_e \widehat{\xi+\zeta} \\ \dot{\xi} &= \tilde{f}(x) \\ \dot{s} &= \varrho(s, u_d) \\ \dot{u}_d &= a_d \\ \dot{a}_d &\in \mathcal{U}(u_d, a_d) \\ \dot{\zeta} &= -\nabla_\nu^\Lambda \zeta - \Lambda^{-1}\big(\mathrm{d}V_q(g_e) + \vartheta_q(\zeta)\big) \\ \dot{\theta}_a &= \mathrm{Proj}(-\Gamma \Phi(g_e, \zeta, \xi, s, u_d, a_d)^\mathsf{T} \xi, \theta_a) \end{aligned}\right\} & x \in \widetilde{C} \\ (q^+, s^+) \in \widetilde{G}(g_e, q, s) & x \in \widetilde{D}, \end{cases} \tag{6.28}$$

where

$$\tilde{f}(x) \coloneqq -M^{-1}\Phi(g_e, \zeta, \xi, s, u_d, a_d)\theta_e - \nabla_\nu^M \xi - M^{-1}(\mathrm{d}V_q(g_e) + \varphi_q(\xi)). \tag{6.29}$$

Moreover, the jump map $\widetilde{G} : \mathcal{G} \times Q \times \mathcal{I} \rightrightarrows Q \times \mathcal{I}$ is defined as

$$\widetilde{G}(g_e, q, s) \coloneqq \begin{cases} (G(g_e, q), s)\,, & (g_e, q, s) \in D \times (\mathcal{I} \backslash \{1\}) \\ \{(G(g_e, q), s)\,, (q, 0)\} & (g_e, q, s) \in D \times \{1\} \\ (q, 0), & (g_e, q, s) \in (C \backslash D) \times \{1\} \end{cases} \tag{6.30}$$

while the flow set $\widetilde{C}$ and jump set $\widetilde{D}$ are defined by

$$\widetilde{C} \coloneqq \{x \in \mathcal{X} : (g_e, q) \in C\}, \tag{6.31}$$

$$\widetilde{D} \coloneqq \{x \in \mathcal{X} : (g_e, q) \in D\} \cup \{x \in \mathcal{X} \colon s = 1\}. \tag{6.32}$$

Lemma 6.3. The closed-loop system $\mathcal{H}$ satisfies the hybrid basic conditions.

Proof. From Lemma 6.1, Assumption 6.2 and the definitions of the jump map, flow set and jump set, it follows that all of the assumptions in [61, Lemma 2.21] are satisfied. □

Theorem 6.4. *Let Assumption 6.3 hold. Given a 5-tuple $(\mathcal{A}, C, D, G, V)$ satisfying Assumption 6.2, the compact set*

$$\mathcal{A}_1 = \{x \in \mathcal{X} : (g_e, q) \in \mathcal{A}, \xi = 0, \zeta = 0, \theta_a = \theta\}, \tag{6.33}$$

is uniformly globally stable for the system $\mathcal{H}$ and every solution to $\mathcal{H}$ converges to

$$\mathcal{A}_2 = \{x \in \mathcal{X} : (g_e, q) \in \mathcal{A}, \xi = 0, \zeta = 0, \Phi(g_e, 0, 0, s, u_d, a_d)\theta_e = 0\}. \tag{6.34}$$

Proof. Let $\breve{\mathcal{H}}$ denote the hybrid system $\mathcal{H}$ with each jump set $\widetilde{D}$ replaced by $\breve{D} = \{x \in \mathcal{X} : (g_e, q) \in C \cap D\} \cup \{x \in \mathcal{X} \colon s = 1\}$ and consider the continuously differentiable function

$$W(g_e, q, \xi, \zeta, \theta_a) = V_q(g_e) + \frac{1}{2}\langle \xi, M\xi \rangle + \frac{1}{2}\langle \zeta, \Lambda\zeta \rangle + \frac{1}{2}\langle \theta_e, \Gamma^{-1}\theta_e \rangle. \tag{6.35}$$

For all $x \in \widetilde{C}$, the change in W along the solutions of $\breve{\mathcal{H}}$ is

$$\begin{aligned} &\langle \mathrm{d}V_q(g_e), \nu_e \rangle + \langle \zeta, -\mathrm{d}V_q(g_e) - \vartheta_q(\zeta) \rangle \\ &+ \langle \xi, -\Phi\theta_e - M\nabla_\nu^M \xi - \mathrm{d}V_q(g_e) - \varphi_q(\xi) \rangle \\ &- \langle \theta_e, \Gamma^{-1}\mathrm{Proj}(-\Gamma\Phi^\mathsf{T}\xi, \theta_a) \rangle, \end{aligned} \tag{6.36}$$

which simplifies to

$$\begin{aligned} &- \langle \xi, \varphi_q(\xi) \rangle - \langle \zeta, \vartheta_q(\zeta) \rangle - \langle \theta_e, \Gamma^{-1}\mathrm{Proj}(-\Gamma\Phi^\mathsf{T}\xi, \theta_a) + \Phi^\mathsf{T}\xi \rangle \\ &\leq -\langle \xi, \varphi_q(\xi) \rangle - \langle \zeta, \vartheta_q(\zeta) \rangle \\ &\leq 0, \end{aligned} \tag{6.37}$$

where the first inequality follows from (P3) in Lemma 6.2. For any $x \in \breve{D}$ and $(w, m) \in \widetilde{G}(g_e, q, s)$, the change in W across jumps is

$$W(g_e, w, \xi, \zeta, \theta_a) - W(g_e, q, \xi, \zeta, \theta_a) = V_w(g_e) - V_q(g_e),$$

which is clearly equal to zero when $(g_e, q, s) \in (C \backslash D) \times \{1\}$, i.e. when $w = q$. Otherwise, it follows from Assumption 6.2 that $V_w(g_e) - V_q(g_e) \leq 0$ for all $(q, w) \in Q \times \pi_1(\widetilde{G}(g_e, q, s))$. Consequently, the growth of W along solutions to $\breve{\mathcal{H}}$ is bounded by

$$u_c(x) = \begin{cases} -\langle \xi, \varphi_q(\xi) \rangle - \langle \zeta, \vartheta_q(\zeta) \rangle, & \text{if } x \in \widetilde{C} \\ -\infty, & \text{otherwise} \end{cases} \tag{6.38}$$

$$u_d(x) = \begin{cases} 0, & \text{if } x \in \breve{D} \\ -\infty, & \text{otherwise} \end{cases} \tag{6.39}$$

along flows and across jumps, respectively. It follows from Assumption 6.2 and (6.35) that W is proper and positive definite on $\widetilde{C} \cup \breve{D}$ with respect to the compact set $\mathcal{A}_1$. Hence, the proof of [90, Theorem 3.18] implies that $\mathcal{A}_1$ is uniformly globally stable for the hybrid system $\breve{\mathcal{H}}$. Observe that the system $\breve{\mathcal{H}}$ permits at most two consecutive jumps before a nonzero time of flow follows. Thus, since W is continuous, $\breve{\mathcal{H}}$ satisfies the hybrid basic conditions, and every maximal solution to $\breve{\mathcal{H}}$ is complete, it follows from [90, Corollary 8.7 (b)] that each solution to $\breve{\mathcal{H}}$ converges to the largest weakly invariant subset Ψ contained in

$$W^{-1}(r) \cap \overline{u_c^{-1}(0)}, \tag{6.40}$$

for some $r \in \mathbb{R}$, where

$$\overline{u_c^{-1}(0)} = \{x \in \mathcal{X} : \xi = 0, \zeta = 0, (g_e, q) \in C\}. \tag{6.41}$$

Moreover, the closed-loop system (6.28) is such that $\zeta \equiv 0$ implies $\mathrm{d}V_q(g_e) \equiv 0$, and it follows from Assumption 6.2 that $\mathrm{d}V_q(g_e) = 0$ implies $(g_e, q) \in \mathcal{A}$. Thus, $(\xi, \zeta) \equiv 0$ implies that $\Phi(g_e, 0, 0, s, u_d, a_d)\theta_e \equiv 0$, which results in

$$\Psi \subset W^{-1}(r) \cap \overline{u_c^{-1}(0)} \subset W^{-1}(r) \cap \mathcal{A}_2 \subset \mathcal{A}_2.$$

Consequently, since every solution is complete and bounded, every solution to $\breve{\mathcal{H}}$ converges to $\mathcal{A}_2$. Solutions to $\mathcal{H}$ that are not solutions to $\breve{\mathcal{H}}$ are those with initial values x^* such that $(g_e^*, q^*) \in D \backslash C$. However, it follows from (A5) that such solutions exhibit $1 \leq K \leq N$ immediate and consecutive jumps from q^* to some $w \in \overline{G}^K(g_e^*, q^*)$ satisfying $(g_e^*, w) \in C \backslash D$, after which the solutions coincide with a solution to $\breve{\mathcal{H}}$. Consequently, we conclude that $\mathcal{A}_1$ is uniformly globally stable for the hybrid system $\mathcal{H}$ and that every solution to the hybrid system $\mathcal{H}$ converges to $\mathcal{A}_2$. □

We remark that Theorem 6.4 implies that the problem statement is solved. Furthermore, note that uniform global asymptotic stability of the compact set

$$\widetilde{\mathcal{B}} = \{x \in \mathcal{X} : (g_e, q) \in \mathcal{A}, \zeta = 0, \xi = 0\}, \tag{6.42}$$

for the closed-loop system $\mathcal{H}$ implies that $\mathcal{B}$ is uniformly globally asymptotically stable for the error system $\mathcal{N}$. However, without further assumptions on the nature of the parametrized loop and commanded input speed, it is not possible to show that (6.26) uniformly globally asymptotically stabilizes the compact set $\widetilde{\mathcal{B}}$ for the closed-loop system $\mathcal{H}$. However, a trivial modification of the proof of Theorem 6.4 clearly shows that the non-adaptive hybrid control law (6.16) uniformly globally asymptotically stabilizes the compact set $\widetilde{\mathcal{B}}$ for the closed-loop system $\mathcal{H}$ with $\dot{\theta}_a = 0$ and $\theta_e = 0$, implying that $\mathcal{B}$ is uniformly globally asymptotically stable for the error system $\mathcal{N}$.

We remark that a trivial modification of the proof of Theorem 6.4 shows that the non-adaptive hybrid control law (6.16) uniformly globally asymptotically stabilizes the compact set $\widetilde{\mathcal{B}}$ for the closed loop system $\mathcal{H}$ with $\dot{\theta}_a = 0$ and $\theta_e = 0$, implying that $\mathcal{B}$ is uniformly globally asymptotically stable for the error system $\mathcal{N}$.

6.4 Potential Functions for Marine Vehicles

In this section we construct potential functions and derive 5-tuples $(\mathcal{A}, C, D, G, V)$ satisfying Assumption 6.2 for a surface vehicle and an underwater vehicle. This 5-tuple determines the proportional control action and the switching mechanism through the potential functions V and the flow set, jump set and jump map C, D, G, respectively.

6.4.1 Potential functions on SE(2)

The configuration of a surface vehicle can be identified with the matrix Lie group $\mathrm{SE}(2) = \mathbb{R}^2 \rtimes \mathrm{SO}(2)$. An element $g = (p, R) \in \mathrm{SE}(2)$ contains the position $p = (x, y) \in \mathbb{R}^2$ and orientation $R \in \mathrm{SO}(2)$ of a vehicle-fixed frame with respect to an inertial frame.

Using the linear action of $\mathrm{SO}(2)$ on $\mathbb{R}^2$ defined by $(p, R) \mapsto Rp$, the semidirect product $\mathrm{SE}(2) = \mathbb{R}^2 \rtimes \mathrm{SO}(2)$ yields the natural error on $\mathrm{SE}(2)$

$$g_e = g_d^{-1} g = (p_e, R_e) = (R_d^{\mathsf{T}}(p - p_d), R_d^{\mathsf{T}} R). \tag{6.43}$$

The goal is to construct potential functions and a switching mechanism for stabilization of the configuration corresponding to the compact set

$$\mathcal{A}^{\bullet} = \{g_e \in \mathrm{SE}(2) : p_e = 0, R_e = e\}. \tag{6.44}$$

To this end, we let $\delta > 0$, and define the functions $\rho_1 : \mathcal{D}_1 \to \mathbb{R}$, $\rho_2 : \mathcal{D}_2 \to \mathbb{R}$ and $\rho_3 : \mathcal{D}_3 \to \mathbb{R}$, where $\mathcal{D}_1 = \mathcal{D}_2 := \{R \in \mathrm{SO}(2) : \widetilde{\log} R \in [\delta, \pi] \cup (-\pi, -\delta]\}$ and $\mathcal{D}_3 := \mathrm{SO}(2)$ by

$$\rho_1(R) := \begin{cases} \widetilde{\log} R, & \text{if } \widetilde{\log} R \in [\delta, \pi] \\ \widetilde{\log} R + 2\pi, & \text{if } \widetilde{\log} R \in (-\pi, -\delta] \end{cases} \tag{6.45a}$$

$$\rho_2(R) := \begin{cases} \widetilde{\log} R, & \text{if } \widetilde{\log} R \in (-\pi, -\delta] \\ \widetilde{\log} R - 2\pi, & \text{if } \widetilde{\log} R \in [\delta, \pi] \end{cases} \tag{6.45b}$$

$$\rho_3(R) := \widetilde{\log} R, \tag{6.45c}$$

where $\widetilde{\log} R = \mathrm{atan2}(R_{21}, R_{11})$ is the principal logarithm of $R \in \mathrm{SO}(2)$, which corresponds to the heading angle $\psi \in (-\pi, \pi]$ in practice. Now, for each $q \in Q = \{1, 2, 3\}$, we define the potential functions $V_q : \mathcal{D}_q \times \mathbb{R}^2 \to \mathbb{R}_{\geq 0}$ by

$$V_q(g_e) := \tfrac{1}{2} k_q \rho_q(R_e)^2 + \tfrac{1}{2} p_e^\mathsf{T} K p_e + o_q, \tag{6.46}$$

where $K = K^\mathsf{T} > 0$, $k_1 = k_2 = k > 0$, $k_3 > 0$, $o_1 = o_2 = o$ and $o_3 = 0$. Due to the topology of $\mathrm{SO}(2)$, at least two potential functions are required to design a globally asymptotically stable hybrid control law. However, by using three potential functions we obtain improved transient performance by encoding smaller proportional gains into the global controllers ($q \in \{1, 2\}$) relative to the local controller ($q = 3$). To this end, the role of the offsets is to enable $k_3 > k$, i.e., a larger proportional gain locally around $R_e = I$. A visualization of the rotational part of the potential functions is shown in Figure 6.1.

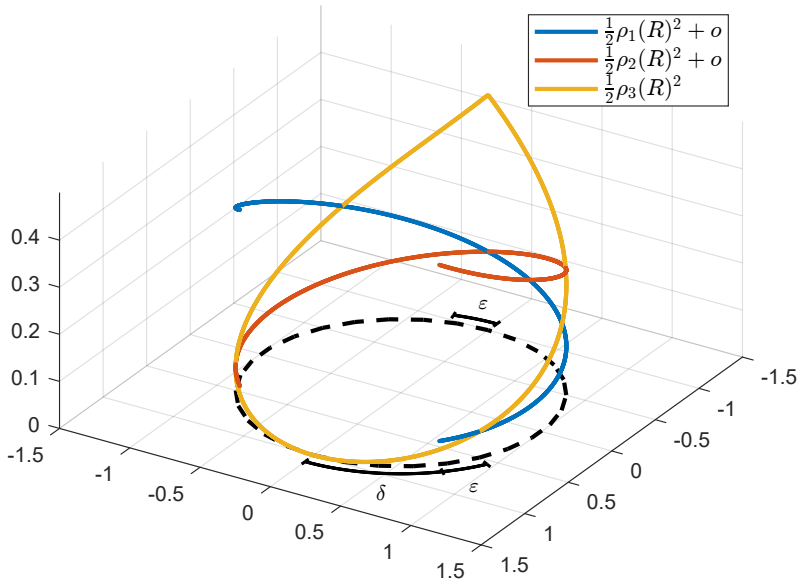

Figure 6.1: The rotational part of the potential functions $\{V_q\}_{q \in Q}$ with $k = \frac{1}{(2\pi)^2}$, $k_3 = \frac{4}{(2\pi)^2}$, $\delta = \frac{\pi}{4}$, $\varepsilon = \frac{\pi}{12}$, and $o = \frac{1}{2}(\delta + \varepsilon)^2(k_3 - k)$.

The switching mechanism is defined by the flow and jump sets $C, D \subset \mathrm{SE}(2) \times Q$ and the jump map $G\colon D \rightrightarrows Q$ associated with the potential functions $\{V_q\}_{q\in Q}$. We define the flow and jump sets by

$$C \coloneqq \bigcup_{q\in Q} C_q \times \{q\}, \tag{6.47a}$$

$$D \coloneqq \bigcup_{q\in Q} D_q \times \{q\}, \tag{6.47b}$$

where

$$C_1 \coloneqq \{g_e \in \mathrm{SE}(2) : \delta \leq \rho_1(R_e) \leq \pi + \varepsilon\}, \tag{6.48a}$$

$$C_2 \coloneqq \{g_e \in \mathrm{SE}(2) : \delta \leq -\rho_2(R_e) \leq \pi + \varepsilon\}, \tag{6.48b}$$

$$C_3 \coloneqq \{g_e \in \mathrm{SE}(2) : |\rho_3(R_e)| \leq \delta + \varepsilon\}. \tag{6.48c}$$

and

$$\begin{aligned} D_1 \coloneqq &\{g_e \in \mathrm{SE}(2)\colon \pi + \varepsilon \leq \rho_1(R_e) \leq 2\pi - \delta\} \\ &\cup \{g_e \in \mathrm{SE}(2)\colon |\rho_3(R_e)| \leq \delta\} \end{aligned} \tag{6.49a}$$

$$\begin{aligned} D_2 \coloneqq &\{g_e \in \mathrm{SE}(2)\colon \pi + \varepsilon \leq -\rho_2(R_e) \leq 2\pi - \delta\} \\ &\cup \{g_e \in \mathrm{SE}(2)\colon |\rho_3(R_e)| \leq \delta\} \end{aligned} \tag{6.49b}$$

$$D_3 \coloneqq \{g_e \in \mathrm{SE}(2)\colon |\rho_3(R_e)| \geq \delta + \varepsilon\}. \tag{6.49c}$$

In (6.48) and (6.49), $\delta > 0$ determines the switching point between the local and global controllers while $\varepsilon > 0$ denotes the hysteresis half-width between the global controllers. Finally, we define the set-valued jump map for all $(g_e, q) \in D$ by

$$G(g_e, q) \coloneqq \{w \in Q \setminus \{q\} : g_e \in C_w \cap D_q\}. \tag{6.50}$$

The following lemma provides conditions on the gains and offsets in (6.46), ensuring that V is nonincreasing across jumps.

Lemma 6.4. Let $\mathcal{A} = \mathcal{A}^\bullet \times \{3\}$. If $k_3 \geq k, \delta + 2\varepsilon < \pi$ and

$$\tfrac{1}{2}\delta^2(k_3 - k) \leq o \leq \tfrac{1}{2}(\delta + \varepsilon)^2(k_3 - k), \tag{6.51}$$

then the 5-tuple $(\mathcal{A}, C, D, G, V)$ satisfies Assumption 6.2.

Proof. (A1-A2) $\mathcal{A}$ is compact since it is finite, while C and D are closed subsets of $\mathrm{SE}(2) \times Q$ since each ρ_q is continuous and the sublevel sets of a continuous function are closed. Moreover, $\bigcup_{q\in Q} C_q = \mathrm{SE}(2)$ and $C_q \cup D_q = \mathrm{SE}(2)$ for each $q \in Q$. Hence, (A1)-(A2) hold.

(A3) Observe that G is locally bounded since $\operatorname{rge} G = Q$ is compact. Moreover, it follows from (A2) that G nonempty for all $(g_e, q) \in D$. Since $G^{-1}(w) = \bigcup_{q\neq w} (C_w \cap D_q) \times \{q\}$ is closed, $\operatorname{gph} G^{-1} = \bigcup_{w\in Q} G^{-1}(w) \times \{w\}$ and the intersection of closed sets are closed, it follows from [102, Theorem 5.7 (a)] that G^{-1} is outer semicontinuous everywhere, and hence that G is outer semicontinuous everywhere.

(A4) Let $g_e \in C_q \cap D_q$ and $w \in G(g_e, q)$. Consider the case where $q \in \{1, 2\}$. If $w = 3$, then it follows that $|\rho_3(R_e)| = \delta$, and hence that $g_e \in C_3 \setminus D_3$. Otherwise,

$w = 3 - q$ and it follows that $|\rho_q(R_e)| = \pi + \varepsilon$, which implies that $|\rho_w(R_e)| = \pi - \varepsilon$ and hence that $g_e \in C_{3-q} \backslash D_{3-q}$. Finally, consider that $q = 3$. Then, $g_e \in C_q \cap D_q$ implies that $|\rho_3(R_e)| = \delta + \varepsilon$, which further implies that $g_e \in C_w \backslash D_w$.

(A5) Let $(g_e, q) \in D \backslash C$. Then, $g_e \in C_w$ for some $w \in G(g_e, q)$. Consequently, $g_e \in C_w \backslash D_w$ or $g_e \in C_w \cap D_w$. It follows from (A4) that (A5) holds with $N = 2$.

(A6) V is clearly continuously differentiable on $\mathcal{O}$ and positive definite with respect to $\mathcal{A}$. Moreover, since the function $\tilde{V} : \mathcal{D} \to \mathbb{R}$, where $\mathcal{D} = \bigcup_{q \in Q} \mathcal{D}_q \times \{q\}$ defined by $(R, q) \mapsto \frac{1}{2} k_q \rho_q(R)^2$ is continuous, $\pi_1(\mathcal{D}) = \mathrm{SO}(2)$, and $\mathrm{SO}(2)$ is compact, it follows that $\tilde{V}_q$ is proper. Additionally, the function $\check{V}_q : \mathbb{R}^2 \to \mathbb{R}$ defined by $p \mapsto \frac{1}{2} p^{\mathsf{T}} K p$ is radially unbounded. Consequently, $V_q(g_e) = \tilde{V}_q(R_e) + \check{V}_q(p_e)$ is a proper map.

To prove (A7), consider $g_e \in C_q \cap D_q$, $q \in \{1, 2\}$, $w = 3 - q$, and $0 < \varepsilon < \pi$. It follows immediately from the definitions of ρ_1 and ρ_2 that $V_{3-q}(g_e) - V_q(g_e) < 0$. When $g_e \in C_q \cap D_q$, $q \in \{1, 2\}$, $w = 3$, $0 < \varepsilon < \pi$ and $0 < \delta < \pi$, it holds that $\rho_3(R_e)^2 \leq \rho_q(R_e)^2$, which implies that

$$V_3(g_e) - V_q(g_e) \leq \frac{1}{2}(k_3 - k)\rho_3(R_e)^2 - o.$$

Since $k_3 - k \geq 0$ and $\rho_3(R_e)^2 \leq \delta^2$, the lower bound $o \geq \frac{1}{2}(k_3 - k)\delta^2$ follows. Let $g_e \in C_3 \cap D_3$ and $w \in G(g_e, 3)$. Then $\delta + 2\varepsilon < \pi$ implies that $\rho_w(R_e)^2 = \rho_3(R_e)^2$, and hence

$$V_w(g_e) - V_3(g_e) \leq \frac{1}{2}(k - k_3)\rho_3(R_e)^2 + o.$$

Using $k - k_3 \leq 0$ and $\rho_3(R_e)^2 \geq \delta + \varepsilon > 0$, it holds that $o \leq \frac{1}{2}(k_3 - k)(\delta + \varepsilon)^2$.

(A8) For all $(g_e, q) \in C$, it is clear that $\mathrm{d}V_q(g_e) = (R_e^{\mathsf{T}} K p_e, k_q \rho_q(R_e)) = 0$ if and only if $(g_e, q) \in \mathcal{A}$. □

6.4.2 Potential functions on $\widetilde{\mathrm{SE}}(3)$

Analogous to the surface vehicle case, we can identify the configuration of an underwater vehicle with the matrix Lie group $\mathrm{SE}(3) = \mathbb{R}^3 \rtimes \mathrm{SO}(3)$. An element $g = (p, R) \in \mathrm{SE}(3)$ contains the position $p \in \mathbb{R}^3$ and orientation $R \in \mathrm{SO}(3)$ of a vehicle-fixed frame with respect to an inertial frame.

The goal is to construct potential functions and a switching mechanism for stabilization of the configuration corresponding to the compact set

$$\mathcal{A}_0 = \{g_e \in \mathrm{SE}(3) : p_e = 0, R_e = I\}, \tag{6.52}$$

However, working with 3×3 rotation matrices can be cumbersome in practice. Unfortunately, there does not exist any globally nonsingular three-parameter representation of $\mathrm{SO}(3)$. As a result, practical state estimation and control applications normally utilize a globally nonsingular four-parameter unit quaternion representation of the vehicle orientation.

Unit quaternions $z = (\eta, \epsilon) \in \mathbb{S}^3$, where $\eta \in \mathbb{R}$ and $\epsilon \in \mathbb{R}^3$, map to the Lie group $\mathrm{SU}(2)$ through the isomorphism $z \mapsto Z$ defined by

$$Z \coloneqq \begin{pmatrix} \eta + i\epsilon_3 & -\epsilon_2 + i\epsilon_1 \\ \epsilon_2 + i\epsilon_1 & \eta - i\epsilon_3 \end{pmatrix} \in \mathbb{C}^{2\times 2}, \tag{6.53}$$

and an element $\omega = (\omega_1, \omega_2, \omega_3) \in \mathbb{R}^3$ maps to $\mathfrak{su}(2)$ through the isomorphism $\widehat{\cdot}^{\mathfrak{su}(2)} \colon \mathbb{R}^3 \to \mathfrak{su}(2)$ defined by

$$\widehat{\omega}^{\mathfrak{su}(2)} \coloneqq \frac{1}{2}\begin{pmatrix} i\omega_3 & -\omega_2 + i\omega_1 \\ \omega_2 + i\omega_1 & -i\omega_3 \end{pmatrix}. \tag{6.54}$$

The Lie algebras of $\mathfrak{su}(2)$ and $\mathfrak{so}(3)$ are isomorphic. Hence, the surjective homomorphism $\mathrm{Ad} \colon \mathrm{SU}(2) \to \mathrm{SO}(3)$ given by

$$\mathrm{Ad}_Z \coloneqq I + 2\eta\epsilon^\times + 2\epsilon^\times\epsilon^\times, \tag{6.55}$$

is a covering map, where $(\,\cdot\,)^\times \colon \mathbb{R}^3 \to \mathfrak{so}(3)$ is defined by

$$\epsilon^\times \coloneqq \begin{pmatrix} 0 & -\epsilon_3 & \epsilon_2 \\ \epsilon_3 & 0 & -\epsilon_1 \\ -\epsilon_2 & \epsilon_1 & 0 \end{pmatrix}. \tag{6.56}$$

Note that $\mathrm{Ad} : \mathrm{SU}(2) \to \mathrm{SO}(3)$ is globally two-to-one and satisfies $\mathrm{Ad}_Z = \mathrm{Ad}_{-Z}$ because $\mathrm{SU}(2)$ is the double cover of $\mathrm{SO}(3)$. In practice, this implies that $\pm Z$ corresponds to the same physical orientation.

Using the adjoint action of $\mathrm{SU}(2)$ on $\mathbb{R}^3$ given by $(p, Z) \mapsto \mathrm{Ad}_Z\, p$, the semidirect product $\mathbb{R}^3 \rtimes \mathrm{SU}(2)$ implies that the natural error on $\widetilde{\mathrm{SE}}(3) \coloneqq \mathbb{R}^3 \rtimes \mathrm{SU}(2)$ is [99]

$$g_e = g_d^{-1} g = (p_e, Z_e) = (\mathrm{Ad}_{Z_d^{-1}}(p - p_d), Z_d^{-1} Z). \tag{6.57}$$

We remark that $\widetilde{\mathrm{SE}}(3)$ is the universal covering group of $\mathrm{SE}(3)$. Due to the double cover property of $\mathrm{SU}(2)$, stabilizing the set $\{g_e \in \widetilde{\mathrm{SE}}(3) : p_e = 0, Z_e = I\}$ using the gradient of a potential function either leads to unwinding, where the control law unnecessarily performs a full rotation of the rigid body, or it may lead to very poor convergence properties around $\mathrm{tr}(Z_e) = 2\eta_e = 0$ [71, 92, 136]. Consequently, to prevent unwinding and obtain global convergence properties, we must stabilize the compact set of disconnected points

$$\mathcal{A}^\bullet = \{g_e \in \widetilde{\mathrm{SE}}(3) : Z_e = \pm I\}. \tag{6.58}$$

To this end, we define the set $Q \coloneqq \{-1, 1\}$ and the potential functions $V_q \colon \widetilde{\mathrm{SE}}(3) \to \mathbb{R}_{\geq 0}$ as in [71] by

$$\begin{aligned} V_q(g_e) &\coloneqq k\,\mathrm{tr}(I - qZ_e) + \tfrac{1}{2} p_e^\mathsf{T} K p_e \\ &= 2k(1 - q\eta_e) + \tfrac{1}{2} p_e^\mathsf{T} K p_e, \end{aligned} \tag{6.59}$$

where $k > 0$ and $K = K^\mathsf{T} > 0$. Let $\varepsilon \in (0, 1)$ denote the hysteresis half-width and define the flow and jump sets by

$$C \coloneqq \{(g_e, q) \in \widetilde{\mathrm{SE}}(3) \times Q : q\eta_e \geq -\varepsilon\} \tag{6.60a}$$

$$D \coloneqq \{(g_e, q) \in \widetilde{\mathrm{SE}}(3) \times Q : q\eta_e \leq -\varepsilon\}. \tag{6.60b}$$

Finally, the jump map is defined as

$$G(q) \coloneqq -q. \tag{6.61}$$

Observe that the preceding definitions ensure that the switching is hysteretic since $q\eta_e \leq -\varepsilon$ implies that $G(q)\eta_e \geq \varepsilon$.

Lemma 6.5. Let $\mathcal{A} \coloneqq \{(g_e, q) \in \widetilde{\mathrm{SE}}(3) \times Q : \eta_e = q\}$. The 5-tuple $(\mathcal{A}, C, D, G, V)$ satisfies Assumption 6.2.

Proof. The proof is a straightforward extension of the results of [71, Lemma 5.1, Theorem 5.2]. It is clear that the function $\check{V}_q : \mathbb{R}^3 \to \mathbb{R}$ defined by $p \mapsto \frac{1}{2} p^\mathsf{T} K p$ is continuously differentiable, radially unbounded and positive definite with respect to $\pi_2(\mathcal{A})$, where $\mathcal{A}$ is regarded as a subset of $\mathrm{SU}(2) \times \mathbb{R}^3 \times Q$. Moreover, C and D are clearly closed subsets of $\widetilde{\mathrm{SE}}(3) \times Q$, $\mathcal{A}$ is compact, and for all $(g_e, q) \in C$, it holds that $\mathrm{d}V_q(g_e) = (R_e^\mathsf{T} K p_e, kq\epsilon_e) = 0$ if and only if $p_e = 0, \epsilon_e = 0$ which implies that $\eta = \pm 1$, i.e., $(g_e, q) \in \mathcal{A}$. □

6.5 Experimental Results

In this section we report the results of three experiments conducted in the Marine Cybernetics Laboratory (MC Lab) [137] at the Norwegian University of Science and Technology (NTNU) in Trondheim. The main purpose of the experiments is to demonstrate the applicability of the devised controllers in realistic scenarios for surface and submerged marine vehicles. The first two experiments were conducted using a scale model tug boat and the third experiment was conducted with a remotely operated underwater vehicle.

In the MC Lab, a local positioning system comprises sets of cameras mounted above and below the water surface and the Qualisys Track Manager (QTM) software. Light emitted by the cameras is reflected by a set of optical markers mounted on the vehicle to be tracked. These measurements are then processed with QTM, which outputs the position and orientation estimates at a rate of 100 Hz. A multiplicative extended Kalman filter (MEKF) [24, Section 14.4.3] is employed to reconstruct the velocities and filter the position and orientation. The MEKF is augmented with linear acceleration and angular velocity measurements for the underwater vehicle experiments.

Figure 6.2: The Marine Cybernetics Lab at NTNU

6.5.1 Cybership Enterprise

Cybership Enterprise (CSE) is a 1:50 scale model tug boat with a length of 1.105 m and beam of 0.248 m. CSE is equipped with two Voith Schneider propellers (VSPs) and one bow thruster. The configuration of CSE is described by $g = (p, R) \in \mathrm{SE}(2)$, where

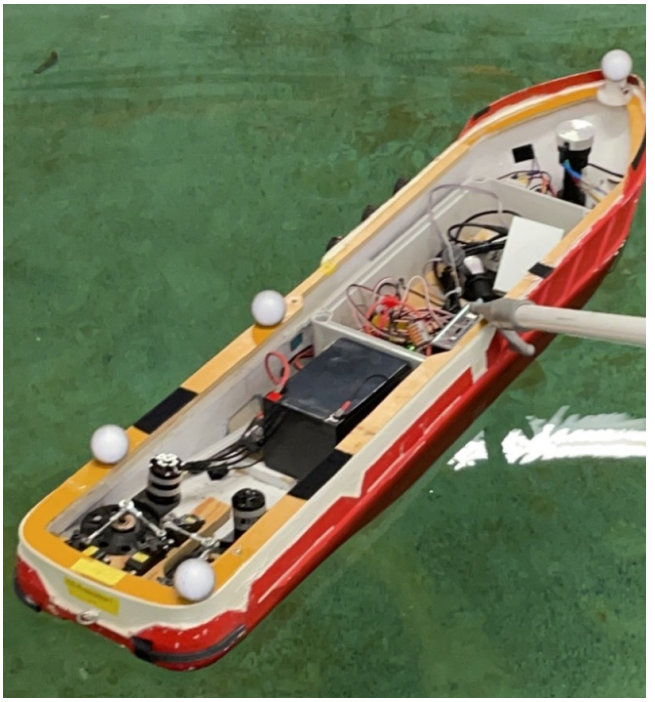

Figure 6.3: Cybership Enterprise in the MC-Lab

elements in SE(2) admit a homogeneous matrix representation through the injective homomorphism $\mathrm{SE}(2) \to \mathrm{GL}(3)$ defined by [99]

$$g \coloneqq \begin{pmatrix} R & p \\ 0 & 1 \end{pmatrix} \in \mathbb{R}^{3\times 3}. \tag{6.62}$$

Denoting the vehicle-fixed linear and angular velocities by $v \in \mathbb{R}^2$ and $\omega \in \mathbb{R}$, respectively, define the vehicle-fixed velocity as $\nu \coloneqq (v, \omega) \in \mathbb{R}^3$. An element $\nu \in \mathbb{R}^3$ maps to $\mathfrak{se}(2)$ through the isomorphism $\widehat{\cdot}\colon \mathbb{R}^3 \to \mathfrak{se}(2)$ defined by

$$\widehat{\nu} \coloneqq \begin{pmatrix} S\omega & v \\ 0 & 0 \end{pmatrix} \in \mathbb{R}^{3\times 3}, \quad S \coloneqq \begin{pmatrix} 0 & -1 \\ 1 & 0 \end{pmatrix}. \tag{6.63}$$

Let $\theta \in \mathbb{R}^{15}$ denote the model parameters. The equations of motion for a surface vehicle can be formulated by (6.1) with

$$M = \begin{pmatrix} \theta_1 & 0 & 0 \\ 0 & \theta_2 & \theta_3 \\ 0 & \theta_3 & \theta_4 \end{pmatrix}, \quad f(g) = b, \tag{6.64}$$

$$d(\nu) = \begin{pmatrix} -\theta_5\nu_1 \\ -\theta_6\nu_2 - \theta_8\omega \\ -\theta_9\nu_2 - \theta_7\omega \end{pmatrix} + \begin{pmatrix} -\theta_{10}|\nu_1|\nu_1 \\ -\theta_{11}|\nu_2|\nu_2 \\ -\theta_{12}|\omega|\omega \end{pmatrix} \tag{6.65}$$

where $b = (\theta_{13}, \theta_{14}, \theta_{15}) \in \mathbb{R}^3$ is a constant bias. We remark that the expression for the regressor Φ follows from (6.17) together with (6.64) and (6.65).

The generalized forces are calculated using (6.26), where the adjoint actions of $\mathrm{SE}(2)$ and $\mathfrak{se}(2)$ on $\mathbb{R}^3$ for $g = (p, R) \in \mathrm{SE}(2)$ and $\nu = (v, \omega) \in \mathbb{R}^3$ are given by

$$\mathrm{Ad}_g = \begin{pmatrix} R & -Sp \\ 0 & 1 \end{pmatrix}, \quad \mathrm{ad}_\nu = \begin{pmatrix} S\omega & -Sv \\ 0 & 0 \end{pmatrix}. \tag{6.66}$$

The generalized forces $\tau \in \mathbb{R}^3$ map to the actuator inputs $(\alpha, u) \in \mathbb{R}^2 \times \mathbb{R}^3$ through

$$\tau = B(\alpha)Ku, \tag{6.67}$$

where $\alpha = (\alpha_1, \alpha_2)$ are the VSP angles and $u = (u_1, u_2, u_3)$ are the thruster inputs. Specifically, (u_1, u_2) corresponds to the VSPs, and u_3 is the bow thruster.

Using the transformation $(\alpha, u) \mapsto (\check{u}_1, \check{u}_2, \check{u}_3)$, where

$$\check{u}_1 = \begin{pmatrix} \cos(\alpha_1)u_1 \\ \sin(\alpha_1)u_1 \end{pmatrix}, \check{u}_2 = \begin{pmatrix} \cos(\alpha_2)u_2 \\ \sin(\alpha_2)u_2 \end{pmatrix}, \check{u}_3 = u_3. \tag{6.68}$$

we can rewrite (6.67) as $\tau = \check{B}\check{K}\check{u}$, which is solved using the Moore-Penrose pseudoinverse

$$\check{u}_* = (\check{B}\check{K})^\dagger \tau, \tag{6.69}$$

for a given $\tau \in \mathbb{R}^3$. The actuator control inputs (α, u) are then obtained by inverting the transformation (6.68). Note that the BT input is constrained to the interval $[-1, 1]$, while the VSP inputs are constrained to $[0, 1]$. The desired path is given by $\gamma(s) = (\gamma_1(s), \gamma_2(s)) \in \mathrm{SE}(2)$ where

$$\gamma_1(s) = \begin{pmatrix} x_d(s) \\ y_d(s) \end{pmatrix}, \gamma_2(s) = \exp(S\psi_d(s)), \tag{6.70}$$

where $\psi_d(s) = \mathrm{atan2}(y_d'(s), x_d'(s))$.

The hysteresis width and control gains are chosen according to Table 6.1 with $\vartheta_q(\zeta) = K_d\zeta$ and $\varphi_q(\xi) = K_d\xi$. Moreover, the adaptation gain and bounds on $\theta \in \mathbb{R}^{15}$ are given by

$$\begin{aligned} \Gamma &= \mathrm{blkdiag}(50, 40, 5, 20, 5I_{4\times4}, 10I_{9\times9}, 0.025, 0.1, 0.01), \\ \underline{\theta} &= (10, 15, 1, -3, 0_{7\times1}, -1, -4, -4, -4), \\ \overline{\theta} &= (20, 30, 5, 3, 10_{7\times1}, 10, 4, 4, 4), \end{aligned}$$

and the parameters are initialized as

$$\theta_0 = (10, 15, 1, 0_{12\times1}). \tag{6.71}$$

Two two experiments are performed using different parametrized loops; the first loop is a circle, and the second is a lemniscate.

Circle

The circle is centered at $O = (1\,\mathrm{m}, 0)$ with a radius of $R = 1.2\,\mathrm{m}$ and is represented by the parametric equation

$$\gamma_1(s) = \begin{pmatrix} R\cos(s) \\ R\sin(s) \end{pmatrix} + O. \tag{6.72}$$

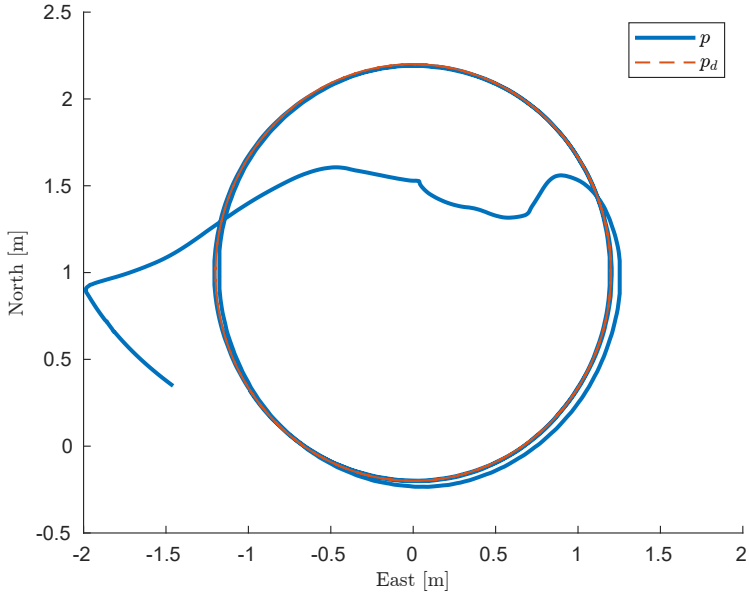

Figure 6.4: North-East plot showing the North-East position $p = (x, y)$ and the desired position $p_d = (x_d, y_d)$.

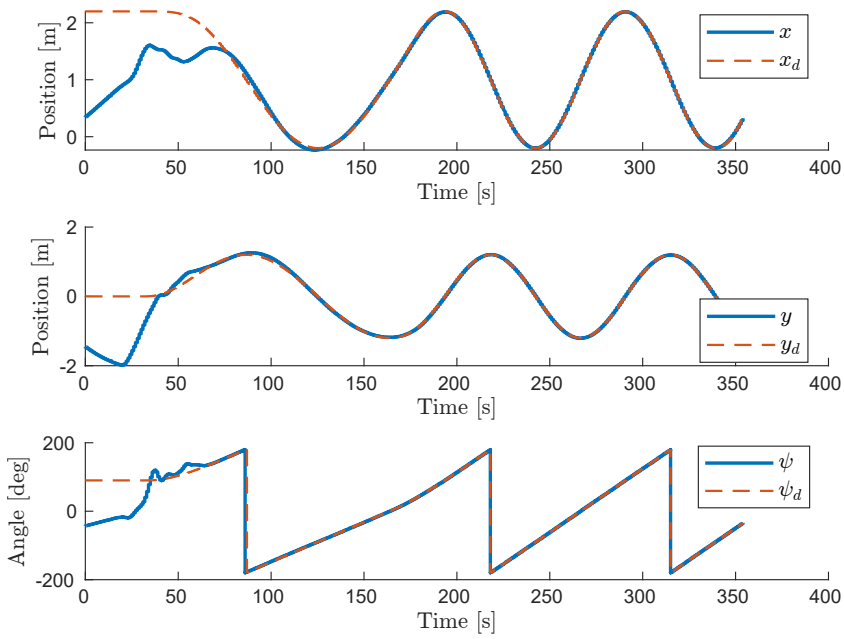

Figure 6.5: The configuration $p = (x, y), R = \exp(S\psi)$ and the desired configuration $p_d = (x_d, y_d), R_d = \exp(S\psi_d)$.

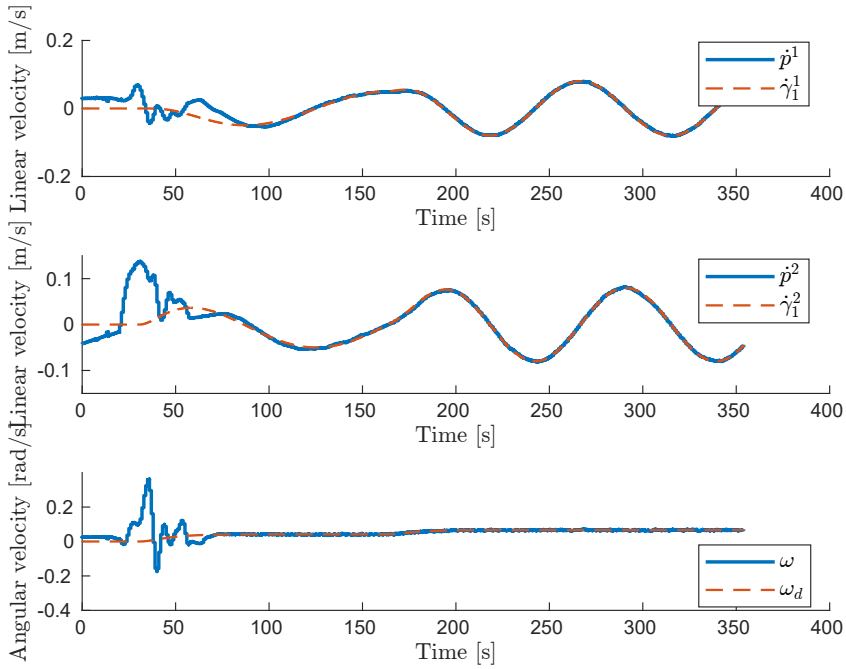

Figure 6.6: The velocity estimates $(\dot{p}, \omega)$ and the desired velocity references $(\dot{\gamma}_1, \omega_d)$.

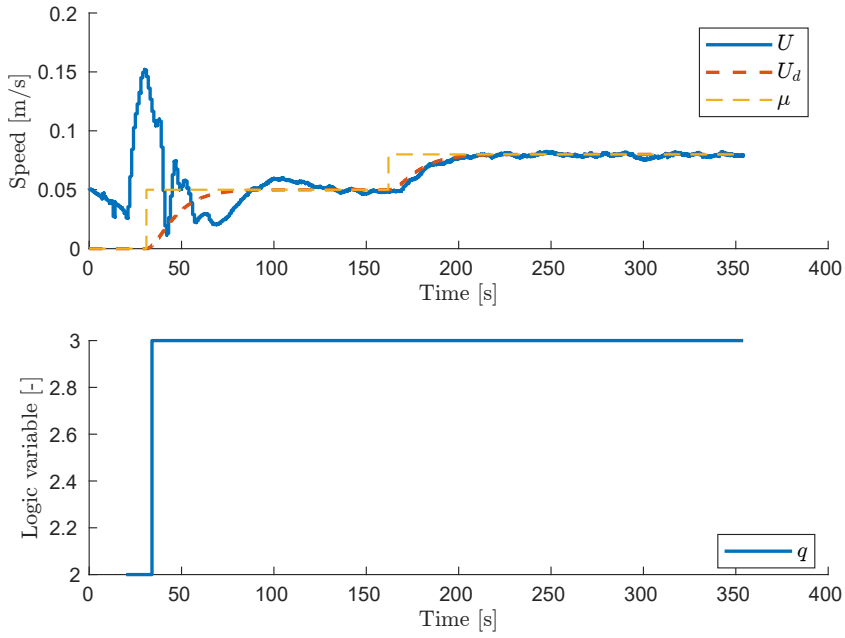

Figure 6.7: The speed U, desired speed u_d, commanded input speed μ and logic variable q.

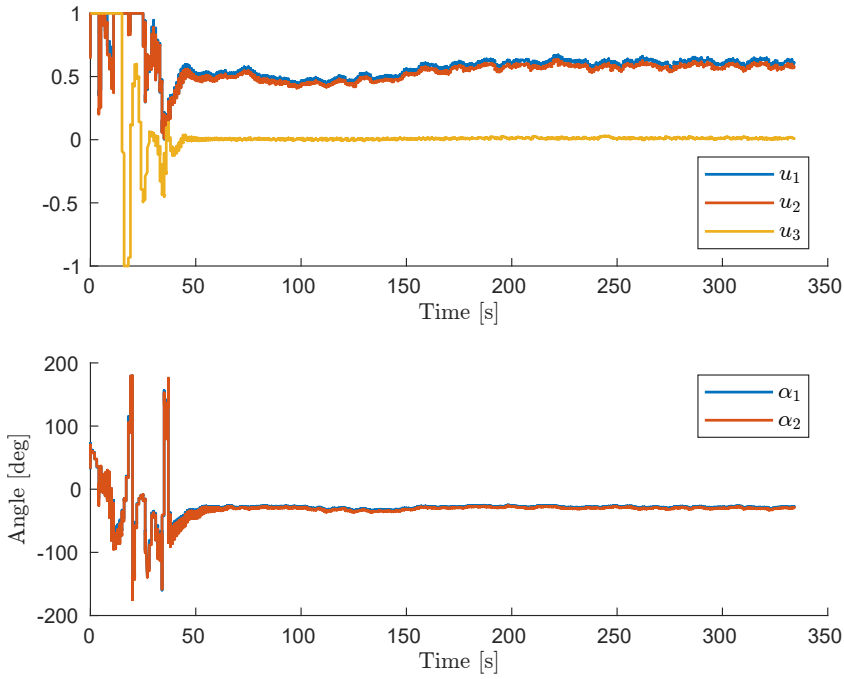

Figure 6.8: The VSP control inputs $u_1, u_2 \in [0, 1]$, the BT control input $u_3 \in [-1, 1]$ and VSP angle inputs α_1, α_2.

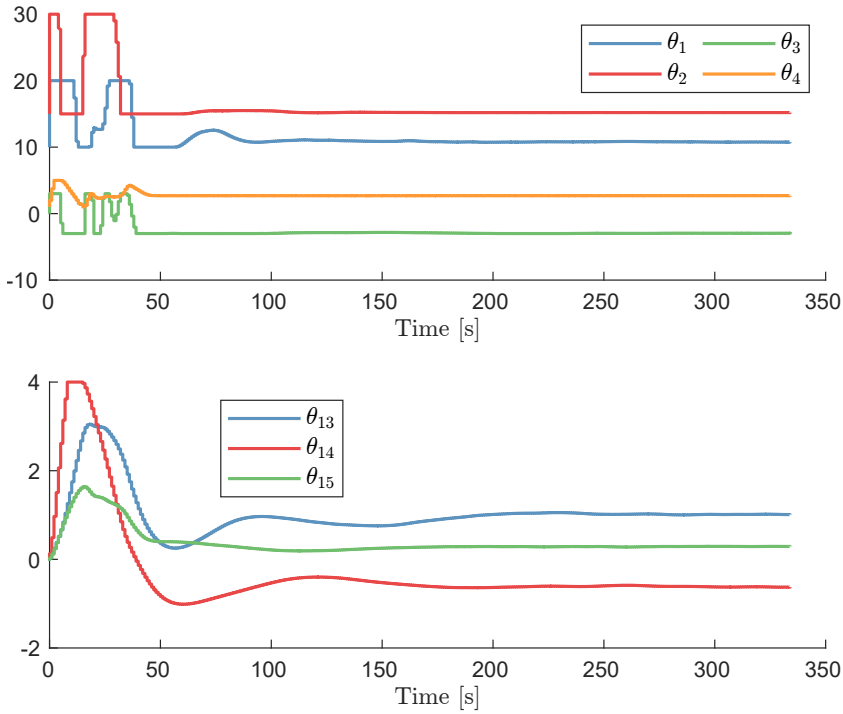

Figure 6.9: The inertia and bias parameters.

Table 6.1: Control Parameters

Circle		**Lemniscate**	
δ	$\pi/6$	δ	$\pi/18$
ε	$\pi/18$	ε	$\pi/18$
K_p	$\text{diag}(1.7, 1.7)$	K_p	$\text{diag}(1.45, 1.45)$
k	0.5	k	0.5
k_3	1.2	k_3	1.5
K_d	$\text{diag}(.7, .6, .6)$	K_d	$\text{diag}(1.25, 1.25, 1)$
Λ	I_3	Λ	I_3

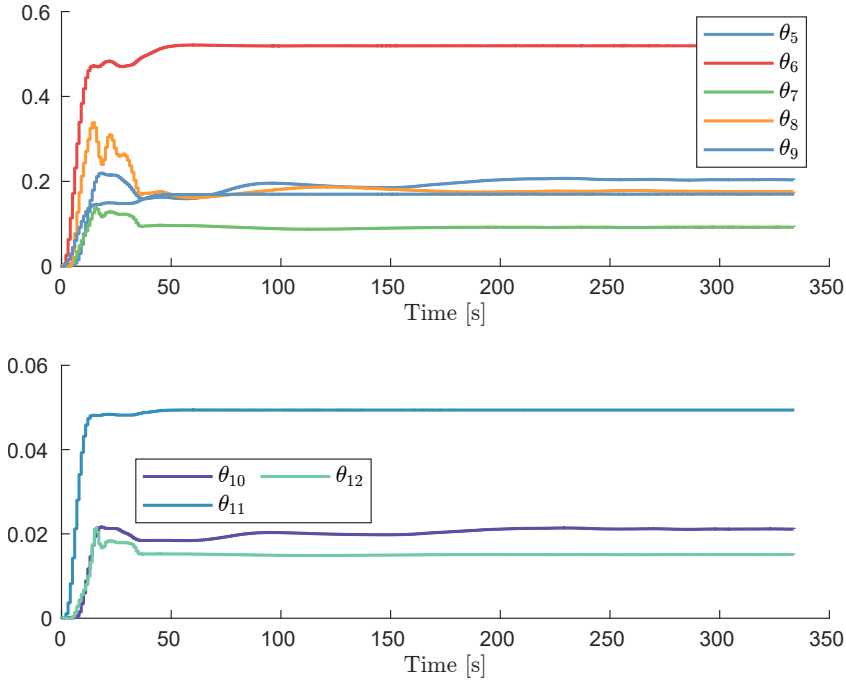

Figure 6.10: The damping parameters associated with the linear and nonlinear damping.

Experimental results are presented in Figures 6.4 to 6.10. The ship was initialized at $p(0) = (0.35\,\text{m}, -1.46\,\text{m})$ with $\psi = -42°$. At this point in time, the orientation error was $\rho_3(R_e(t))|_{t=0} = -\pi\frac{106}{180} \geq \delta + \varepsilon$, and it follows from (6.46) that $\rho_2^2(R_e(t))|_{t=0} < \rho_1^2(R_e(t))|_{t=0}$. In other words, the orientation error was in the jump set corresponding to $q = 3$ and the jump map (6.50) implies that the global controller corresponding to $q^+ = 2$ was activated, which is what we observe in the lower plot in Figure 6.7. Then, at $t \approx 33\,\text{s}$, the commanded input speed μ was set to $0.08\,\text{m/s}$ as seen in Figure 6.7. Figures 6.4 and 6.5 shows that CSE accurately tracked the path after an initial transient due to the significant initial configuration error, even though the actuator inputs saturate until $t \approx 25\,\text{s}$ as seen in Figure 6.8. Figure 6.6 depicts the

system velocities and desired velocities, while Figure 6.7 shows the commanded input speed $\mu(t)$, the desired speed $u_d(t)$ and the estimated speed $U(t) = \|v(t)\|$. Therefore, it is clear that the speed and velocities are tracked with sufficient accuracy.

Lemniscate

The lemniscate is centered at $O = (2\,\mathrm{m}, 0)$ and is represented by the parametric equation

$$\gamma_1(s) = \begin{pmatrix} R_1 \dfrac{\cos s}{1 + \sin^2 s} \\ R_2 \dfrac{\sqrt{2} \sin 2s}{1 + \sin^2 s} \end{pmatrix} + O, \tag{6.73}$$

where $R_1 = 2\,\mathrm{m}$, $R_2 = 2.4\,\mathrm{m}$.

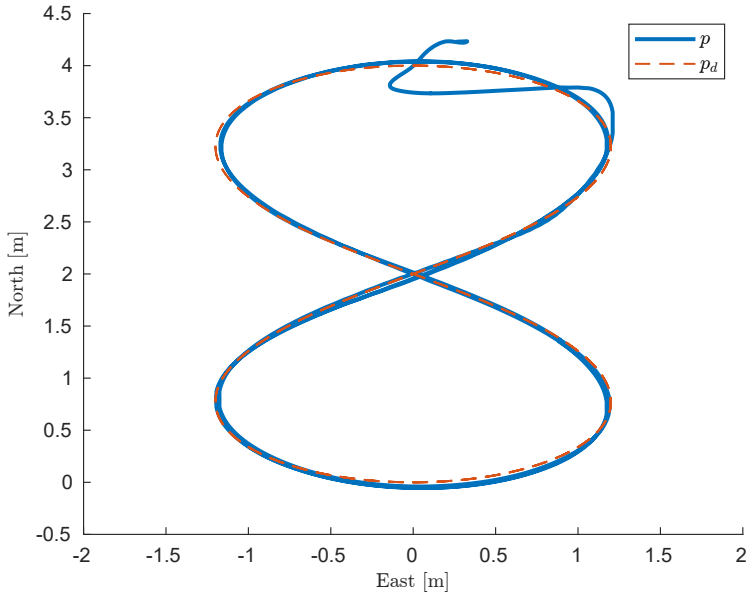

Figure 6.11: North-East plot showing the position p and the desired position p_d.

Experimental results are presented in Figures 6.11 to 6.17. The ship was initialized at $p(0) = (4.2\,\mathrm{m}, 0.3\,\mathrm{m})$ with a heading of $\psi = 130°$. Since the lemniscate loop given by (6.73) does not result in a constant acceleration with respect to the body-fixed frame for nonzero commanded input speeds, the control gains must be increased to compensate for the inaccuracies in the dynamic model and obtain similar performance to the circular trajectory.

By comparing Figures 6.9 and 6.10 with Figures 6.16 and 6.17, it is clear that the parameters do not converge to any 'true' value. This cannot be expected because we have not provided any persistency of excitation condition; that is, we have not given any conditions under which (6.26) uniformly globally asymptotically stabilizes the compact set $\widetilde{\mathcal{B}}$ for the closed-loop system $\mathcal{H}$. However, even if such conditions were provided, a constant bias in the vehicle-fixed frame will not fully capture the

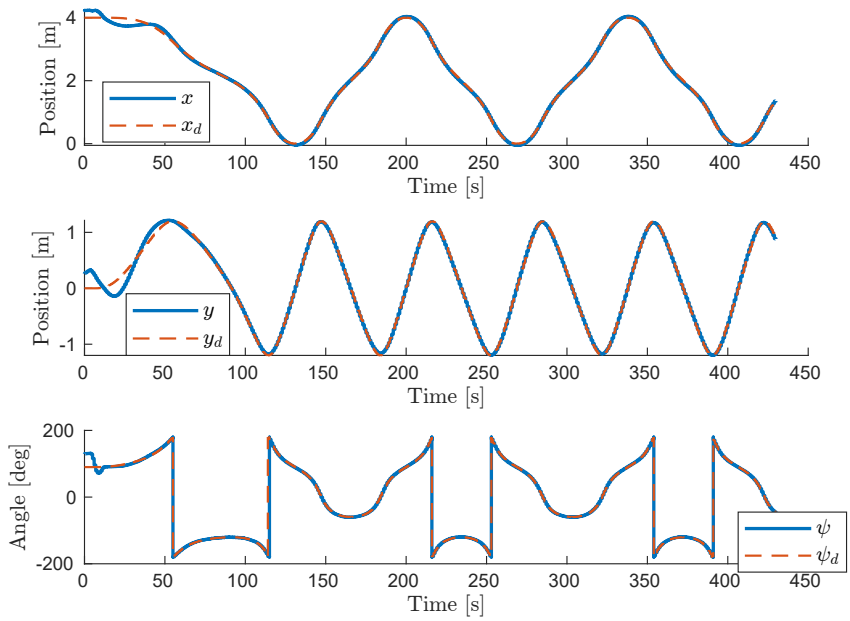

Figure 6.12: The configuration $p = (x, y), R = \exp(S\psi)$ and the desired configuration $p_d = (x_d, y_d), R_d = \exp(S\psi_d)$.

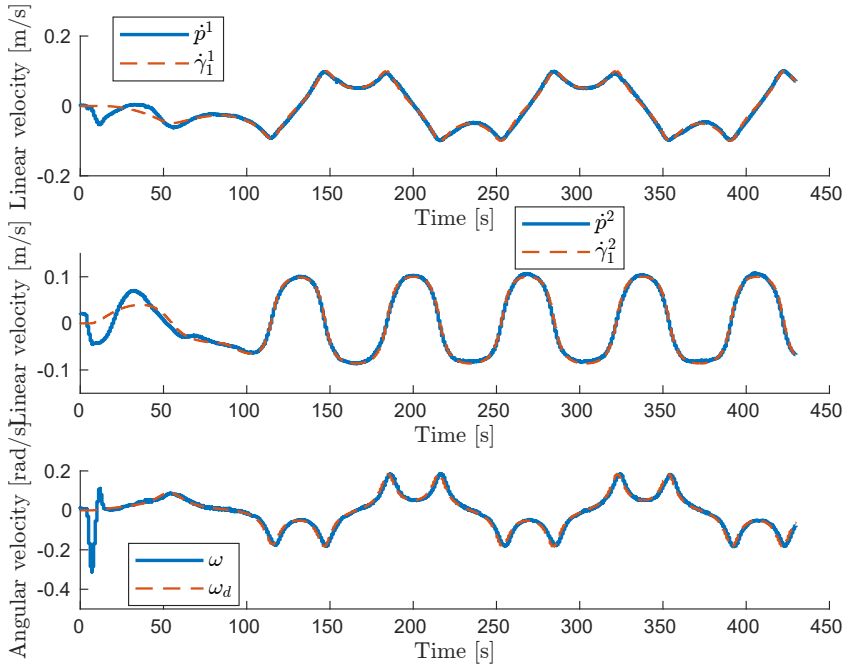

Figure 6.13: The velocity estimates $(\dot{p}, \omega)$ and the desired velocity references $(\dot{\gamma}_1, \omega_d)$.

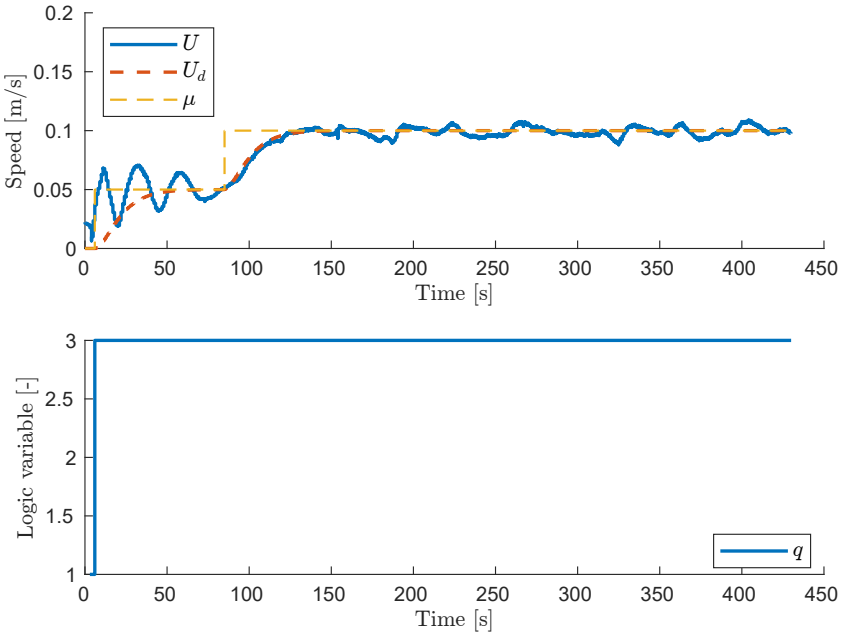

Figure 6.14: The speed U, desired speed u_d, commanded input speed μ and logic variable q.

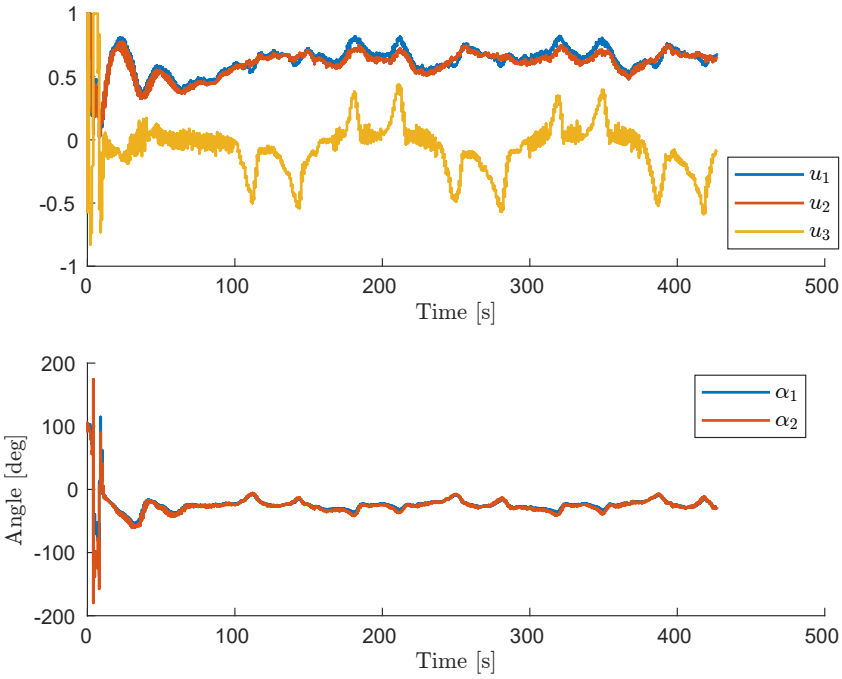

Figure 6.15: The VSP control inputs $u_1, u_2 \in [0, 1]$, the BT control input $u_3 \in [-1, 1]$ and VSP angle inputs α_1, α_2.

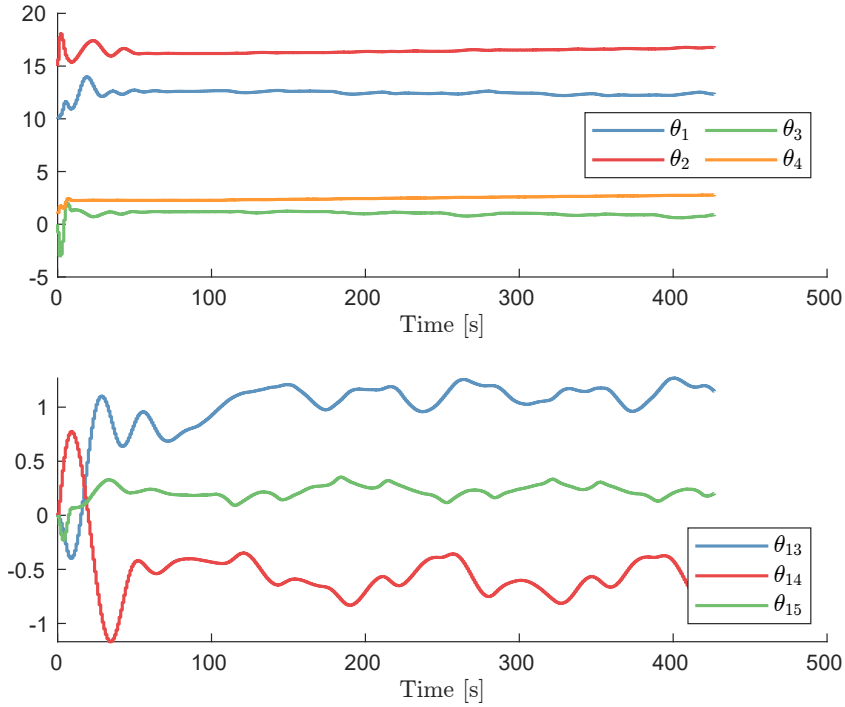

Figure 6.16: The inertia and bias parameters.

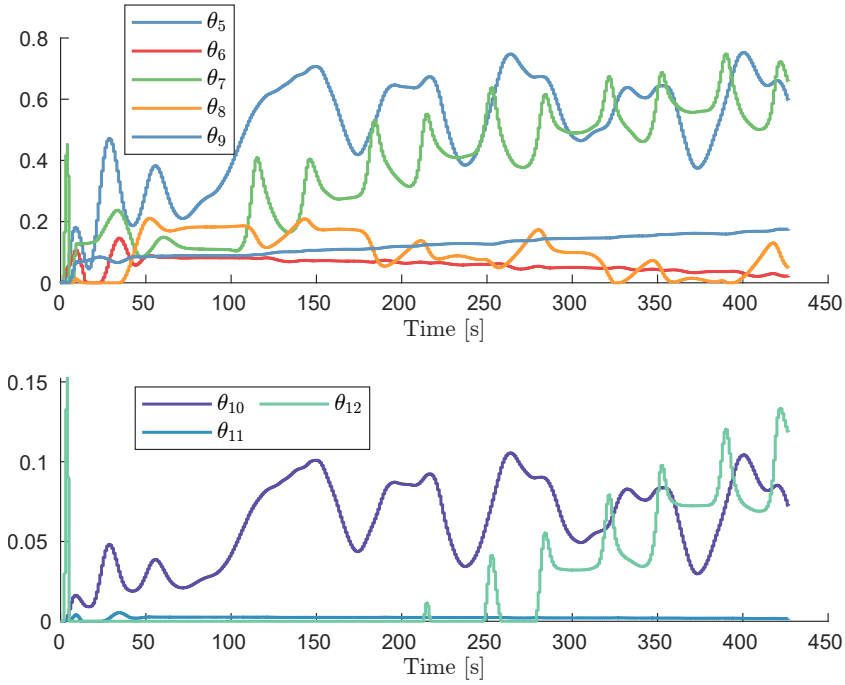

Figure 6.17: The damping parameters associated with the linear and nonlinear damping.

inaccuracies in the mapping between the forces produced by the actuators and their inputs. As a consequence, the desired forces and torque computed by the control law are significantly different from the actual forces and torque produced by the actuators. In turn, this leads to a tracking error, which induces parameter adaptation. Since this adaptation occurs due to unmodeled effects that are not correctly captured by our assumed model structure, we cannot expect to accurately identify the mass and damping model parameters for this system. Instead, due to the presence of a constant bias in our dynamic model, our control law is more reminiscent of a PID controller with adaptive feedforward. To see this, note that the bias feedforward term can be written as $-\int_0^t(\nu_e(\tau)-\zeta(\tau))\mathrm{d}\tau$, and that (6.14) can be interpreted as a multiple-input multiple-output low-pass filter with input $-\mathrm{d}V_q$ and output ζ. Thus, when the velocity error ν_e is zero, the bias feedforward term can be interpreted as the integral of the output of a low-pass filter whose input is the configuration error.

Finally, we observe that the parameters converge for the circular trajectory. This is a consequence of the steady-state nature of the circular trajectory, that is, constant desired velocities with respect to the desired frame when u_d has converged to the commanded input speed μ. For the lemniscate trajectory, however, the desired velocities are not constant even if the desired speed has converged to the commanded input speed. Hence, considering the inaccuracies in the mappings between the desired forces and torque and the produced forces and torque, it is not surprising that the parameters do not converge to any specific values and that the damping and bias parameters change more rapidly when the ship is in a turning maneuver, as seen in Figures 6.12, 6.16 and 6.17. Despite these structural modeling inaccuracies, the ship's position remains within 4 cm of the desired position after converging to the path, as seen in Figures 6.11 and 6.12. Moreover, from Figure 6.13 and Figure 6.14, we observe that the desired velocities and the desired speed are tracked with sufficient accuracies.

6.5.2 BlueROV2

The BlueROV2 is a remotely operated underwater vehicle developed by Blue Robotics. The experiments were conducted using the heavy configuration BlueROV2 with eight thrusters, depicted in Fig. 6.18.

Elements $g = (p, Z) \in \widetilde{\mathrm{SE}}(3)$ admit a matrix representation using the injective homomorphism $\widetilde{\mathrm{SE}}(3) \to \mathrm{GL}(6, \mathbb{C})$ given by

$$g = \begin{pmatrix} \mathrm{Ad}_Z & p & 0 \\ 0 & 1 & 0 \\ 0 & 0 & Z \end{pmatrix} \in \mathbb{C}^{6\times 6} \tag{6.74}$$

Denoting the vehicle-fixed linear and angular velocities by $v \in \mathbb{R}^3$ and $\omega \in \mathbb{R}^3$, respectively, define the vehicle-fixed velocity as $\nu \coloneqq (v, \omega) \in \mathbb{R}^6$. An element $\nu \in \mathbb{R}^6$ maps to $\widetilde{\mathfrak{se}}(3)$ through the isomorphism $\widehat{\cdot}\colon \mathbb{R}^6 \to \widetilde{\mathfrak{se}}(3)$ defined by

$$\widehat{\nu} = \begin{pmatrix} \omega^\times & v & 0 \\ 0 & 0 & 0 \\ 0 & 0 & \widehat{\omega}^{\mathfrak{su}} \end{pmatrix} \in \mathbb{C}^{6\times 6}. \tag{6.75}$$

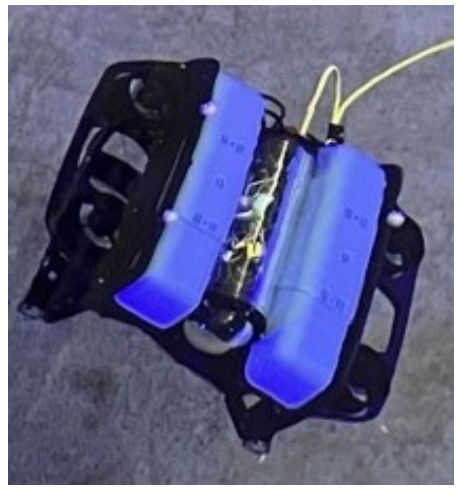

Figure 6.18: The BlueROV2 in the MC-Lab.

The equations of motion for an underwater vehicle can then be formulated by (6.1) with

$$f(g) = \beta(Z) + b, \tag{6.76}$$

where $\beta(Z) = (\theta_7 \operatorname{Ad}_Z^{\mathsf{T}} e_3, e_3^{\times} \operatorname{Ad}_Z^{\mathsf{T}} \theta_{8:10})$ contains gravitational and buoyancy forces and $b = (\theta_1, \ldots, \theta_6) \in \mathbb{R}^6$ is a constant bias. Moreover, by assuming port/starboard and fore/aft symmetry, the inertia matrix is parametrized by

$$M = \begin{pmatrix} \theta_{11} & 0 & 0 & 0 & \theta_{17} & 0 \\ 0 & \theta_{12} & 0 & \theta_{18} & 0 & 0 \\ 0 & 0 & \theta_{13} & 0 & 0 & 0 \\ 0 & \theta_{18} & 0 & \theta_{14} & 0 & 0 \\ \theta_{17} & 0 & 0 & 0 & \theta_{15} & 0 \\ 0 & 0 & 0 & 0 & 0 & \theta_{16} \end{pmatrix} \tag{6.77}$$

while the hydrodynamic drag forces are assumed to satisfy

$$d_i(\nu) = \theta_{18+i}\nu_i + \theta_{24+i}|\nu_i|\nu_i, \tag{6.78}$$

for $i \in \{1, \ldots, 6\}$. We remark that the expression for the regressor Φ follows from (6.17) together with (6.76), (6.77) and (6.78). The generalized forces are calculated using the control law (6.26), where the adjoint actions of $\widetilde{\mathrm{SE}}(3)$ and $\widetilde{\mathfrak{se}}(3)$ on $\mathbb{R}^6$ for $g = (p, Z) \in \widetilde{\mathrm{SE}}(3)$ and $\nu = (v, \omega) \in \mathbb{R}^6$ are given by

$$\operatorname{Ad}_g = \begin{pmatrix} \operatorname{Ad}_Z & p^{\times} \operatorname{Ad}_Z \\ 0 & \operatorname{Ad}_Z \end{pmatrix}, \quad \operatorname{ad}_\nu = \begin{pmatrix} \omega^{\times} & v^{\times} \\ 0 & \omega^{\times} \end{pmatrix}. \tag{6.79}$$

The generalized forces $\tau \in \mathbb{R}^6$ map to the desired thrust $u \in \mathbb{R}^8$ through $\tau = Ku$, where each column of K is

$$K_i = \begin{pmatrix} r_i \\ L_i \times r_i \end{pmatrix}, \tag{6.80}$$

where $r_i \in \mathbb{R}^3$ is a unit vector pointing in the direction of thrust and $L_i \in \mathbb{R}^3$ is the position of the thruster relative to the body frame. Using (6.26), the actuator control inputs are then found from the expression $u = K^\dagger \tau$.

The desired path is given by $\gamma(s) = (p_d(s), Z_d(s)) \in \widetilde{\mathrm{SE}}(3)$, with

$$p_d(s) = \begin{pmatrix} L_1 \frac{\cos s}{1+\sin^2 s} \\ L_2 \frac{\sqrt{2}\sin 2s}{1+\sin^2 s} \\ L_3 \frac{2\sin s}{1+\sin^2 s} \end{pmatrix} + O, \; z_d(s) = \begin{pmatrix} \cos(\psi(s)/2) \\ 0 \\ 0 \\ \sin(\psi(s)/2) \end{pmatrix}$$

where z_d is a unit quaternion that maps to SU(2) through the isomorphism $z_d \mapsto Z_d$ defined in (6.53). Moreover, $O = (0.2\,\mathrm{m}, -0.3\,\mathrm{m}, -0.55\,\mathrm{m})$, $L_1 = 1\,\mathrm{m}$, $L_2 = 0.6\,\mathrm{m}$, $L_3 = 0.25\,\mathrm{m}$ and $\psi(s) = \mathrm{atan2}(y_d'(s), x_d'(s))$.

The desired speed reference is given by

$$\mu = \begin{cases} 0.1\,\mathrm{m/s}, & 5 \leq t < 125 \\ 0.2\,\mathrm{m/s}, & t \geq 125 \end{cases}, \tag{6.81}$$

while the hysteresis half-width is $\varepsilon = 0.1$. The control gains are chosen as $K_p = \mathrm{diag}(50, 50, 70), k = 16, \varphi_q(\xi) = K_d\xi, \vartheta_q(\zeta) = K_d\zeta$, $K_d = \mathrm{diag}(40, 40, 30, 7, 7, 7)$, and $\Lambda = I_6$. Moreover, the adaptation gain and bounds on $\theta \in \mathbb{R}^{30}$ are given by

$$\begin{aligned} \Gamma &= \mathrm{blkdiag}(\Gamma_1, \Gamma_2, \Gamma_3), \\ \Gamma_1 &= \mathrm{diag}(1.5, 1.5, 1.5, 1.2, 1.2, 1.2), \\ \Gamma_2 &= \mathrm{diag}(2.5, 2, 2, 2), \\ \Gamma_3 &= \mathrm{diag}(7, 7, 7, 4, 4, 4, 5, 5, 20, 20, 20, 5, 5, 5, 20, 20, 20, 5, 5, 5), \\ \underline{\theta} &= (-40, -10_{9\times 1}, 0_{7\times 1}, -2, 0_{12\times 1}), \\ \overline{\theta} &= (10_{10\times 1}, 50_{6\times 1}, 2, 0, 50_{12\times 1}), \end{aligned}$$

and the parameters are initialized as

$$\begin{aligned} \theta_0 = (&0_{10\times 1}, 19.17, 26.37, 28.24, 0.28, 0.28, \\ &0.28, 0.23, -0.23, 4.03, 6.22, 5.1, \\ &0.07, 0.07, 0.07, 18.18, 21.66, 36.99, \\ &1.55, 1.55, 1.55) \end{aligned} . \tag{6.82}$$

Experimental results are presented in Figures 6.19 to 6.27. Due to limitations in the hardware implementation, the controller activates a few seconds before the data logger and actuator driver do. As a result, the bias and gravitational parameters have already adapted for several seconds by the time the control signals are sent to the actuators. This can be observed in the upper plot in Figure 6.27, where θ_1 and θ_3, i.e., the x and z components of the bias, are already saturated at $t \approx 4\,\mathrm{s}$ when the actuator driver is activated and the control inputs are converted to pulse width modulated actuator signals. Remarkably, this has little effect on the transient performance, as observed in Figure 6.21. This occurs despite the fact that the BlueROV2 was initialized at the bottom of the pool at a distance $\|p_e\| \approx 1.36\,\mathrm{m}$ away from the desired position with no initial knowledge of the gravitational- and buoyancy-related parameters.

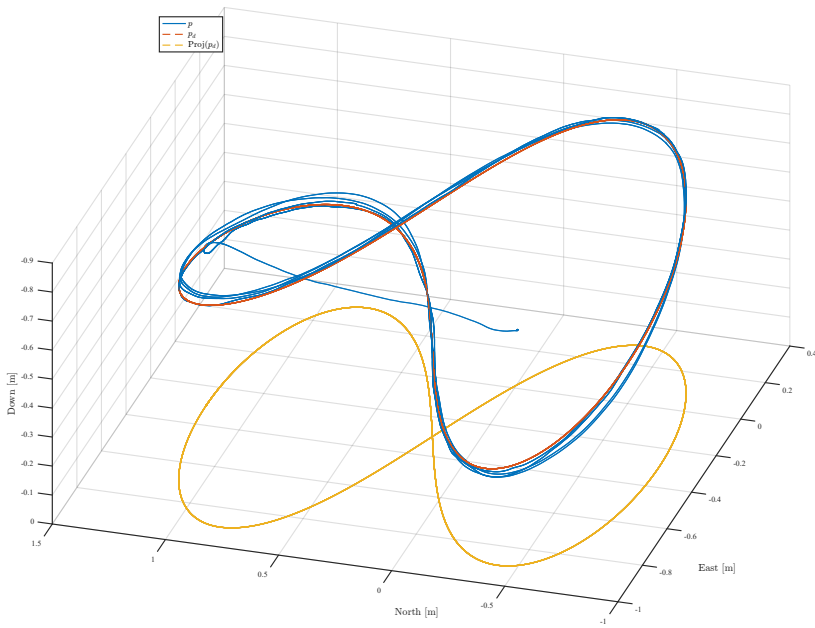

Figure 6.19: North-East-Down plot showing the position p, the desired position p_d and the projection of p_d onto the North-East plane.

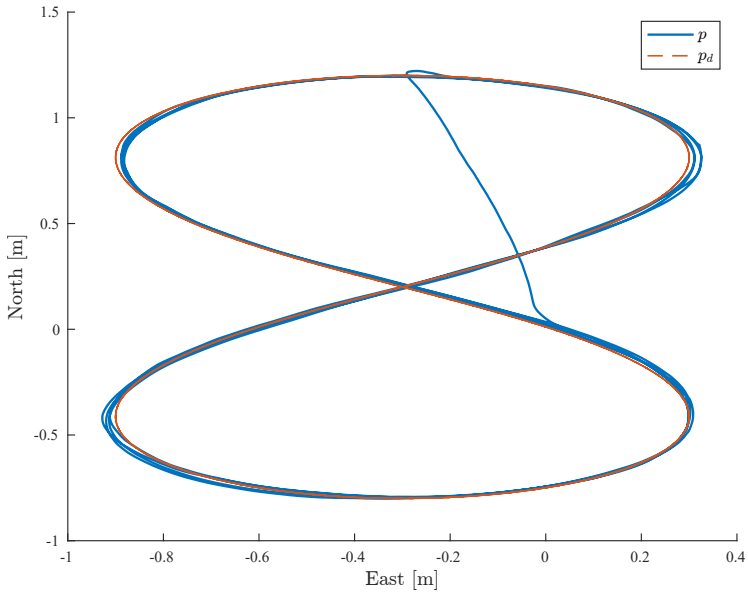

Figure 6.20: North-East plot of the position and desired position

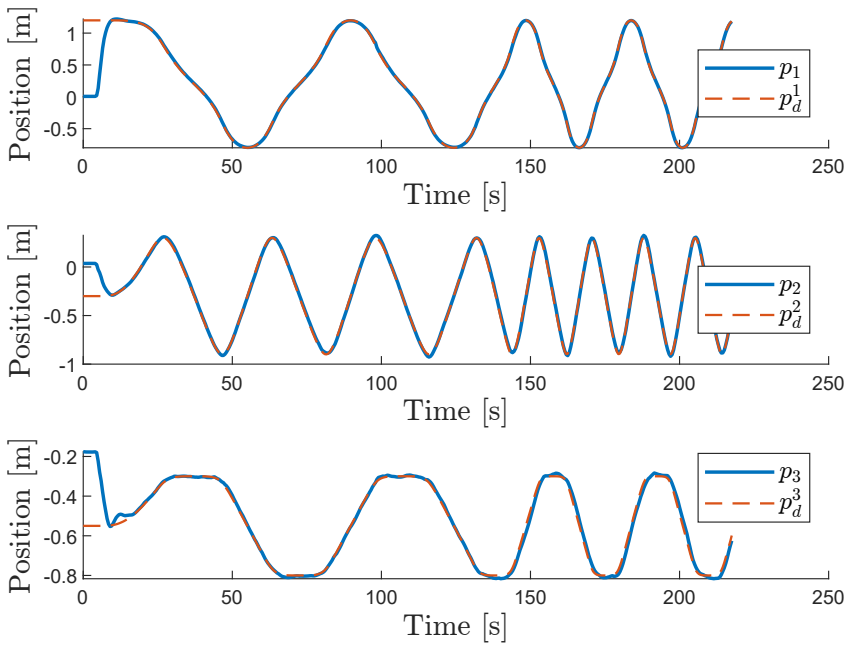

Figure 6.21: The position $p = (p_1, p_2, p_3)$ and desired position $p_d = (p_d^1, p_d^2, p_d^3)$.

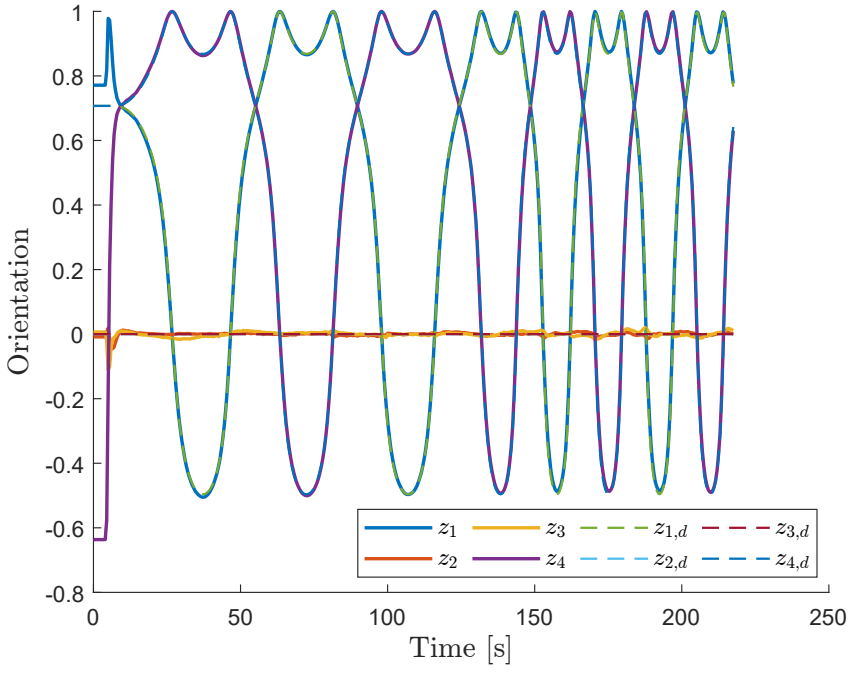

Figure 6.22: The orientation and desired orientation, represented by the unit quaternions z and z_d, respectively.

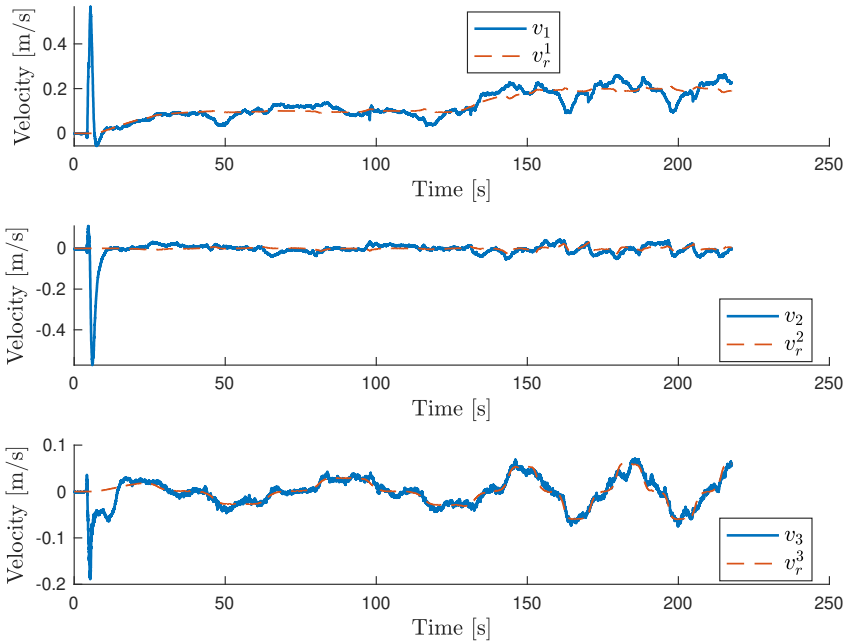

Figure 6.23: The linear velocities v and the desired linear velocities v_r, decomposed in the body frame.

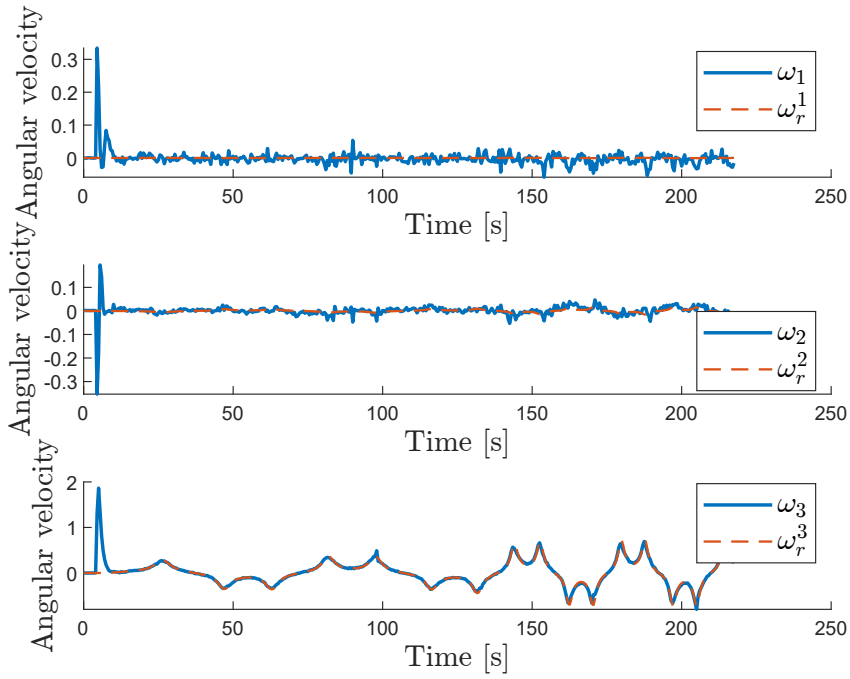

Figure 6.24: The angular velocities ω and the desired angular velocities ω_r decomposed in the body frame.

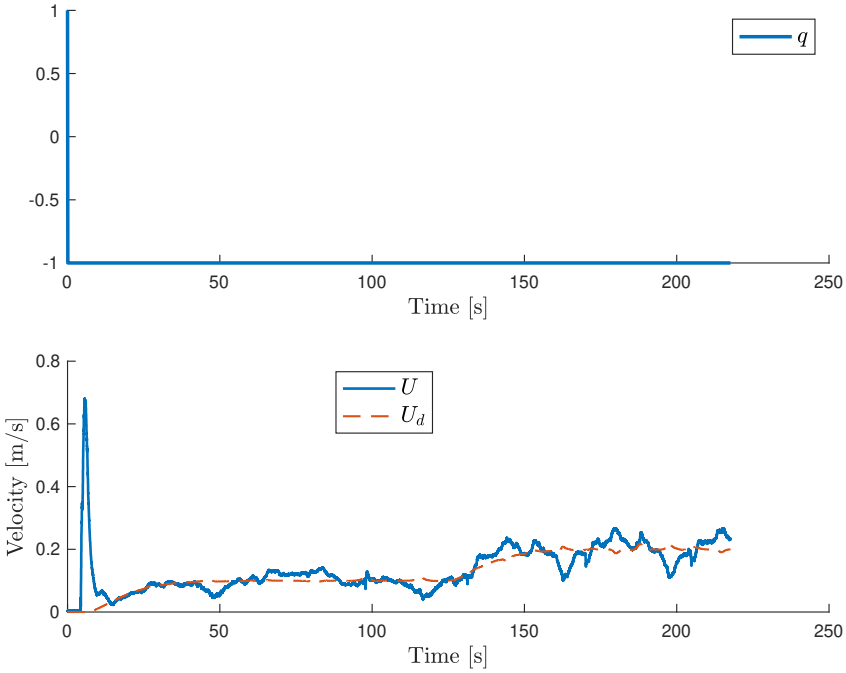

Figure 6.25: The logic variable q, the speed U, and the desired speed $U_d = |\dot{\gamma}_1|$

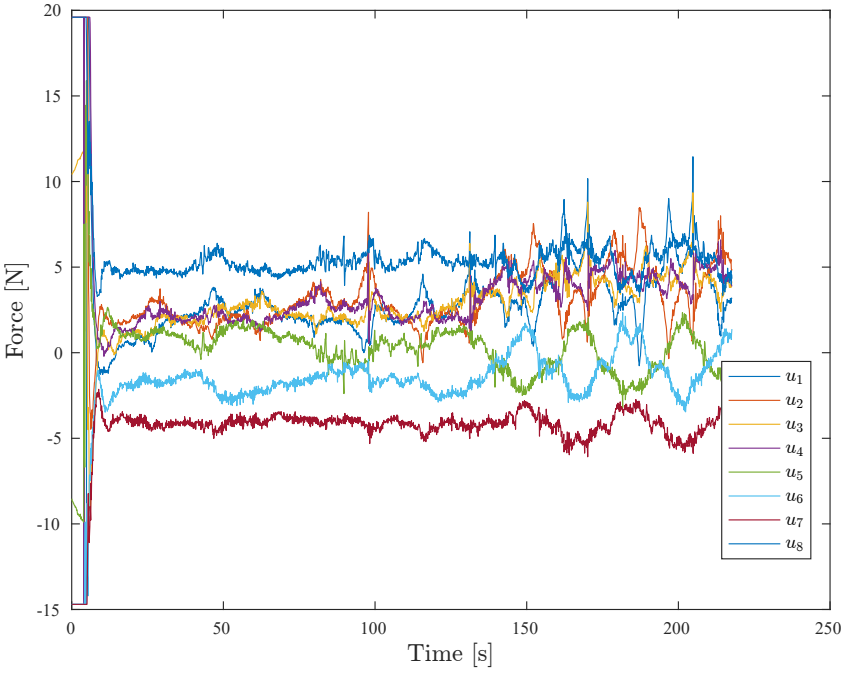

Figure 6.26: The control inputs u corresponding to the eight thrusters.

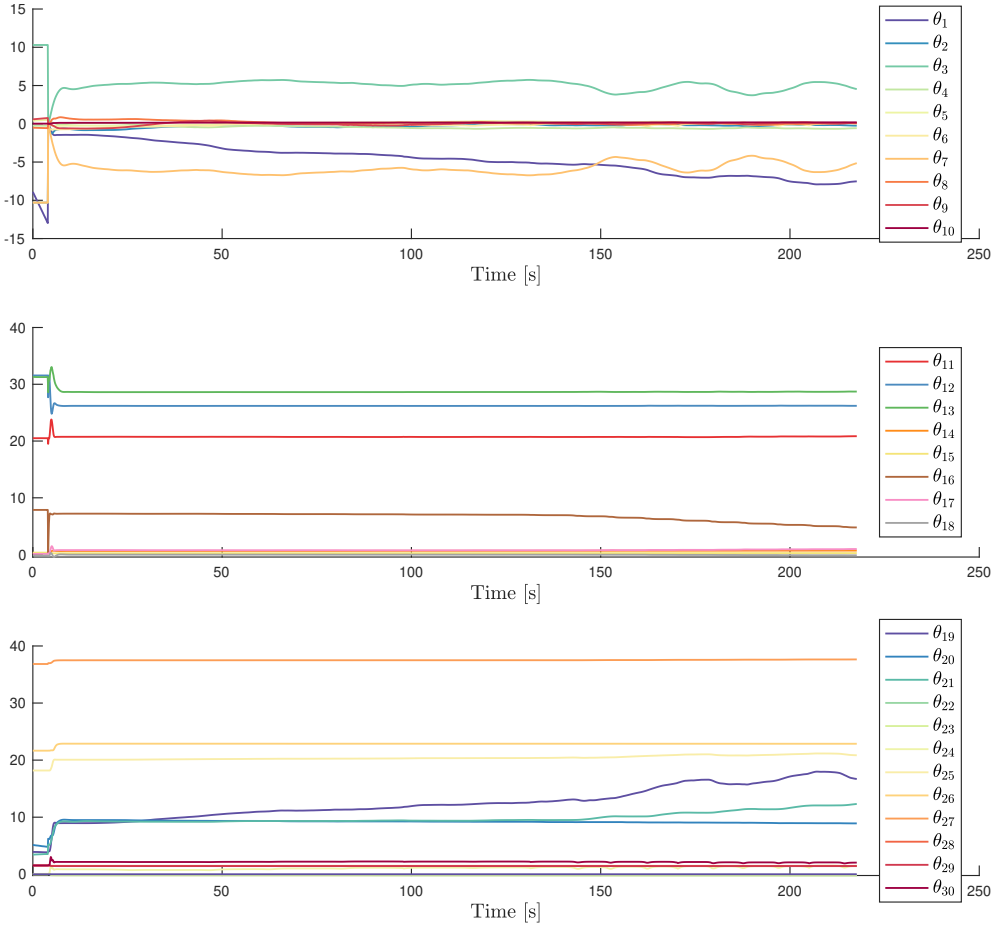

Figure 6.27: The bias and gravitational/buoyancy related parameters, the inertia matrix parameters and the damping parameters.

The initial quaternion error satisfies $\eta_e \leq -\varepsilon$, which entails that a switch from the initial value of $q = 1$ to $q = -1$ occurs at the first time step of the controller. Since the logger was initialized after the controller, although no control inputs were sent to the actuators, we have changed first logged value of the logic variable to $q = 1$ to highlight the fact that a switch has in fact occurred.

From Figures 6.19, 6.21 and 6.22, we observe that the ROV successfully tracks the position and orientation references with satisfactory accuracy. Moreover, from Figures 6.23 and 6.24, we see that the desired velocities $\nu_r = \mathrm{Ad}_{g_e}^{-1} \nu_d$ are tracked with satisfactory accuracy. However, we remark that v_3 contains significantly more noise compared to the other linear velocities. Moreover, the x-component of the linear velocity, v_1, exhibits spikes that coincide with the minima of p_3, i.e. the z-component of the position vector. This is due to poor tracking of the ROV from the camera-based underwater positioning system, which either loses track of the ROV and/or outputs noisy and inaccurate position measurements (especially in the z-direction). This can be mitigated by further restricting the operating region of the ROV and/or lowering

the weight of the camera-based position measurements relative to the accelerometer measurements in the Kalman filter.

Chapter 7

Hysteretic Control Lyapunov Functions

In this chapter, we present a new class of control Lyapunov functions for hybrid feedback control of continuous-time systems, referred to as hysteretic control Lyapunov functions (HCLFs). HCLFs include a hysteresis-based switching mechanism and result in a hybrid control law, transforming the continuous-time system into a hybrid control system. We show that the existence of a family of HCLFs satisfying the small control property implies global stabilizability of a compact set. The hybrid feedback consists of a collection of continuous feedback laws and a hysteresis-based switching mechanism. Moreover, we prove that optimization-based hybrid feedback laws can be constructed under minor assumptions on the objective functions. The collection of optimization-based feedback laws are continuous, implying that the hybrid basic conditions hold such that the stability is robust.

The material in this chapter is based on [92].

7.1 Introduction

Control Lyapunov functions (CLFs) constitute a powerful tool for constructive nonlinear control design, since they can be utilized to determine a stabilizing control law from Lyapunov inequalities [138, 139]. General control laws for stabilization of nonlinear systems using CLFs were first introduced in [140] through Sontag's universal formula, and later in [89]. The control law in [89] is notable in the sense that it pointwise minimizes the norm of the control input with respect to the CLF. More recently, CLFs have been extended to hybrid systems with and without disturbances in [141] and [142], respectively. However, for global asymptotic stabilization of dynamical systems defined on non-contractible state-spaces, there does not exist a continuously differentiable CLF [143].

The remainder of this chapter is organized as follows. Section 7.2 defines a family of hysteretic CLFs, and proves that a family of continuous feedback laws derived from the feasible set-valued map of control inputs defined by the HCLFs results in global asymptotic stability of any compact set. We subsequently introduce synergistic control Lyapunov functions in Section 7.3 and characterize their relationship with SCLFs. Then, Section 7.4 presents sufficient conditions for the existence of a family

of continuous control selections from the feasible set-valued map. Given a collection of level-bounded and strictly convex objective functions, we present an optimization-based hybrid feedback law that pointwise minimizes the objective functions subject to the stability constraints imposed by the HCLFs. Finally, Section 7.5 presents a HCLF-based control design for an underwater vehicle guaranteeing global asymptotic tracking. The theoretical developments are verified with simulations.

7.2 Hysteretic Control Lyapunov Functions

In this section, we define hysteretic control Lyapunov functions for the following class of continuous-time systems

$$\dot{x} = f(x, r, u), \quad (x, r, u) \in \mathcal{X} \times \mathcal{R} \times \mathcal{U}, \tag{7.1}$$

where $u \in \mathcal{U}$ describes the input and $r \in \mathcal{R}$ describes a known exogenous reference signal. Throughout this chapter, the data of (7.1) is taken to satisfy the following assumptions.

Assumption 7.1.

(N1) The state space $\mathcal{X} \subset \mathbb{R}^n$ is closed.
(N2) The exogenous reference space $\mathcal{R} \subset \mathbb{R}^k$ is compact.
(N3) The input space $\mathcal{U} \subset \mathbb{R}^m$ is closed and convex.
(N4) The mapping $f \colon \mathcal{X} \times \mathcal{R} \times \mathcal{U} \to \mathbb{R}^n$ is continuous.

Systems of this form adequately describe a wide range of tracking problems for mechanical systems.

Definition 7.2 (HCLF Family)**.** *Let $\mathcal{A} \subset \mathcal{X}$ be compact and $\mathcal{Q} \subset \mathbb{Z}$ be finite. A collection of functions $\{V_q\}_{q\in\mathcal{Q}}$ is a family of hysteretic control Lyapunov functions for the system (7.1) relative to $\mathcal{A}$ with negativity margins $\{\gamma_q\}_{q\in\mathcal{Q}}$ if there exist collections of sets $\{\mathcal{I}_q\}_{q\in\mathcal{Q}}$, $\{\mathcal{O}_q\}_{q\in\mathcal{Q}}$, and $\{\mathcal{M}_q\}_{q\in\mathcal{Q}}$ such that*

(H1) $\{\mathcal{I}_q\}_{q\in\mathcal{Q}}$ covers $\mathcal{X}$, and for each $q \in \mathcal{Q}$, $\mathcal{I}_q$ is closed in $\mathcal{X}$, $\mathcal{O}_q$ is open in $\mathcal{X}$, $\mathcal{M}_q$ is closed in $\mathcal{X}$, and $\mathcal{I}_q \subset \mathcal{O}_q \subset \mathcal{M}_q$;

(H2) for every $q \in \mathcal{Q}$, $V_q : \mathcal{M}_q \to \mathbb{R}_{\geq 0}$ is continuous on $\mathcal{M}_q$ and continuously differentiable on $\mathcal{M}_q \setminus \mathcal{A}$, the zero set of V_q satisfies $\operatorname{Zero} V_q = \mathcal{A} \cap \mathcal{M}_q$, and for each $c > 0$, the set $\{x \in \mathcal{M}_q : V_q(x) \leq c\}$ is compact.

(H3) for all $(q, s) \in \mathcal{Q} \times \mathcal{Q}$ and every $x \in (\mathcal{M}_q \setminus \mathcal{O}_q) \cap \mathcal{I}_s$,

$$V_s(x) \leq V_q(x); \tag{7.2}$$

(H4) for every $q \in \mathcal{Q}$, $\gamma_q : \mathcal{M}_q \setminus \mathcal{A} \to \mathbb{R}_{>0}$ is continuous, and for every $x \in \mathcal{M}_q \setminus \mathcal{A}$ and every $r \in \mathcal{R}$, there exists $u \in \mathcal{U}$ such that

$$\langle \nabla V_q(x), f(x, r, u) \rangle + \gamma_q(x) < 0. \tag{7.3}$$

A family of HCLFs is a tool that allows the design of a hybrid feedback controller of the form

$$\begin{cases} \dot{q} = 0 & (x, r) \in C_q, \\ q^+ \in G_q(x) & (x, r) \in D_q, \\ u = \kappa_q(x, r) \end{cases} \tag{7.4}$$

where $\{\kappa_q\}_{q\in\mathcal{Q}}$ is a collection of continuous feedback control laws and the controller flow set, jump set, and jump map are defined by

$$C_q \coloneqq \mathcal{M}_q \times \mathcal{R}, \tag{7.5}$$
$$D_q \coloneqq (\mathcal{X} \setminus \mathcal{O}_q) \times \mathcal{R}, \tag{7.6}$$
$$G_q(x) \coloneqq \{s \in \mathcal{Q} : x \in \mathcal{I}_s \setminus \mathcal{O}_q\}, \tag{7.7}$$

respectively. We remark that the smallest possible $\mathcal{M}_q$ is the closure of $\mathcal{O}_q$. In this case, the set $\mathcal{M}_q \setminus \mathcal{O}_q$ that appears in (H3) in Definition 7.2 becomes $\overline{\mathcal{O}}_q \setminus \mathcal{O}_q$. Since every $\mathcal{O}_q$ is relatively open in $\mathcal{X}$, this set may be interpreted as the relative boundary of $\mathcal{O}_q$ in $\mathcal{X}$.

A hybrid system describing the resulting closed-loop dynamics when the hybrid feedback controller (7.4) is applied to the system (7.1) that takes into account all admissible exogenous reference signals is given by

$$\begin{cases} \dot{x} \in F(x,q) & (x,q) \in C, \\ q^+ \in G(x,q) & (x,q) \in D, \end{cases} \tag{7.8}$$

where the closed-loop flow set, flow map, jump set, and jump map are defined by

$$C \coloneqq \bigcup_{q\in\mathcal{Q}} \mathcal{M}_q \times \{q\}, \tag{7.9}$$
$$F(x,q) \coloneqq \overline{\operatorname{con}}\{f(x,r,\kappa_q(x,r)) : r \in \mathcal{R}\}, \tag{7.10}$$
$$D \coloneqq \bigcup_{q\in\mathcal{Q}} (\mathcal{X} \setminus \mathcal{O}_q) \times \{q\}, \tag{7.11}$$
$$G(x,q) \coloneqq G_q(x), \tag{7.12}$$

respectively, and $\overline{\operatorname{con}}$ denotes the closed convex hull of a set. For convenience of notation, the flow map (jump map) of a state in a hybrid system is omitted if it remains unchanged along flows (across jumps). The closed-loop data has the following desired properties.

Lemma 7.1. The hybrid system (7.8) satisfies the hybrid basic conditions (Assumption 2.16).

Proof. Since C and D are finite unions of closed sets, it follows that C and D are closed. The set-valued mapping $(x,q) \mapsto \{f(x,r,\kappa_q(x,r)) : r \in \mathcal{R}\}$ is outer semicontinuous and locally bounded relative to C by [103, Proposition 1.4.14]. In particular, $(x,r,q) \mapsto f(x,r,\kappa_q(x,r))$ is continuous on $\mathcal{X}\times\mathcal{R}\times\mathcal{Q}$ and $(x,q) \mapsto \mathcal{R}$ is outer semicontinuous and locally bounded when regarded as a set-valued mapping. Taking the closed convex hull preserves local boundedness and outer semicontinuity of mappings (this follows from [90, Lemma 5.17]) and ensures that F is convex-valued. Lastly, it holds that

$$\begin{aligned} \operatorname{gph} G &= \{(x,q,s) \in \mathcal{X}\times\mathcal{Q}\times\mathcal{Q} : x \in \mathcal{I}_s \setminus \mathcal{O}_q\} \\ &= \bigcup_{q\in\mathcal{Q}} \bigcup_{s\in\mathcal{Q}} (\mathcal{I}_s \setminus \mathcal{O}_q) \times \{q\} \times \{s\}, \end{aligned} \tag{7.13}$$

which is closed as it is a finite union of closed sets. Consequently, G is outer semicontinuous relative to D by Lemma 2.2. □

The definition of an HCLF family naturally leads to a collection of feasible set-valued mappings for the input. Defining, for every $q \in \mathcal{Q}$, the compact set

$$\mathcal{B}_q \coloneqq (\mathcal{A} \times \mathcal{R}) \cap C_q, \tag{7.14}$$

we can for every $q \in \mathcal{Q}$ define the feasible set-valued mapping $\mathcal{F}_q : C_q \setminus \mathcal{B}_q \rightrightarrows \mathcal{U}$,

$$\mathcal{F}_q(x,r) \coloneqq \big\{u \in \mathcal{U} : \langle \nabla V_q(x), f(x,r,u)\rangle + \gamma_q(x) \leq 0\big\}. \tag{7.15}$$

The fact that $\mathcal{F}_q$ is takes nonempty values on $C_q \setminus \mathcal{B}_q$ follows readily from (H4) in Definition 7.2. With (7.15) in place, we now define a feasible family of control laws.

Definition 7.3. *A collection of control laws $\{\kappa_q\}_{q\in\mathcal{Q}}$ is feasible if for every $q \in \mathcal{Q}$, $\kappa_q : C_q \times \mathcal{R} \to \mathcal{U}$ is continuous and $\kappa_q(x,r) \in \mathcal{F}_q(x,r)$ for all $(x,r) \in C_q \setminus \mathcal{B}_q$.*

A feasible collection of control laws ensures that $\langle \nabla V_q(x), f(x,r,\kappa_q(x,r))\rangle + \gamma_q(x) \leq 0$ for every $q \in \mathcal{Q}$ and all $(x,r) \in C_q \setminus \mathcal{B}_q$. Hence, the negativity margins control the decrease of the HCLF family along flows and should therefore be viewed as design parameters. The next result shows that the regularized set-valued flow map F as defined by (7.10) inherits this property.

Lemma 7.2. Let $\{V_q\}_{q\in\mathcal{Q}}$ be an HCLF family for (7.1) relative to $\mathcal{A}$ with negativity margins $\{\gamma_q\}_{q\in\mathcal{Q}}$. If $\{\kappa_q\}_{q\in\mathcal{Q}}$ is a feasible collection of control laws, then $\langle \nabla V_q(x), \varphi\rangle + \gamma_q(x) \leq 0$ for every $\varphi \in F(x,q)$ and all $(x,q) \in C \setminus (\mathcal{A} \times \mathcal{Q})$.

Proof. Let $F_\kappa(x,q) \coloneqq \{f(x,r,\kappa_q(x,r)) : r \in \mathcal{R})\}$ such that $F(x,q) = \overline{\operatorname{con}} F_\kappa(x,q)$ for all $(x,q) \in C$. Let $F_\circ(x,q) \coloneqq \{\varphi \in \mathbb{R}^n : \langle \nabla V_q(x), \varphi\rangle + \gamma_q(x) \leq 0\}$. Since $F_\circ(x,q)$ is the sublevel set of an affine function, it is closed and convex for all $(x,q) \in C$. Since the controllers are feasible, it holds that $F_\kappa(x,q) \subset F_\circ(x,q)$ for all $(x,q) \in C \setminus (\mathcal{A} \times \mathcal{Q})$. Consequently, $F(x,q) = \overline{\operatorname{con}} F_\kappa(x,q) \subset \overline{\operatorname{con}} F_\circ(x,q) = F_\circ(x,q)$ for all $(x,q) \in C \setminus (\mathcal{A} \times \mathcal{Q})$. □

We now prove that if $\{\kappa_q\}_{q\in\mathcal{Q}}$ is a feasible collection of control laws, then the compact set $\mathcal{A} \times Q$ is globally pre-asymptotically stable for the closed-loop system (7.8). This stability is robust to perturbations in the sense of [90, Definition 7.15], as seen from [90, Proposition 7.21].

Theorem 7.4. *Let $\{V_q\}_{q\in\mathcal{Q}}$ be an HCLF family for (7.1) relative to $\mathcal{A}$ with negativity margins $\{\gamma_q\}_{q\in\mathcal{Q}}$. If $\{\kappa_q\}_{q\in\mathcal{Q}}$ is a feasible collection of control laws, then $\mathcal{A} \times \mathcal{Q}$ is globally pre-asymptotically stable for the closed-loop system (7.8).*

Proof. Consider the hybrid system

$$\begin{cases} \dot{x} \in F(x,q) & (x,q) \in C, \\ q^+ \in G(x,q) & (x,q) \in C \cap D, \end{cases} \tag{7.16}$$

that is, the closed-loop system (7.8) with jump set D replaced by $C \cap D$. Since $C \cap D \subset D$ is closed, it follows from Lemma 7.1 that (7.16) satisfies the hybrid basic conditions (Assumption 2.16). We claim that $V(x,q) \coloneqq V_q(x)$ can be used as a Lyapunov function for (7.16) relative to $\mathcal{A} \times \mathcal{Q}$. It follows from (H2) in Definition 7.2 that $V : C \to \mathbb{R}_{\geq 0}$ is continuously differentiable on $C \setminus (\mathcal{A} \times \mathcal{Q})$ and positive definite with respect to $\mathcal{A} \times \mathcal{Q}$.

Furthermore, the set $\{(x,q) \in C : V(x,q) \leq c\}$ is compact for every $c > 0$. It follows from Lemma 7.2 that the decrease of V along flows of (7.16) is strict on $C \setminus (\mathcal{A} \times \mathcal{Q})$. Since $C \cap D = \bigcup_{q \in \mathcal{Q}} (\mathcal{M}_q \setminus \mathcal{O}_q) \times \{q\}$, it follows from (H3) that $V(x,s) - V(x,q) \leq 0$ for all $(x,q) \in C \cap D$ and every $s \in G(x,q)$. Furthermore, jumping out of $\mathcal{A} \times \mathcal{Q}$ is not possible. Lastly, since $(x,q) \in C \cap D$ and $s \in G(x,q)$ implies that $x \in \mathcal{I}_s$, and $\mathcal{I}_s \subset \mathcal{O}_s$, we have that $(x,s) \in C \setminus D$. Consequently, solutions to (7.16) always jump out of $C \cap D$ and into $C \setminus D$. It then follows from [106, Theorem 23] that $\mathcal{A} \times \mathcal{Q}$ is globally pre-asymptotically stable for the system (7.16). Solutions to (7.8) that are not solutions to (7.16) are those initiated in $D \setminus C$. Such a solution must immediately jump into $C \setminus D$, after which it coincides with a solution to (7.8). Since the distance of the solution to $\mathcal{A} \times \mathcal{Q}$ is unchanged by such a jump and $\mathcal{A} \times \mathcal{Q}$ is globally pre-asymptotically stable for (7.16), it follows that $\mathcal{A} \times \mathcal{Q}$ is globally pre-asymptotically stable for (7.8). □

We now illustrate the presented theory with a simple example.

Example 7.5. Let $\mathcal{X} \coloneqq \mathbb{R}$, $\mathcal{R} \coloneqq [-1,1]$, $\mathcal{U} \coloneqq \mathbb{R}$, and $f : \mathcal{X} \times \mathcal{R} \times \mathcal{U} \to \mathbb{R}$ be defined by $f(x,r,u) = -r + u$. Furthermore, let $\mathcal{Q} \coloneqq \{-1,1\}$, and $\mathcal{A} \coloneqq \{-1,1\}$, and for every $q \in \mathcal{Q}$,

$$\begin{aligned} \mathcal{I}_q &\coloneqq \{x \in \mathbb{R} : qx \geq 0\}, \\ \mathcal{O}_q &\coloneqq \{x \in \mathbb{R} : qx > -\tfrac{1}{4}\}, \\ \mathcal{M}_q &\coloneqq \{x \in \mathbb{R} : qx \geq -\tfrac{1}{2}\}, \end{aligned} \tag{7.17}$$

$$V_q(x) \coloneqq (qx-1)^2. \tag{7.18}$$

It is clear that the sets (7.17) satisfy (H1) in Definition 7.2. It is also readily seen from Figure 7.1 that (H2) in Definition 7.2 is satisfied. Furthermore,

$$\mathcal{I}_s \cap (\mathcal{M}_q \setminus \mathcal{O}_q) = \begin{cases} \emptyset & s = q \\ \{x \in \mathbb{R} : -\frac{1}{2} \leq qx \leq -\frac{1}{4}\} & s = -q \end{cases} \tag{7.19}$$

from which it follows that $V_s(x) \leq \frac{9}{16}$ and $V_q(x) \geq \frac{25}{16}$ for every $x \in \mathcal{I}_s \cap (\mathcal{M}_q \setminus \mathcal{O}_q)$ and every $q \in \mathcal{Q}$. Hence, (H3) in Definition 7.2 is satisfied. Lastly, we find that

$$\langle \nabla V_q(x), f(x,r,u) \rangle = 2(x-q)(-r+u) \tag{7.20}$$

such that (H4) in Definition 7.2 holds with negativity margins $\{\gamma_q\}_{q \in \mathcal{Q}}$ defined by $\gamma_q(x) \coloneqq 2k(qx-1)^2$, where $k > 0$. Then $\{\kappa_q\}_{q \in \mathcal{Q}}$, where every κ_q is defined by $\kappa_q(x,r) \coloneqq r - k(x-q)$, is a feasible family of control laws.

7.3 Synergistic Control Lyapunov Functions

HCLFs are closely related to the notions of synergistic functions and synergistic Lyapunov function and feedback pairs (SLFFs) from Chapter 5 and Chapter 8. Recall that every continuous function $V : \mathcal{X} \times \mathcal{Q} \to \mathbb{R}_{\geq 0}$ has an associated continuous synergy gap $\mu_V : \mathcal{X} \times \mathcal{Q} \to \mathbb{R}_{\geq 0}$, defined by

$$\mu_V(x,q) \coloneqq V(x,q) - \min_{s \in \mathcal{Q}} V(x,s). \tag{7.21}$$

We now introduce the notion of a synergistic control Lyapunov function (SCLF).

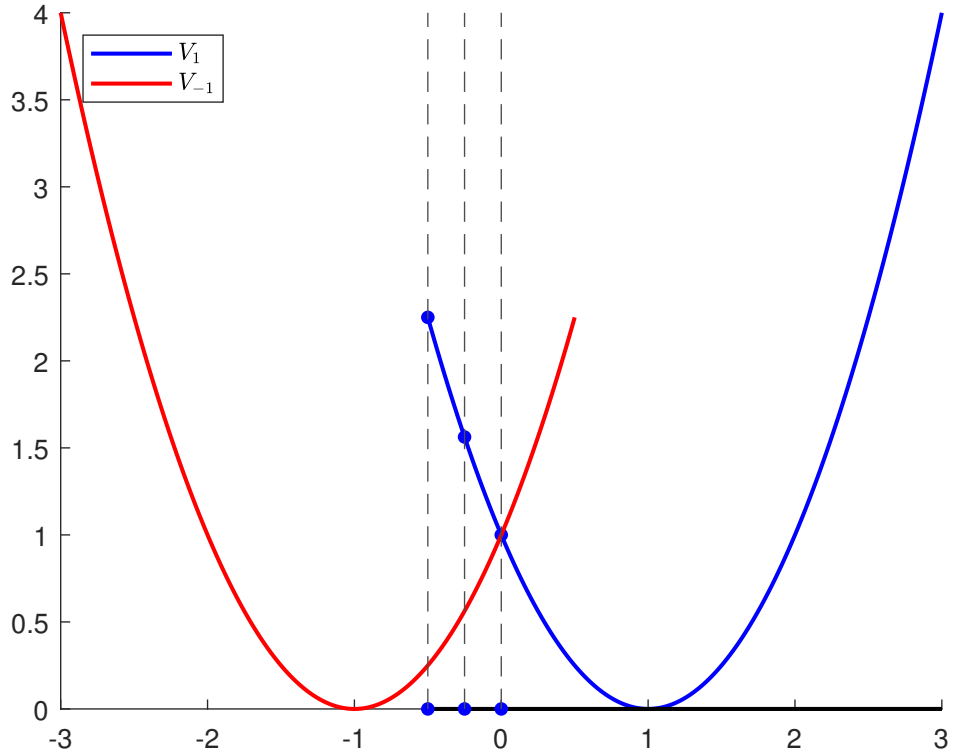

Figure 7.1: A plot of $\{V_q\}_{q\in\mathcal{Q}}$.

Definition 7.6 (SCLF)**.** *Let $\mathcal{Q}\subset\mathbb{Z}$ be finite, $\mathcal{M}\subset\mathcal{X}\times\mathcal{Q}$ be closed, and $\mathcal{A}\subset\mathcal{X}$ be compact. A function V is a synergistic control Lyapunov function for the system (7.1) relative to $\mathcal{A}$ with negativity margin γ and gap exceeding ρ if V satisfies*

(S1) $V:\mathcal{X}\times\mathcal{Q}\to\mathbb{R}_{\geq 0}$ is proper, V is continuously differentiable on $\mathcal{M}$, and the zero set of V satisfies $\pi_1(\operatorname{Zero}V)=\mathcal{A}$;

(S2) there exist continuous functions $\gamma:\mathcal{M}\to\mathbb{R}_{\geq 0}$ and $\rho:\mathcal{X}\times\mathcal{Q}\to\mathbb{R}_{\geq 0}$, $\operatorname{Zero}\rho\subset\operatorname{Zero}V$, and the synergy gap satisfies

$$\mu_V(x,q)>\rho(x,q) \text{ for all } (x,q)\in\left(\mathcal{P}_\gamma\cup(\mathcal{A}\times\mathcal{Q})\cup\overline{(\mathcal{X}\times\mathcal{Q})\setminus\mathcal{M}}\right)\setminus\operatorname{Zero}V,$$

where

$$\mathcal{P}_\gamma:=\{(x,q)\in\mathcal{M}:\inf_{u\in\mathcal{U}}\max_{r\in\mathcal{R}}\langle\nabla V(x,q),f(x,r,u)\rangle+\gamma(x,q)\geq 0\}\cup\operatorname{Zero}\gamma. \tag{7.22}$$

Let V be an SCLF for the system (7.1) relative to $\mathcal{A}$ with negativity margin γ and gap exceeding ρ, and define, for each $q\in\mathcal{Q}$,

$$\begin{aligned}\mathcal{I}_q&:=\{x\in\mathcal{X}:\mu_V(x,q)=0\},\\ \mathcal{O}_q&:=\{x\in\mathcal{X}:\mu_V(x,q)<\rho(x,q)\},\\ \mathcal{M}_q&:=\{x\in\mathcal{X}:\mu_V(x,q)\leq\rho(x,q)\}.\end{aligned} \tag{7.23}$$

If $\rho(x,q) > 0$ for all $(x,q) \in \mathcal{X} \times \mathcal{Q}$, then it follows from the continuity of μ_V that the sets in (7.23) satisfy (H1) in Definition 7.2. Define then, for every $q \in \mathcal{Q}$, $V_q : \mathcal{M}_q \to \mathbb{R}_{\geq 0}$ by $V_q(x) \coloneqq V(x,q)$ and $\gamma_q : \mathcal{M}_q \setminus \mathcal{A} \to \mathbb{R}_{>0}$ by $\gamma_q(x) \coloneqq \gamma(x,q)$. It is then straightforward to verify that $\{V_q\}_{q\in\mathcal{Q}}$ is an HCLF family for (7.1) relative to $\mathcal{A}$ with negativity margins $\{\gamma_q\}_{q\in\mathcal{Q}}$. The requirement that $\rho(x,q) > 0$ for all $(x,q) \in \mathcal{X} \times \mathcal{Q}$ is due to the fact that having $\rho(x,q) = 0$ for some $(x,q) \in \operatorname{Zero} V$ leads to the possibility of consecutive jumps in the synergistic framework. In the hysteretic framework, consecutive jumping is impossible by design; every jump leaves the jump set. We note that the results that are introduced in Section 7.4 also hold for an SCLF in the absence of this additional restriction on ρ.

7.4 Hysteretic Feedback Control Design

Let $\{V_q\}_{q\in\mathcal{Q}}$ be an HCLF family for (7.1) relative to $\mathcal{A}$ with negativity margins $\{\gamma_q\}_{q\in\mathcal{Q}}$. The following theorem provides sufficient conditions for the existence of a feasible collection of control laws.

Theorem 7.7 (Continuous Selection)**.** *Let $\{V_q\}_{q\in\mathcal{Q}}$ be an HCLF family for (7.1) relative to $\mathcal{A}$ with negativity margins $\{\gamma_q\}_{q\in\mathcal{Q}}$. If it holds that,*

(C1) for every $q \in \mathcal{Q}$ and all $(x,r) \in C_q$, the mapping

$$u \mapsto \langle \nabla V_q(x), f(x,r,u) \rangle, \tag{7.24}$$

is convex on $\mathcal{U}$;

(C2) there exists a collection of mappings $\{\theta_q\}_{q\in\mathcal{Q}}$ such that for every $q \in \mathcal{Q}$, $\theta_q \colon \mathcal{B}_q \to \mathcal{U}$ is continuous and the set-valued mapping $\mathcal{K}_q : C_q \rightrightarrows \mathcal{U}$,

$$\mathcal{K}_q(x,r) \coloneqq \begin{cases} \{\theta_q(x,r)\}, & \text{if } (x,r) \in \mathcal{B}_q \\ \mathcal{F}_q(x,r), & \text{if } (x,r) \in C_q \setminus \mathcal{B}_q, \end{cases} \tag{7.25}$$

is inner semicontinuous relative to C_q at all $(x,r) \in \mathcal{B}_q$,

then there exists a feasible collection of feedback control laws $\{\kappa_q\}_{q\in\mathcal{Q}}$.

Proof. It follows directly from (H4) of Definition 7.2 that the set-valued mapping $\mathcal{S}_q : C_q \setminus \mathcal{B}_q \rightrightarrows \mathcal{U}$ defined by

$$S_q(x,r) \coloneqq \{u \in \mathcal{U} : \langle \nabla V_q(x), f(x,r,u) \rangle + \gamma_q(x) < 0\},$$

is nonempty-valued on $C_q \setminus \mathcal{B}_q$. Furthermore, since f, every ∇V_q, and every γ_q are continuous, it follows directly from [89, Corollary 2.13] that, for every $q \in \mathcal{Q}$, S_q is inner semicontinuous relative to $C_q \setminus \mathcal{B}_q$. From (C1), [144, Theorem 7.6], and the fact that taking closures preserves inner semicontinuity, it follows that for every $q \in \mathcal{Q}$ and all $(x,r) \in C_q \setminus \mathcal{B}_q$

$$\begin{aligned} \overline{S_q(x,r)} &= \{u \in \mathcal{U} : \langle \nabla V_q(x), f(x,r,u) \rangle + \gamma_q(x) \leq 0\} \\ &= \mathcal{F}_q(x,r), \end{aligned}$$

is closed-convex-valued and inner semicontinuous relative to $C_q \backslash \mathcal{B}_q$. A similar result is also found in [103, Proposition 1.5.2], which can be adapted from the affine to the convex case.

Since every $C_q \setminus \mathcal{B}_q$ is relatively open in C_q, it holds that every $\mathcal{K}_q$ is inner semicontinuous relative to C_q at all $(x, r) \in C_q \setminus \mathcal{B}_q$. It now follows directly from (C2) that $\mathcal{K}_q$ is inner semicontinuous relative to C_q for every $q \in \mathcal{Q}$. Then, Theorem 2.14 implies the existence of a collection of functions $\{\kappa_q\}_{q\in\mathcal{Q}}$ such that $\kappa_q : C_q \to \mathcal{U}$ is continuous and $\kappa_q(x, r) \in \mathcal{K}_q(x, r)$ for every $q \in \mathcal{Q}$ and all $(x, r) \in C_q$. In other words, there exists a collection of feasible control laws. □

Condition (C1) always holds when the mapping $u \mapsto f(x, r, u)$ is affine for all $(x, r) \in \mathcal{X} \times \mathcal{R}$. Additionally, (C2) is recognized as the small control property [89]. Theorem 7.7 states sufficient conditions for the existence of a feasible collection of control laws. However, it is neither constructive nor optimal. The following theorem enables us to take continuous selections from $\mathcal{K}_q$ minimizing a specified objective function.

Theorem 7.8 (Optimal Selection)**.** *Let $\{V_q\}_{q\in\mathcal{Q}}$ be an HCLF family for (7.1) relative to $\mathcal{A}$ with negativity margins $\{\gamma_q\}_{q\in\mathcal{Q}}$. If condition (C1) in Theorem 7.7 holds and there exists a collection of functions $\{h_q\}_{q\in\mathcal{Q}}$ such that,*

(O1) for every $q \in \mathcal{Q}$, $h_q : C_q \times \mathcal{U} \to \mathbb{R}$ is continuous, $u \mapsto h_q(x, r, u)$ is strictly convex on $\mathcal{U}$ for all $(x, r) \in C_q$, and for every compact set $K \subset C_q$ and every $k \in \mathbb{R}$, the set

$$\{u \in \mathcal{U} : (x, r) \in K, h_q(x, r, u) \leq k\} \tag{7.26}$$

is bounded;

(O2) condition (C2) in Theorem 7.7 holds with $\theta_q : \mathcal{B}_q \to \mathcal{U}$ defined by

$$\theta_q(x, r) \coloneqq \arg\min_{u\in\mathcal{U}} h_q(x, r, u), \tag{7.27}$$

then the collection of control laws $\{\kappa_q\}_{q\in\mathcal{Q}}$ defined by

$$\kappa_q(x, r) = \arg\min_{u\in\mathcal{K}_q(x,r)} h_q(x, r, u), \tag{7.28}$$

where $\mathcal{K}_q$ is defined by (7.25), is feasible.

Proof. For all $(x, r) \in C_q$ and every $q \in \mathcal{Q}$, it holds $\mathcal{K}_q(x, r)$ is closed and that $u \to h_q(x, r, u)$ is continuous and level bounded on $\mathcal{K}_q(x, r)$. It follows from [102, Theorem 1.9] that the set $\arg\min_{u\in\mathcal{K}_q(x,r)} h_q(x, r, q)$ is nonempty and compact for all $(x, r) \in C_q$ and every $q \in \mathcal{Q}$. Furthermore, since every $\mathcal{K}_q(x, r)$ is convex and $u \to h_q(x, r, u)$ is strictly convex on $\mathcal{K}_q(x, r)$, it follows from [102, Theorem 2.6] that the set $\arg\min_{u\in\mathcal{K}_q(x,r)} h_q(x, r, q)$ is a singleton. Consequently,

$$\begin{aligned} \underline{h}_q(x, r) &\coloneqq \inf_{u\in\mathcal{K}_q(x,r)} h_q(x, r, u) \\ &= \min_{u\in\mathcal{K}_q(x,r)} h_q(x, r, u) \\ &= h_q(x, r, \kappa_q(x, r)). \end{aligned} \tag{7.29}$$

Since every $\mathcal{K}_q$ is inner semicontinuous relative to C_q, it follows from [103, Theorem 1.4.16] that every $\underline{h}_q$ is upper semicontinuous. Continuity of every h_q and upper semicontinuity of every $\underline{h}_q$ ensure that the set-valued mappings $R_q : C_q \rightrightarrows \mathcal{U}$ defined by

$$R_q(x,r) \coloneqq \{u \in \mathcal{U} : h_q(x,r,u) \leq \underline{h}_q(x,r)\} \tag{7.30}$$

are outer semicontinuous relative to C_q. By definition of κ_q, it holds that $\kappa_q(x,r) = \mathcal{K}_q(x,r) \cap R_q(x,r)$ for all $(x,r) \in C_q$. Since every $\underline{h}_q$ is upper semicontinuous, they are upper bounded on compacts. Consequently, for every $q \in \mathcal{Q}$ and every compact set $K \subset C_q$, there exists $k \in \mathbb{R}$ such that

$$\begin{aligned} R_q(K) &= \{u \in \mathcal{U} : (x,r) \in K, h_q(x,r,u) \leq \underline{h}_q(x,r)\} \\ &\subset \{u \in \mathcal{U} : (x,r) \in K, h_q(x,r,u) \leq k\}, \end{aligned} \tag{7.31}$$

In light of (O1), it can be concluded that $R_q(K)$ is bounded for every compact set $K \subset C_q$. It follows that every R_q is locally bounded relative to C_q, and consequently that every κ_q is locally bounded. Since every V_q is continuously differentiable and every γ_q is continuous on $\mathcal{M}_q \setminus \mathcal{A}$, and f is continuous on $\mathcal{X} \times \mathcal{R} \times \mathcal{U}$, we find for every $q \in \mathcal{Q}$ that

$$\begin{aligned} &\operatorname{gph} \mathcal{K}_q \cap [(C_q \setminus \mathcal{B}_q) \times \mathbb{R}^m] = \\ &\qquad \{(x,r,u) \in (C_q \setminus \mathcal{B}_q) \times \mathcal{U} : \langle \nabla V_q(x), f(x,r,u) \rangle + \gamma_q(x) \leq 0\} \end{aligned} \tag{7.32}$$

is relatively closed in $(C_q \setminus \mathcal{B}_q) \times \mathbb{R}^m$. It follows that

$$\begin{aligned} \operatorname{gph} \kappa_q &= \operatorname{gph} \mathcal{K}_q \cap \operatorname{gph} R_q \\ &= \overline{\operatorname{gph} \mathcal{K}_q} \cap \operatorname{gph} R_q \end{aligned} \tag{7.33}$$

is closed, and every κ_q is therefore outer semicontinuous when regarded as a set-valued mapping. Since every κ_q is outer semicontinuous and locally bounded, they are in fact continuous. □

The main difficulty in applying Theorem 7.8 appears to be how to verify that the HCLF family satisfies the small control property (C2) defined in Theorem 7.7. It turns out that if (C1) holds, then the existence of a feasible collection of control laws for the HCLF family implies that the small control property holds, as shown in the following result.

Lemma 7.3. Let $\{V_q\}_{q \in \mathcal{Q}}$ be an HCLF family for (7.1) relative to $\mathcal{A}$ with negativity margins $\{\gamma_q\}_{q \in \mathcal{Q}}$ satisfying (C1) in Theorem 7.7. If there exists a feasible collection of control laws $\{\kappa_q\}_{q \in \mathcal{Q}}$ such that $\kappa_q(x,r) = \theta_q(x,r)$ for all $(x,r) \in \mathcal{B}_q$ and every $q \in \mathcal{Q}$, then $\mathcal{K}_q$ as defined in (7.25) is inner semicontinuous relative to C_q for every $q \in \mathcal{Q}$.

Proof. We have already shown in the proof of Theorem 7.7 that every $\mathcal{K}_q$ is inner semicontinuous relative to C_q at all $(x,r) \in C_q \setminus \mathcal{B}_q$. Let $(\bar{x},\bar{r}) \in \mathcal{B}_q$. By continuity of κ_q, there exists for every neighborhood V of $\theta_q(\bar{x},\bar{r})$ a neighborhood U of $(\bar{x},\bar{r})$ such that $U \cap C_q \subset \kappa_q^{-1}(V)$. Moreover, since $\kappa_q(x,r) \in \mathcal{K}_q(x,r)$ for all $(x,r) \in C_q$ and every $q \in \mathcal{Q}$, it holds that $U \cap C_q \subset \mathcal{K}_q^{-1}(V)$. Consequently, $\mathcal{K}_q$ is inner semicontinuous relative to C_q at $(\bar{x},\bar{r})$ by Definition 2.11. This approach works for all $(\bar{x},\bar{r}) \in \mathcal{B}_q$ and every $q \in \mathcal{Q}$. Consequently, every $\mathcal{K}_q$ is inner semicontinuous relative to C_q. □

7.5 Trajectory Tracking for Underwater Vehicles

In the remaining part of this chapter we will illustrate how the results of the previous sections can be applied. Specifically, we will construct a family of HCLFs and synthesize a hybrid control law ensuring global asymptotic tracking for an underwater vehicle with configuration described by $\widetilde{\mathrm{SE}}(3)$.

7.5.1 Control Model

We denote by $p \in \mathbb{R}^3$ the position of the vehicle with respect to the inertial frame origin, and by $z = (\eta, \epsilon) \in \mathbb{S}^3$ a unit quaternion such that the rotation matrix $\mathrm{rot}(z)$ specifies the orientation of the vehicle with respect to the inertial frame. Defining $\widehat{\mathrm{SE}}(3) \coloneqq \{(p, z) \in \mathbb{R}^7 : p \in \mathbb{R}^3, z \in \mathbb{S}^3\}$, and denoting by $\nu = (v, \omega) \in \mathbb{R}^6$ the body velocity of the vehicle, the fundamental kinematic relation reads

$$\dot{\varphi} = T(\varphi)\nu, \quad (\varphi, \nu) \in \widehat{\mathrm{SE}}(3) \times \mathbb{R}^6 \tag{7.34}$$

where the transformation $T : \widehat{\mathrm{SE}}(3) \to \mathbb{R}^{7\times 6}$ is defined by $T(\varphi) \coloneqq \mathrm{blkdiag}(\mathrm{rot}\, z, \mathrm{atr}\, z)$ with $\mathrm{atr} : \mathbb{S}^3 \to \mathbb{R}^{4\times 3}$ defined by

$$\mathrm{atr}\, z \coloneqq \frac{1}{2}\begin{pmatrix} -\epsilon^{\mathsf{T}} \\ \eta I + \epsilon^{\times} \end{pmatrix}. \tag{7.35}$$

When equipped with the group operation $\circledcirc : \widehat{\mathrm{SE}}(3) \times \widehat{\mathrm{SE}}(3) \to \widehat{\mathrm{SE}}(3)$ defined by $\varphi_1 \circledcirc \varphi_2 \coloneqq (\mathrm{rot}(z_1)p_2 + p_1, z_1 \odot z_2)$ and group inverse $\varphi^{-1} = (-\mathrm{rot}(z)^{\mathsf{T}}p, z^{-1})$, where $\odot$ denotes the quaternion product and $z^{-1} = (\eta, -\epsilon)$ denotes the quaternion conjugate of $z = (\eta, \epsilon)$, then $\widehat{\mathrm{SE}}(3)$ is a Lie group. The identity element of the group becomes $\varphi_I = (0, z_I)$, where $z_I = (1, 0)$ is the identity quaternion. It can be shown that $\widehat{\mathrm{SE}}(3)$ and $\widetilde{\mathrm{SE}}(3)$ are isomorphic as Lie groups.

We consider the underwater vehicle model

$$\left.\begin{aligned} \dot{\varphi} &= T(\varphi)\nu \\ M\dot{\nu} &= \mathrm{ad}_{\nu}^{\mathsf{T}} M\nu + d(\nu) + \chi(g) + Bu \end{aligned}\right\} (\varphi, \nu, u) \in \widehat{\mathrm{SE}}(3) \times \mathbb{R}^6 \times \mathbb{R}^m, \tag{7.36}$$

where $M \in \mathbb{R}^{6\times 6}$ is the total inertia matrix of the vehicle, $d : \mathbb{R}^6 \to \mathbb{R}^6$ is the hydrodynamic damping wrench, $\chi : \widehat{\mathrm{SE}} \to \mathbb{R}^6$ is hydrostatic wrench, $B \in \mathbb{R}^{6\times m}$ is the thruster configuration matrix, and $u \in \mathbb{R}^m$ is the thruster control signal. It is assumed that M is symmetric and positive definite, that d and χ are continuous, and that B has full rank. Since $\widetilde{\mathrm{SE}}(3)$ and $\widehat{\mathrm{SE}}(3)$ are isomorphic, the model (7.36) is equivalent to the control model of Section 3.6 provided $b = 0$ and $\tau = Bu$.

A bounded reference trajectory for the vehicle configuration, velocity and acceleration is generated from the exogenous system

$$\left.\begin{aligned} \dot{\varphi}_d &= T(\varphi_d)\nu_d \\ \dot{\nu}_d &= \alpha_d \end{aligned}\right\} (\varphi_d, \nu_d, \alpha_d) \in \Omega \times c\mathbb{B} \times l\mathbb{B}, \tag{7.37}$$

where $\Omega \subset \widehat{\mathrm{SE}}(3)$ is compact and $c, l > 0$. Here $\varphi_d \in \widehat{\mathrm{SE}}(3)$ represents the desired configuration, $\nu_d \in \mathbb{R}^6$ the desired velocity, and $\alpha_d \in \mathbb{R}^6$ the desired acceleration. It

can be verified that the reference system is equivalent to the reference system (5.2) used in Chapter 5 for $\mathcal{G} = \widehat{\mathrm{SE}}(3)$.

Given a configuration $\varphi \in \widehat{\mathrm{SE}}(3)$ and a desired configuration $\varphi_d \in \widehat{\mathrm{SE}}(3)$, we define analogously to Chapter 5 the the error configuration $\varphi_e \coloneqq \varphi_d^{-1} \circledcirc \varphi$. Then, $\varphi_e = \varphi_I$ if and only if $\varphi = \varphi_d$. With the error configuration φ_e, we can associate the error velocity

$$\nu_e \coloneqq \nu - \mathrm{Ad}_{\varphi_e}^{-1} \nu_d, \tag{7.38}$$

where, for every $\varphi = (p, z) \in \widehat{\mathrm{SE}}(3)$, $\mathrm{Ad}_\varphi \in \mathbb{R}^{6\times 6}$ is defined by

$$\mathrm{Ad}_\varphi \coloneqq \begin{pmatrix} \mathrm{rot}(z) & p^\times \mathrm{rot}(z) \\ 0 & \mathrm{rot}(z) \end{pmatrix}. \tag{7.39}$$

It is then easily verified that

$$\mathrm{Ad}_\varphi^{-1} \coloneqq \begin{pmatrix} \mathrm{rot}(z)^\mathsf{T} & -\mathrm{rot}(z)^\mathsf{T} p^\times \\ 0 & \mathrm{rot}(z)^\mathsf{T} \end{pmatrix}. \tag{7.40}$$

We perform the change of variables $(\varphi, \nu, u, \varphi_d, \nu_d, \alpha_d) \mapsto (\varphi_e, \nu_e, u, \varphi_d, \nu_d, \alpha_d)$, and restrict the desired configuration, desired velocity, and desired acceleration as done in (7.37). This results in the tracking error system

$$\begin{aligned} \dot{\varphi}_e &= T(\varphi_e)\nu_e \\ \dot{\nu}_e &= M^{-1}[\mathrm{ad}_\nu^\mathsf{T} M\nu + d(\nu) + \chi(\varphi) + Bu] \\ &\quad - \mathrm{Ad}_{g_e}^{-1} \alpha_d + \mathrm{ad}_{\nu_e} \mathrm{Ad}_{g_e}^{-1} \nu_d \\ \dot{\varphi}_d &= T(\varphi_d)\nu_d \\ \dot{\nu}_d &= \alpha_d \end{aligned} \tag{7.41}$$

$$(\varphi_e, \nu_e, u, \varphi_d, \nu_d, \alpha_d) \in \widehat{\mathrm{SE}}(3) \times \mathbb{R}^6 \times \mathbb{R}^m \times \Omega \times c\mathbb{B} \times l\mathbb{B}$$

Finally, we can make the identifications

$$\begin{aligned} \mathcal{X} &= \widehat{\mathrm{SE}}(3) \times \mathbb{R}^6 \times \Omega \times c\mathbb{B}, \\ x &= (\varphi_e, \nu_e, \varphi_d, \nu_d), \\ \mathcal{R} &= l\mathbb{B}, \\ r &= \alpha_d, \\ \mathcal{U} &= \mathbb{R}^m, \end{aligned} \tag{7.42}$$

$$f(x, r, u) = \begin{pmatrix} T(\varphi_e)\nu_e \\ M^{-1}[\mathrm{ad}_\nu^\mathsf{T} M\nu + d(\nu) + \chi(\varphi) + Bu] - \mathrm{Ad}_{g_e}^{-1} r + \mathrm{ad}_{\nu_e} \mathrm{Ad}_{g_e}^{-1} \nu_d \\ T(\varphi_d)\nu_d \\ r \end{pmatrix},$$

which place the error system (7.41) firmly in the scope of the present chapter. In particular, $\mathcal{X} \subset \mathbb{R}^{26}$ is closed because it is a product of closed sets, $\mathcal{R} \subset \mathbb{R}^6$ is a closed ball of radius $l > 0$ and therefore compact, and $\mathcal{U} = \mathbb{R}^m$ is closed and convex. Lastly, since d and χ are assumed continuous, it follows that f is continuous.

7.5.2 Hysteretic Control Design

This section constructs HCLFs for trajectory tracking of an underwater vehicle. The HCLFs are subsequently employed to synthesize an optimization-based hybrid feedback control law.

Let $\mathcal{Q} = \{-1, 1\}$, and define for every $q \in \mathcal{Q}$, $W_{1,q} : \widehat{\mathrm{SE}}(3) \to \mathbb{R}_{\geq 0}$,

$$W_{1,q}(\varphi_e) \coloneqq \frac{1}{2} k_1 |p_e|^2 + 2k_2(1 - q\eta_e), \tag{7.43}$$

where $k_1 > 0$ and $k_2 > 0$ are gains. It is straightforward to show that

$$T(\varphi_e)^\mathsf{T} \nabla W_{1,q}(\varphi_e) = \begin{pmatrix} k_1 \operatorname{rot}(z_e)^\mathsf{T} p_e \\ k_2 q \epsilon_e \end{pmatrix}. \tag{7.44}$$

Differentiating (7.43) along the error kinematics yields

$$\langle \nabla W_{1,q}(\varphi_e), T(\varphi_e)\nu_e \rangle = -\langle K_2 \alpha_q(\varphi_e), \nu_e \rangle. \tag{7.45}$$

where $K_2 = \operatorname{blkdiag}(k_3 I, k_4 I) \in \mathbb{R}^{6\times 6}$ with $k_3 > 0$ and $k_4 > 0$, and $\alpha_q : \widehat{\mathrm{SE}}(3) \to \mathbb{R}^6$ is defined by

$$\alpha_q(\varphi_e) \coloneqq -\begin{pmatrix} \frac{k_1}{k_3} \operatorname{rot}(z_e)^\mathsf{T} p_e \\ \frac{k_2}{k_4} q \epsilon_e \end{pmatrix} = -K_2^{-1} T(\varphi_e)^\mathsf{T} \nabla W_{1,q}(\varphi_e). \tag{7.46}$$

Utilizing the fact that $q^2 = 1$, (7.45) may be rewritten as

$$\langle \nabla W_{1,q}(\varphi_e), T(\varphi_e)\nu_e \rangle = -\langle K_2 \alpha_1(\varphi_e), \alpha_1(\varphi_e) \rangle - \langle \nu_e - \alpha_q(\varphi_e), K_2 \alpha_q(\varphi_e) \rangle. \tag{7.47}$$

We then augment $W_{1,q}$ with a positive definite term in $\nu_e - \alpha_q(\varphi_e)$. In particular, we define $W_q : \widehat{\mathrm{SE}}(3) \times \mathbb{R}^6 \to \mathbb{R}_{\geq 0}$ by

$$W_q(x) = W_{1,q}(\varphi_e) + \frac{1}{2} \langle M(\nu_e - \alpha_q(\varphi_e)), \nu_e - \alpha_q(\varphi_e) \rangle \tag{7.48}$$

which is smooth and proper. Furthermore, it holds that

$$\operatorname{Zero} W_q = \{ x \in \mathcal{X} : p_e = 0, q\eta_e = 1, \nu_e = 0 \}. \tag{7.49}$$

Differentiating W_q along flows yields

$$\begin{aligned} \langle \nabla W_q(x), f(x, r, u) \rangle = &-\langle K_2 \alpha_q(\varphi_e), \alpha_q(\varphi_e) \rangle - \langle \nu_e - \alpha_q(\varphi_e), K_2 \alpha_q(\varphi_e) \rangle \\ &- \langle \nu_e - \alpha_q(\varphi_e), M \dot{\alpha}_q(\varphi_e, \nu_e) \rangle \\ &- \langle \nu_e - \alpha_q(\varphi_e), M \operatorname{Ad}_{g_e}^{-1} r - M \operatorname{ad}_{\nu_e} \operatorname{Ad}_{g_e}^{-1} \nu_d \rangle \\ &+ \langle \nu_e - \alpha_q(\varphi_e), \operatorname{ad}_\nu^\mathsf{T} M\nu + d(\nu) + \chi(\varphi) + Bu \rangle, \end{aligned} \tag{7.50}$$

where we for readability defined $\dot{\alpha}_q(\varphi_e, \nu_e) \coloneqq \mathrm{D}\alpha_q(\varphi_e) T(\varphi_e)\nu_e$.

Note that the set $\mathcal{Q}$ only consists of two elements. Thus, the only possible switching strategy for the logic variable is $q^+ = -q$, and we set in what follows $s = -q$. In order

to derive the sets $\{\mathcal{I}_q\}_{q\in\mathcal{Q}}, \{\mathcal{O}_q\}_{q\in\mathcal{Q}}$, and $\{\mathcal{M}_q\}_{q\in\mathcal{Q}}$ that in turn define the flow and jump sets, we calculate the change in W_q along jumps as

$$\begin{aligned} W_s(x) - W_q(x) = W_{1,s}(\varphi_e) - W_{1,q}(\varphi_e) - \langle M\nu_e, \alpha_s(\varphi_e) - \alpha_q(\varphi_e)\rangle \\ + \frac{1}{2}\langle M\alpha_s(\varphi_e), \alpha_s(\varphi_e)\rangle - \frac{1}{2}\langle M\alpha_q(\varphi_e), \alpha_q(\varphi_e)\rangle. \end{aligned} \tag{7.51}$$

We partition the inertia matrix M in terms of $M_i \in \mathbb{R}^{3\times 3}$, $i \in \{1,2,3\}$, as

$$M = \begin{pmatrix} M_1 & M_2^{\mathsf{T}} \\ M_2 & M_3 \end{pmatrix}. \tag{7.52}$$

Then, straightforward computations give

$$\begin{aligned} W_{1,s}(\varphi_e) - W_{1,q}(\varphi_e) &= 4k_2 q\eta_e, \\ \langle M\nu_e, \alpha_s(\varphi_e) - \alpha_q(\varphi_e)\rangle &= -2q\langle \overline{M}_1\nu_e, \alpha_1(\varphi_e)\rangle, \\ \langle M\alpha_s(\varphi_e), \alpha_s(\varphi_e)\rangle - \langle M\alpha_q(\varphi_e), \alpha_q(\varphi_e)\rangle &= -2q\langle \overline{M}_2\alpha_1(\varphi_e), \alpha_1(\varphi_e)\rangle, \end{aligned} \tag{7.53}$$

where

$$\overline{M}_1 \coloneqq \begin{pmatrix} 0 & 0 \\ M_2 & M_3 \end{pmatrix}, \qquad \overline{M}_2 \coloneqq \begin{pmatrix} 0 & M_2^{\mathsf{T}} \\ M_2 & 0 \end{pmatrix}. \tag{7.54}$$

Let $\Psi(x) : \mathcal{X} \to \mathbb{R}$ be defined by

$$\Psi(x) \coloneqq \eta_e + \frac{1}{2k_2}\langle \overline{M}_1\nu_e, \alpha_1(\varphi_e)\rangle - \frac{1}{4k_2}\langle \overline{M}_2\alpha_1(\varphi_e), \alpha_1(\varphi_1)\rangle, \tag{7.55}$$

such that $W_s(x) - W_q(x) = 4k_2 q\Psi(x)$. Then, we define the sets

$$\begin{aligned} \mathcal{I}_q &\coloneqq \{x \in \mathcal{X} : q\Psi(x) \le 0\}, \\ \mathcal{O}_q &\coloneqq \{x \in \mathcal{X} : q\Psi(x) < \delta\}, \\ \mathcal{M}_q &\coloneqq \{x \in \mathcal{X} : q\Psi(x) \le \delta\}, \end{aligned} \tag{7.56}$$

where $\delta \in (0,1)$ is the hysteresis half-width. We claim that $\{V_q\}_{q\in\mathcal{Q}}$, where every $V_q : \mathcal{M}_q \to \mathbb{R}_{\ge 0}$ is defined by $V_q(x) = W_q(x)$, is an HCLF family for the system (7.41) relative to

$$\mathcal{A} \coloneqq \{x \in \mathcal{X} : p_e = 0, \eta_e = \pm 1, \nu_e = 0\} \tag{7.57}$$

with negativity margins $\{\gamma_q\}_{q\in\mathcal{Q}}$ defined by

$$\gamma_q(x) \coloneqq \varepsilon\langle K_2\alpha_1(\varphi_e), \alpha_1(\varphi_e)\rangle + \varepsilon\langle K_3(\nu_e - \alpha_q(\varphi_e)), \nu_e - \alpha_q(\varphi_e)\rangle, \tag{7.58}$$

where $K_3 \in \mathbb{R}^{6\times 6}$ is positive definite and $\varepsilon \in (0,1)$. Indeed, it follows from the definition of Ψ that the sets defined by (7.56) satisfy (H1) in Definition 7.2. Since every V_q is a restriction of the corresponding W_q to $\mathcal{M}_q$, condition (H2) in Definition 7.2 is also seen to hold. Furthermore, (H3) holds (strictly) by construction of the sets (7.56) since $V_s(x) - V_q(x) \le -4k_2\delta$ for every $x \in (\mathcal{M}_q \backslash \mathcal{O}_q) \cap \mathcal{I}_s$ and every $q \in \mathcal{Q}$. From

(7.50), it is straightforward to verify that (H4) holds, since the family of control laws $\{\mu_q\}_{q\in\mathcal{Q}}$, where every $\mu_q : C_q \to \mathbb{R}^m$ is defined by

$$\begin{aligned}\mu_q(x,r) \coloneqq B^\dagger[M\dot{\alpha}_q(\varphi_e,\nu_e) + M\,\mathrm{Ad}_{g_e}^{-1} r - M\,\mathrm{ad}_{\nu_e}\,\mathrm{Ad}_{g_e}^{-1}\nu_d - \mathrm{ad}_\nu^\mathsf{T} M\nu] \\ + B^\dagger[-\chi(\varphi) - d(\nu) + K_2\alpha_q(\varphi_e) - K_3(\nu - \alpha_q(\varphi_e))],\end{aligned} \tag{7.59}$$

and $B^\dagger \in \mathbb{R}^{m\times 6}$ is the Moore-Penrose inverse of B, results in

$$\langle \nabla V_q(x), f(x,r,\mu_q(x,r))\rangle + \gamma_q(x) \leq -\frac{1-\varepsilon}{\varepsilon}\gamma_q(x) \tag{7.60}$$

which is strictly negative for all $(x,r) \in (\mathcal{M}_q \setminus \mathcal{A}) \times \mathcal{R}$ and every $q \in \mathcal{Q}$.

In order to use Theorem 7.8 to synthesize an optimization-based hybrid control law, we first define the mapping $\vartheta : \mathcal{X} \times \mathcal{R} \to \mathbb{R}^m$ by

$$\vartheta(x,r) = B^\dagger[Mr - \mathrm{ad}_{\nu_d}^\mathsf{T} M\nu_d - d(\nu_d) - \chi(\varphi_d)]. \tag{7.61}$$

We then claim that property (C2) in Theorem 7.7 holds if, for every $q \in \mathcal{Q}$, $\theta_q(x,r) \coloneqq \vartheta(x,r)$. Indeed, the feasible family of control laws defined by (7.59) satisfies $\mu_q(x,r) = \vartheta(x,r)$ for all $(x,r) \in \mathcal{B}_q$ and every $q \in \mathcal{Q}$ such that inner semicontinuity of $\mathcal{K}_q$ relative to C_q follows from Lemma 7.3. Hence, by defining the family of objective functions $\{h_q\}_{q\in\mathcal{Q}}$, $h_q : C_q \times \mathbb{R}^m \to \mathbb{R}$, by

$$h_q(x,r,u) \coloneqq |u - \vartheta(x,r)|, \tag{7.62}$$

all of the conditions in Theorem 7.8 are satisfied. It follows that a family of feasible control laws $\{\kappa_q\}_{q\in\mathcal{Q}}$ can be obtained by solving the quadratic program

$$\begin{cases} \kappa_q(x,r) = \underset{u\in\mathbb{R}^m}{\arg\min}\ \langle u,u\rangle - 2\langle u, \vartheta(x,r)\rangle \\ \text{subject to} \\ \langle a_q(x,r), u\rangle \leq b_q(x,r) \end{cases} \tag{7.63}$$

where

$$a_q(x,r) \coloneqq B^\mathsf{T}(\nu - \alpha_q(x,r)) \tag{7.64}$$

$$\begin{aligned} b_q(x,r) \coloneqq\ & \langle \nu_e - \alpha_q(\varphi_e), M\dot{\alpha}_q(\varphi_e,\nu_e) + M\,\mathrm{Ad}_{g_e}^{-1} r - M\,\mathrm{ad}_{\nu_e}\,\mathrm{Ad}_{g_e}^{-1}\nu_d\rangle \\ & - \langle \nu_e - \alpha_q(\varphi_e), \mathrm{ad}_\nu^\mathsf{T} M\nu + d(\nu) + \chi(\varphi) - K_2\alpha_q(\varphi_e)\rangle \\ & + (1-\varepsilon)\langle K_2\alpha_q(\varphi_e), \alpha_q(\varphi_e)\rangle - \varepsilon\langle K_3(\nu_e - \alpha_q(\varphi_e)), \nu_e - \alpha_q(\varphi_e)\rangle. \end{aligned}$$

7.5.3 Simulation Case Study

In this section, we verify the theoretical results in simulation for the underwater vehicle ODIN, we refer to [45] for the model parameters. The system is initialized at the configuration $\varphi_0 = (0, z_0)$, where $z_0 = (\eta_0, \epsilon_0)$, $\eta_0 = 0$, and $\epsilon_0 = \frac{1}{\sqrt{50}}(3,4,5)$, and at the initial velocity $\nu_0 = (0, 1.2\epsilon_0)$. The desired position and orientation is obtained from the exogenous system in (7.37), initialized at $\varphi_{d,0} = (0, z_I)$ and $\nu_{d,0} = 0$. The desired acceleration r is generated from the low-pass filter

$$T_e\dot{r} + r = \xi(t), \tag{7.65}$$

with time constant $T_e \coloneqq 15\,\mathrm{s}$ and the reference acceleration

$$\xi(t) \coloneqq \begin{cases} (0.1, 0.06, -0.07, 0, 0, 0), & 0 \leq t < 5 \\ 0_{6\times 1}, & 5 \leq t < 10 \\ (0_{3\times 1}, 0.05, -0.1, 0.02) & 10 \leq t < 15 \\ (0_{4\times 1}, -0.1, 0.02) & 15 \leq t. \end{cases} \tag{7.66}$$

The control gains are chosen as $k_1 = k_2 = k_3 = k_4 = 1$ and $K = \frac{1}{2}I$. The system is simulated with Simulink, using the o1e15 solver with a maximum step-size of 0.01. Simulation results are presented in Figures 7.2 to 7.4. Observe that the only jump occurs at $t = 0$, which is due to the initial angular velocity. Moreover, note that the control input is continuous for all $t > 0$. To emphasize the necessity of the small control property for continuity of the resulting control laws, Figure 7.5 depicts the control inputs for the same control scenario with objective functions $\overline{h}_q(x, r, u) \coloneqq |u|^2$. It is easily seen that

$$\arg\min_{u\in\mathbb{R}^m} \overline{h}_q(x, r, u) = 0, \tag{7.67}$$

such that (O2) in Theorem 7.8 is not satisfied. From Figure 7.5, it is apparent that the control input exhibits significant chattering when the state is near $\mathcal{A}$ at approximately $t > 20\,\mathrm{s}$.

In order to highlight the benefits of the optimization-based control law obtained from (7.63), Figures 7.6 to 7.8 depict simulation results for the same control scenario using $u = \mu_q(x, r)$ given by (7.59). From Figures 7.2, 7.3, 7.6 and 7.7, it is clear that the optimization-based control law achieves faster convergence to the desired orientation with less control effort.

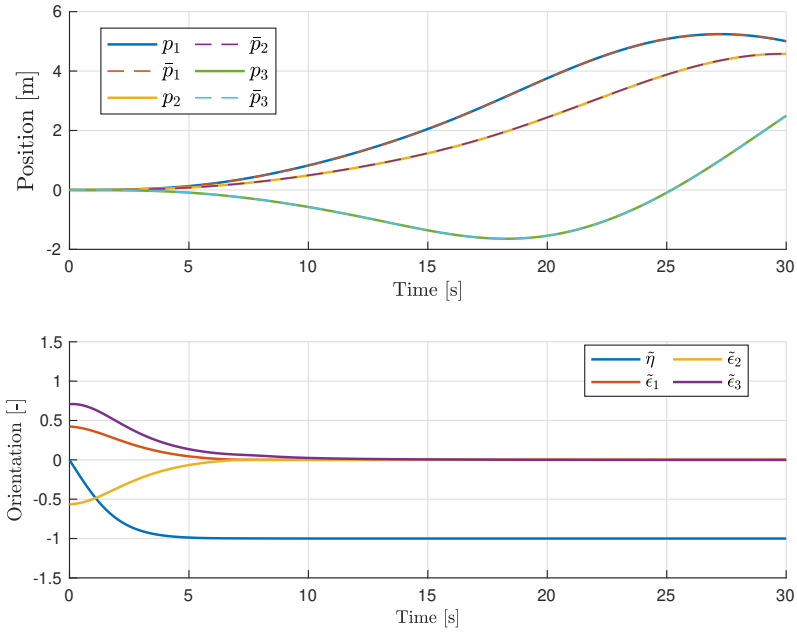

Figure 7.2: The position p, the desired position p_d and the unit quaternion orientation error $z_e = (\eta_e, \epsilon_e)$.

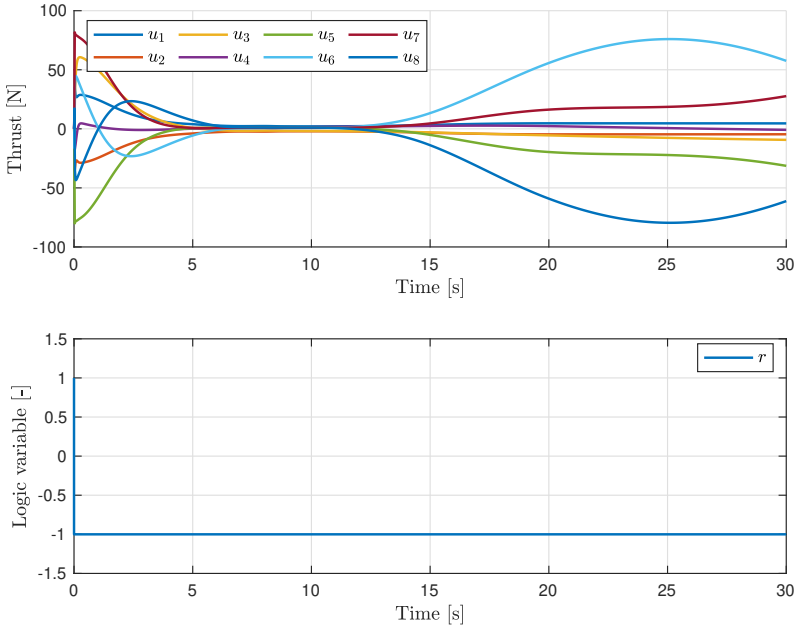

Figure 7.3: The thruster control inputs u, and the logic variable q.

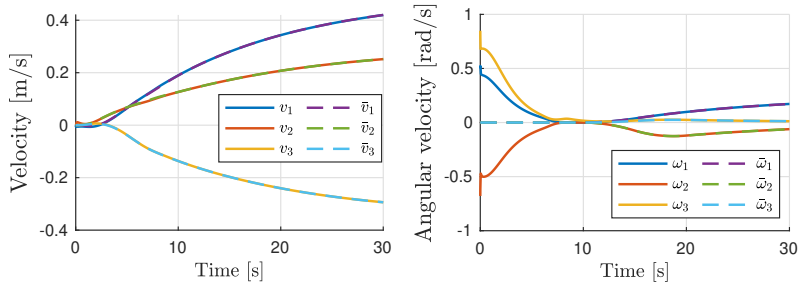

Figure 7.4: The linear and angular velocities v and ω, and their desired values v_d and ω_d, respectively.

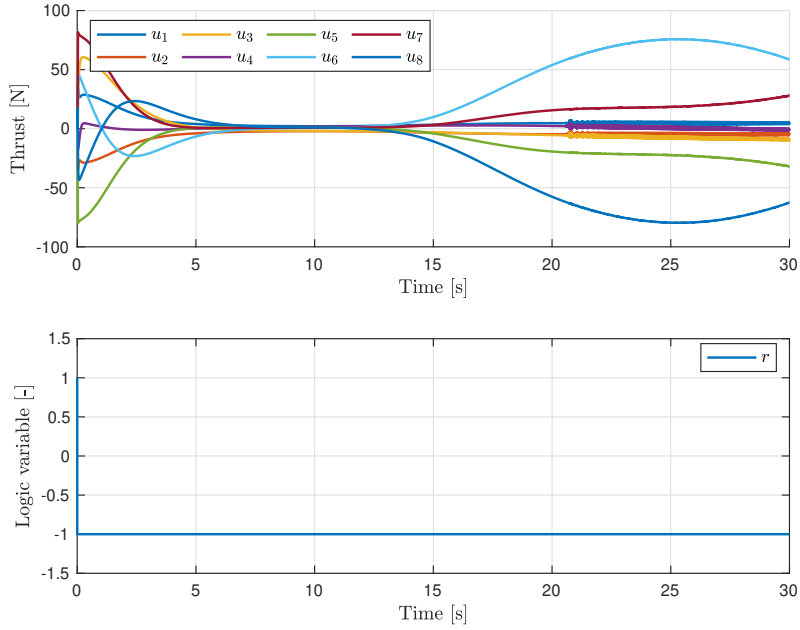

Figure 7.5: The thruster control inputs u with $h_q = |u|^2$ and the logic variable q.

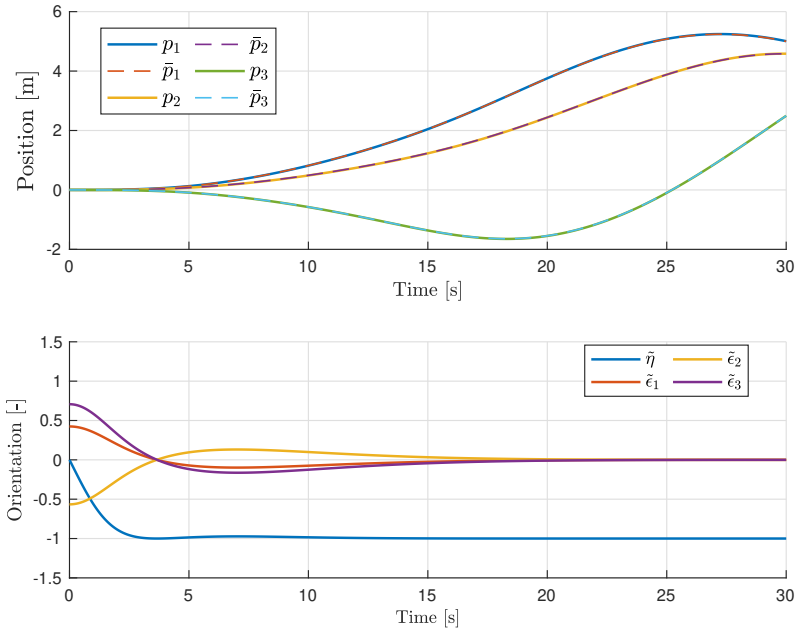

Figure 7.6: The position p, the desired position p_d and the unit quaternion orientation error $z_e = (\eta_e, \epsilon_e)$ using (7.59).

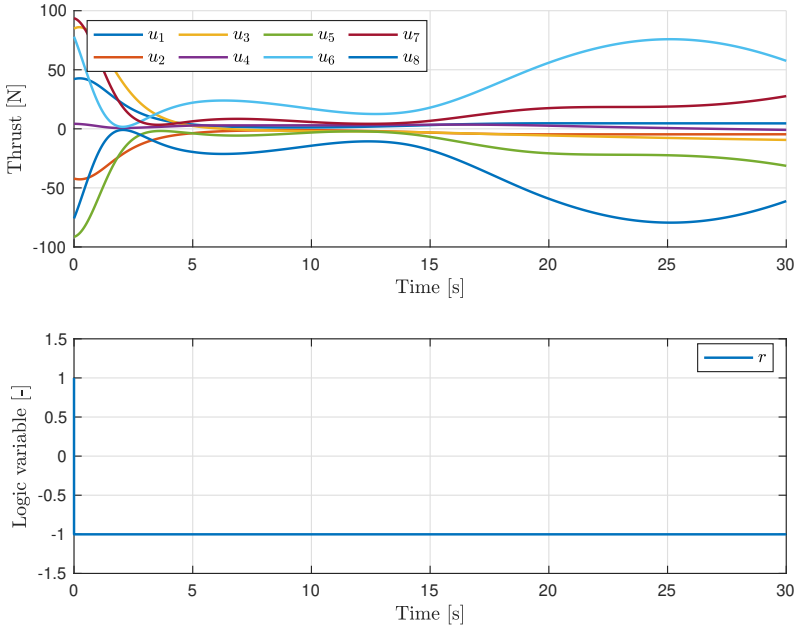

Figure 7.7: The thruster control inputs u, and the logic variable q using (7.59).

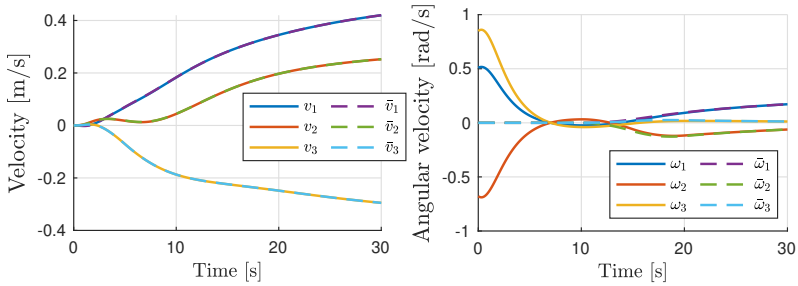

Figure 7.8: The linear and angular velocities v and ω, and their desired values v_d and ω_d, respectively, using (7.59).

Chapter 8

Synergistic Lyapunov Function and Feedback Triples

In this chapter, we extend the SLFF definition from [77]. The proposed generalization allows the logic variable, now referred to as the synergy variable, to be vector-valued and possess flow dynamics. Moreover, since the synergy variable is vector-valued, we define synergy gaps relative to components of product sets. These synergy gaps enable us to define flow and jump sets and jump conditions in the form of synergy gaps for different components of the synergy variable. As a result, we can show that the output feedback control method for rigid-body scheme outlined in [71] is synergistic. The proposed generalization also encompasses the results for SO(3) and SE(3) in [70], in which the scalar logic variable is also allowed to change during flows. However, our proposed framework also includes path-following control scenarios in which the path variable exhibits jump dynamics, such as instantaneously moving the desired state closer to the actual state. As a result, ship maneuvering control as outlined in [84] and [85] can be augmented with discrete path dynamics and combined with a traditional synergistic control approach such as [75] to ensure global asymptotic stability within the proposed framework.

The material in this chapter is based on [93].

8.1 Introduction

Consider a continuous-time system

$$\dot{x} = f(x, u) \quad (x, v) \in X \times \mathbb{R}^k, \tag{8.1}$$

where $x \in X \subset \mathbb{R}^n$ is the state, $v \in \mathbb{R}^k$ is the input and $f : X \times \mathbb{R}^k \to \mathbb{R}^n$ is continuous. The following definition of an SLFF pair is the starting point of this chapter and is a slight modification of [61, Definition 7.3].

Definition 8.1 (Synergistic Lyapunov function and feedback pair)**.** *Given a system* (8.1)*, a compact set* $\mathcal{A} \subset X \times Q$*, a continuously differentiable function* $V : X \times Q \to \mathbb{R}_{\geq 0}$ *and a continuous function* $\kappa : X \to \mathbb{R}^k$ *define*

$$\mu_V(x, q) \coloneqq V(x, q) - \min_{p \in Q} V(x, p). \tag{8.2}$$

The pair (V, κ) is a synergistic Lyapunov function and feedback pair relative to $\mathcal{A}$ with synergy gap exceeding $\rho > 0$ for (8.1) if

1. *V is proper and positive definite with respect to $\mathcal{A}$;*
2. *for all $(x, q) \in X \times Q$, it holds that*

$$\langle \nabla_1 V(x,q), f(x, \kappa(x,q)) \rangle \leq 0; \tag{8.3}$$

3. *$\mu_V(x,q) > \rho$ for each $(x,q) \in \mathcal{I} \setminus \mathcal{A}$, where $\mathcal{I}$ is the largest weakly invariant subset for the system*

$$\begin{aligned} \dot{x} &= f(x, \kappa(x,q)) \\ \dot{q} &= 0 \end{aligned} \qquad (x,q) \in \mathcal{E} \tag{8.4}$$

and

$$\mathcal{E} \coloneqq \{(x,q) \in X \times Q : \langle \nabla_1 V(x,q), f(x, \kappa(x,q)) \rangle = 0\}. \tag{8.5}$$

The remainder of this chapter is organized as follows. In Section 8.2, we extend the definition of SLFF pairs to SLFF triples, for which the synergy variables are allowed to have flow dynamics and be vector-valued. Moreover, we show how the hybrid feedback controller induced by an SLFF triple renders a given compact set globally pre-asymptotically stable. Section 8.3 introduces the notion of synergy gaps relative to components of product sets, which is a distinct feature of vector-valued synergy variables. Then, Section 8.4 introduces a weaker notion of SLFF triples, and we show that if an affine control system admits a weak SLFF triple, then the same system augmented with an integrator at the input admits a (non-weak) SLFF triple. Section 8.5 presents a case study which combines the classical synergistic control approach of [63] using the synergistic Lyapunov functions in [75] with the ship maneuvering control of [84].

8.2 Synergistic Lyapunov Function and Feedback

This section extends the definition of an SLFF pair in Definition 8.1 by augmenting the SLFF definition with a feedback representing the flow dynamics of the synergy variables. Moreover, we show that the hybrid feedback control law induced by an SLFF triple renders a given compact set globally pre-asymptotically stable.

Our goal is to design generalized synergistic controllers with state $\theta \in \Theta \subset \mathbb{R}^m$ of the form

$$\begin{aligned} \dot{\theta} &= \nu(x,\theta) \quad (x,\theta) \in C \\ \theta^+ &\in G(x,\theta) \quad (x,\theta) \in D \\ v &= \kappa(x,\theta) \end{aligned} \tag{8.6}$$

where $C \subset X \times \Theta$, $D \subset X \times \Theta$, $\nu : X \times \Theta \to \mathbb{R}^m$, and $G : X \times \Theta \rightrightarrows \Theta$ are the flow set, jump set, flow map and jump map of the controller, respectively. The controller state θ is also referred to as the synergy variable. We assume the following throughout the chapter.

Assumption 8.2.

1. $X \subset \mathbb{R}^n$ is closed;
2. $f : X \times \mathbb{R}^k \to \mathbb{R}^n$ is continuous;
3. $\Theta \subset \mathbb{R}^m$ is closed.

In the following, we generalize the notion of a synergy gap of a nonnegative and proper function V introduced in [77]. In particular, we evaluate the minimum of V over a set $\Psi \subset \Theta$ which need not be finite (or even compact).

Definition 8.3. *Let $V : X \times \Theta \to \mathbb{R}_{\geq 0}$ be proper, and let $\Psi \subset \Theta$ be closed and nonempty. The synergy gap of V with respect to Ψ is the function $\mu_{V,\Psi} : X \times \Theta \to \mathbb{R}$ defined by*

$$\mu_{V,\Psi}(x,\theta) \coloneqq V(x,\theta) - \min_{\psi \in \Psi} V(x,\psi). \tag{8.7}$$

The set-valued solution mapping associated with $\mu_{V,\Psi}$ is $G_{V,\Psi} : X \times \Theta \rightrightarrows \Theta$, defined as

$$G_{V,\Psi}(x,\theta) \coloneqq \{\psi \in \Psi : \mu_{V,\Psi}(x,\psi) = 0\}. \tag{8.8}$$

The fact that V is nonnegative, continuous, and proper is sufficient for its synergy gap relative to any nonempty and closed set $\Psi \subset \Theta$ to be continuous. Moreover, the associated solution mapping has the key properties it has in traditional synergistic control. Specifically, nonemptiness, outer semicontinuity, and local boundedness. Consequently, even when Ψ is not compact, the set of points where $\theta \mapsto V(x,\theta)$ attains its minimum on Ψ is compact for each $x \in X$.

Proposition 8.4. *The synergy gap $\mu_{V,\Psi}$ is continuous. The associated set-valued solution mapping $G_{V,\Psi}$ is nonempty-valued, outer semicontinuous, and locally bounded.*

Proof. The claims follow from [102, Corollary 7.42]. □

The following definition extends the notion of SLFF pairs from [77]. In addition to utilizing the generalized notion of synergy gap from Definition 8.3, we allow the synergy variable θ to flow.

Definition 8.5. *Let $\mathcal{A} \subset X \times \Theta$ be compact. A continuously differentiable function $V : X \times \Theta \mapsto \mathbb{R}_{\geq 0}$ and continuous functions $\kappa : X \times \Theta \to \mathbb{R}^k$ and $\nu : X \times \Theta \to \mathbb{R}^m$ define a synergistic Lyapunov function and feedback triple (V, κ, ν) relative to $\mathcal{A}$ with synergy gap relative to Ψ exceeding $\rho > 0$ for the system (8.1) if*

1. *V is proper and positive definite with respect to $\mathcal{A}$;*
2. *The closed loop system*

$$\begin{pmatrix} \dot{x} \\ \dot{\theta} \end{pmatrix} = \underbrace{\begin{pmatrix} f(x,\kappa(x,\theta)) \\ \nu(x,\theta) \end{pmatrix}}_{F_c(x,\theta)} \qquad (x,\theta) \in X \times \Theta \tag{8.9}$$

satisfies

$$\langle \nabla V(x,\theta), F_c(x,\theta) \rangle \leq 0, \quad \forall (x,\theta) \in X \times \Theta; \tag{8.10}$$

3. $\mu_{V,\Psi}(x,\theta) > \rho$ *for each* $(x,\theta) \in \mathcal{I} \setminus \mathcal{A}$, *where* $\mathcal{I}$ *is the largest weakly invariant subset for the system*

$$\begin{aligned} \dot{x} &= f(x,\theta,\kappa(x,\theta)) \\ \dot{\theta} &= \nu(x,\theta) \end{aligned} \qquad (x,\theta) \in \mathcal{E} \tag{8.11}$$

and

$$\mathcal{E} \coloneqq \{(x,\theta) \in X \times \Theta : \langle \nabla V(x,\theta), F_c(x,\theta) \rangle = 0\}. \tag{8.12}$$

We remark that if $\nu(x,\theta) = 0$ for all $(x,\theta) \in X \times \Theta$ and $\Theta = \Psi$ is finite, then Definition 8.5 reduces to the definition of an SLFF pair given in [77]. If $\Theta = \mathbb{R}$, and $\Psi \subset \mathbb{R}$ is finite, then Definition 8.5 encompasses the class of potential functions recently introduced in [70].

Analogous to SLFF pairs [77, Theorem 7], the existence of an SLFF triple relative to $\mathcal{A}$ with synergy gap relative to Ψ exceeding $\rho > 0$ guarantees global pre-asymptotic stability of $\mathcal{A}$ for a synergistic closed loop system resulting from (8.1).

Proposition 8.6. *Let* (V,κ,ν) *be an SLFF triple relative to* $\mathcal{A}$ *with synergy gap relative to* Ψ *exceeding* $\rho > 0$. *Then* $\mathcal{A}$ *is globally pre-asymptotically stable for the system*

$$\left.\begin{aligned} \dot{x} &= f(x,\kappa(x,\theta)) \\ \dot{\theta} &= \nu(x,\theta) \end{aligned}\right\} \quad (x,\theta) \in C$$
$$\theta^+ \in G(x,\theta) \qquad (x,\theta) \in D \tag{8.13}$$

where

$$\begin{aligned} C &\coloneqq \{(x,\theta) \in X \times \Theta : \mu_{V,\Psi}(x,\theta) \leq \rho\}, \\ D &\coloneqq \{(x,\theta) \in X \times \Theta : \mu_{V,\Psi}(x,\theta) \geq \rho\}, \\ G(x,\theta) &\coloneqq G_{V,\Psi}(x,\theta). \end{aligned} \tag{8.14}$$

Proof. The sets C and D are closed since $\mu_{V,\Psi}$ is continuous by Proposition 8.4. Moreover, the closed-loop flow map F_c is continuous, and G is nonempty-valued, outer semicontinuous, and locally bounded by Proposition 8.4. Consequently, the system (8.13) satisfies the hybrid basic conditions [90, Assumption 6.5] and is therefore well posed. From the definition of the jump set and jump map in (8.14), V decreases strictly across jumps by at least ρ. Since V is proper and positive definite with respect to $\mathcal{A}$ by 1) of Definition 8.5 and V does not grow along solutions to the system (8.13) by 2) of Definition 8.5 and the nonincrease of V across jumps, it follows that $\mathcal{A}$ is stable and that all solutions are bounded. Since V must vanish in $\mathcal{A}$ by 1) of Definition 8.5, it holds that $\mu_{V,\Psi}$ vanishes in $\mathcal{A}$ as well. Consequently, $\mathcal{A} \subset C$. From 3) of Definition 8.5, it then follows that $\mathcal{I} \cap C \subset \mathcal{A}$. The invariance principle [90, Corollary 8.4] then guarantees that complete solutions converge to $\mathcal{A}$. It follows that $\mathcal{A}$ is globally pre-asymptotically stable. □

Completeness of maximal solutions (and global asymptotic stability of $\mathcal{A}$ for (8.13)) is guaranteed if, in addition to the conditions of Proposition 8.6, it also holds that

$$F_c(x,\theta) \in T_{X\times\Theta}(x,\theta) \tag{8.15}$$

for all (x, θ) such that $\mu_{V,\Psi}(x, \theta) < \rho$, where $T_{X\times\Theta}(x, \theta)$ is the tangent cone to $X \times \Theta$ at (x, θ). Indeed, $T_{X\times\Theta}(x, \theta) = T_C(x, \theta)$ at these points, and the claim follows from [90, Proposition 6.10]. It should also be remarked that $T_{X\times\Theta} \neq T_X \times T_\Theta$ in general. See [102, Chapter 6], and in particular Proposition 6.41, for further results on this matter.

8.3 Synergy Gaps Relative to Components of Product Sets

The control approach covered in Proposition 8.6 updates the whole synergy variable θ when the instantaneous synergy gap is equal to or exceeds the threshold ρ. This approach offers relatively little flexibility in shaping the jump sets. When Θ is a product set, one can formulate the synergy gap and associated solution mapping relative to the components of Θ. For simplicity, it is assumed that Θ comprises two components, although the approach outlined in this section can be further generalized.

Assumption 8.7.

4) $\Theta = \Theta_a \times \Theta_b$, where Θ_a and Θ_b are closed.

We now adapt Definition 8.3 to exploit the additional structure of Θ induced by this assumption.

Definition 8.8. *Let $V : X \times \Theta \to \mathbb{R}_{\geq 0}$ be proper, and let $\Psi = \Psi_a \times \Psi_b$ such that $\Psi_a \subset \Theta_a$ and $\Psi_b \subset \Theta_b$ are nonempty and closed. The synergy gap of V with respect to Ψ_a is defined as*

$$\mu_{V,\Psi_a}(x, \theta) \coloneqq V(x, \theta) - \min_{\psi_a \in \Psi_a} V(x, (\psi_a, \theta_b)). \tag{8.16}$$

The synergy gap of V with respect to Ψ_b is defined as

$$\mu_{V,\Psi_b}(x, \theta) \coloneqq V(x, \theta) - \min_{\psi_b \in \Psi_b} V(x, (\theta_a, \psi_b)). \tag{8.17}$$

The set-valued solution mapping associated with μ_{V,Ψ_a}, $G_{V,\Psi_a} : X \times \Theta \rightrightarrows \Theta$ is

$$G_{V,\Psi_a}(x, \theta) \coloneqq \{\psi_a \in \Psi_a : \mu_{V,\Psi_a}(x, (\psi_a, \theta_b)) = 0\} \times \{\theta_b\}. \tag{8.18}$$

The objects introduced in Definition 8.8 have similar properties as the ones introduced in Definition 8.3.

Proposition 8.9. *The synergy gaps μ_{V,Ψ_a} and μ_{V,Ψ_b} are continuous. The set-valued solution mapping G_{V,Ψ_a} is nonempty-valued, outer semicontinuous, and locally bounded.*

Proof. Apply [102, Corollary 7.42] with (x, θ_b) as parameters and θ_a as optimization variable to show the claims for μ_{V,Ψ_a} and G_{V,Ψ_a}. Continuity of μ_{V,Ψ_b} is shown similarly. □

Consequently, we may specialize the notion of an SLFF triple to the case where Θ is product set.

Definition 8.10. *Let $\mathcal{A} \subset X \times \Theta$ be compact, and (V, κ, ν) satisfy 1) and 2) in Definition 8.5 for the system (8.1). We say that (V, κ, ν) is a synergistic Lyapunov function and feedback triple relative to $\mathcal{A}$ with synergy gap relative to Ψ_a exceeding $\rho_a > 0$ if*

3a) $\mu_{V,\Psi_a}(x, \theta) > \rho_a$ for each $(x, \theta) \in \mathcal{I} \setminus \mathcal{A}$.

We say that (V, κ, ν) is a synergistic Lyapunov function and feedback triple relative to $\mathcal{A}$ with synergy gap relative to (Ψ_a, Ψ_b) exceeding (ρ_a, ρ_b) with $\rho_a, \rho_b > 0$ if

3b) $\mu_{V,\Psi_a}(x, \theta) > \rho_a$ or $\mu_{V,\Psi_b}(x, \theta) > \rho_b$ for each $(x, \theta) \in \mathcal{I} \setminus \mathcal{A}$.

In both cases, $\mathcal{I}$ is defined as in Definition 8.5.

It is clear that if (V, κ, ν) has synergy gap relative to Ψ_a exceeding $\rho_a > 0$, then it has synergy gap relative to Ψ exceeding ρ_a. If instead (V, κ, ν) has a synergy gap relative to to (Ψ_a, Ψ_b) exceeding (ρ_a, ρ_b), with $\rho_a, \rho_b > 0$, then it has a synergy gap relative to Ψ exceeding $\min(\rho_a, \rho_b) > 0$. The last part of item 3b) ensures that (V, κ, ν) is not an SLFF triple relative to $\mathcal{A}$ with synergy gap relative to Ψ_a or Ψ_b, and hence that ρ_a and ρ_b are well-defined.

8.3.1 Optional Jumps

When (V, κ, ν) is an SLFF triple relative to $\mathcal{A}$ with synergy gap relative to Ψ_a exceeding $\rho_a > 0$, it is not necessary to update θ_b to avoid the invariant sets where solutions may get stuck. Jumping θ_b may nonetheless increase the performance of the closed-loop system. We therefore define a closed-loop system in which jumps of θ_b are optional.

Proposition 8.11. *Let (V, κ, ν) be a synergistic Lyapunov function and feedback triple relative to $\mathcal{A}$ with synergy gap relative to Ψ_a exceeding $\rho_a > 0$. Then $\mathcal{A}$ is globally pre-asymptotically stable for the system (8.13) with*

$$
\begin{aligned}
C &:= \{(x, \theta) \in X \times \Theta : \mu_{V,\Psi_a}(x, \theta) \leq \rho_a\}, \\
D &:= \{(x, \theta) \in X \times \Theta : \mu_{V,\Psi_a}(x, \theta) \geq \rho_a \text{ or } \mu_{V,\Psi}(x, \theta) \geq \rho\} \\
G(x, \theta) &:= \begin{cases}
G_{V,\Psi_a}(x, \theta), & \mu_{V,\Psi_a}(x, \theta) \geq \rho_a \text{ and } \mu_{V,\Psi}(x, \theta) < \rho, \\
(G_{V,\Psi_a} \cup G_{V,\Psi})(x, \theta), & \mu_{V,\Psi_a}(x, \theta) \geq \rho_a \text{ and } \mu_{V,\Psi}(x, \theta) \geq \rho, \\
G_{V,\Psi}(x, \theta), & \mu_{V,\Psi_a}(x, \theta) < \rho_a \text{ and } \mu_{V,\Psi}(x, \theta) \geq \rho, \\
\emptyset & \text{otherwise,}
\end{cases}
\end{aligned} \tag{8.19}
$$

where $\rho \geq \rho_a$.

Proof. It is clear that C and the sets

$$D_{\Psi_a} := \{(x, \theta) \in X \times \Theta : \mu_{V,\Psi_a}(x, \theta) \geq \rho_a\} \tag{8.20}$$

$$D_{\Psi} := \{(x, \theta) \in X \times \Theta : \mu_{V,\Psi}(x, \theta) \geq \rho\} \tag{8.21}$$

are closed since μ_{V,Ψ_a} and $\mu_{V,\Psi}$ are continuous. Therefore, $D = D_{\Psi_a} \cup D_{\Psi}$ is closed. The closed-loop flow map is continuous on $X \times \Theta$. We know that G_{V,Ψ_a} and $G_{V,\Psi}$ are nonempty-valued, outer semicontinuous, and locally bounded. Denote then by $\widetilde{G}_{V,\Psi_a}$ and $\widetilde{G}_{V,\Psi}$ the restrictions of G_{V,Ψ_a} and $G_{V,\Psi}$ to D_{Ψ_a} and D_{Ψ}, respectively. These

restrictions are also outer semicontinuous and locally bounded. Now, G is defined such that $\operatorname{gph} G = \operatorname{gph} \widetilde{G}_{V,\Psi_a} \cup \operatorname{gph} \widetilde{G}_{V,\Psi}$. Thus, G is nonempty-valued on D. Since outer semicontinuity of a set-valued mapping is equivalent to its graph being closed, it also follows that G is outer semicontinuous. Moreover, the union of two locally bounded set-valued mappings is locally bounded. Consequently, G is locally bounded. Hence, the closed loop system (8.13) with data defined by (8.19) satisfies the hybrid basic conditions. The remainder of the proof proceeds as the proof of Proposition 8.6, with the strict decrease of V across jumps now being at least ρ_a. □

Completeness of maximal solutions to the closed-loop system with data (8.19) is guaranteed if the tangent cone condition (8.15) holds for all (x, θ) such that $\mu_{V,\Psi_a}(x, \theta) < \rho_a$. In this case, the system always admits complete solutions over the course of which θ_b does not jump.

8.3.2 Independently Triggered Jumps

The following proposition introduces the concept of independentely triggered jumps, where both components of θ jump when either of their jump conditions are met.

Proposition 8.12. *Let (V, κ, ν) be a synergistic Lyapunov function and feedback triple relative to $\mathcal{A}$ with synergy gap relative to (Ψ_a, Ψ_b) exceeding (ρ_a, ρ_b), with $\rho_a, \rho_b > 0$. Then $\mathcal{A}$ is globally pre-asymptotically stable for the system (8.13) with*

$$\begin{aligned} C &:= \{(x,\theta) \in X \times \Theta : \mu_{V,\Psi_a}(x,\theta) \leq \rho_a \text{ and } \mu_{V,\Psi_b}(x,\theta) \leq \rho_b\}, \\ D &:= \{(x,\theta) \in X \times \Theta : \mu_{V,\Psi_a}(x,\theta) \geq \rho_a \text{ or } \mu_{V,\Psi_b}(x,\theta) \geq \rho_b\}, \\ G(x,\theta) &:= G_{V,\Psi}(x,\theta). \end{aligned} \tag{8.22}$$

The proof of Proposition 8.12 is very similar to the proofs of Proposition 8.6 and Proposition 8.11 and is therefore omitted. An example where independently triggered switching is used is furnished by the quaternion output feedback control scheme for rigid-body orientation in [71, Section V-B]. In this work, θ_a corresponds to a traditional synergy variable for a feedback controller, and θ_b corresponds to a traditional synergy variable for an observer, while $\nu(x, \theta) = 0$ for all $(x, \theta) \in X \times \Theta$.

8.4 Backstepping

This section begins by introducing a weaker notion of SLFF triples for affine control systems. Then, given a system that admits a weak SLFF triple, we construct a (non-weak) SLFF triple for the same system augmented with an integrator at the input.

By assuming that (8.1) is affine in the control input v, we obtain the system

$$\dot{x} = f_0(x) + g_0(x)v \quad (x, v) \in X \times \mathbb{R}^k \tag{8.23}$$

Definition 8.13. *Let $\mathcal{A} \subset X \times \Theta$ be compact. A continuously differentiable function $V : X \times \Theta \mapsto \mathbb{R}_{\geq 0}$ and continuous functions $\kappa : X \times \Theta \to \mathbb{R}^k$ and $\nu : X \times \Theta \to \mathbb{R}^m$ define a weak synergistic Lyapunov function and feedback triple (V, κ, ν) relative to $\mathcal{A}$ with a weak synergy gap relative to Ψ exceeding $\rho > 0$ for (8.23) if*

1. *V is proper and positive definite with respect to $\mathcal{A}$;*

2. *The closed loop system*

$$\begin{pmatrix}\dot{x}\\ \dot{\theta}\end{pmatrix} = \underbrace{\begin{pmatrix} f_0(x) + g_0(x)\kappa(x,\theta) \\ \nu(x,\theta)\end{pmatrix}}_{F_0(x,\theta)} \qquad (x,\theta) \in X \times \Theta \tag{8.24}$$

satisfies

$$\langle \nabla V(x,\theta), F_0(x,\theta)\rangle \leq 0, \quad \forall (x,\theta) \in X \times \Theta; \tag{8.25}$$

3. $\mu_{V,\Psi}(x,\theta) > \rho$ *for each* $(x,\theta) \in \mathcal{I} \setminus \mathcal{A}$, *where* $\mathcal{I}$ *is the largest weakly invariant subset for the system*

$$\left.\begin{aligned}\dot{x} &= f_0(x) + g_0(x)\kappa(x,\theta)\\ \dot{\theta} &= \nu(x,\theta)\end{aligned}\right\} (x,\theta) \in \mathcal{E} \cap \mathcal{W} \tag{8.26}$$

where $\mathcal{E}$ *is given in Definition 8.5, and*

$$\mathcal{W} \coloneqq \{(x,q) \in X \times \Theta : g_0(x)^{\mathsf{T}} \nabla_1 V(x,\theta) = 0\}. \tag{8.27}$$

Augmenting the system (8.23) with an integrator at the input results in the control system

$$\dot{z} = f_1(z) + g_1(z)u \quad (z,u) \in Z \times \mathbb{R}^k \tag{8.28}$$

where $z = (x,v) \in Z \coloneqq X \times \mathbb{R}^k$, $u \in \mathbb{R}^k$ is the control input and

$$f_1(z) = \begin{pmatrix} f_0(x) + g_0(x)v \\ 0\end{pmatrix}, g_1(z) = \begin{pmatrix}0\\ I\end{pmatrix}. \tag{8.29}$$

Now, let (V_0, κ_0, ν_0) be a weak SLFF triple relative to the compact set $\mathcal{A}_0 \subset X \times \Theta$, define the set

$$\mathcal{A}_1 = \{(z,\theta) \in Z \times \Theta : (x,\theta) \in \mathcal{A}_0, v = \kappa(x,\theta)\}, \tag{8.30}$$

and consider the following SLFF triple

$$V_1(z,\theta) = V_0(x,\theta) + \frac{1}{2}|v - \kappa_0(x,\theta)|^2_\Gamma, \tag{8.31a}$$

$$\begin{aligned}\kappa_1(z,\theta) = {} & \nabla_1\kappa_0(x,\theta)\left(f_0(x) + g_0(x)v\right)\\ & + \nabla_2\kappa_0(x,\theta)\nu_0(x,\theta) - \gamma_1(v - \kappa_0(x,\theta))\\ & - \Gamma^{-1}g_0(x)^{\mathsf{T}}\nabla_1 V_0(x,\theta),\end{aligned} \tag{8.31b}$$

$$\nu_1(z,\theta) = \nu_0(x,\theta) - \vartheta_1(\nabla_2 V_1(z,\theta)), \tag{8.31c}$$

where $\Gamma \in \mathbb{R}^{k\times k}$ is positive definite, $\gamma_1 : \mathbb{R}^k \to \mathbb{R}^k$ is continuous and satisfies $\langle \gamma_1(v), v\rangle > 0$ for every $v \in \mathbb{R}^k \setminus \{0\}$, and $\vartheta_1 : \mathbb{R}^m \to \mathbb{R}^m$ is continuous and satisfies $\langle \vartheta_1(\nu), \nu\rangle \geq 0$ for every $\nu \in \mathbb{R}^m$. The following proposition establishes that (V_1, κ_1, ν_1) is an SLFF triple for the system (8.28) with synergy gap exceeding $\rho > 0$ relative to Ψ.

Proposition 8.14. *If (V_0, κ_0, ν_0) is a weak synergistic Lyapunov function and feedback triple for the system (8.23) relative to $\mathcal{A}_0$, with a weak synergy gap relative to Ψ exceeding $\rho > 0$, then (V_1, κ_1, ν_1) is a (non-weak) synergistic Lyapunov function and feedback triple for the system (8.28) relative to $\mathcal{A}_1$ with a (non-weak) synergy gap relative to Ψ exceeding $\rho > 0$.*

Proof. The derivative of V_1 along the solutions of (8.23) is

$$\begin{aligned}
\dot{V}_1 &= \langle \nabla_1 V_1(z,\theta), f_1(z) + g_1(z)\kappa_1(z,\theta)\rangle \\
&\quad + \langle \nabla_2 V_1(z,\theta), \nu_1(z,\theta)\rangle \\
&= \langle \nabla_1 V_0(x,\theta), f_0(x) + g_0(x)\kappa_0(x,\theta)\rangle \\
&\quad - \langle v - \kappa_0(x,\theta), \Gamma\gamma_1(v - \kappa_0(x,\theta)\rangle \\
&\quad - \langle v - \kappa_0(x,\theta), \Gamma\nabla_2\kappa_0(x,\theta)(\nu_1(z,\theta) - \nu_0(x,\theta))\rangle \\
&\quad + \langle \nabla_2 V_0(x,\theta), \nu_1(z,\theta)\rangle \\
&= \langle \nabla_1 V_0(x,\theta), f_0(x) + g_0(x)\kappa_0(x,\theta)\rangle \\
&\quad - \langle v - \kappa_0(x,\theta), \Gamma\gamma_1(v - \kappa_0(x,\theta)\rangle \\
&\quad + \langle \nabla_2 V_0(x,\theta), \nu_0(x,\theta)\rangle \\
&\quad - \langle \nabla_2 V_1(z,\theta), \vartheta_1(\nabla_2 V_1(z,\theta))\rangle \\
&\leq 0.
\end{aligned} \tag{8.32}$$

Define $\mathcal{E}_0, \mathcal{W}_0$ and $\mathcal{E}_1, \mathcal{W}_1$ according to (8.12) and (8.27) for the systems (8.23) and (8.28), respectively. It follows from (8.32) that

$$\begin{aligned}
\mathcal{E}_1 &= \{(z,\theta) \in X \times \Theta : (x,\theta) \in \mathcal{E}_0, v = \kappa_0(x,\theta), \vartheta_1(\nabla_2 V_1(z,\theta)) = 0\} \\
&\subset \mathcal{W}_1.
\end{aligned} \tag{8.33}$$

Let $\mathcal{I}_1 \subset \mathcal{E}_1$ denote the largest weakly invariant subset for the system

$$\left.\begin{aligned}
\dot{z} &= f_1(z) + g_1(z)\kappa_1(z,\theta) \\
\dot{\theta} &= \nu_1(z,\theta)
\end{aligned}\right\} (z,\theta) \in \mathcal{E}_1 \tag{8.34}$$

It follows that

$$\mathcal{I}_1 = \big\{(z,\theta) \in Z \times \Theta : (x,\theta) \in \Omega_0, v = \kappa_0(x,\theta), \vartheta_1(\nabla_2 V_1(z,\theta)) = 0\big\}. \tag{8.35}$$

From Definition 8.3 and 3) in Definition 8.13 it holds that

$$\begin{aligned}
\mu_{V_1,\Psi} &\geq \mu_{V_0,\Psi}(x,\theta) + \frac{1}{2}|v - \kappa_0(x,\theta)|_\Gamma^2 \\
&\quad - \min_{\psi\in\Psi} \frac{1}{2}|v - \kappa_0(x,\psi)|_\Gamma^2 \\
&\geq \mu_{V_0,\Psi}(x,\theta) && (8.36) \\
&> \rho. && (8.37)
\end{aligned}$$

Consequently, (V_1, κ_1, ν_1) is an SLFF triple with synergy gap relative to Ψ exceeding $\rho > 0$. □

8.5 Synergistic Maneuvering for Ships

In this section, the proposed theory is exemplified by combining the traditional synergistic control approach of [63], [75] with the ship maneuvering control of [84], [85], where we augment the path variable with jump dynamics. The configuration space of a ship can be reasonably described by $\mathrm{SE}(2) = \mathbb{R}^2 \rtimes \mathrm{SO}(2)$. Configurations of the ship are then represented as $x = (p, R)$, where $p \in \mathbb{R}^2$ represents the ship position and $R \in \mathrm{SO}(2)$ represents the ship heading.

The desired position of the ship is described in terms of a sufficiently smooth planar path.

Definition 8.15. *A planar C^r-path is a C^r-mapping $\eta : [0,1] \to \mathbb{R}^2$. If $r \geq 1$, we say that a planar C^r-path is regular if $\eta'(s) \neq 0$ for all $s \in [0,1]$.*

Given a regular C^3-path η in $\mathbb{R}^2$, we synthesize a C^2-path in $\mathrm{SE}(2)$ by requiring that the heading of the ship is tangential to the path. Such a path has the form $s \mapsto (p_d(s), R_d(s))$, where

$$\begin{aligned} p_d(s) &\coloneqq \eta(s) \\ R_d(s) &\coloneqq \frac{1}{|\eta'(s)|} \begin{pmatrix} \eta'(s) & S\eta'(s) \end{pmatrix}. \end{aligned} \tag{8.38}$$

A desired speed assignment for $\dot{s}$ along the path, $u_d : [0,1] \to \mathbb{R}$, is chosen as

$$u_d(s) \coloneqq \frac{U_d(s)}{|p_d'(s)|}, \tag{8.39}$$

where $U_d : [0,1] \to \mathbb{R}$ is a continuously differentiable signed desired ship speed along the path. In particular, u_d is defined such that if $\dot{s} = u_d(s)$, then $\dot{p}_d(s) = \frac{p_d'(s)}{|p_d'(s)|} U_d(s)$. A two times continuously differentiable path in the configuration space $x_d : [0,1] \to \mathrm{SE}(2)$ can now be defined as $x_d(s) \coloneqq (p_d(s), R_d(s))$. We define the desired tangent $\tau_d : [0,1] \to \mathbb{R}^3$ such that $\widehat{\tau}_d = x_d(s)^{-1} x_d'(s)$ for all $s \in [0,1]$.

We denote by $v = (\zeta, \omega) \in \mathbb{R}^3$ the velocity of the ship, where $\zeta \in \mathbb{R}^2$ is its linear velocity and $\omega \in \mathbb{R}$ is its angular velocity. A model for the ship kinematics and dynamics is [24, Chapter 6.5]

$$\left.\begin{aligned} \dot{x} &= x\widehat{v} \\ \dot{v} &= -\gamma(v) + M^{-1}(d(v) + u) \end{aligned}\right\} (x, v, u) \in \mathrm{SE}(2) \times \mathbb{R}^3 \times \mathbb{R}^3, \tag{8.40}$$

where $M = M^{\mathsf{T}} > 0$ is the ship inertia tensor (including hydrodynamic inertia), $\gamma : \mathbb{R}^3 \to \mathbb{R}^3$ describes the Coriolis and centripetal accelerations associated with M, $d : \mathbb{R}^3 \to \mathbb{R}^3$ describes the hydrodynamic drag forces acting on the ship, and u are idealized input forces produced by the actuators.

The general ship maneuvering problem is then split into a geometric task that represents convergence to this path, and a dynamic task that represents the attainment of the speed assignment u_d on this path.

Problem Statement (Maneuvering Problem [85])**.**

- **Geometric Task:** Force the position and heading of the ship to converge to the desired path,

$$\lim_{(t+j)\to\infty} \|x_d(s(t,j))^{-1}x(t,j) - I\| = 0. \tag{8.41}$$

- **Dynamic Task:** Force the path speed to converge to the desired speed assignment:

$$\lim_{(t+j)\to\infty} |\dot{s}(t,j) - u_d(s(t,j))| = 0. \tag{8.42}$$

8.5.1 Backstepping Controller

We set $X = \mathrm{SE}(2)$ and $\Theta = \Theta_a \times \Theta_b$, where $\Theta_a = \{-1, 1\}$, $\Theta_b = [0, 1]$ and $\theta = (\theta_a, \theta_b) = (q, s)$. In particular, q is a classical synergistic logic variable and s is a path variable utilized in the ship maneuvering control problem. Then, the kinematics of the ship and the flow of q and s may be cast as a system of the form (8.23),

$$\dot{x} = x\widehat{v} \quad (x, v) \in \mathrm{SE}(2) \times \mathbb{R}^3. \tag{8.43}$$

The set $\mathcal{A}_0 \subset X \times \Theta$ is now chosen as

$$\mathcal{A}_0 = \{(x, \theta) \in X \times \Theta : x = x_d(s)\}. \tag{8.44}$$

Compactness of $\mathcal{A}_0$ holds because the mapping $(q, s) \mapsto x_d(s)$ is continuous and Θ is compact.

We now introduce a synergistic potential function which is similar to [75] for the heading control of the ship. In particular, let $P : \mathrm{SO}(2) \times [0, 1] \to \mathbb{R}$ and, with $\rho_a > 0$, the mapping $T : \mathrm{SO}(2) \times \Theta \to \mathrm{SO}(2)$

$$P(R, s) \coloneqq (1 - \langle e_1, R_d(s)^\mathsf{T} R e_1 \rangle), \tag{8.45}$$

$$T(R, \theta) \coloneqq \exp(\rho_a q P(R, s) S) R_d(s)^\mathsf{T} R. \tag{8.46}$$

Let $k_0 > 0$ and let $K_0 = K_0^\mathsf{T}$ be a positive definite matrix. Then, (V_0, κ_0, ν_0) defined as

$$V_0(x, \theta) = \frac{1}{2}|R_d^\mathsf{T}(p - p_d(s))|^2_{K_0} + k_0 P(T(R, \theta), s) \tag{8.47a}$$

$$\kappa_0(x, \theta) = \mathrm{Ad}^{-1}_{x_d(s)^{-1}x}\, \tau_d(s) u_d(s) - K\, \mathrm{d}_1 V_0(x, \theta) \tag{8.47b}$$

$$\nu_0(x, \theta) = \begin{pmatrix} 0 \\ u_d(s) \end{pmatrix}, \tag{8.47c}$$

where $K = K^\mathsf{T}$ is a positive definite matrix, is an SLFF triple for (8.43) with synergy gap relative to $\{-1, 1\}$ exceeding $\frac{1}{2}$.

We now augment (8.43) with the ship dynamics

$$\left.\begin{aligned} \dot{x} &= x\widehat{v} \\ \dot{v} &= -\gamma(v) + M^{-1}(d(v) + u) \end{aligned}\right\} (z, u) \in (\mathrm{SE}(2) \times \mathbb{R}^3) \times \mathbb{R}^3, \tag{8.48}$$

and define

$$\mathcal{A}_1 = \{(x, v, \theta) : (x, \theta) \in \mathcal{A}_0, v = \kappa_0(x, \theta)\}. \tag{8.49}$$

It then follows directly from Proposition 8.14 that

$$V_1(z, \theta) = V_0(x, \theta) + \frac{1}{2}|v - \kappa_0(x, \theta)|_M^2, \tag{8.50a}$$

$$\begin{aligned}\kappa_1(z, \theta) = {} & M\,\mathrm{d}_1\kappa_0(x, \theta)v + M\nabla_2\kappa_0(x, \theta)\nu_0(x, \theta) \\ & + M\gamma(v) - d(v) \\ & - \gamma_1(v - \kappa_0(x, \theta)) \\ & - \mathrm{d}_1 V_0(x, \theta),\end{aligned} \tag{8.50b}$$

$$\nu_1(z, \theta) = \nu_0(x, \theta), \tag{8.50c}$$

is an SLFF triple for the system (8.48) relative to $\mathcal{A}_1$ with synergy gap relative to $\{-1, 1\}$ exceeding $\frac{1}{2}$. Consequently, the synergistic controller

$$\dot{\theta} = \nu_1(z, \theta) \qquad (z, \theta) \in C, \tag{8.51}$$

$$\theta^+ \in G(z, \theta) \qquad (z, \theta) \in D, \tag{8.52}$$

$$u = \kappa_1(z, \theta), \tag{8.53}$$

where (C, D, G) are given by (8.19), renders $\mathcal{A}_1$ globally pre-asymptotically stable for the resulting closed-loop system by Proposition 8.11. Moreover, if $u_d(s) \in T_{\Theta_b}(s)$ for all $s \in \Theta_b$, then all maximal solutions are complete and $\mathcal{A}_1$ is globally asymptotically stable for the resulting closed-loop system, which implies that the problem statement is solved.

8.5.2 Simulations

Simulation results are presented in Figures 8.1 to 8.5. The model parameters can be found in [86]. In the simulations, we have chosen $\delta = 0.1$, $\rho_a = \delta k_0$, $\rho = 1.2\rho_a$, $k_0 = 5$, $K_0 = 5I_2$, $K = 0.05I_3$ and $\gamma_1 = \mathrm{diag}(10, 10, 7)$. The chosen path is given by $p_d(s) \coloneqq 5(\cos(\pi s), \sin(\pi s))$. The ship is initialized at $p = (5, 2)$ with an initial heading of $\psi = -85°$, an initial velocity of $v = 0$ and a desired speed of $U_d = 0.3\,\mathrm{m/s}$.

From Figure 8.1 we observe that the position references are successfully tracked after an initial transient phase. An optional jump is immediately triggered such that q is mapped to -1 and s is mapped to approximately 0.08. An optional jump is triggered around $t \approx 2\,\mathrm{s}$ as seen in Figure 8.1. The error in the x-direction is slightly decreased while the error in the y-direction is slightly increased. Moreover, from Figure 8.2 we note that the difference between ζ_1 and $\kappa_{0,1}$ decreases over the jump in s. In Figure 8.4, we observe that s is decreased over the jump, while q remains the same. Moreover, from Figure 8.5, we observe a discontinuity in u_2 at the time of the jump.

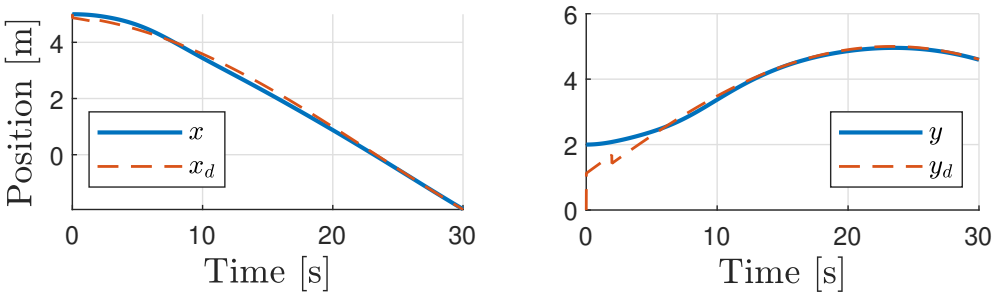

Figure 8.1: The position $p = (x, y)$ and desired position $p_d = (x_d, y_d)$.

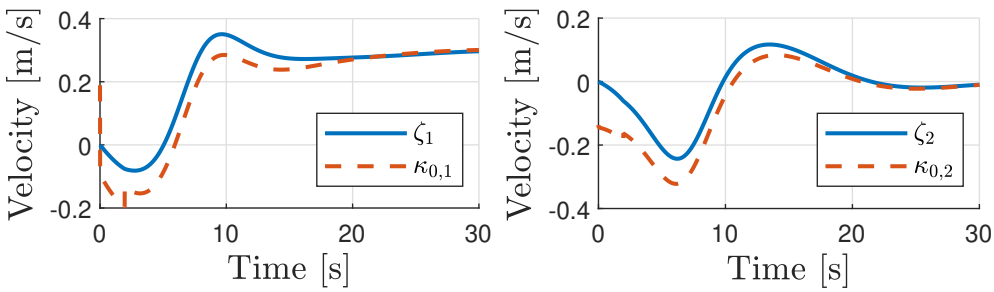

Figure 8.2: The body linear velocity ζ_1 and ζ_2 and the first and second component of κ_0.

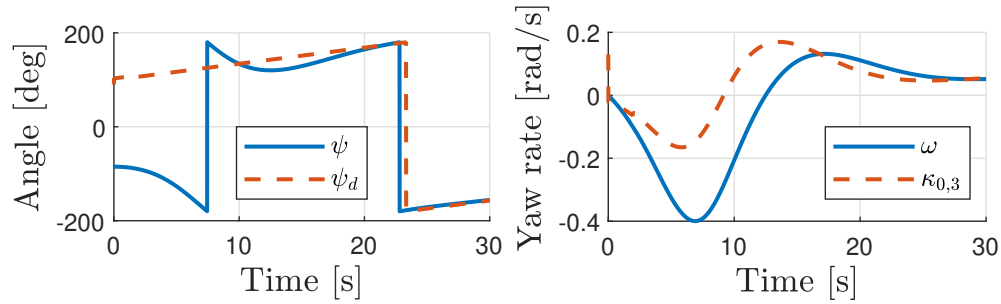

Figure 8.3: The heading angle $\psi = \text{atan2}(R_{21}, R_{11})$, desired heading angle $\psi_d = \text{atan2}(R_{d,21}, R_{d,11})$, angular velocity ω and the third component of κ_0.

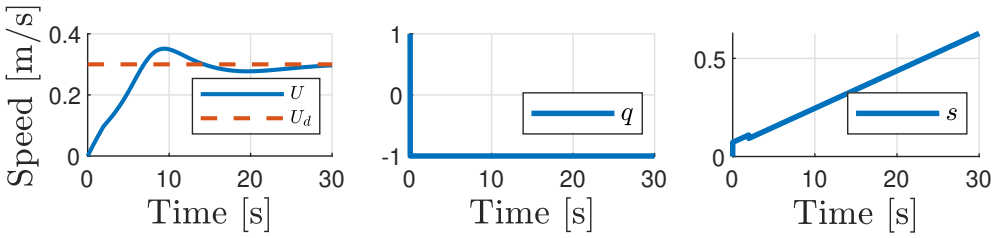

Figure 8.4: The speed $U = (\zeta_1^2 + \zeta_2^2)^{\frac{1}{2}}$, desired speed U_d and synergistic variables q and s.

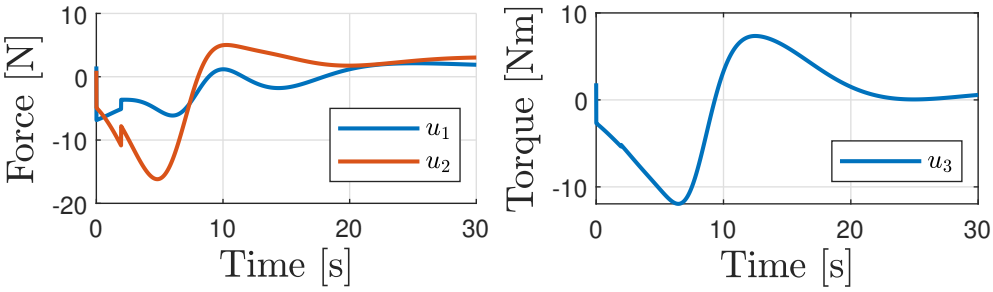

Figure 8.5: The control forces and moment u.

Chapter 9

Conclusions and Future Work

This thesis has presented several new results on modeling of underwater vehicles and hybrid feedback control of nonlinear systems. While not all results pertaining to hybrid feedback control focus directly on underwater vehicle control, all of them are applicable in this domain.

In Chapter 3, a matrix Lie group approach to the modeling of rigid underwater vehicles was presented. Furthermore, we introduced the notion of monotone dissipativity and showed its connection with convex Rayleigh dissipation functions. Building on established results from hydrodynamics, we also provided a modern symmetry principle for hydrodynamic inertia and damping effects that can be used to simplify underwater vehicle models. An important avenue for further work is to include the influence of additional submerged bodies in the fluid. The presented model takes its relatively simple form in large part because it is assumed that the underwater vehicle constitutes the only bounding surface of the fluid. Since underwater vehicles often work in close proximity to the seafloor or subsea installations, this assumption is strictly speaking rarely satisfied. The presence of other bodies in the fluid makes it necessary to consider configuration-dependent expressions for hydrodynamic mass and damping effects. The symmetry principle should in this case also be extended to give simplifications due to left-invariance of the wrenches with respect to the symmetry group of the other submerged bodies. Another avenue for further work is to extend the hydrodynamic symmetry principle to also address wrenches generated by the vehicle's thrusters and control surfaces.

In Chapter 4, we have extended the modeling approach outlined in Chapter 3 to multibody underwater vehicles with tree-topology. It was demonstrated how such an approach could be useful for expressing and computing kinematic and dynamic quantities of interest. The equations of motion in a global matrix-form were derived, and the most important properties of the resulting system matrices given. We presented a generalized Newton-Euler algorithm that can be used for the implementation of control algorithms that rely on a parametrization of the $C_\circ$-matrix possessing the skew property. Furthermore, it was shown how efficient methods from the field of multibody dynamics could be adapted to simulate multibody underwater vehicles. One avenue for further research is a modification of the generalized Newton-Euler algorithm to compute other parametrizations of the $C_\circ$-matrix, and in particular the one associated with the generalized Christoffel symbols [101, Section 3.8.2]. Another interesting

topic, similar to the one mentioned for the preceding chapter, is an investigation of the effect of hydrodynamic couplings between the bodies composing the vehicle.

In Chapter 5, we have introduced multiple synergistic control designs for mechanical systems on matrix Lie groups. Specifically, we have proposed synergistic PD, output feedback, and PID type control laws ensuring global asymptotic tracking of a desired bounded reference trajectory. The PID type control laws achieve global asymptotic tracking also when there is a constant disturbance present in the system dynamics. Given the importance of integral action for the control of underwater vehicles, there is ample reason to pursue this topic further. The presented PID control laws do not utilize the same feedforward control as the presented PD and output feedback control laws, and do therefore not exploit the system properties fully. The cross-terms involving the velocity error and the bias error present in the Lyapunov functions for the PID control laws also makes the utilization of the synergistic smoothing approach outlined in for instance [65] impossible without modification. Improving these aspects of the presented PID control laws is of high importance. Furthermore, all control laws presented in this chapter assume full actuation of the mechanical system. This assumption does of course not hold for a wide range of underwater vehicles, and further research in this direction is required to achieve greater practical applicability of the presented control laws.

In Chapter 6, we have proposed an adaptive hybrid feedback control law for marine vehicles. The control law tracks a hybrid reference system constructed from a parametrized loop and a speed assignment for the motion along the path and achieves global asymptotic tracking of the loop at a time-varying desired speed. The proposed hybrid feedback control law was implemented on a scale model tug boat and a remotely operated underwater vehicle, and laboratory experiments demonstrated the effectiveness of the proposed control law. The particular structure of this control law and the relatively simple expressions of the Lyapunov functions utilized in its stability analysis makes it possible to apply it to other mechanical systems defined on general matrix Lie groups. This includes systems that do not posses a left-invariant metric, provided that the feedforward control is modified to also include certain terms stemming from derivatives of the metric. One example from the class of systems that is then within reach is furnished by traditional robot manipulators. Indeed, several robot manipulators have joints that allow full rotation such that topological obstructions to global asymptotic stabilization exist. More generally, the control law could be applied to the fairly general class of underwater vehicles presented in Chapter 4, if the current is modeled as a bias.

In Chapter 7, we have presented hysteretic control Lyapunov functions for a class of nonlinear continuous-time systems. We have stated sufficient conditions for the existence of a feasible collection of feedback control laws that globally asymptotically stabilize a compact set. Moreover, we have shown how a collection of optimization-based feedback laws can be derived from a family of HCLFs under mild assumptions on the objective function. As a result, HCLFs can serve as a tool for synthesis of optimal feedback laws ensuring global asymptotic tracking of spatial rigid-bodies such as underwater vehicles. Further work related to the control of underwater vehicles could focus on showing that the HCLF decrease conditions can be satisfied for underwater vehicle error systems with bounded inputs, and investigating whether the "Lyapunov-based thrust allocation" that the optimization-based control laws essentially constitute in this context is an effective form of thrust allocation.

In Chapter 8, we have generalized the definition of synergistic Lyapunov function and feedback pairs introduced in [77, 78] to synergistic Lyapunov function and feedback triples by allowing the traditional logic variable to change during flows. We have introduced two approaches to triggering jumps in the closed-loop system within the synergistic framework, which we referred to as optional jumps and independently triggered jumps. Furthermore, we have showed that SLFF triples, just like SLFF pairs, are amenable to integrator backstepping for input-affine systems. Finally, we have applied the presented theory to the maneuvering control of ships, were optional jumps in the path-variable where introduced. We consider further work to be a complete integration of the maneuvering problem presented in [85, 132] into the synergistic framework.

References

[1] G. Kirchhoff, "Ueber die bewegung eines rotationskörpers in einer flüssigkeit.," *Journal für die reine und angewandte Mathematik*, vol. 1870, no. 71, pp. 237–262, 1870.

[2] W. Thomson, "Hydrokinetic solutions and observations," *The London, Edinburgh, and Dublin Philosophical Magazine and Journal of Science*, vol. 42, no. 281, pp. 362–377, 1871.

[3] W. Thomson and P. G. Tait, *Treatise on natural philosophy*. Claredon Press, 1867, vol. 1.

[4] M. Howe, "On the force and moment on a body in an incompressible fluid, with application to rigid bodies and bubbles at high and low reynolds numbers," *The Quarterly Journal of Mechanics and Applied Mathematics*, vol. 48, no. 3, pp. 401–426, 1995.

[5] L. Quartapelle and M. Napolitano, "Force and moment in incompressible flows," *AIAA journal*, vol. 21, no. 6, pp. 911–913, 1983.

[6] M. Howe, "On unsteady surface forces, and sound produced by the normal chopping of a rectilinear vortex," *Journal of Fluid Mechanics*, vol. 206, pp. 131–153, 1989.

[7] C.-C. Chang, "Potential flow and forces for incompressible viscous flow," *Proceedings of the Royal Society of London. Series A: Mathematical and Physical Sciences*, vol. 437, no. 1901, pp. 517–525, 1992.

[8] L. Wakaba and S. Balachandar, "On the added mass force at finite reynolds and acceleration numbers," *Theoretical and Computational fluid dynamics*, vol. 21, no. 2, pp. 147–153, 2007.

[9] M. Gertler and G. R. Hagen, "Standard equations of motion for submarine simulation," David W. Taylor Naval Ship Research and Development Center Bethesda MD, Tech. Rep., 1967.

[10] K. Fedyaevsky and G. Sobolev, "Control and stability in ship design," 1964.

[11] M. A. Abkowitz, "Lectures on ship hydrodynamics–steering and manoeuvrability," Tech. Rep., 1964.

[12] R. J. Boncal, "A study of model based maneuvering controls for autonomous underwater vehicles," Naval Postgraduate School, Tech. Rep., 1987.

[13] A. J. Healey and D. Lienard, "Multivariable sliding mode control for autonomous diving and steering of unmanned underwater vehicles," *IEEE journal of Oceanic Engineering*, vol. 18, no. 3, pp. 327–339, 1993.

[14] K. R. Goheen, "The modelling and control of remotely operated underwater vehicles," Ph.D. dissertation, University of London, 1986.

[15] K. R. Goheen, "Modeling methods for underwater robotic vehicle dynamics," *Journal of Robotic Systems*, vol. 8, no. 3, pp. 295–317, 1991.

[16] J. J. Craig, "Introduction to robotics machanics and control," 1986.

[17] S. I. Sagatun and T. I. Fossen, "Lagrangian formulation of underwater vehicles' dynamics," in *IEEE International Conference on Systems, Man, and Cybernetics*, IEEE, 1991, pp. 1029–1034.

[18] T. I. Fossen, "Nonlinear modelling and control of underwater vehicles," Ph.D. dissertation, Norwegian Institute of Technology, 1991.

[19] S. I. Sagatun, "Modeling and control of underwater vehicles. a lagrangian approach," Ph.D. dissertation, Norwegian Institute of Technology, 1992.

[20] J.-J. E. Slotine and W. Li, "On the adaptive control of robot manipulators," *The international journal of robotics research*, vol. 6, no. 3, pp. 49–59, 1987.

[21] T. I. Fossen and S. I. Sagatun, "Adaptive control of nonlinear underwater robotic systems," in *Proc. 1991 IEEE International Conference on Robotics and Automation*, Sacramento, CA, USA, 1991.

[22] T. I. Fossen and O.-E. Fjellstad, "Nonlinear modelling of marine vehicles in 6 degrees of freedom," *Mathematical Modelling of Systems*, vol. 1, no. 1, pp. 17–27, 1995.

[23] T. I. Fossen, *Guidance and control of ocean vehicles*. John Wiley & Sons, 1999.

[24] T. I. Fossen, *Handbook of Marine Craft Hydrodynamics and Motion Control*, 2nd. Wiley, 2020.

[25] J. Larmor, "On hydrokinetic symmetry," *Quarterly Journal for Pure and Applied Mathematics*, vol. 20, pp. 261–266, 1884.

[26] H. Lamb, *Hydrodynamics*. Cambridge university press, 1993.

[27] D. Ribas, N. Palomeras, P. Ridao, M. Carreras, and A. Mallios, "Girona 500 auv: From survey to intervention," *IEEE/ASME Transactions on mechatronics*, vol. 17, no. 1, pp. 46–53, 2011.

[28] E. Simetti, G. Casalino, S. Torelli, A. Sperinde, and A. Turetta, "Floating underwater manipulation: Developed control methodology and experimental validation within the Trident project," *Journal of Field Robotics*, vol. 31, no. 3, pp. 364–385, 2014.

[29] I.-L. G. Borlaug, K. Y. Pettersen, and J. T. Gravdahl, "Tracking control of an articulated intervention autonomous underwater vehicle in 6dof using generalized super-twisting: Theory and experiments," *IEEE Transactions on Control Systems Technology*, vol. 29, no. 1, pp. 353–369, 2020.

[30] J. R. Morison, M. P. O'Brien, J. W. Johnson, and S. A. Schaaf, "The force exerted by surface waves on piles," *Journal of Petroleum Technology*, vol. 2, no. 05, pp. 149–154, 1950.

[31] N. Salvesen, E. Tuck, and O. Faltinsen, "Ship motions and sea loads," 1970.

[32] K. Ioi and K. Itoh, "Modelling and simulation of an underwater manipulator," *Advanced Robotics*, vol. 4, no. 4, pp. 303–317, 1989.

[33] B. Lévesque and M. J. Richard, "Dynamic analysis of a manipulator in a fluid environment," *The International Journal of Robotics Research*, vol. 13, no. 3, pp. 221–231, 1994.

[34] I. Schjølberg and T. I. Fossen, "Modelling and control of underwater vehicle-manipulator systems," in *Proceedings of 3rd Conference on Marine Craft maneuvering and control*, 1994.

[35] S. McMillan, D. E. Orin, and R. B. McGhee, "Efficient dynamic simulation of an underwater vehicle with a robotic manipulator," *IEEE Transactions on Systems, Man, and Cybernetics*, vol. 25, no. 8, pp. 1194–1206, 1995.

[36] T. J. Tarn, G. Shoults, and S. Yang, "A dynamic model of an underwater vehicle with a robotic manipulator using Kane's method," *Autonomous robots*, vol. 3, no. 2-3, pp. 269–283, 1996.

[37] M. Dunnigan and G. T. Russell, "Evaluation and reduction of the dynamic coupling between a manipulator and an underwater vehicle," *IEEE Journal of Oceanic Engineering*, vol. 23, no. 3, pp. 260–273, 1998.

[38] T. W. McLain and S. M. Rock, "Development and experimental validation of an underwater manipulator hydrodynamic model," *The International Journal of Robotics Research*, vol. 17, no. 7, pp. 748–759, 1998.

[39] R. Featherstone, "The calculation of robot dynamics using articulated-body inertias," *The international journal of robotics research*, vol. 2, no. 1, pp. 13–30, 1983.

[40] R. Featherstone, *Rigid Body Dynamics Algorithms*. Springer, 2014.

[41] H. Huang, Q. Tang, H. Li, L. Liang, W. Li, and Y. Pang, "Vehicle-manipulator system dynamic modeling and control for underwater autonomous manipulation," *Multibody System Dynamics*, vol. 41, pp. 125–147, 2017.

[42] I. Schjølberg, "Modeling and control of underwater robotic systems," Ph.D. dissertation, Norwegian University of Science and Technology, 1996.

[43] P. J. From, V. Duindam, K. Y. Pettersen, J. T. Gravdahl, and S. Sastry, "Singularity-free dynamic equations of vehicle–manipulator systems," *Simulation Modelling Practice and Theory*, vol. 18, no. 6, pp. 712–731, 2010.

[44] O. Egeland and K. Y. Pettersen, "Free-floating robotic systems," in *Control Problems in Robotics and Automation*, Springer, 1998, pp. 119–134.

[45] G. Antonelli, *Underwater Robots*, 4th. Springer, 2018, ISBN: 9783319778990.

[46] P. J. From, J. T. Gravdahl, and K. Y. Pettersen, *Vehicle-Manipulator Systems*. Springer, Aug. 23, 2016, 412 pp., ISBN: 1447170717.

[47] T. R. Kane and C. Wang, "On the derivation of equations of motion," *Journal of the Society for Industrial and Applied Mathematics*, vol. 13, no. 2, pp. 487–492, 1965.

[48] T. R. Kane and D. A. Levinson, *Dynamics, theory and applications*. McGraw Hill, 1985.

[49] N. Sarkar and T. K. Podder, "Coordinated motion planning and control of autonomous underwater vehicle-manipulator systems subject to drag optimization," *IEEE Journal of Oceanic Engineering*, vol. 26, no. 2, pp. 228–239, 2001.

[50] L. Meirovitch, *Methods of analytical dynamics*. Dover, 2010.

[51] G. Hamel, "Über die virtuellen verschiebungen in der mechanik," *Mathematische Annalen*, vol. 59, no. 3, pp. 416–434, 1904.

[52] G. Hamel, "Die lagrange-euler'schen gleichungen der mechanik," *Zeitschrift für Mathematik und Physik*, vol. 50, 1904.

[53] A. Bloch, J. Baillieul, P. Crouch, J. E. Marsden, D. Zenkov, P. S. Krishnaprasad, and R. M. Murray, *Nonholonomic Mechanics and Control*. Springer, 2003, vol. 24.

[54] S. P. Bhat and D. S. Bernstein, "A topological obstruction to continuous global stabilization of rotational motion and the unwinding phenomenon," *Systems & Control Letters*, vol. 39, no. 1, pp. 63–70, 2000, ISSN: 0167-6911.

[55] C. G. Mayhew and A. R. Teel, "On the topological structure of attraction basins for differential inclusions," *Systems & Control Letters*, vol. 60, no. 12, pp. 1045–1050, 2011.

[56] A. R. Teel, "Robust hybrid control systems: An overview of some recent results," in *Advances in Control Theory and Applications*, C. Bonivento, A. Isidori, L. Marconi, and C. Rossi, Eds., Springer, 2007, pp. 279–302, ISBN: 978-3-540-70701-1. DOI: 10.1007/978-3-540-70701-1_15.

[57] C. Prieur, "Asymptotic controllability and robust asymptotic stabilizability," *SIAM Journal on Control and Optimization*, vol. 43, no. 5, pp. 1888–1912, 2005.

[58] C. Prieur, R. Goebel, and A. R. Teel, "Hybrid feedback control and robust stabilization of nonlinear systems," *IEEE Transactions on Automatic Control*, vol. 52, no. 11, pp. 2103–2117, 2007.

[59] R. Goebel, C. Prieur, and A. R. Teel, "Smooth patchy control Lyapunov functions," *Automatica*, vol. 45, no. 3, pp. 675–683, 2009.

[60] P. Casau, R. Cunha, R. G. Sanfelice, and C. Silvestre, "Hybrid control for robust and global tracking on smooth manifolds," *IEEE Transactions on Automatic Control*, vol. 65, no. 5, pp. 1870–1885, 2020.

[61] R. G. Sanfelice, *Hybrid Feedback Control*. Princeton University Press, Princeton, NJ, 2021.

[62] C. G. Mayhew, "Hybrid control for topologically constrained systems," Ph.D. dissertation, University of California, Santa Barbara, 2010.

[63] C. G. Mayhew and A. R. Teel, "Synergistic potential functions for hybrid control of rigid-body attitude," in *Proc. 2011 American Control Conf.*, San Francisco, CA, USA, Jun. 2011, pp. 875–880. DOI: 10.1109/ACC.2011.5990826.

[64] D. E. Koditschek, "The application of total energy as a Lyapunov function for mechanical control systems," *Contemporary Mathematics*, vol. 97, p. 131, 1989.

[65] C. G. Mayhew and A. R. Teel, "Synergistic hybrid feedback for global rigid-body attitude tracking on SO(3)," *IEEE Transactions on Automatic Control*, vol. 58, no. 11, pp. 2730–2742, Nov. 2013, ISSN: 2334-3303. DOI: 10.1109/TAC.2013.2266852.

[66] S. Berkane and A. Tayebi, "Construction of synergistic potential functions on SO(3) with application to velocity-free hybrid attitude stabilization," *IEEE Transactions on Automatic Control*, vol. 62, no. 1, pp. 495–501, 2017.

[67] S. Berkane, A. Abdessameud, and A. Tayebi, "Hybrid global exponential stabilization on so (3)," *Automatica*, vol. 81, pp. 279–285, 2017.

[68] T. Lee, "Exponential stability of an attitude tracking control system on so (3) for large-angle rotational maneuvers," *Systems & Control Letters*, vol. 61, no. 1, pp. 231–237, 2012.

[69] T. Lee, "Global exponential attitude tracking controls on $\mathsf{SO}(3)$," *IEEE Transactions on Automatic Control*, vol. 60, no. 10, 2015.

[70] M. Wang and A. Tayebi, "Hybrid feedback for global tracking on matrix lie groups SO(3) and SE(3)," *IEEE Transactions on Automatic Control*, 2021. DOI: 10.1109/TAC.2021.3097704.

[71] C. G. Mayhew, R. G. Sanfelice, and A. R. Teel, "Quaternion-based hybrid control for robust global attitude tracking," *IEEE Transactions on Automatic Control*, vol. 56, no. 11, 2011.

[72] R. Schlanbusch, E. I. Grøtli, A. Loria, and P. J. Nicklasson, "Hybrid attitude tracking of rigid bodies without angular velocity measurement," *Systems & Control Letters*, vol. 61, no. 4, pp. 595–601, 2012.

[73] P. Casau, R. G. Sanfelice, R. Cunha, D. Cabecinhas, and C. Silvestre, "Robust global trajectory tracking for a class of underactuated vehicles," *Automatica*, vol. 58, pp. 90–98, 2015, ISSN: 0005-1098.

[74] C. G. Mayhew and A. R. Teel, "Global stabilization of spherical orientation by synergistic hybrid feedback with application to reduced-attitude tracking for rigid bodies," *Automatica*, vol. 49, no. 7, pp. 1945–1957, 2013.

[75] C. G. Mayhew and A. R. Teel, "Hybrid control of planar rotations," in *Proc. 2010 American Control Conf.*, Baltimore, MD, USA, 2010.

[76] P. Casau, C. G. Mayhew, R. G. Sanfelice, and C. Silvestre, "Robust global exponential stabilization on the n-dimensional sphere with applications to trajectory tracking for quadrotors," *Automatica*, vol. 110, p. 108 534, 2019.

[77] C. G. Mayhew, R. G. Sanfelice, and A. R. Teel, "Synergistic Lyapunov functions and backstepping hybrid feedbacks," in *Proc. 2011 American Control Conf.*, San Francisco, CA, USA, Jun. 2011, pp. 3203–3208.

[78] C. G. Mayhew, R. G. Sanfelice, and A. R. Teel, "Further results on synergistic Lyapunov functions and hybrid feedback design through backstepping," in *Proc. 50th IEEE Conf. on Decision and Control*, Orlando, FL, USA, 2011, pp. 7428–7433.

[79] C. Cai, A. R. Teel, and R. Goebel, "Smooth lyapunov functions for hybrid systems—part i: Existence is equivalent to robustness," *IEEE Transactions on Automatic Control*, vol. 52, no. 7, pp. 1264–1277, 2007.

[80] C. Cai, A. R. Teel, and R. Goebel, "Smooth lyapunov functions for hybrid systems part ii:(pre) asymptotically stable compact sets," *IEEE Transactions on Automatic Control*, vol. 53, no. 3, pp. 734–748, 2008.

[81] P. Casau, R. G. Sanfelice, and C. Silvestre, "Adaptive backstepping of synergistic hybrid feedbacks with application to obstacle avoidance," in *Proc. 2019 American Control Conf.*, Philadelphia, PA, USA, 2019, pp. 1730–1735.

[82] H. M. Schmidt-Didlaukies, A. J. Sørensen, and K. Y. Pettersen, "Modeling of articulated underwater robots for simulation and control," in *2018 IEEE/OES Autonomous Underwater Vehicle Workshop (AUV)*, IEEE, 2018, pp. 1–7.

[83] E. A. Basso, H. M. Schmidt-Didlaukies, K. Y. Pettersen, and J. T. Gravdahl, "Synergistic pid and output feedback control on matrix lie groups," in *Proc. 12th IFAC Symposium on Nonlinear Control Systems*, Canberra, Australia, Jan. 2022.

[84] R. Skjetne, T. I. Fossen, and P. V. Kokotović, "Robust output maneuvering for a class of nonlinear systems," *Automatica*, 2004, ISSN: 0005-1098. DOI: https://doi.org/10.1016/j.automatica.2003.10.010.

[85] R. Skjetne, "The maneuvering problem," Ph.D. dissertation, Norwegian University of Science and Technology, 2005.

[86] E. A. Basso, H. M. Schmidt-Didlaukies, K. Y. Pettersen, and A. J. Sørensen, "Global asymptotic tracking for marine surface vehicles using hybrid feedback in the presence of parametric uncertainties," in *Proc. 2021 American Control Conf.*, New Orleans, LA, USA, 2021, pp. 1432–1437. DOI: 10.23919/ACC50511.2021.9483419.

[87] E. A. Basso, H. M. Schmidt-Didlaukies, K. Y. Pettersen, and A. J. Sorensen, "Global asymptotic tracking for marine vehicles using adaptive hybrid feedback," *IEEE Transactions on Automatic Control*, 2022. DOI: 10.1109/TAC.2022.3161372.

[88] R. A. Freeman and P. V. Kokotovic, "Inverse optimality in robust stabilization," *SIAM journal on control and optimization*, vol. 34, no. 4, pp. 1365–1391, 1996.

[89] R. A. Freeman and P. Kokotović, *Robust Nonlinear Control Design*. Birkhäuser Boston, 1996.

[90] R. Goebel, R. G. Sanfelice, and A. R. Teel, *Hybrid Dynamical Systems: Modeling Stability, and Robustness*. Princeton University Press, Princeton, NJ, 2012.

[91] C. G. Mayhew, R. G. Sanfelice, and A. R. Teel, "Robust global asymptotic stabilization of a 6-DOF rigid body by quaternion-based hybrid feedback," in *Proc. 48h IEEE Conf. on Decision and Control*, Shanghai, China, Dec. 2009. DOI: 10.1109/CDC.2009.5400338.

[92] E. A. Basso, H. M. Schmidt-Didlaukies, and K. Y. Pettersen, "Hysteretic control Lyapunov functions with application to global asymptotic tracking for underwater vehicles," in *Proc. 59th Conf. on Decision and Control*, Jeju Island, Republic of Korea, 2020.

[93] H. M. Schmidt-Didlaukies, E. A. Basso, and K. Y. Pettersen, "A generalization of synergistic hybrid feedback control with application to maneuvering control of ships," in *Proc. 61st IEEE Conference on Decision and Control*, Cancún, Mexico, Dec. 2022. [Online]. Available: https://bit.ly/3AvhAoA.

[94] J. R. Munkres, *Analysis on manifolds*. CRC Press, 2018.

[95] M. Spivak, *Calculus on manifolds: a modern approach to classical theorems of advanced calculus*. CRC press, 2018.

[96] J. M. Lee, *Introduction to Smooth Manifolds*. Springer, 2012.

[97] B. C. Hall, *Lie Groups, Lie Algebras, and Representations*. Springer, 2015, ISBN: 978-3-319-13466-6.

[98] R. M. Murray, Z. Li, and S. S. Sastry, *A Mathematical Introduction to Robotic Manipulation*. Taylor & Francis, 1994, ISBN: 9780849379819.

[99] J. M. Selig, *Geometric Fundamentals of Robotics*. Springer, 2004.

[100] K. M. Lynch and F. C. Park, *Modern Robotics*. Cambridge University Press, 2017.

[101] F. Bullo and A. D. Lewis, *Geometric Control of Mechanical Systems*. Springer, 2005.

[102] R. T. Rockafellar and R. J.-B. Wets, *Variational Analysis*. Springer, 2009.

[103] J. P. Aubin and H. Frankowska, *Set-Valued Analysis* (Systems & control). Birkhäuser Boston, 1990. DOI: 10.1007/978-0-8176-4848-0.

[104] J. P. Aubin, *Mutational and Morphological Analysis: Tools for Shape Evolution and Morphogenesis*. Birkhäuser Boston, 2012, ISBN: 9781461215769.

[105] E. Michael, "Continuous selections. I," *Annals of Mathematics*, 1956.

[106] R. Goebel, R. G. Sanfelice, and A. R. Teel, "Hybrid dynamical systems," *IEEE Control Systems Magazine*, vol. 29, no. 2, pp. 28–93, 2009. DOI: 10.1109/MCS.2008.931718.

[107] J. E. Marsden and T. Ratiu, *Introduction to Mechanics and Symmetry: A Basic Exposition of Classical Mechanical Systems*. Springer Science & Business Media, 2013, vol. 17.

[108] D. Medková, *The Laplace Equation*. Springer, 2018.

[109] J. N. Newman, *Marine hydrodynamics*. The MIT press, 2018.

[110] A. Galper and T. Miloh, "Generalized kirchhoff equations for a deformable body moving in a weakly non-uniform flow field," *Proceedings of the Royal Society of London. Series A: Mathematical and Physical Sciences*, vol. 446, no. 1926, pp. 169–193, 1994.

[111] A. Galper and T. Miloh, "Dynamic equations of motion for a rigid or deformable body in an arbitrary non-uniform potential flow field," *Journal of Fluid Mechanics*, vol. 295, pp. 91–120, 1995.

[112] O. Faltinsen, *Sea loads on ships and offshore structures*. Cambridge University Press, 1993.

[113] T. Sarpkaya, *Wave forces on offshore structures*. Cambridge university press, 2010.

[114] Ø. Hegrenæs and O. Hallingstad, "Model-aided ins with sea current estimation for robust underwater navigation," *IEEE Journal of Oceanic Engineering*, vol. 36, no. 2, pp. 316–337, 2011.

[115] M. Arcak and P. Kokotović, "Nonlinear observers: A circle criterion design and robustness analysis," *Automatica*, vol. 37, no. 12, pp. 1923–1930, 2001.

[116] X. Fan and M. Arcak, "Observer design for systems with multivariable monotone nonlinearities," *Systems & Control Letters*, vol. 50, no. 4, pp. 319–330, 2003.

[117] J. E. Refsnes, A. J. Sorensen, and K. Y. Pettersen, "Model-based output feedback control of slender-body underactuated auvs: Theory and experiments," *IEEE Transactions on control systems technology*, vol. 16, no. 5, pp. 930–946, 2008.

[118] J. W. Strutt, "Some general theorems relating to vibrations," *Proceedings of the London Mathematical Society*, vol. s1-4, no. 1, pp. 357–368, 1871.

[119] S. Stramigioli, *Modeling and IPC Control of Interactive Mechanical Systems - A Coordinate-Free Approach*. Springer London, Mar. 23, 2001, 296 pp., ISBN: 1852333952.

[120] S. R. Ploen, "Geometric algorithms for the dynamics and control of multibody systems," Ph.D. dissertation, University of California, Irvine, 1997.

[121] E. Kanso, J. E. Marsden, C. W. Rowley, and J. B. Melli-Huber, "Locomotion of articulated bodies in a perfect fluid," *Journal of Nonlinear Science*, vol. 15, no. 4, pp. 255–289, 2005.

[122] A. Munnier, "On the self-displacement of deformable bodies in a potential fluid flow," *Mathematical Models and Methods in Applied Sciences*, vol. 18, no. 11, pp. 1945–1981, 2008.

[123] P. From, J. Gravdahl, and K. Pettersen, *Vehicle-Manipulator Systems: Modeling for Simulation, Analysis, and Control*. Jan. 2014, ISBN: 978-1-4471-5462-4.

[124] D. Maithripala and J. M. Berg, "An intrinsic pid controller for mechanical systems on Lie groups," *Automatica*, vol. 54, pp. 189–200, 2015, ISSN: 0005-1098.

[125] Z. Zhang, A. Sarlette, and Z. Ling, "Integral control on Lie groups," *Systems & Control Letters*, 2015.

[126] T. I. Fossen and O.-E. Fjellstad, "Robust adaptive control of underwater vehicles: A comparative study," in *Proc. 3rd IFAC Workshop on Control Applications in Marine Systems*, Trondheim, Norway, 1995.

[127] O.-E. Fjellstad and T. I. Fossen, "Position and attitude tracking of AUV's: A quaternion feedback approach," *IEEE Journal of Oceanic Engineering*, vol. 19, no. 4, pp. 512–518, 1994. DOI: 10.1109/48.338387.

[128] G. Antonelli, F. Caccavale, S. Chiaverini, and G. Fusco, "A novel adaptive control law for underwater vehicles," *IEEE Transactions on control systems technology*, vol. 11, no. 2, pp. 221–232, 2003.

[129] G. Antonelli, S. Chiaverini, N. Sarkar, and M. West, "Adaptive control of an autonomous underwater vehicle: Experimental results on ODIN," *IEEE Transactions on Control Systems Technology*, vol. 9, no. 5, pp. 756–765, 2001. DOI: 10.1109/87.944470.

[130] J.-M. Godhavn, T. I. Fossen, and S. P. Berge, "Non-linear and adaptive backstepping designs for tracking control of ships," *International Journal of Adaptive Control and Signal Processing*, 1998.

[131] R. Skjetne, O. Smogeli, and T. Fossen, "A nonlinear ship manoeuvering model: Identification and adaptive control with experiments for a model ship," *Modeling, Identification and Control*, vol. 25, pp. 3–27, 2004. DOI: 10.4173/mic.2004.1.1.

[132] R. Skjetne, T. I. Fossen, and P. V. Kokotović, "Adaptive maneuvering, with experiments, for a model ship in a marine control laboratory," *Automatica*, vol. 41, no. 2, pp. 289–298, 2005, ISSN: 0005-1098.

[133] A. H. Brodtkorb, S. A. Værnø, A. R. Teel, A. J. Sørensen, and R. Skjetne, "Hybrid controller concept for dynamic positioning of marine vessels with experimental results," *Automatica*, 2018, ISSN: 0005-1098. DOI: https://doi.org/10.1016/j.automatica.2018.03.047.

[134] B. Paden and R. Panja, "Globally asymptotically stable PD+ controller for robot manipulators," *International Journal of Control*, 1988.

[135] M. Krstic, P. V. Kokotovic, and I. Kanellakopoulos, *Nonlinear and Adaptive Control Design*. John Wiley & Sons, 1995, ISBN: 0471127329.

[136] C. G. Mayhew, R. G. Sanfelice, and A. R. Teel, "On path-lifting mechanisms and unwinding in quaternion-based attitude control," *IEEE Transactions on Automatic Control*, vol. 58, no. 5, pp. 1179–1191, 2013. DOI: 10.1109/TAC.2012.2235731.

[137] Marine Cybernetics Lab, (Accessed Oct. 14th, 2021). [Online]. Available: https://www.ntnu.edu/imt/lab/cybernetics.

[138] Z. Artstein, "Stabilization with relaxed controls," *Nonlinear Analysis: Theory, Methods & Applications*, vol. 7, no. 11, pp. 1163–1173, 1983.

[139] E. D. Sontag, "A Lyapunov-like characterization of asymptotic controllability," *SIAM Journal on Control and Optimization*, vol. 21, no. 3, pp. 462–471, 1983.

[140] E. D. Sontag, "A universal construction of Artstein's theorem on nonlinear stabilization," *Systems & Control Letters*, vol. 13, no. 2, 1989.

[141] R. G. Sanfelice, "On the existence of control Lyapunov functions and state-feedback laws for hybrid systems," *IEEE Transactions on Automatic Control*, vol. 58, no. 12, pp. 3242–3248, 2013.

[142] R. G. Sanfelice, "Robust asymptotic stabilization of hybrid systems using control Lyapunov functions," in *Proc. 19th International Conference on Hybrid Systems: Computation and Control*, Vienna, Austria, 2016, pp. 235–244.

[143] H. Nakamura and Y. Satoh, "Étale backstepping for control Lyapunov function design on manifold," *Automatica*, vol. 83, pp. 100–107, 2017, ISSN: 0005-1098. DOI: https://doi.org/10.1016/j.automatica.2017.05.010.

[144] R. T. Rockafellar, *Convex Analysis*. Princeton University Press, 1970.

Previous PhD theses published at the Department of Marine Technology

Previous PhD theses published at the Department of Marine Technology (earlier: Faculty of Marine Technology)
NORWEGIAN UNIVERSITY OF SCIENCE AND TECHNOLOGY

Report No.	Author	Title
	Kavlie, Dag	Optimization of Plane Elastic Grillages, 1967
	Hansen, Hans R.	Man-Machine Communication and Data-Storage Methods in Ship Structural Design, 1971
	Gisvold, Kaare M.	A Method for non-linear mixed -integer programming and its Application to Design Problems, 1971
	Lund, Sverre	Tanker Frame Optimalization by means of SUMT-Transformation and Behaviour Models, 1971
	Vinje, Tor	On Vibration of Spherical Shells Interacting with Fluid, 1972
	Lorentz, Jan D.	Tank Arrangement for Crude Oil Carriers in Accordance with the new Anti-Pollution Regulations, 1975
	Carlsen, Carl A.	Computer-Aided Design of Tanker Structures, 1975
	Larsen, Carl M.	Static and Dynamic Analysis of Offshore Pipelines during Installation, 1976
UR-79-01	Brigt Hatlestad, MK	The finite element method used in a fatigue evaluation of fixed offshore platforms. (Dr.Ing. Thesis)
UR-79-02	Erik Pettersen, MK	Analysis and design of cellular structures. (Dr.Ing. Thesis)
UR-79-03	Sverre Valsgård, MK	Finite difference and finite element methods applied to nonlinear analysis of plated structures. (Dr.Ing. Thesis)
UR-79-04	Nils T. Nordsve, MK	Finite element collapse analysis of structural members considering imperfections and stresses due to fabrication. (Dr.Ing. Thesis)
UR-79-05	Ivar J. Fylling, MK	Analysis of towline forces in ocean towing systems. (Dr.Ing. Thesis)
UR-79- x	Finn Gunnar Nielsen, MH	Hydrodynamic problems related to oil barriers for offshore application
UR-80-06	Nils Sandsmark, MM	Analysis of Stationary and Transient Heat Conduction by the Use of the Finite Element Method. (Dr.Ing. Thesis)
UR-80-09	Sverre Haver, MK	Analysis of uncertainties related to the stochastic modeling of ocean waves. (Dr.Ing. Thesis)

UR-81-15	Odland, Jonas	On the Strength of welded Ring stiffened cylindrical Shells primarily subjected to axial Compression
UR-82-17	Engesvik, Knut	Analysis of Uncertainties in the fatigue Capacity of Welded Joints
UR-82-18	Rye, Henrik	Ocean wave groups
UR-83-30	Eide, Oddvar Inge	On Cumulative Fatigue Damage in Steel Welded Joints
UR-83-33	Mo, Olav	Stochastic Time Domain Analysis of Slender Offshore Structures
UR-83-34	Amdahl, Jørgen	Energy absorption in Ship-platform impacts
UR-84-37	Mørch, Morten	Motions and mooring forces of semi submersibles as determined by full-scale measurements and theoretical analysis
UR-84-38	Soares, C. Guedes	Probabilistic models for load effects in ship structures
UR-84-39	Aarsnes, Jan V.	Current forces on ships
UR-84-40	Czujko, Jerzy	Collapse Analysis of Plates subjected to Biaxial Compression and Lateral Load
UR-85-46	Alf G. Engseth, MK	Finite element collapse analysis of tubular steel offshore structures. (Dr.Ing. Thesis)
UR-86-47	Dengody Sheshappa, MP	A Computer Design Model for Optimizing Fishing Vessel Designs Based on Techno-Economic Analysis. (Dr.Ing. Thesis)
UR-86-48	Vidar Aanesland, MH	A Theoretical and Numerical Study of Ship Wave Resistance. (Dr.Ing. Thesis)
UR-86-49	Heinz-Joachim Wessel, MK	Fracture Mechanics Analysis of Crack Growth in Plate Girders. (Dr.Ing. Thesis)
UR-86-50	Jon Taby, MK	Ultimate and Post-ultimate Strength of Dented Tubular Members. (Dr.Ing. Thesis)
UR-86-51	Walter Lian, MH	A Numerical Study of Two-Dimensional Separated Flow Past Bluff Bodies at Moderate KC-Numbers. (Dr.Ing. Thesis)
UR-86-52	Bjørn Sortland, MH	Force Measurements in Oscillating Flow on Ship Sections and Circular Cylinders in a U-Tube Water Tank. (Dr.Ing. Thesis)
UR-86-53	Kurt Strand, MM	A System Dynamic Approach to One-dimensional Fluid Flow. (Dr.Ing. Thesis)
UR-86-54	Arne Edvin Løken, MH	Three Dimensional Second Order Hydrodynamic Effects on Ocean Structures in Waves. (Dr.Ing. Thesis)
UR-86-55	Sigurd Falch, MH	A Numerical Study of Slamming of Two-

		Dimensional Bodies. (Dr.Ing. Thesis)
UR-87-56	Arne Braathen, MH	Application of a Vortex Tracking Method to the Prediction of Roll Damping of a Two-Dimension Floating Body. (Dr.Ing. Thesis)
UR-87-57	Bernt Leira, MK	Gaussian Vector Processes for Reliability Analysis involving Wave-Induced Load Effects. (Dr.Ing. Thesis)
UR-87-58	Magnus Småvik, MM	Thermal Load and Process Characteristics in a Two-Stroke Diesel Engine with Thermal Barriers (in Norwegian). (Dr.Ing. Thesis)
MTA-88-59	Bernt Arild Bremdal, MP	An Investigation of Marine Installation Processes – A Knowledge - Based Planning Approach. (Dr.Ing. Thesis)
MTA-88-60	Xu Jun, MK	Non-linear Dynamic Analysis of Space-framed Offshore Structures. (Dr.Ing. Thesis)
MTA-89-61	Gang Miao, MH	Hydrodynamic Forces and Dynamic Responses of Circular Cylinders in Wave Zones. (Dr.Ing. Thesis)
MTA-89-62	Martin Greenhow, MH	Linear and Non-Linear Studies of Waves and Floating Bodies. Part I and Part II. (Dr.Techn. Thesis)
MTA-89-63	Chang Li, MH	Force Coefficients of Spheres and Cubes in Oscillatory Flow with and without Current. (Dr.Ing. Thesis
MTA-89-64	Hu Ying, MP	A Study of Marketing and Design in Development of Marine Transport Systems. (Dr.Ing. Thesis)
MTA-89-65	Arild Jæger, MH	Seakeeping, Dynamic Stability and Performance of a Wedge Shaped Planing Hull. (Dr.Ing. Thesis)
MTA-89-66	Chan Siu Hung, MM	The dynamic characteristics of tilting-pad bearings
MTA-89-67	Kim Wikstrøm, MP	Analysis av projekteringen for ett offshore projekt. (Licenciat-avhandling)
MTA-89-68	Jiao Guoyang, MK	Reliability Analysis of Crack Growth under Random Loading, considering Model Updating. (Dr.Ing. Thesis)
MTA-89-69	Arnt Olufsen, MK	Uncertainty and Reliability Analysis of Fixed Offshore Structures. (Dr.Ing. Thesis)
MTA-89-70	Wu Yu-Lin, MR	System Reliability Analyses of Offshore Structures using improved Truss and Beam Models. (Dr.Ing. Thesis)
MTA-90-71	Jan Roger Hoff, MH	Three-dimensional Green function of a vessel with forward speed in waves. (Dr.Ing. Thesis)
MTA-90-72	Rong Zhao, MH	Slow-Drift Motions of a Moored Two-Dimensional Body in Irregular Waves. (Dr.Ing. Thesis)
MTA-90-73	Atle Minsaas, MP	Economical Risk Analysis. (Dr.Ing. Thesis)

MTA-90-74	Knut-Aril Farnes, MK	Long-term Statistics of Response in Non-linear Marine Structures. (Dr.Ing. Thesis)
MTA-90-75	Torbjørn Sotberg, MK	Application of Reliability Methods for Safety Assessment of Submarine Pipelines. (Dr.Ing. Thesis)
MTA-90-76	Zeuthen, Steffen, MP	SEAMAID. A computational model of the design process in a constraint-based logic programming environment. An example from the offshore domain. (Dr.Ing. Thesis)
MTA-91-77	Haagensen, Sven, MM	Fuel Dependant Cyclic Variability in a Spark Ignition Engine - An Optical Approach. (Dr.Ing. Thesis)
MTA-91-78	Løland, Geir, MH	Current forces on and flow through fish farms. (Dr.Ing. Thesis)
MTA-91-79	Hoen, Christopher, MK	System Identification of Structures Excited by Stochastic Load Processes. (Dr.Ing. Thesis)
MTA-91-80	Haugen, Stein, MK	Probabilistic Evaluation of Frequency of Collision between Ships and Offshore Platforms. (Dr.Ing. Thesis)
MTA-91-81	Sødahl, Nils, MK	Methods for Design and Analysis of Flexible Risers. (Dr.Ing. Thesis)
MTA-91-82	Ormberg, Harald, MK	Non-linear Response Analysis of Floating Fish Farm Systems. (Dr.Ing. Thesis)
MTA-91-83	Marley, Mark J., MK	Time Variant Reliability under Fatigue Degradation. (Dr.Ing. Thesis)
MTA-91-84	Krokstad, Jørgen R., MH	Second-order Loads in Multidirectional Seas. (Dr.Ing. Thesis)
MTA-91-85	Molteberg, Gunnar A., MM	The Application of System Identification Techniques to Performance Monitoring of Four Stroke Turbocharged Diesel Engines. (Dr.Ing. Thesis)
MTA-92-86	Mørch, Hans Jørgen Bjelke, MH	Aspects of Hydrofoil Design: with Emphasis on Hydrofoil Interaction in Calm Water. (Dr.Ing. Thesis)
MTA-92-87	Chan Siu Hung, MM	Nonlinear Analysis of Rotordynamic Instabilities in Highspeed Turbomachinery. (Dr.Ing. Thesis)
MTA-92-88	Bessason, Bjarni, MK	Assessment of Earthquake Loading and Response of Seismically Isolated Bridges. (Dr.Ing. Thesis)
MTA-92-89	Langli, Geir, MP	Improving Operational Safety through exploitation of Design Knowledge - an investigation of offshore platform safety. (Dr.Ing. Thesis)
MTA-92-90	Sævik, Svein, MK	On Stresses and Fatigue in Flexible Pipes. (Dr.Ing. Thesis)
MTA-92-91	Ask, Tor Ø., MM	Ignition and Flame Growth in Lean Gas-Air Mixtures. An Experimental Study with a Schlieren

		System. (Dr.Ing. Thesis)
MTA-86-92	Hessen, Gunnar, MK	Fracture Mechanics Analysis of Stiffened Tubular Members. (Dr.Ing. Thesis)
MTA-93-93	Steinebach, Christian, MM	Knowledge Based Systems for Diagnosis of Rotating Machinery. (Dr.Ing. Thesis)
MTA-93-94	Dalane, Jan Inge, MK	System Reliability in Design and Maintenance of Fixed Offshore Structures. (Dr.Ing. Thesis)
MTA-93-95	Steen, Sverre, MH	Cobblestone Effect on SES. (Dr.Ing. Thesis)
MTA-93-96	Karunakaran, Daniel, MK	Nonlinear Dynamic Response and Reliability Analysis of Drag-dominated Offshore Platforms. (Dr.Ing. Thesis)
MTA-93-97	Hagen, Arnulf, MP	The Framework of a Design Process Language. (Dr.Ing. Thesis)
MTA-93-98	Nordrik, Rune, MM	Investigation of Spark Ignition and Autoignition in Methane and Air Using Computational Fluid Dynamics and Chemical Reaction Kinetics. A Numerical Study of Ignition Processes in Internal Combustion Engines. (Dr.Ing. Thesis)
MTA-94-99	Passano, Elizabeth, MK	Efficient Analysis of Nonlinear Slender Marine Structures. (Dr.Ing. Thesis)
MTA-94-100	Kvålsvold, Jan, MH	Hydroelastic Modelling of Wetdeck Slamming on Multihull Vessels. (Dr.Ing. Thesis)
MTA-94-102	Bech, Sidsel M., MK	Experimental and Numerical Determination of Stiffness and Strength of GRP/PVC Sandwich Structures. (Dr.Ing. Thesis)
MTA-95-103	Paulsen, Hallvard, MM	A Study of Transient Jet and Spray using a Schlieren Method and Digital Image Processing. (Dr.Ing. Thesis)
MTA-95-104	Hovde, Geir Olav, MK	Fatigue and Overload Reliability of Offshore Structural Systems, Considering the Effect of Inspection and Repair. (Dr.Ing. Thesis)
MTA-95-105	Wang, Xiaozhi, MK	Reliability Analysis of Production Ships with Emphasis on Load Combination and Ultimate Strength. (Dr.Ing. Thesis)
MTA-95-106	Ulstein, Tore, MH	Nonlinear Effects of a Flexible Stern Seal Bag on Cobblestone Oscillations of an SES. (Dr.Ing. Thesis)
MTA-95-107	Solaas, Frøydis, MH	Analytical and Numerical Studies of Sloshing in Tanks. (Dr.Ing. Thesis)
MTA-95-108	Hellan, Øyvind, MK	Nonlinear Pushover and Cyclic Analyses in Ultimate Limit State Design and Reassessment of Tubular Steel Offshore Structures. (Dr.Ing. Thesis)
MTA-95-109	Hermundstad, Ole A., MK	Theoretical and Experimental Hydroelastic Analysis of High Speed Vessels. (Dr.Ing. Thesis)

MTA-96-110	Bratland, Anne K., MH	Wave-Current Interaction Effects on Large-Volume Bodies in Water of Finite Depth. (Dr.Ing. Thesis)
MTA-96-111	Herfjord, Kjell, MH	A Study of Two-dimensional Separated Flow by a Combination of the Finite Element Method and Navier-Stokes Equations. (Dr.Ing. Thesis)
MTA-96-112	Æsøy, Vilmar, MM	Hot Surface Assisted Compression Ignition in a Direct Injection Natural Gas Engine. (Dr.Ing. Thesis)
MTA-96-113	Eknes, Monika L., MK	Escalation Scenarios Initiated by Gas Explosions on Offshore Installations. (Dr.Ing. Thesis)
MTA-96-114	Erikstad, Stein O., MP	A Decision Support Model for Preliminary Ship Design. (Dr.Ing. Thesis)
MTA-96-115	Pedersen, Egil, MH	A Nautical Study of Towed Marine Seismic Streamer Cable Configurations. (Dr.Ing. Thesis)
MTA-97-116	Moksnes, Paul O., MM	Modelling Two-Phase Thermo-Fluid Systems Using Bond Graphs. (Dr.Ing. Thesis)
MTA-97-117	Halse, Karl H., MK	On Vortex Shedding and Prediction of Vortex-Induced Vibrations of Circular Cylinders. (Dr.Ing. Thesis)
MTA-97-118	Igland, Ragnar T., MK	Reliability Analysis of Pipelines during Laying, considering Ultimate Strength under Combined Loads. (Dr.Ing. Thesis)
MTA-97-119	Pedersen, Hans-P., MP	Levendefiskteknologi for fiskefartøy. (Dr.Ing. Thesis)
MTA-98-120	Vikestad, Kyrre, MK	Multi-Frequency Response of a Cylinder Subjected to Vortex Shedding and Support Motions. (Dr.Ing. Thesis)
MTA-98-121	Azadi, Mohammad R. E., MK	Analysis of Static and Dynamic Pile-Soil-Jacket Behaviour. (Dr.Ing. Thesis)
MTA-98-122	Ulltang, Terje, MP	A Communication Model for Product Information. (Dr.Ing. Thesis)
MTA-98-123	Torbergsen, Erik, MM	Impeller/Diffuser Interaction Forces in Centrifugal Pumps. (Dr.Ing. Thesis)
MTA-98-124	Hansen, Edmond, MH	A Discrete Element Model to Study Marginal Ice Zone Dynamics and the Behaviour of Vessels Moored in Broken Ice. (Dr.Ing. Thesis)
MTA-98-125	Videiro, Paulo M., MK	Reliability Based Design of Marine Structures. (Dr.Ing. Thesis)
MTA-99-126	Mainçon, Philippe, MK	Fatigue Reliability of Long Welds Application to Titanium Risers. (Dr.Ing. Thesis)
MTA-99-127	Haugen, Elin M., MH	Hydroelastic Analysis of Slamming on Stiffened Plates with Application to Catamaran Wetdecks. (Dr.Ing. Thesis)
MTA-99-	Langhelle, Nina K., MK	Experimental Validation and Calibration of

128		Nonlinear Finite Element Models for Use in Design of Aluminium Structures Exposed to Fire. (Dr.Ing. Thesis)
MTA-99-129	Berstad, Are J., MK	Calculation of Fatigue Damage in Ship Structures. (Dr.Ing. Thesis)
MTA-99-130	Andersen, Trond M., MM	Short Term Maintenance Planning. (Dr.Ing. Thesis)
MTA-99-131	Tveiten, Bård Wathne, MK	Fatigue Assessment of Welded Aluminium Ship Details. (Dr.Ing. Thesis)
MTA-99-132	Søreide, Fredrik, MP	Applications of underwater technology in deep water archaeology. Principles and practice. (Dr.Ing. Thesis)
MTA-99-133	Tønnessen, Rune, MH	A Finite Element Method Applied to Unsteady Viscous Flow Around 2D Blunt Bodies With Sharp Corners. (Dr.Ing. Thesis)
MTA-99-134	Elvekrok, Dag R., MP	Engineering Integration in Field Development Projects in the Norwegian Oil and Gas Industry. The Supplier Management of Norne. (Dr.Ing. Thesis)
MTA-99-135	Fagerholt, Kjetil, MP	Optimeringsbaserte Metoder for Ruteplanlegging innen skipsfart. (Dr.Ing. Thesis)
MTA-99-136	Bysveen, Marie, MM	Visualization in Two Directions on a Dynamic Combustion Rig for Studies of Fuel Quality. (Dr.Ing. Thesis)
MTA-2000-137	Storteig, Eskild, MM	Dynamic characteristics and leakage performance of liquid annular seals in centrifugal pumps. (Dr.Ing. Thesis)
MTA-2000-138	Sagli, Gro, MK	Model uncertainty and simplified estimates of long term extremes of hull girder loads in ships. (Dr.Ing. Thesis)
MTA-2000-139	Tronstad, Harald, MK	Nonlinear analysis and design of cable net structures like fishing gear based on the finite element method. (Dr.Ing. Thesis)
MTA-2000-140	Kroneberg, André, MP	Innovation in shipping by using scenarios. (Dr.Ing. Thesis)
MTA-2000-141	Haslum, Herbjørn Alf, MH	Simplified methods applied to nonlinear motion of spar platforms. (Dr.Ing. Thesis)
MTA-2001-142	Samdal, Ole Johan, MM	Modelling of Degradation Mechanisms and Stressor Interaction on Static Mechanical Equipment Residual Lifetime. (Dr.Ing. Thesis)
MTA-2001-143	Baarholm, Rolf Jarle, MH	Theoretical and experimental studies of wave impact underneath decks of offshore platforms. (Dr.Ing. Thesis)
MTA-2001-144	Wang, Lihua, MK	Probabilistic Analysis of Nonlinear Wave-induced Loads on Ships. (Dr.Ing. Thesis)
MTA-2001-145	Kristensen, Odd H. Holt, MK	Ultimate Capacity of Aluminium Plates under Multiple Loads, Considering HAZ Properties.

		(Dr.Ing. Thesis)
MTA-2001-146	Greco, Marilena, MH	A Two-Dimensional Study of Green-Water Loading. (Dr.Ing. Thesis)
MTA-2001-147	Heggelund, Svein E., MK	Calculation of Global Design Loads and Load Effects in Large High Speed Catamarans. (Dr.Ing. Thesis)
MTA-2001-148	Babalola, Olusegun T., MK	Fatigue Strength of Titanium Risers – Defect Sensitivity. (Dr.Ing. Thesis)
MTA-2001-149	Mohammed, Abuu K., MK	Nonlinear Shell Finite Elements for Ultimate Strength and Collapse Analysis of Ship Structures. (Dr.Ing. Thesis)
MTA-2002-150	Holmedal, Lars E., MH	Wave-current interactions in the vicinity of the sea bed. (Dr.Ing. Thesis)
MTA-2002-151	Rognebakke, Olav F., MH	Sloshing in rectangular tanks and interaction with ship motions. (Dr.Ing. Thesis)
MTA-2002-152	Lader, Pål Furset, MH	Geometry and Kinematics of Breaking Waves. (Dr.Ing. Thesis)
MTA-2002-153	Yang, Qinzheng, MH	Wash and wave resistance of ships in finite water depth. (Dr.Ing. Thesis)
MTA-2002-154	Melhus, Øyvin, MM	Utilization of VOC in Diesel Engines. Ignition and combustion of VOC released by crude oil tankers. (Dr.Ing. Thesis)
MTA-2002-155	Ronæss, Marit, MH	Wave Induced Motions of Two Ships Advancing on Parallel Course. (Dr.Ing. Thesis)
MTA-2002-156	Økland, Ole D., MK	Numerical and experimental investigation of whipping in twin hull vessels exposed to severe wet deck slamming. (Dr.Ing. Thesis)
MTA-2002-157	Ge, Chunhua, MK	Global Hydroelastic Response of Catamarans due to Wet Deck Slamming. (Dr.Ing. Thesis)
MTA-2002-158	Byklum, Eirik, MK	Nonlinear Shell Finite Elements for Ultimate Strength and Collapse Analysis of Ship Structures. (Dr.Ing. Thesis)
IMT-2003-1	Chen, Haibo, MK	Probabilistic Evaluation of FPSO-Tanker Collision in Tandem Offloading Operation. (Dr.Ing. Thesis)
IMT-2003-2	Skaugset, Kjetil Bjørn, MK	On the Suppression of Vortex Induced Vibrations of Circular Cylinders by Radial Water Jets. (Dr.Ing. Thesis)
IMT-2003-3	Chezhian, Muthu	Three-Dimensional Analysis of Slamming. (Dr.Ing. Thesis)
IMT-2003-4	Buhaug, Øyvind	Deposit Formation on Cylinder Liner Surfaces in Medium Speed Engines. (Dr.Ing. Thesis)
IMT-2003-5	Tregde, Vidar	Aspects of Ship Design: Optimization of Aft Hull with Inverse Geometry Design. (Dr.Ing. Thesis)

IMT-2003-6	Wist, Hanne Therese	Statistical Properties of Successive Ocean Wave Parameters. (Dr.Ing. Thesis)
IMT-2004-7	Ransau, Samuel	Numerical Methods for Flows with Evolving Interfaces. (Dr.Ing. Thesis)
IMT-2004-8	Soma, Torkel	Blue-Chip or Sub-Standard. A data interrogation approach of identity safety characteristics of shipping organization. (Dr.Ing. Thesis)
IMT-2004-9	Ersdal, Svein	An experimental study of hydrodynamic forces on cylinders and cables in near axial flow. (Dr.Ing. Thesis)
IMT-2005-10	Brodtkorb, Per Andreas	The Probability of Occurrence of Dangerous Wave Situations at Sea. (Dr.Ing. Thesis)
IMT-2005-11	Yttervik, Rune	Ocean current variability in relation to offshore engineering. (Dr.Ing. Thesis)
IMT-2005-12	Fredheim, Arne	Current Forces on Net-Structures. (Dr.Ing. Thesis)
IMT-2005-13	Heggernes, Kjetil	Flow around marine structures. (Dr.Ing. Thesis
IMT-2005-14	Fouques, Sebastien	Lagrangian Modelling of Ocean Surface Waves and Synthetic Aperture Radar Wave Measurements. (Dr.Ing. Thesis)
IMT-2006-15	Holm, Håvard	Numerical calculation of viscous free surface flow around marine structures. (Dr.Ing. Thesis)
IMT-2006-16	Bjørheim, Lars G.	Failure Assessment of Long Through Thickness Fatigue Cracks in Ship Hulls. (Dr.Ing. Thesis)
IMT-2006-17	Hansson, Lisbeth	Safety Management for Prevention of Occupational Accidents. (Dr.Ing. Thesis)
IMT-2006-18	Zhu, Xinying	Application of the CIP Method to Strongly Nonlinear Wave-Body Interaction Problems. (Dr.Ing. Thesis)
IMT-2006-19	Reite, Karl Johan	Modelling and Control of Trawl Systems. (Dr.Ing. Thesis)
IMT-2006-20	Smogeli, Øyvind Notland	Control of Marine Propellers. From Normal to Extreme Conditions. (Dr.Ing. Thesis)
IMT-2007-21	Storhaug, Gaute	Experimental Investigation of Wave Induced Vibrations and Their Effect on the Fatigue Loading of Ships. (Dr.Ing. Thesis)
IMT-2007-22	Sun, Hui	A Boundary Element Method Applied to Strongly Nonlinear Wave-Body Interaction Problems. (PhD Thesis, CeSOS)
IMT-2007-23	Rustad, Anne Marthine	Modelling and Control of Top Tensioned Risers. (PhD Thesis, CeSOS)
IMT-2007-24	Johansen, Vegar	Modelling flexible slender system for real-time

		simulations and control applications
IMT-2007-25	Wroldsen, Anders Sunde	Modelling and control of tensegrity structures. (PhD Thesis, CeSOS)
IMT-2007-26	Aronsen, Kristoffer Høye	An experimental investigation of in-line and combined inline and cross flow vortex induced vibrations. (Dr. avhandling, IMT)
IMT-2007-27	Gao, Zhen	Stochastic Response Analysis of Mooring Systems with Emphasis on Frequency-domain Analysis of Fatigue due to Wide-band Response Processes (PhD Thesis, CeSOS)
IMT-2007-28	Thorstensen, Tom Anders	Lifetime Profit Modelling of Ageing Systems Utilizing Information about Technical Condition. (Dr.ing. thesis, IMT)
IMT-2008-29	Refsnes, Jon Erling Gorset	Nonlinear Model-Based Control of Slender Body AUVs (PhD Thesis, IMT)
IMT-2008-30	Berntsen, Per Ivar B.	Structural Reliability Based Position Mooring. (PhD-Thesis, IMT)
IMT-2008-31	Ye, Naiquan	Fatigue Assessment of Aluminium Welded Box-stiffener Joints in Ships (Dr.ing. thesis, IMT)
IMT-2008-32	Radan, Damir	Integrated Control of Marine Electrical Power Systems. (PhD-Thesis, IMT)
IMT-2008-33	Thomassen, Paul	Methods for Dynamic Response Analysis and Fatigue Life Estimation of Floating Fish Cages. (Dr.ing. thesis, IMT)
IMT-2008-34	Pákozdi, Csaba	A Smoothed Particle Hydrodynamics Study of Two-dimensional Nonlinear Sloshing in Rectangular Tanks. (Dr.ing.thesis, IMT/ CeSOS)
IMT-2007-35	Grytøyr, Guttorm	A Higher-Order Boundary Element Method and Applications to Marine Hydrodynamics. (Dr.ing.thesis, IMT)
IMT-2008-36	Drummen, Ingo	Experimental and Numerical Investigation of Nonlinear Wave-Induced Load Effects in Containerships considering Hydroelasticity. (PhD thesis, CeSOS)
IMT-2008-37	Skejic, Renato	Maneuvering and Seakeeping of a Singel Ship and of Two Ships in Interaction. (PhD-Thesis, CeSOS)
IMT-2008-38	Harlem, Alf	An Age-Based Replacement Model for Repairable Systems with Attention to High-Speed Marine Diesel Engines. (PhD-Thesis, IMT)
IMT-2008-39	Alsos, Hagbart S.	Ship Grounding. Analysis of Ductile Fracture, Bottom Damage and Hull Girder Response. (PhD-thesis, IMT)
IMT-2008-40	Graczyk, Mateusz	Experimental Investigation of Sloshing Loading and Load Effects in Membrane LNG Tanks Subjected to Random Excitation. (PhD-thesis, CeSOS)

IMT-2008-41	Taghipour, Reza	Efficient Prediction of Dynamic Response for Flexible amd Multi-body Marine Structures. (PhD-thesis, CeSOS)
IMT-2008-42	Ruth, Eivind	Propulsion control and thrust allocation on marine vessels. (PhD thesis, CeSOS)
IMT-2008-43	Nystad, Bent Helge	Technical Condition Indexes and Remaining Useful Life of Aggregated Systems. PhD thesis, IMT
IMT-2008-44	Soni, Prashant Kumar	Hydrodynamic Coefficients for Vortex Induced Vibrations of Flexible Beams, PhD thesis, CeSOS
IMT-2009-45	Amlashi, Hadi K.K.	Ultimate Strength and Reliability-based Design of Ship Hulls with Emphasis on Combined Global and Local Loads. PhD Thesis, IMT
IMT-2009-46	Pedersen, Tom Arne	Bond Graph Modelling of Marine Power Systems. PhD Thesis, IMT
IMT-2009-47	Kristiansen, Trygve	Two-Dimensional Numerical and Experimental Studies of Piston-Mode Resonance. PhD-Thesis, CeSOS
IMT-2009-48	Ong, Muk Chen	Applications of a Standard High Reynolds Number Model and a Stochastic Scour Prediction Model for Marine Structures. PhD-thesis, IMT
IMT-2009-49	Hong, Lin	Simplified Analysis and Design of Ships subjected to Collision and Grounding. PhD-thesis, IMT
IMT-2009-50	Koushan, Kamran	Vortex Induced Vibrations of Free Span Pipelines, PhD thesis, IMT
IMT-2009-51	Korsvik, Jarl Eirik	Heuristic Methods for Ship Routing and Scheduling. PhD-thesis, IMT
IMT-2009-52	Lee, Jihoon	Experimental Investigation and Numerical in Analyzing the Ocean Current Displacement of Longlines. Ph.d.-Thesis, IMT.
IMT-2009-53	Vestbøstad, Tone Gran	A Numerical Study of Wave-in-Deck Impact usin a Two-Dimensional Constrained Interpolation Profile Method, Ph.d.thesis, CeSOS.
IMT-2009-54	Bruun, Kristine	Bond Graph Modelling of Fuel Cells for Marine Power Plants. Ph.d.-thesis, IMT
IMT 2009-55	Holstad, Anders	Numerical Investigation of Turbulence in a Sekwed Three-Dimensional Channel Flow, Ph.d.-thesis, IMT.
IMT 2009-56	Ayala-Uraga, Efren	Reliability-Based Assessment of Deteriorating Ship-shaped Offshore Structures, Ph.d.-thesis, IMT
IMT 2009-57	Kong, Xiangjun	A Numerical Study of a Damaged Ship in Beam Sea Waves. Ph.d.-thesis, IMT/CeSOS.
IMT 2010-58	Kristiansen, David	Wave Induced Effects on Floaters of Aquaculture Plants, Ph.d.-thesis, CeSOS.

IMT 2010-59	Ludvigsen, Martin	An ROV-Toolbox for Optical and Acoustic Scientific Seabed Investigation. Ph.d.-thesis IMT.
IMT 2010-60	Hals, Jørgen	Modelling and Phase Control of Wave-Energy Converters. Ph.d.thesis, CeSOS.
IMT 2010- 61	Shu, Zhi	Uncertainty Assessment of Wave Loads and Ultimate Strength of Tankers and Bulk Carriers in a Reliability Framework. Ph.d. Thesis, IMT/ CeSOS
IMT 2010-62	Shao, Yanlin	Numerical Potential-Flow Studies on Weakly-Nonlinear Wave-Body Interactions with/without Small Forward Speed, Ph.d.thesis,CeSOS.
IMT 2010-63	Califano, Andrea	Dynamic Loads on Marine Propellers due to Intermittent Ventilation. Ph.d.thesis, IMT.
IMT 2010-64	El Khoury, George	Numerical Simulations of Massively Separated Turbulent Flows, Ph.d.-thesis, IMT
IMT 2010-65	Seim, Knut Sponheim	Mixing Process in Dense Overflows with Emphasis on the Faroe Bank Channel Overflow. Ph.d.thesis, IMT
IMT 2010-66	Jia, Huirong	Structural Analysis of Intect and Damaged Ships in a Collission Risk Analysis Perspective. Ph.d.thesis CeSoS.
IMT 2010-67	Jiao, Linlin	Wave-Induced Effects on a Pontoon-type Very Large Floating Structures (VLFS). Ph.D.-thesis, CeSOS.
IMT 2010-68	Abrahamsen, Bjørn Christian	Sloshing Induced Tank Roof with Entrapped Air Pocket. Ph.d.thesis, CeSOS.
IMT 2011-69	Karimirad, Madjid	Stochastic Dynamic Response Analysis of Spar-Type Wind Turbines with Catenary or Taut Mooring Systems. Ph.d.-thesis, CeSOS.
IMT - 2011-70	Erlend Meland	Condition Monitoring of Safety Critical Valves. Ph.d.-thesis, IMT.
IMT – 2011-71	Yang, Limin	Stochastic Dynamic System Analysis of Wave Energy Converter with Hydraulic Power Take-Off, with Particular Reference to Wear Damage Analysis, Ph.d. Thesis, CeSOS.
IMT – 2011-72	Visscher, Jan	Application of Particla Image Velocimetry on Turbulent Marine Flows, Ph.d.Thesis, IMT.
IMT – 2011-73	Su, Biao	Numerical Predictions of Global and Local Ice Loads on Ships. Ph.d.Thesis, CeSOS.
IMT – 2011-74	Liu, Zhenhui	Analytical and Numerical Analysis of Iceberg Collision with Ship Structures. Ph.d.Thesis, IMT.
IMT – 2011-75	Aarsæther, Karl Gunnar	Modeling and Analysis of Ship Traffic by Observation and Numerical Simulation. Ph.d.Thesis, IMT.

Imt – 2011-76	Wu, Jie	Hydrodynamic Force Identification from Stochastic Vortex Induced Vibration Experiments with Slender Beams. Ph.d.Thesis, IMT.
Imt – 2011-77	Amini, Hamid	Azimuth Propulsors in Off-design Conditions. Ph.d.Thesis, IMT.
IMT – 2011-78	Nguyen, Tan-Hoi	Toward a System of Real-Time Prediction and Monitoring of Bottom Damage Conditions During Ship Grounding. Ph.d.thesis, IMT.
IMT- 2011-79	Tavakoli, Mohammad T.	Assessment of Oil Spill in Ship Collision and Grounding, Ph.d.thesis, IMT.
IMT- 2011-80	Guo, Bingjie	Numerical and Experimental Investigation of Added Resistance in Waves. Ph.d.Thesis, IMT.
IMT- 2011-81	Chen, Qiaofeng	Ultimate Strength of Aluminium Panels, considering HAZ Effects, IMT
IMT- 2012-82	Kota, Ravikiran S.	Wave Loads on Decks of Offshore Structures in Random Seas, CeSOS.
IMT- 2012-83	Sten, Ronny	Dynamic Simulation of Deep Water Drilling Risers with Heave Compensating System, IMT.
IMT- 2012-84	Berle, Øyvind	Risk and resilience in global maritime supply chains, IMT.
IMT- 2012-85	Fang, Shaoji	Fault Tolerant Position Mooring Control Based on Structural Reliability, CeSOS.
IMT- 2012-86	You, Jikun	Numerical studies on wave forces and moored ship motions in intermediate and shallow water, CeSOS.
IMT- 2012-87	Xiang ,Xu	Maneuvering of two interacting ships in waves, CeSOS
IMT- 2012-88	Dong, Wenbin	Time-domain fatigue response and reliability analysis of offshore wind turbines with emphasis on welded tubular joints and gear components, CeSOS
IMT- 2012-89	Zhu, Suji	Investigation of Wave-Induced Nonlinear Load Effects in Open Ships considering Hull Girder Vibrations in Bending and Torsion, CeSOS
IMT- 2012-90	Zhou, Li	Numerical and Experimental Investigation of Station-keeping in Level Ice, CeSOS
IMT- 2012-91	Ushakov, Sergey	Particulate matter emission characteristics from diesel enignes operating on conventional and alternative marine fuels, IMT
IMT- 2013-1	Yin, Decao	Experimental and Numerical Analysis of Combined In-line and Cross-flow Vortex Induced Vibrations, CeSOS

IMT-2013-2	Kurniawan, Adi	Modelling and geometry optimisation of wave energy converters, CeSOS
IMT-2013-3	Al Ryati, Nabil	Technical condition indexes doe auxiliary marine diesel engines, IMT
IMT-2013-4	Firoozkoohi, Reza	Experimental, numerical and analytical investigation of the effect of screens on sloshing, CeSOS
IMT-2013-5	Ommani, Babak	Potential-Flow Predictions of a Semi-Displacement Vessel Including Applications to Calm Water Broaching, CeSOS
IMT-2013-6	Xing, Yihan	Modelling and analysis of the gearbox in a floating spar-type wind turbine, CeSOS
IMT-7-2013	Balland, Océane	Optimization models for reducing air emissions from ships, IMT
IMT-8-2013	Yang, Dan	Transitional wake flow behind an inclined flat plate-----Computation and analysis, IMT
IMT-9-2013	Abdillah, Suyuthi	Prediction of Extreme Loads and Fatigue Damage for a Ship Hull due to Ice Action, IMT
IMT-10-2013	Ramìrez, Pedro Agustìn Pèrez	Ageing management and life extension of technical systems- Concepts and methods applied to oil and gas facilities, IMT
IMT-11-2013	Chuang, Zhenju	Experimental and Numerical Investigation of Speed Loss due to Seakeeping and Maneuvering. IMT
IMT-12-2013	Etemaddar, Mahmoud	Load and Response Analysis of Wind Turbines under Atmospheric Icing and Controller System Faults with Emphasis on Spar Type Floating Wind Turbines, IMT
IMT-13-2013	Lindstad, Haakon	Strategies and measures for reducing maritime CO2 emissons, IMT
IMT-14-2013	Haris, Sabril	Damage interaction analysis of ship collisions, IMT
IMT-15-2013	Shainee, Mohamed	Conceptual Design, Numerical and Experimental Investigation of a SPM Cage Concept for Offshore Mariculture, IMT
IMT-16-2013	Gansel, Lars	Flow past porous cylinders and effects of biofouling and fish behavior on the flow in and around Atlantic salmon net cages, IMT
IMT-17-2013	Gaspar, Henrique	Handling Aspects of Complexity in Conceptual Ship Design, IMT
IMT-18-2013	Thys, Maxime	Theoretical and Experimental Investigation of a Free Running Fishing Vessel at Small Frequency of Encounter, CeSOS
IMT-19-2013	Aglen, Ida	VIV in Free Spanning Pipelines, CeSOS

IMT-1-2014	Song, An	Theoretical and experimental studies of wave diffraction and radiation loads on a horizontally submerged perforated plate, CeSOS
IMT-2-2014	Rogne, Øyvind Ygre	Numerical and Experimental Investigation of a Hinged 5-body Wave Energy Converter, CeSOS
IMT-3-2014	Dai, Lijuan	Safe and efficient operation and maintenance of offshore wind farms ,IMT
IMT-4-2014	Bachynski, Erin Elizabeth	Design and Dynamic Analysis of Tension Leg Platform Wind Turbines, CeSOS
IMT-5-2014	Wang, Jingbo	Water Entry of Freefall Wedged – Wedge motions and Cavity Dynamics, CeSOS
IMT-6-2014	Kim, Ekaterina	Experimental and numerical studies related to the coupled behavior of ice mass and steel structures during accidental collisions, IMT
IMT-7-2014	Tan, Xiang	Numerical investigation of ship's continuous- mode icebreaking in leverl ice, CeSOS
IMT-8-2014	Muliawan, Made Jaya	Design and Analysis of Combined Floating Wave and Wind Power Facilities, with Emphasis on Extreme Load Effects of the Mooring System, CeSOS
IMT-9-2014	Jiang, Zhiyu	Long-term response analysis of wind turbines with an emphasis on fault and shutdown conditions, IMT
IMT-10-2014	Dukan, Fredrik	ROV Motion Control Systems, IMT
IMT-11-2014	Grimsmo, Nils I.	Dynamic simulations of hydraulic cylinder for heave compensation of deep water drilling risers, IMT
IMT-12-2014	Kvittem, Marit I.	Modelling and response analysis for fatigue design of a semisubmersible wind turbine, CeSOS
IMT-13-2014	Akhtar, Juned	The Effects of Human Fatigue on Risk at Sea, IMT
IMT-14-2014	Syahroni, Nur	Fatigue Assessment of Welded Joints Taking into Account Effects of Residual Stress, IMT
IMT-1-2015	Bøckmann, Eirik	Wave Propulsion of ships, IMT
IMT-2-2015	Wang, Kai	Modelling and dynamic analysis of a semi-submersible floating vertical axis wind turbine, CeSOS
IMT-3-2015	Fredriksen, Arnt Gunvald	A numerical and experimental study of a two-dimensional body with moonpool in waves and current, CeSOS
IMT-4-2015	Jose Patricio Gallardo Canabes	Numerical studies of viscous flow around bluff bodies, IMT

IMT-5-2015	Vegard Longva	Formulation and application of finite element techniques for slender marine structures subjected to contact interactions, IMT
IMT-6-2015	Jacobus De Vaal	Aerodynamic modelling of floating wind turbines, CeSOS
IMT-7-2015	Fachri Nasution	Fatigue Performance of Copper Power Conductors, IMT
IMT-8-2015	Oleh I Karpa	Development of bivariate extreme value distributions for applications in marine technology,CeSOS
IMT-9-2015	Daniel de Almeida Fernandes	An output feedback motion control system for ROVs, AMOS
IMT-10-2015	Bo Zhao	Particle Filter for Fault Diagnosis: Application to Dynamic Positioning Vessel and Underwater Robotics, CeSOS
IMT-11-2015	Wenting Zhu	Impact of emission allocation in maritime transportation, IMT
IMT-12-2015	Amir Rasekhi Nejad	Dynamic Analysis and Design of Gearboxes in Offshore Wind Turbines in a Structural Reliability Perspective, CeSOS
IMT-13-2015	Arturo Jesùs Ortega Malca	Dynamic Response of Flexibles Risers due to Unsteady Slug Flow, CeSOS
IMT-14-2015	Dagfinn Husjord	Guidance and decision-support system for safe navigation of ships operating in close proximity, IMT
IMT-15-2015	Anirban Bhattacharyya	Ducted Propellers: Behaviour in Waves and Scale Effects, IMT
IMT-16-2015	Qin Zhang	Image Processing for Ice Parameter Identification in Ice Management, IMT
IMT-1-2016	Vincentius Rumawas	Human Factors in Ship Design and Operation: An Experiential Learning, IMT
IMT-2-2016	Martin Storheim	Structural response in ship-platform and ship-ice collisions, IMT
IMT-3-2016	Mia Abrahamsen Prsic	Numerical Simulations of the Flow around single and Tandem Circular Cylinders Close to a Plane Wall, IMT
IMT-4-2016	Tufan Arslan	Large-eddy simulations of cross-flow around ship sections, IMT

IMT-5-2016	Pierre Yves-Henry	Parametrisation of aquatic vegetation in hydraulic and coastal research,IMT
IMT-6-2016	Lin Li	Dynamic Analysis of the Instalation of Monopiles for Offshore Wind Turbines, CeSOS
IMT-7-2016	Øivind Kåre Kjerstad	Dynamic Positioning of Marine Vessels in Ice, IMT
IMT-8-2016	Xiaopeng Wu	Numerical Analysis of Anchor Handling and Fish Trawling Operations in a Safety Perspective, CeSOS
IMT-9-2016	Zhengshun Cheng	Integrated Dynamic Analysis of Floating Vertical Axis Wind Turbines, CeSOS
IMT-10-2016	Ling Wan	Experimental and Numerical Study of a Combined Offshore Wind and Wave Energy Converter Concept
IMT-11-2016	Wei Chai	Stochastic dynamic analysis and reliability evaluation of the roll motion for ships in random seas, CeSOS
IMT-12-2016	Øyvind Selnes Patricksson	Decision support for conceptual ship design with focus on a changing life cycle and future uncertainty, IMT
IMT-13-2016	Mats Jørgen Thorsen	Time domain analysis of vortex-induced vibrations, IMT
IMT-14-2016	Edgar McGuinness	Safety in the Norwegian Fishing Fleet – Analysis and measures for improvement, IMT
IMT-15-2016	Sepideh Jafarzadeh	Energy effiency and emission abatement in the fishing fleet, IMT
IMT-16-2016	Wilson Ivan Guachamin Acero	Assessment of marine operations for offshore wind turbine installation with emphasis on response-based operational limits, IMT
IMT-17-2016	Mauro Candeloro	Tools and Methods for Autonomous Operations on Seabed and Water Coumn using Underwater Vehicles, IMT
IMT-18-2016	Valentin Chabaud	Real-Time Hybrid Model Testing of Floating Wind Tubines, IMT
IMT-1-2017	Mohammad Saud Afzal	Three-dimensional streaming in a sea bed boundary layer
IMT-2-2017	Peng Li	A Theoretical and Experimental Study of Wave-induced Hydroelastic Response of a Circular Floating Collar
IMT-3-2017	Martin Bergström	A simulation-based design method for arctic maritime transport systems

IMT-4-2017	Bhushan Taskar	The effect of waves on marine propellers and propulsion
IMT-5-2017	Mohsen Bardestani	A two-dimensional numerical and experimental study of a floater with net and sinker tube in waves and current
IMT-6-2017	Fatemeh Hoseini Dadmarzi	Direct Numerical Simualtion of turbulent wakes behind different plate configurations
IMT-7-2017	Michel R. Miyazaki	Modeling and control of hybrid marine power plants
IMT-8-2017	Giri Rajasekhar Gunnu	Safety and effiency enhancement of anchor handling operations with particular emphasis on the stability of anchor handling vessels
IMT-9-2017	Kevin Koosup Yum	Transient Performance and Emissions of a Turbocharged Diesel Engine for Marine Power Plants
IMT-10-2017	Zhaolong Yu	Hydrodynamic and structural aspects of ship collisions
IMT-11-2017	Martin Hassel	Risk Analysis and Modelling of Allisions between Passing Vessels and Offshore Installations
IMT-12-2017	Astrid H. Brodtkorb	Hybrid Control of Marine Vessels – Dynamic Positioning in Varying Conditions
IMT-13-2017	Kjersti Bruserud	Simultaneous stochastic model of waves and current for prediction of structural design loads
IMT-14-2017	Finn-Idar Grøtta Giske	Long-Term Extreme Response Analysis of Marine Structures Using Inverse Reliability Methods
IMT-15-2017	Stian Skjong	Modeling and Simulation of Maritime Systems and Operations for Virtual Prototyping using co-Simulations
IMT-1-2018	Yingguang Chu	Virtual Prototyping for Marine Crane Design and Operations
IMT-2-2018	Sergey Gavrilin	Validation of ship manoeuvring simulation models
IMT-3-2018	Jeevith Hegde	Tools and methods to manage risk in autonomous subsea inspection,maintenance and repair operations
IMT-4-2018	Ida M. Strand	Sea Loads on Closed Flexible Fish Cages
IMT-5-2018	Erlend Kvinge Jørgensen	Navigation and Control of Underwater Robotic Vehicles

IMT-6-2018	Bård Stovner	Aided Intertial Navigation of Underwater Vehicles
IMT-7-2018	Erlend Liavåg Grotle	Thermodynamic Response Enhanced by Sloshing in Marine LNG Fuel Tanks
IMT-8-2018	Børge Rokseth	Safety and Verification of Advanced Maritime Vessels
IMT-9-2018	Jan Vidar Ulveseter	Advances in Semi-Empirical Time Domain Modelling of Vortex-Induced Vibrations
IMT-10-2018	Chenyu Luan	Design and analysis for a steel braceless semi-submersible hull for supporting a 5-MW horizontal axis wind turbine
IMT-11-2018	Carl Fredrik Rehn	Ship Design under Uncertainty
IMT-12-2018	Øyvind Ødegård	Towards Autonomous Operations and Systems in Marine Archaeology
IMT-13-2018	Stein Melvær Nornes	Guidance and Control of Marine Robotics for Ocean Mapping and Monitoring
IMT-14-2018	Petter Norgren	Autonomous Underwater Vehicles in Arctic Marine Operations: Arctic marine research and ice monitoring
IMT-15-2018	Minjoo Choi	Modular Adaptable Ship Design for Handling Uncertainty in the Future Operating Context
MT-16-2018	Ole Alexander Eidsvik	Dynamics of Remotely Operated Underwater Vehicle Systems
IMT-17-2018	Mahdi Ghane	Fault Diagnosis of Floating Wind Turbine Drivetrain- Methodologies and Applications
IMT-18-2018	Christoph Alexander Thieme	Risk Analysis and Modelling of Autonomous Marine Systems
IMT-19-2018	Yugao Shen	Operational limits for floating-collar fish farms in waves and current, without and with well-boat presence
IMT-20-2018	Tianjiao Dai	Investigations of Shear Interaction and Stresses in Flexible Pipes and Umbilicals
IMT-21-2018	Sigurd Solheim Pettersen	Resilience by Latent Capabilities in Marine Systems
IMT-22-2018	Thomas Sauder	Fidelity of Cyber-physical Empirical Methods. Application to the Active Truncation of Slender Marine Structures
IMT-23-2018	Jan-Tore Horn	Statistical and Modelling Uncertainties in the Design of Offshore Wind Turbines

IMT-24-2018	Anna Swider	Data Mining Methods for the Analysis of Power Systems of Vessels
IMT-1-2019	Zhao He	Hydrodynamic study of a moored fish farming cage with fish influence
IMT-2-2019	Isar Ghamari	Numerical and Experimental Study on the Ship Parametric Roll Resonance and the Effect of Anti-Roll Tank
IMT-3-2019	Håkon Strandenes	Turbulent Flow Simulations at Higher Reynolds Numbers
IMT-4-2019	Siri Mariane Holen	Safety in Norwegian Fish Farming – Concepts and Methods for Improvement
IMT-5-2019	Ping Fu	Reliability Analysis of Wake-Induced Riser Collision
IMT-6-2019	Vladimir Krivopolianskii	Experimental Investigation of Injection and Combustion Processes in Marine Gas Engines using Constant Volume Rig
IMT-7-2019	Anna Maria Kozlowska	Hydrodynamic Loads on Marine Propellers Subject to Ventilation and out of Water Condition.
IMT-8-2019	Hans-Martin Heyn	Motion Sensing on Vessels Operating in Sea Ice: A Local Ice Monitoring System for Transit and Stationkeeping Operations under the Influence of Sea Ice
IMT-9-2019|	Stefan Vilsen	Method for Real-Time Hybrid Model Testing of Ocean Structures – Case on Slender Marine Systems
IMT-10-2019	Finn-Christian W. Hanssen	Non-Linear Wave-Body Interaction in Severe Waves
IMT-11-2019	Trygve Olav Fossum	Adaptive Sampling for Marine Robotics
IMT-12-2019	Jørgen Bremnes Nielsen	Modeling and Simulation for Design Evaluation
IMT-13-2019	Yuna Zhao	Numerical modelling and dyncamic analysis of offshore wind turbine blade installation
IMT-14-2019	Daniela Myland	Experimental and Theoretical Investigations on the Ship Resistance in Level Ice
IMT-15-2019	Zhengru Ren	Advanced control algorithms to support automated offshore wind turbine installation
IMT-16-2019	Drazen Polic	Ice-propeller impact analysis using an inverse propulsion machinery simulation approach
IMT-17-2019	Endre Sandvik	Sea passage scenario simulation for ship system performance evaluation

IMT-18-2019	Loup Suja-Thauvin	Response of Monopile Wind Turbines to Higher Order Wave Loads
IMT-19-2019	Emil Smilden	Structural control of offshore wind turbines – Increasing the role of control design in offshore wind farm development
IMT-20-2019	Aleksandar-Sasa Milakovic	On equivalent ice thickness and machine learning in ship ice transit simulations
IMT-1-2020	Amrit Shankar Verma	Modelling, Analysis and Response-based Operability Assessment of Offshore Wind Turbine Blade Installation with Emphasis on Impact Damages
IMT-2-2020	Bent Oddvar Arnesen Haugaløkken	Autonomous Technology for Inspection, Maintenance and Repair Operations in the Norwegian Aquaculture
IMT-3-2020	Seongpil Cho	Model-based fault detection and diagnosis of a blade pitch system in floating wind turbines
IMT-4-2020	Jose Jorge Garcia Agis	Effectiveness in Decision-Making in Ship Design under Uncertainty
IMT-5-2020	Thomas H. Viuff	Uncertainty Assessment of Wave-and Current-induced Global Response of Floating Bridges
IMT-6-2020	Fredrik Mentzoni	Hydrodynamic Loads on Complex Structures in the Wave Zone
IMT-7-2020	Senthuran Ravinthrakumar	Numerical and Experimental Studies of Resonant Flow in Moonpools in Operational Conditions
IMT-8-2020	Stian Skaalvik Sandøy	Acoustic-based Probabilistic Localization and Mapping using Unmanned Underwater Vehicles for Aquaculture Operations
IMT-9-2020	Kun Xu	Design and Analysis of Mooring System for Semi-submersible Floating Wind Turbine in Shallow Water
IMT-10-2020	Jianxun Zhu	Cavity Flows and Wake Behind an Elliptic Cylinder Translating Above the Wall
IMT-11-2020	Sandra Hogenboom	Decision-making within Dynamic Positioning Operations in the Offshore Industry – A Human Factors based Approach
IMT-12-2020	Woongshik Nam	Structural Resistance of Ship and Offshore Structures Exposed to the Risk of Brittle Failure
IMT-13-2020	Svenn Are Tutturen Værnø	Transient Performance in Dynamic Positioning of Ships: Investigation of Residual Load Models and Control Methods for Effective Compensation
IMT-14-2020	Mohd Atif Siddiqui	Experimental and Numerical Hydrodynamic Analysis of a Damaged Ship in Waves
IMT-15-2020	John Marius Hegseth	Efficient Modelling and Design Optimization of Large Floating Wind Turbines

IMT-16-2020	Asle Natskår	Reliability-based Assessment of Marine Operations with Emphasis on Sea Transport on Barges
IMT-17-2020	Shi Deng	Experimental and Numerical Study of Hydrodynamic Responses of a Twin-Tube Submerged Floating Tunnel Considering Vortex-Induced Vibration
IMT-18-2020	Jone Torsvik	Dynamic Analysis in Design and Operation of Large Floating Offshore Wind Turbine Drivetrains
IMT-1-2021	Ali Ebrahimi	Handling Complexity to Improve Ship Design Competitiveness
IMT-2-2021	Davide Proserpio	Isogeometric Phase-Field Methods for Modeling Fracture in Shell Structures
IMT-3-2021	Cai Tian	Numerical Studies of Viscous Flow Around Step Cylinders
IMT-4-2021	Farid Khazaeli Moghadam	Vibration-based Condition Monitoring of Large Offshore Wind Turbines in a Digital Twin Perspective
IMT-5-2021	Shuaishuai Wang	Design and Dynamic Analysis of a 10-MW Medium-Speed Drivetrain in Offshore Wind Turbines
IMT-6-2021	Sadi Tavakoli	Ship Propulsion Dynamics and Emissions
IMT-7-2021	Haoran Li	Nonlinear wave loads, and resulting global response statistics of a semi-submersible wind turbine platform with heave plates
IMT-8-2021	Einar Skiftestad Ueland	Load Control for Real-Time Hybrid Model Testing using Cable-Driven Parallel Robots
IMT-9-2021	Mengning Wu	Uncertainty of machine learning-based methods for wave forecast and its effect on installation of offshore wind turbines
IMT-10-2021	Xu Han	Onboard Tuning and Uncertainty Estimation of Vessel Seakeeping Model Parameters
IMT-01-2022	Ingunn Marie Holmen	Safety in Exposed Aquacultrue Operations
IMT-02-2022	Prateek Gupta	Ship Performance Monitoring using In-service Measurements and Big Data Analysis Methods
IMT-03-2022	Sangwoo Kim	Non-linear time domain analysis of deepwater riser vortex-induced vibrations
IMT-04-2022	Jarle Vinje Kramer	Hydrodynamic Aspects of Sail-Assisted Merchant Vessels
IMT-05-2022	Øyvind Rabliås	Numerical and Expermental Studies of Maneuvering in Regular and Irregular Waves

IMT-06-2022	Pramod Ghimire	Simulation-Based Ship Hybrid Power System Conspet Studies and Performance Analyses
IMT-07-2022	Carlos Eduardo Silva de Souza	Structural modelling, coupled dynamics, and design of large floating wind turbines
IMT-08-2022	Lorenzo Balestra	Design of hybrid fuel cell & battery systems for maritime vessels
IMT-09-2022	Sharmin Sultana	Process safety and risk management using system perspectives – A contribution to the chemical process and petroleum industry
IMT-10-2022	Øystein Sture	Autonomous Exploration for Marine Minerals
IMT-11-2022	Tiantian Zhu	Information and Decision-making for Major Accident Prevention – A concept of information-based strategies for accident prevention
IMT-12-2022	Siamak Karimi	Shore-to-Ship Charging Systems for Battery-Electric Ships
IMT-01-2023	Huili Xu	Fish-inspired Propulsion Study: Numerical Hydrodynamics of Rigid/Flexible/Morphing Foils and Observations on Real Fish
IMT-02-2023	Chana Sinsabvarodom	Probabilistic Modelling of Ice-drift and Ice Loading on Fixed and Floating Offshore Structures
IMT-03-2023	Martin Skaldebø	Intelligent low-cost solutions for underwater intervention using computer vision and machine learning
IMT-04-2023	Hans Tobias Slette	Vessel operations in exposed aquaculture – Achieving safe and efficient operation of vessel fleets in fish farm systems experiencing challenging metocean conditions
IMT-05-2023	Ruochen Yang	Methods and models for analyzing and controlling the safety in operations of autonomous marine systems
IMT-06-2023	Tobias Rye Torben	Formal Approaches to Design and Verification of Safe Control Systems for Autonomous Vessels
IMT-07-2023	YoungRong Kim	Modeling Operational Performance for the Global Fleet & Application of an Energy Saving Measure
IMT-08-2023	Henrik Schmidt-Didlaukies	Modeling and Hybrid Feedback Control of Underwater Vehicles